

EVALUATION OF A HEATING SYSTEM
USING A HEAT PUMP AND HEAT STORE

By

MICHAEL JOHN NORREY B.A. (HONS)

A thesis submitted for the Degree of
Master of Philosophy

THE UNIVERSITY OF ASTON
IN BIRMINGHAM

DECEMBER 1987

"This copy of the thesis has been supplied on condition that anyone who consults it is understood to recognise that its copyright rests with its author and that no quotation from the thesis and no information derived from it may be published without the author's prior, written consent".

EVALUATION OF A HEATING SYSTEM
USING A HEAT PUMP AND HEAT STORE

MICHAEL JOHN NORREY

A thesis submitted for the degree of
MASTER OF PHILOSOPHY - 1987

SUMMARY

A commercial model reverse cycle heat pump of split System design having a nominal 8.35 kW heating capacity operating in an air-to-air mode, was modified by the author to operate in an air-to-water mode.

The 240v, single phase unit was incorporated into a purpose designed and constructed hot water storage system. The water circuit comprised the condenser connected via a closed-loop copper pipe network to two direct contact sensible heat stores. The storage vessels, modified to satisfy the basic requirements of a research programme, could be used singly or in parallel.

The system was instrumented throughout for monitoring individual circuit temperatures and pressures. A micro-computer, in conjunction with an Analogue-Digital (A-D) converter unit measured and recorded system conditions. Software used in the computerised control of the data collection was written by the Author.

Performance of the evaporator, condenser and water store was evaluated individually, and collectively, and compared with design performances corrected for prevailing conditions. The refrigerant mass flow rate was calculated based on ASHRAE methods and the air volume through the evaporator was accepted as the manufacturers stated value.

Manufacturers published performance data has been incorporated into the computer evaluation routine.

Theoretical aspects and practical problems associated with sensible heat storage have been examined. Results of promoting thermal stratification in one vessel are compared with the results from a similar, non-stratified vessel.

A mathematical relationship, based on empirical results, for predicting the development of stratification in a thermal store has been produced.

The resultant computer model predicts the amount of energy capable of being stored in a sensible heat store, being supplied from a reverse cycle heat pump, over selected running periods.

The temperature of the store can be predicted along with the instantaneous coefficient of performance (COP) of the overall system

KEY WORDS: Heat Pump; air-to-water; thermal energy store; stratification; computer model.

To my wife Maureen, daughters Ann Marie and Caroline
who's love and sacrifices have been my inspiration.

ACKNOWLEDGEMENTS

To Professor W E J Neal, Emeritus Professor, University of Aston in Birmingham, for the guidance, assistance and intellectual stimulation given throughout the duration of my research activity.

I also gratefully acknowledge the considerable attention and involvement of my supervisor, Mr M Wrenn, of the Department of Electrical and Electronic Engineering and Applied Physics at the University of Aston in Birmingham. My most sincere thanks are also due to Mr J S Phull and Mr R S Bassi who's valuable time was willingly given to discussions during my research work and for providing laboratory assistance whenever it was sought.

I also pay tribute to Mrs Hazel Wright, Departmental Secretary, Physics, who's direction, thoroughly professional services and considerable patience has enabled me to present the following thesis.

CONTENTS

	Page
Summary	2
Dedications	3
Acknowledgements	4
Contents	5
List of Graphs	9
List of Figures	14
List of Tables	20
List of Appendices	21
References	356
 CHAPTER ONE	
1. Introduction	24
1.1 Overall Objectives	24
1.2 Background	26
1.3 Heat Pumps - range of types and sizes currently available	30
1.3.1 Development Potential for heat pumps in the UK	32
1.3.2 Practical System Configurations	37
 CHAPTER TWO	
2. Description of the System Under Test	46
2.1 The Pressure - Enthalpy Cycle	65
2.2 Refrigerating Capacity	68

		Page
2.3	Evaporator Capacity and Performance	75
2.3.1	Evaporator Fan	81
2.4	Condenser	84
2.5	Empirical Laws (Pressure - Enthalpy)	86
2.6	Water Circulating Pump	87
2.7	Sensible Heat Store Vessels	96
2.8	System Monitoring and Instrumentation	106

CHAPTER THREE

3.	Evaporator Performance	
	- Psychrometric Properties	109
3.1	Theoretical Approach Towards Sensible and Latent Heat Availability	110
3.1.2	Design Data - Manufacturers Formulae	117
3.2	Condenser Performance	
	- Manufacturers Design Data	120
3.3	Heat Transfer Mechanisms in Thermal Store Vessels	128
3.4	Jet Entry Theory	134
3.4.1	Dimensionless Group Analysis	137
3.4.2	Heat Transfer Coefficients	142
3.5	Stratification in Sensible Heat Store Vessels	162

	Page
CHAPTER FOUR	
4.0	Heat Pump Components 165
4.1	Evaporator Coil Air Temperature
	Distribution Patterns 165
4.2	Condenser Coil Temperature
	Pattern 168
4.3	System Performance (corrected condenser design capacity) 175
4.3.1	Heat Transfer at Condenser 177
4.3.2	Heat Transfer to Store 179
4.4	Heat Pump Coefficient of Performance 181
4.5	Auxiliary Power Consumption 183
4.6	Overall System Coefficient of Performance (COP_H) 183
4.7	Temperature Distribution in Water Store 185
4.7.1	Fixed Position Thermocouples 185
4.7.2	Variable Position Thermocouples 205
4.7.3	Temperature Distribution along Horizontal Plane (radial distribution) 211
4.7.4	Temperature Patterns with the two Store Vessels in parallel 232
4.7.5	Mathematical model of Store Temperature Patterns 234
4.7.6	Discussion on Test Results 239

CHAPTER FIVE

5.	The Computer Model	252
5.1	The Model - an Overview	252
5.2	Inputs to Model	255
5.2.1	Data Collection	255
5.2.2	Calculation of System Performance	256
5.3	Data Manipulation within Model	257
5.4	Output from Model	268
5.5	Limitations of the Model	270

CHAPTER SIX

6	Possible Improvements to the System	276
6.1	The Heat Pump Unit	276
6.2	The System	278
6.2.1	The System - Condenser Coil	278
6.2.2	The System - Pipework	280
6.2.3	The System - Storage Vessels	281
6.3	Basis of a System for Commercial Application	284

CHAPTER SEVEN

7.	Future Possible Applications for Heat Pumps, with Thermal Storage in the UK	
7.1	System Economics	
7.2	Summary of Main Results	
7.3	Main Conclusions	
7.4	Recommendations for Future Work	

LIST OF GRAPHS

	Page
Graph 1 Water meter calibration and store capacity curves	52
Graph 2 Truco Condenser Coil - conversion factors	123
Graph 3 Actual spatial air temperatures at evaporator inlet and outlet	166
Graph 4 Average air temperatures at evaporator inlet and outlet	167
Graph 5 Condenser refrigerant and water temperatures - flow $1.065 \text{ m}^3 \text{ hr}^{-1}$	169
Graph 6 Condenser refrigerant and water temperatures - flow $1.1038 \text{ m}^3 \text{ hr}^{-1}$	170

	Page
Graph 7 Condenser refrigerant and water temperatures - flow 1.0295 m ³ hr ⁻¹	171
Graph 8 Condenser refrigerant and water temperatures - flow 0.7742 m ³ hr ⁻¹	172
Graph 9 Water store temperatures Vessel 1 (without diffuser) (fixed thermocouples)	186
Graph 10 Water store temperatures Vessel 1 (without diffuser) (fixed thermocouples)	189
Graph 11 Water store temperatures Vessel 1 (without diffuser) (fixed thermocouples - 335 minute run)	191
Graph 12 Water store temperatures Vessel 2 (with diffuser) (fixed thermocouples)	193
Graph 13 Water store temperatures Vessel 2 (with diffuser) (fixed thermocouples)	196

	Page
Graph 14 Water store temperatures Vessel 2 (with diffuser) (fixed thermocouples - 335 minute run)	199
Graph 15 Depthwise temperature distribution of water. (Vessels 1 & 2 - fixed thermocouples)	201
Graph 16 Water store temperatures Vessel 2 (with diffuser) (fixed and variable thermocouples)	206
Graph 17 Store temperature variation at radial positions and three vertical locations. (Vessel 2)	210
Graph 18. Vessel 2 water temperature (with diffuser) (at four vertical heights and five radial positions)	212
Graph 19 Vessel 2 water temperatures (with diffuser) (at three fixed thermocouples)	214

	Page
Graph 20 Vessel 2 water temperature (with diffuser) (mean actual and projected temperatures at four vertical heights)	216
Graph 21 Temperature distribution on horizontal plane at three vertical heights (Vessel 2)	219
Graph 22 Temperature distribution on horizontal plane at two vertical heights (Vessel 2)	221
Graph 23 Temperature distribution on horizontal plane at three vertical heights (Vessel 1)	223
Graph 24 Temperature distribution on horizontal plane at two vertical heights (Vessel 1)	226
Graph 25 Vessel 2 water temperatures (with diffuser) (variable position thermocouples)	228

	Page
Graph 26 Water temperatures - Vessels 1 & 2 (fixed and variable thermocouples)	231
Graph 27 Derivation of first term correction factor (cf) against height of water in vessel (based on Graph 20)	235
Graph 28 Basis for 2nd and 3rd term correction against height of water in vessel (based on Graph 20)	237

LIST OF FIGURES

	Page
Fig.1. Hot tap water heat pump with passive immersion condenser.	39
Fig.2. Hot tap water heat pump with controlled water circulation.	41
Fig.3. 38 CQ split system heat pump outdoor section and original heating cycle circuit, (Air-to-Air mode).	45
Fig.4. Truco coaxial condenser K7-13 WT.	47
Fig.5. Data sheet for Refrigerant R22.	48
Fig.6. 38 CQ split system heat pump circuit modified for air-to-water mode.	49
Fig.7. External view of condenser coil housing in-situ.	51

- Fig.8. View of store vessel with a graduated scale above for indicating the internal location of the variable position thermocouples (The vessel inspection port is also shown). 54
- Fig.9. View of the variable thermocouple carrier arrangement internal to the vessel. (The Vessel 2 velocity diffuser at the top of the vessel is shown). 56
- Fig.10. View showing a CBM model micro-computer, on-line printer and twin floppy disk drive. 58
- Fig.11. Diagrammatic presentation of fixed and variable thermocouple carrier arrangement in the store vessel. 59
- Fig.12. Temperature and pressure recording positions throughout the heat pump circuit. 61

	Page
Fig.13. Pressure/Enthalpy diagram for a basic cycle.	64
Fig.14. Accurator Components - An exploded view of Carlyle expansion valve.	74
Fig.15. Schematic layout of heat pump and thermal energy store.	88
Fig.16. View of vessel inspection port (showing partially filled vessel with thermocouple cables entering from above.	95
Fig.17. Section through vessel top entry arrangement.	97
Fig.18. View of variable position thermocouple carrier with a thermocouple bonded to the radial arm.	99

	Page
Fig.19. View of thermocouple carrier block and vessel dimensions.	101
Fig.20. Vessel 2 velocity diffuser dimensions.	103
Fig.21. Detail of circulating water header assembly.	105
Fig.22. Truco Coil Condenser performance curves.	121
Fig.23. Regimes of natural, forced and mixed convection for flow through vertical tubes.	132
Fig.24. Velocity field at the initial cross-section of a turbulent or submerged jet.	137
Fig.25. Velocity and temperature distribution for forced convection over a heated plate.	143

	Page
Fig.26. Variations in flow regimes at distances from the leading edge of a flat plate.	145
Fig.27. Flow geometries in a tube or duct.	147
Fig.28. Velocity distribution in laminar flow of a liquid with heating or cooling.	149
Fig.29. Diagram showing relationship of viscosity, velocity and temperature in fluid flow.	158
Fig.30. Radial and axial velocity components in fluid flows.	243
Fig.31. Energy loss due to sudden enlargement of pipe diameter (showing region of dead water "Po").	245

	Page
Fig.32. Basic schematic arrangement of vessel with multi-draw- off points (stratified energy store).	283
Fig.33. View of 38 CQ heat pump outdoor section.	309
Fig.34. Truco coaxial condenser K7-13 WT.	316
Fig.35. Location of thermocouples at evaporator air inlet and outlet.	321

LIST OF TABLES

	Page
1. Properties of common fluids.	138
2. Refrigerant temperatures at condenser inlet.	173
3. Rate of heat rejection, refrigerant to water.	174
4. Test data showing averaged store temperature used for compiling Graph 20.	218
5. Calculated values for water temperature in store compared to average recorded temperatures.	229
6. Desired range for setting the A-D unit.	313
7. Air temperatures at evaporator inlet and outlet. (Ref. Fig. 35(a))	323
8. Air temperature at evaporator inlet and outlet. (Ref. Figs 35 (b) (c))	325
9. Air temperature comparisons (averaged spacial viz central position)	328

LIST OF APPENDICES

	Page
1. Heat pump specifications	310
2. Analogue to digital conversion unit - manufacturers material.	312
3. Truco co-axial condenser coil.	317
4. Derived laws for determining absolute pressure - temperature/ enthalpy.	318
5. Air temperature distribution at evaporator coil (inlet and outlet).	320
6. Condenser coil - Derivation of Formulae.	331
7. Sample calculations based on actual test data.	335
8. Heat transfer at store vessel.	341

		Page
9.	Summary of test conditions for a typical test period (Ref. Graph 18).	346
10.	Summary of test conditions (Ref. Graph 25).	348
11.	Summary of equations used in the mathematical model.	350
12.	Output format of test data and typical evaluated results.	353
13.	Summary of parameters monitored during a test.	354
14.	Summarized calculation output format.	355

Big whirls have little whirls,
That feed on their velocity;
And little whirls have lesser whirls,
An so on to viscosity.

L F Richardson.

CHAPTER ONE

1. Introduction

1.1 Overall Objectives

The initial objectives were to design, construct, operate and evaluate a hot water system employing an electrically driven heat pump in conjunction with a sensible heat store, in a closed loop circuit.

The ultimate system design will be assessed for its suitability of use in commercial environments, where the system incorporates compatible standard production components.

In order to achieve the overall objectives the following secondary objectives were pursued.

Modification of the initial system design in light of operational performance in order to promote stratification in a heat store for drawing comparisons with a non-stratified store.

Production of a computer model of the system and a mathematical model of temperature stratification taking place in the sensible heat store vessels.

Assessment of the individual and collective performance of selected component manufacturers equipment using manufacturers published design criteria.

In order to satisfy the above objectives it was essential that the following activities were completed:

- (a) Identification of the important behavioural characteristics of a closed-loop hot water circuit through a direct contact heat store.
- (b) An examination of a heat store performance criteria where water is used as the store medium.
- (c) The development of a monitoring system to provide data for evaluating system operational performance via a computer model.
- (d) To assess the economics of a system capital and operating costs with a view to installing systems in selected commercial environments.

1.2 Background

Stratification in thermal stores has attracted limited attention from researchers to date. The reasons appear to be many and varied.

Tabor H[1], (1981) for example, believed that successful sensible heat storage

"..... raises a wide range of practical questions.....",

the solution to which,

".....meet with little consensus among the various designers".

He also implies that little progress had been made mainly up to 1981 because of the lack of meaningful research material.

A study undertaken by Brinkworth B J [2] (December 1979) of thermal storage in density stratified fluids and phase change materials also concludes that:

"Unresolved problems in thermo-hydrodynamics remain as obstacles to the effective design of thermal energy stores in the form of sensible and latent heat.

Emperical methods enable trial store designs to continue but a better understanding of natural convection is required".

The situation to date (September 1987) has barely changed. A search of the S.T.N. International Data-base, sponsored by the U.S. Department of Energy, and located in Karlsruhe, Germany, reveals that limited research material exists covering systems similar to this thesis material.

Van Koppen C W J^[3] (1982) has drawn a number of conclusions on the problems of sensible heat storage. Though his work refers more to storage in conjunction with solar energy systems, where the storage temperatures are higher than those currently experienced with heat pumps, he observed that for the majority of instances sensible heat stores are necessarily bulky devices. However, solar energy stores have to be significantly large to cater for the uncertainties of the heat supply whereas stores associated with heat pumps can be relatively less bulky because the heat supply can invariably be regulated to suit the system.

The development of suitable sensible heat stores has, according to Van Koppen, been inhibited because;

"The mathematical modelling of unsteady heat conduction and thermal stratification poses considerable problems for which as yet, no generally accepted solution is available".

A further reason for limited developments in sensible heat stores to date is the lack of distinction made between the storage for service hot water, often referred to as domestic hot water (DHW) and storage for space heating systems.

For the former a storage capacity can be readily determined but for the latter, as Van Koppen suggests;

"..... much confused thinking remains",
this no doubt being based on his findings during the early days of solar technology development as,

"..... little finesse is found in theoretical and experimental work".

A parametric study of DHW installations carried out at the University of Wisconsin^[4] (1973) covers some approaches considered appropriate for promoting temperature stratification in energy stores.

According to Wood R.J.^[5] (1981) experimental studies of thermal stratification in sensible heat thermal energy storage systems using water have been undertaken and design correlations suitable for use with cubical storage tanks have been derived.

Wood's analytical predictions of the transient development of the thermocline compare favourably with experimental measurements.

During the ISES Congress^[6] (1981) held in Brighton (England), some available methods for short-term sensible heat storage were presented.

It was, however, generally concluded that the relatively high capital cost of an adequately sized heat pump and system had been a major disincentive for heat pump systems and remained a prime reason for retaining existing, proven, heating units even though revenue costs of conventional systems were greater than for a heat pump system.

A study carried out by Cox A.J., Neal W.E.J. and Yankuba S.C.S.^[7], (1973) at Aston University also concluded that the present capital cost of electrically driven heat pumps made them unattractive for domestic space heating in the U.K. mainly;

"..... since there is little or no cooling requirement during the summer".

They do however state that for a DHW supply

"..... such an application could be a more viable introduction into the domestic and commercial market..... It would then seem appropriate to use electricity for shaft power rather than for resistive heating".

Cox A.J. et al also concluded that the equilibrium properties of the heat pump could be used to predict the non-equilibrium rise in temperature of the store.

In a review Neal W.E.J.^[8] (1981), outlined the types of thermal stores available. These included sensible heat and phase change heat stores. Stores involving chemical reaction were not considered.

Neal cites two examples of long term sensible heat stores in operation in the U.K. One being at the Building Research Establishment, near Watford and the other at the National Centre for Alternative Technology, Machynlleth (Wales).

Todd R W^[9] (1978) reports on the Machynlleth installation whilst Wozniak S T^[10] (1977) details the system installed at Watford.

1.3 Heat Pumps - range of types and sizes currently available

There are two main types of heat pump being currently considered for commercial application. These are classified as:

(a) the vapour-compression type

(b) the absorption cycle type.

The absorption cycle system is in the early stages of development. A prototype model developed by a major company in association with the U.K. Government was investigated - this particular model was aimed at meeting a 6 kw heat demand and was to produce water at approximately 55°C. The overall seasonal efficiency of the system was targeted for 125 to 130 per cent.

The size of available heat pump units ranges from electrically driven units of 1.5 kW output to over 6.0 Mw using gas engines, (Pearson J (1985)) [11]. A maximum output water temperature of approximately 70°C is considered achievable.

The majority of heat pumps used commercially are of the vapour-compression type driven mainly by electricity.

Electrically driven heat pumps have been installed in the U.K. in recent years having an installed capacity of some 25 Mw, according to Witt A M (1985) in an Electricity Council survey^[12].

Another method employed for supplying motive power is the internal combustion engine firing on natural gas, Liquid Petroleum Gas (LPG) or diesel oil.

1.3.1 Development Potential for Heat Pumps in the U.K.

Until recently there has been limited financial incentive for commerce and industry to deploy heat pumps for providing domestic hot water (DHW), or for space heating.

It is only within the last decade that more efficient use of primary energy has been given serious consideration worldwide.

The relatively low cost and high availability of primary fuels, coupled with the higher capital cost of heat pump equipment, has been the major reason for limited use of heat pumps

Pabon-Diaz^[13] (1982) comments on the progress of heat pump usage in the U.K. indicating that the bulk of the models used are of U.S.A. design and construction:-

"They have been used in the U.K. since the mid-1960's for space heating,These machines are electrically driven air-to-air heat pumps and usually require a three phase power supply".

When comparing heat pumps with conventional gas fired boilers, in terms of utilization of primary energy resources Pabon-Diaz states:-

"Studies by the Electricity Council indicate the Coefficient of Performance in the heating mode (COP_H) in the region of 2.3 to 2.5 for present machines in the U.K. climate averaged over one heating season. In fact an electrically driven heat pump with a COP_H of about 2.0 uses the same amount of primary energy to provide the same amount of heat as a gas fired boiler, working at 60% efficiency, using substitute natural gas".

Pabon-Diaz also suggests that several technical problems, associated with heat pump systems, in common use, still exists. Amongst the problems he cites the need for supplementary heat.

"Thus, the conventional air-to-air heat pump must be augmented by a fossil fuel appliance if the building demand exceeds the heat pump output".

Contrary to Pabon-Diaz assertions the use of supplementary heat can be considered more an economic expedient than a technical problem. The inclusion of supplementary heat not only contains system capital cost of installation but performs a necessary function during heat pump defrost periods.

A bivalent system also assists in maximising heat pump operating periods.

The employment of heat pumps operating in an air-to-water mode, in conjunction with a thermal store would overcome many of the problems identified by Pabon-Diaz, especially as the interest in heat pumps for providing some heating/cooling requirements is now gaining momentum.

The majority of heat pumps in use today operate at low condenser heat transfer fluid temperatures, that is, lower than is possible with conventional hot water systems. Heat pumps coupled directly to "wet" systems, i.e. those systems employing water filled radiators, suffer from several significant disadvantages - some of which have been identified by McDonnell T^[14], (1983).

One problem is that heat pump heating systems using water as the distribution medium operate at relatively low water temperatures, namely in the region of 50°C to 60°C,

and are therefore slow to raise the temperature of the environment when compared with a more conventional boiler/radiator system.

Larger than conventionally required radiator surface areas would, of course, partly overcome this relatively sluggish behaviour of the low thermal capacity heating system.

The higher operating temperature range of a conventional boiler can tolerate the low thermal capacity systems.

A further disadvantage of heat pumps connected directly to a "wet" system would be one of "wear and tear" of mechanical components.

The heat pump condenser unit transfers heat to the water faster than the radiators dissipate heat to the surrounding environment, consequently the heat pump, when operating in a direct mode - coupled directly to the radiator system - would be subjected to many cyclic (on-off) operations.

Frequent cyclic operations would have a greater adverse effect on the heat pump compressor than on a conventional boiler unit.

The stress on a compressor would promote mechanical breakdown at an early stage. For this reason alone it would be appropriate to include a thermal energy store in a heat pump hot water system.

The store would allow for longer periods of continuous heat pump operation and could possibly assist in confining some of the running period to the lower cost electricity tariff times.

However, improvements in design of the compressor, which is a major component in the Rankine compression cycle heat pump unit, and the continued development in refrigeration engineering, has ensured that the modern compressor unit is now a robust and reliable piece of equipment.

The recent, (1987) introduction to the commercial market of the rotary compressor along with an inverter in the mains electricity supply enables load-matching to take place which, in turn, reduces further the previously referred to cyclic operation.

Load matching is basically that of regulating the speed, hence output, of the heat pump to meet the demand placed upon it.

A mathematical model for determining the performance of variable speed air-to-water heat pump systems is described by Tassou S A [15] et al (June 1982).

The progress in refrigeration technology has also ensured the development of suitable refrigerants for heat pump applications.

The results of tests on a heat pump and thermal energy store presented in this thesis form part of a programme of work on the applications of heat pumps being undertaken in the Department of Electrical and Electronic Engineering and Applied Physics.

1.3.2 Practical System Configurations

Domestic hot water is an essential commodity more-or-less worldwide whereas the usefulness of space heating facilities, whether provided by water or by other means, is not a universal requirement.

Space cooling however is a desirable feature in many areas of the world. Domestic hot water and space heating/cooling can be readily accommodated by a heat pump based system. Electrically driven heat pumps would be

beneficial for reducing energy consumption and operating costs in instances where DHW and space heating/cooling is currently provided by electrical energy.

A 1982 publication by the U.K. Heat Pump and Air Conditioning Bureau[16] states:

"Experience has shown that where the heat pump installation is well designed, the equipment properly installed, commissioned and used, an average coefficient of seasonal performance of the order 2.5 to 1 can be achieved".

Pabon-Diaz[13] has calculated that, within the U.K, savings in annual national consumption of primary energy could amount to 7% and approximately 2% (space heating and DHW production) respectively, assuming the present annual domestic space heating load of the country could be met by electrically driven heat pumps working with an overall efficiency of 81%.

The savings in DHW production assume an annual net demand for useful energy of 12GJ (3336 Kwh) per dwelling and an electrically driven heat pump having a COP_H of 2.0 - overall efficiency of 54%.

Anderson J A [17] (1985) et al concluded from their own studies that the deployment of an air-water vapour-compression, electrically driven heat pump along with a

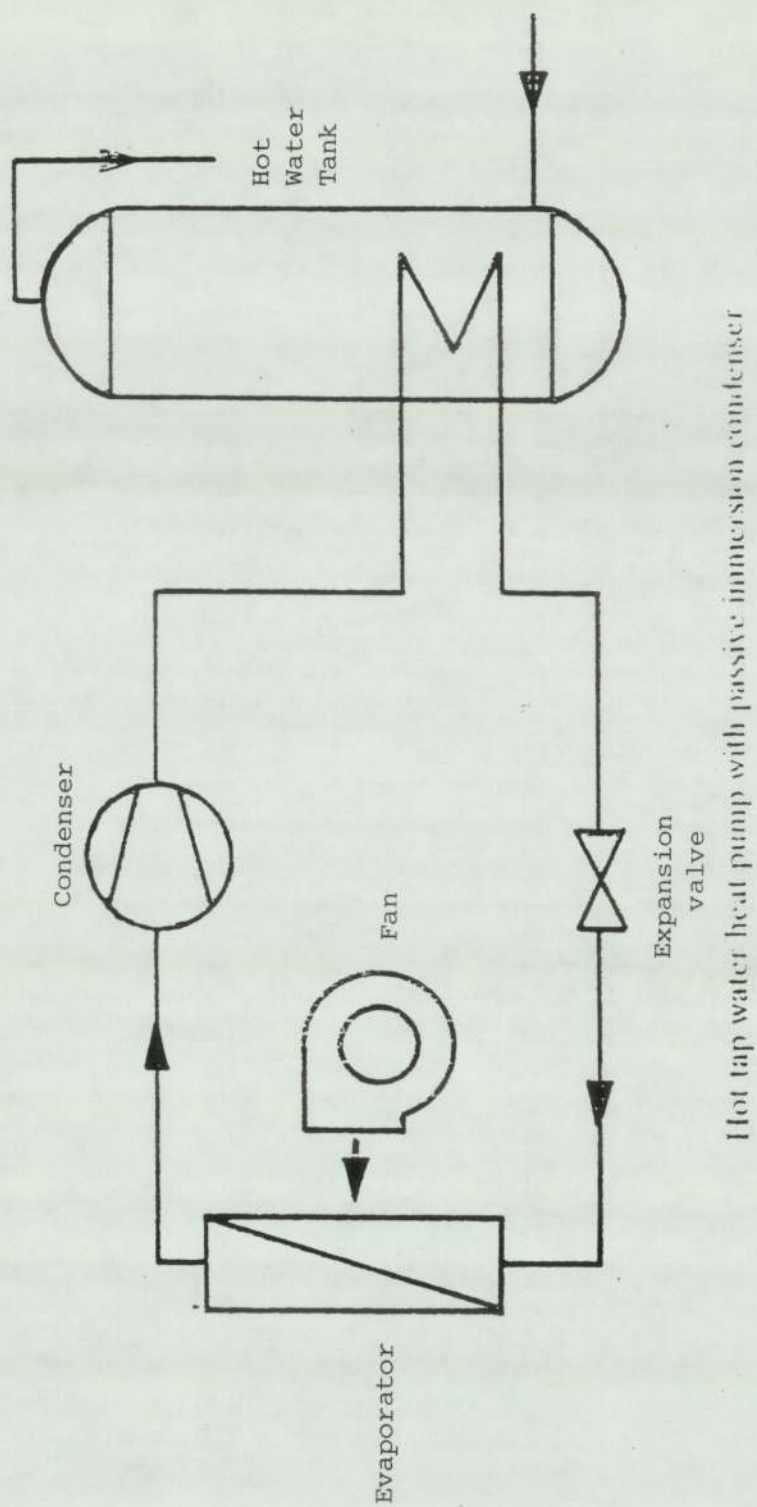


Fig.1.

thermal energy store, for providing DHW, can achieve electricity consumption savings, over nationally derived average consumption values, - of between 50% and 58%.

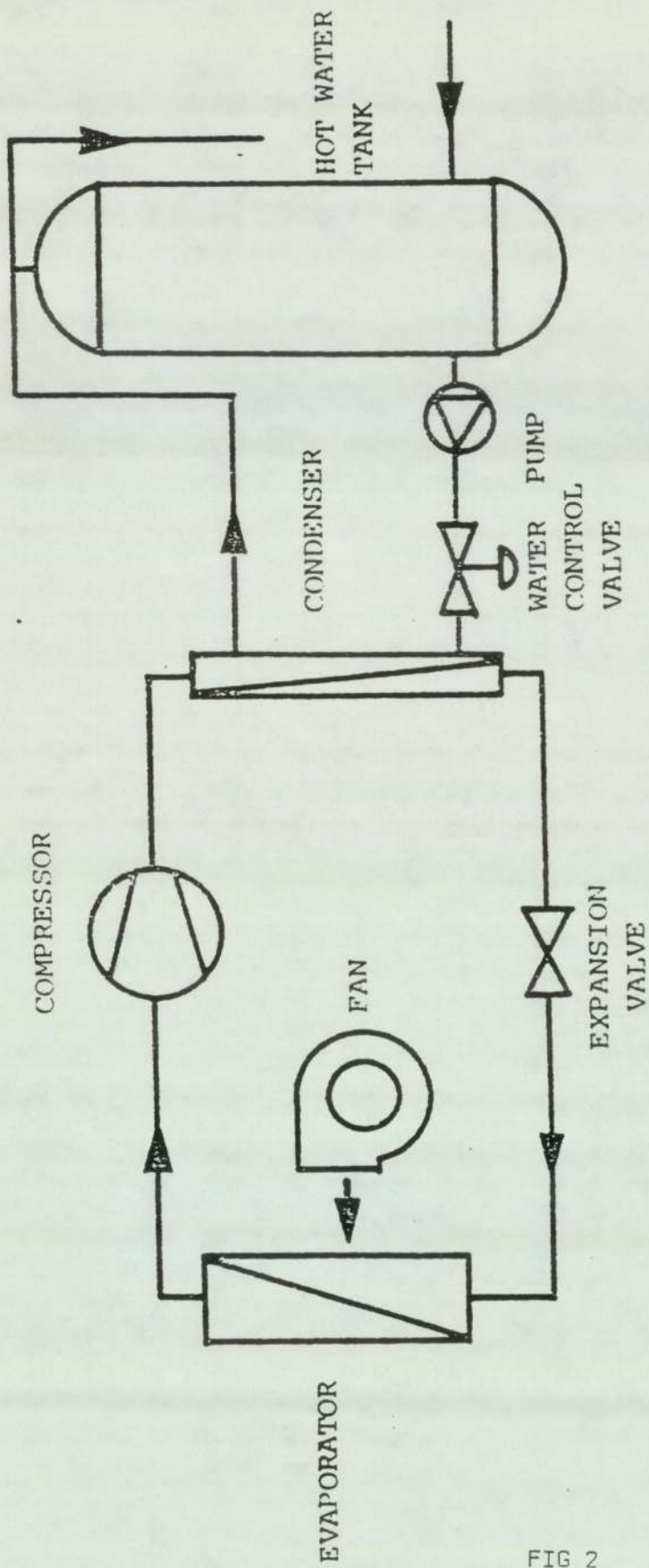
The inclusion of a thermal energy store into a system using a heat pump could therefore be of some commercial significance.

Thermal energy stores should, if correctly designed and operated, allow associated heat pump(s) to run for significant periods of time for obtaining optimum efficiency performance. This type of operating regime would reduce to a minimum the adverse effects referred to earlier of cyclic operation. The operating costs would, as suggested also be usefully controlled.

The thermal energy store design and performance is therefore a critical feature of such a system.

Carrington^[18] (1983) considered two designs for hot water producing heat pumps. In one system a condenser coil was situated internally to the water store vessel, - see Figure 1 - whilst the second operation was based on the water being actively pumped from the tank to the heat pump condenser and back to the tank, - see Figure 2.

The second approach, according to Carrington, is not in general use,



Hot tap water heat pump with controlled water circulation

FIG 2

"..... even though it has advantages over option one". The major disadvantage of these options in the UK, is that they would not meet current U.K. statutory requirements for prevention of refrigerant leakage into a domestic water source.

Carrington also states that for his options - Figures 1 and 2.

"In terms of thermodynamic efficiency there is no obvious advantage in one system or the other".

The introduction of two heat exchangers would, however, be a more acceptable approach for meeting U.K. statutory requirements but increases the system heat transfer losses and reduce operating efficiency.

The system used for the tests upon which this thesis is based, employs the second of Carrington's approaches, i.e. pumped water from a direct-contact storage vessel through a condensing coil and returning to the storage vessel.

An understanding of the behaviour of a thermal energy store is paramount if such systems are to become universally acceptable. Problems of thermal stratification in store vessels have been investigated by Channey S.R. [19], (1984) et al.

Whilst the studies of Channey have suggested that

"single medium thermocline energy storage (THES) systems are commercially attractive devices for off-peak storage of surplus energy in power generation systems".

their studies did not encompass the domestic/commercial type system requirements.

They do, however, state that:

"The practical realization of a THES system depends on the extent to which a hot layer of fluid can be stably stratified over a colder layer and both be made to flow without seriously eroding the temperature difference resulting at the hot-cold interface",

The difficulties of achieving these stable conditions have, as yet, not been fully overcome.

This thesis reviews an approach developed for promoting stratification in thermal energy stores, the benefits or otherwise in so doing and a means for modelling store temperature distribution patterns.


Comparisons of energy store effectiveness are also drawn with a similar vessel where storage stratification is not promoted.

It is anticipated that the commercial development of a practical system configuration combining a heat pump and energy store using an air-water system, may be further advanced through greater awareness of the advantages gained from employing thermal storage.

The problems associated with a complete evaluation of thermal store characteristics are known to be considerable and any practical system will contain elements which will be difficult to model.

The present experimental system enabled certain parameters to be evaluated but it must be realised that because of unavoidable restrictions on system design and construction there are limitations which preclude the evaluation of a perfect system.

The major physical construction limitations of the system employed are referred to in Chapter 2 of this thesis.

	Carlyle Air Conditioning Company Ltd.	38CQ Split System Heat Pump Outdoor Sections Heating 7180 - 10200 kcal/h Cooling 5680 - 9450 kcal/h 50 Hz
---	---	--

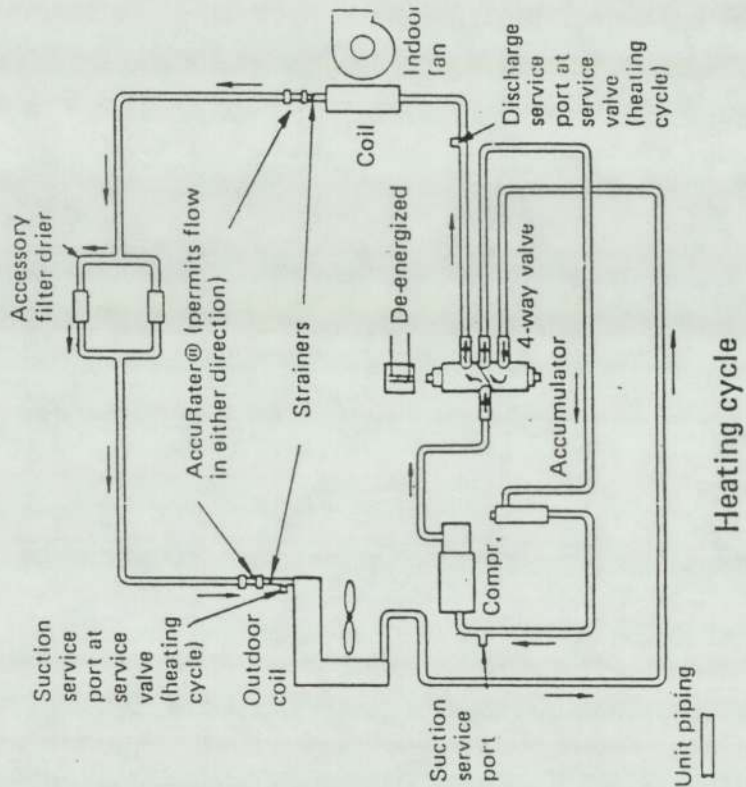
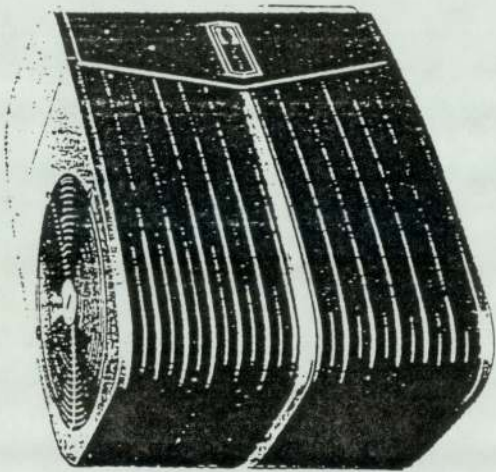


FIG 3

CHAPTER TWO

2. Description of the system under test

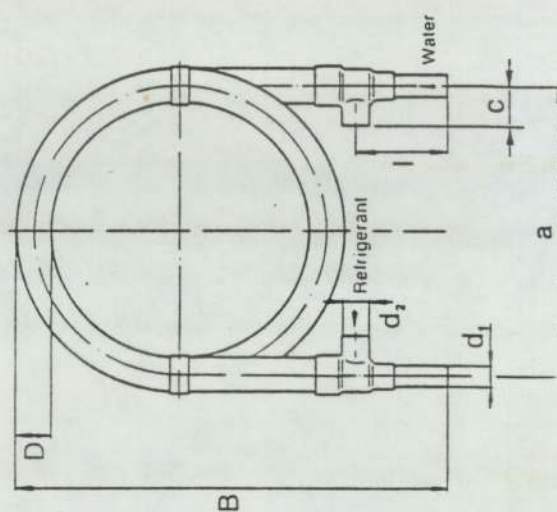
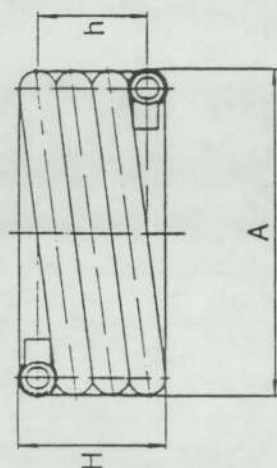
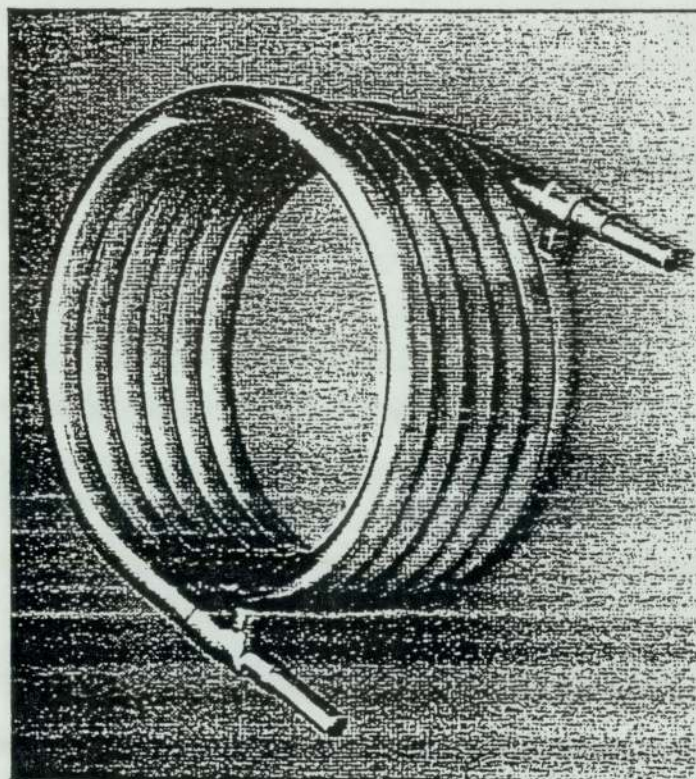
A major component of the system comprise a floor mounted outdoor unit of a standard commercial split-unit air-to-air heat pump of nominal heating capacity 8.35 kw, which was modified to an air-to-water unit for the purpose of this research project. The manufacturers specification for the original unit is included as Appendix 1. Fig. 3 shows the unit and refrigerant circuit for the heating cycle.

A counterflow co-axial condenser coil was built into the refrigerant circuit with the water side of the condenser being coupled to a thermal store. Details of the condenser coil are shown as Fig. 4.

The heat pump working fluid was refrigerant R22-mono-chloridifluoromethane (CH Cl F_2). a data sheet of which is presented as Fig 5. The line diagram of Fig 6 shows the modified refrigerant circuit layout.

The standard outdoor section of the heat pump contains:

Truco coaxial condenser K 7-13 WT



Dimensions		All dimensions in mm									
Truco coaxial condenser	Connection dimensions Water / Refrigerant	Maximum insulation dimensions	Outer dimensions	Outer dimensions	Outer dimensions	Outer dimensions	Outer dimensions	Outer dimensions	Outer dimensions	Outer dimensions	Outer dimensions
K 1-3 WT	15	151 ø	240	245	90	210	19	55	90	22	2
K 3-5 WT	15	151 ø	310	315	110	280	19	80	100	22	4
K 5-9 WT	18	181 ø	335	325	180	285	22	145	105	26	7
K 7-13 WT	22	221 ø	360	355	310	315	29	265	110	35	17
K 11-19 WT	28	281 ø	500	545	305	450	42	255	120	39	26
K 15-30 WT	35.1 ø	28	500	545	260	430	-	190	80	54	30
K 25-50 WT	42.1 ø	28	600	655	470	520	-	345	80	62	80

FIG 4

DATA SHEET FOR R 22					
C H F ₂ Cl		MONOCHLORODIFLUOROMETHANE		Molecular Wt. 86.5	
Pressure		Temperature		Volume	Density
50.3	kg/cm ²	96 ° C	205 ° F	1.904 l/kg	.525 kg/l.
716	psia	369 ° K	655 ° R	.0305 ft ³ /lb	32.8 lbs/ft ³
AT CRITICAL POINT					2.98 Air=1
Discharge Pressure		30° C 86° F		Discharge Temperature	
12.2	kg/cm ²			53 ° C	128 ° F
173	psia			326 ° K	588 ° R
Inlet Pressure		-15° C +5° F		Normal Boiling Point	
3.02	kg/cm ²			-40.8 ° C	-41.4 ° F
42.9	psia			232 ° K	418 ° R
		Refrigerating Effect		Triple Point	
		501 kcal/m ³ 56.4 Btu/ft ³		-160 ° C	-256 ° F
				113 ° K	204 ° R
Latent Heat at NBP	56 kcal/kg	4844 /kg mol	100.7 Btu/lb	8710 /lb mol	
Trouton's No.	20.85	Gas Constant	9.80 kg.m/kg/° K	17.78 ft.lbs/lb/° R	
Specific Heat Liquid at 30° C 86° F Fig 13			Gas C _p .157	C _p /C _v 1.184 at 25°C	
Liquid at 30° C 86° F Density		.117 kg/l.	73.3 lbs/ft ³	Viscosity	.18 cp
Reduced Form at NBP Pressure		.0205	1 / Temperature 1.629		
Reduced value of 1/T		2.02	1.169	1.37	
when Reduced Pressure is		a) .001	b) .01	c) .1	

(Meacock- Refrigeration Processes)

Fig.5.

- A saturated liquid at condensing pressure/temperature
 A-A' saturated liquid rejecting heat from unlagged pipework
 B liquid-vapour mixture
 C saturated vapour at vapourizing pressure/temperature
 C-C' saturated vapour absorbing heat
 D superheated vapour at condensing pressure/temperature
 E saturated vapour

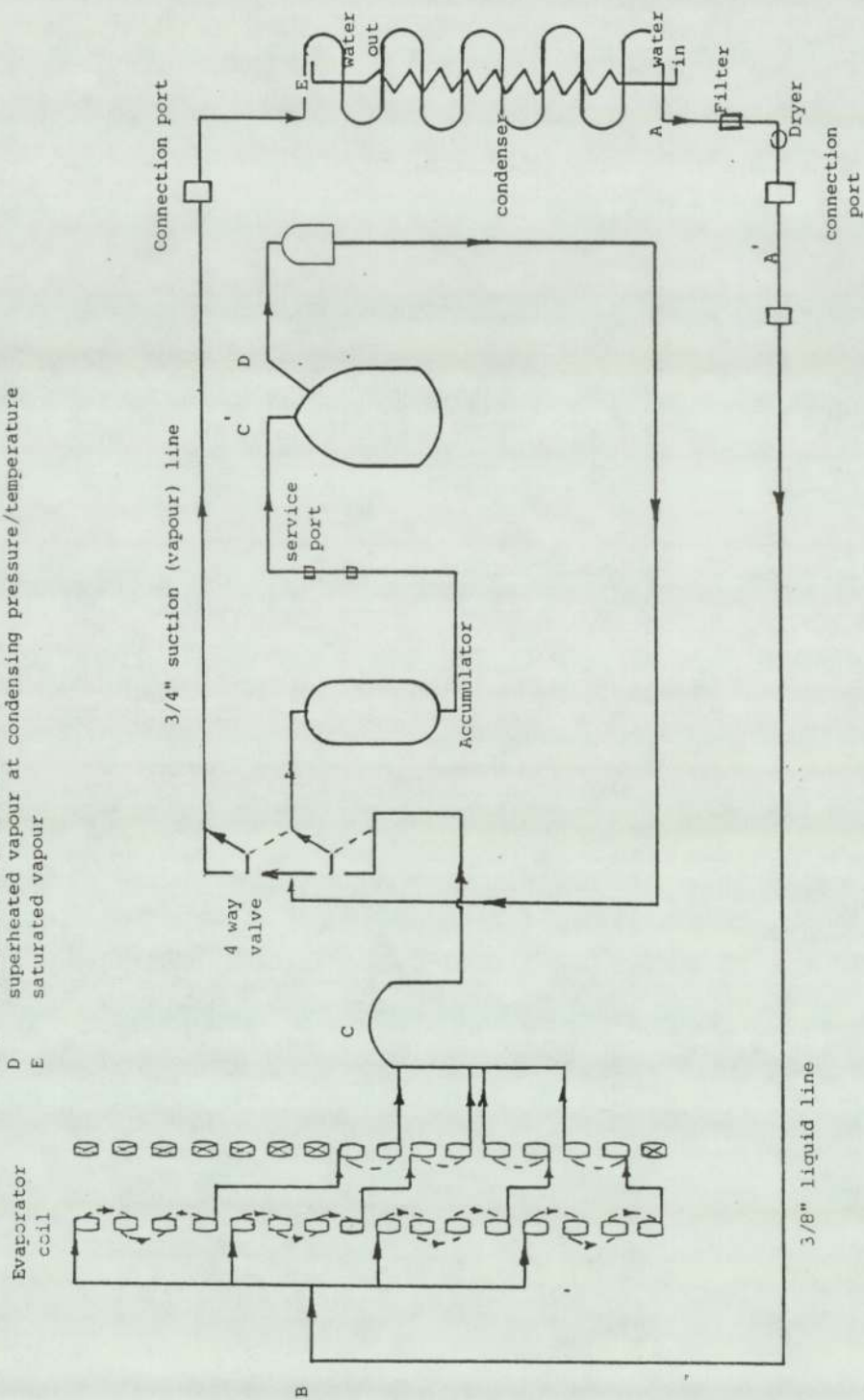


Fig. 6.

- (i) the evaporator coil
- (ii) the evaporator fan
- (iii) the hermetically sealed reciprocating compressor
- (iv) a refrigerant control valve
- (v) a 4-way reversing valve.

The condenser unit, of the counterflow type, has refrigerant circulating in the free space between the inner finned tube and the outer tube.

This particular type of coil was selected for its rated capacity - being closely matched with the output from the heat pump.

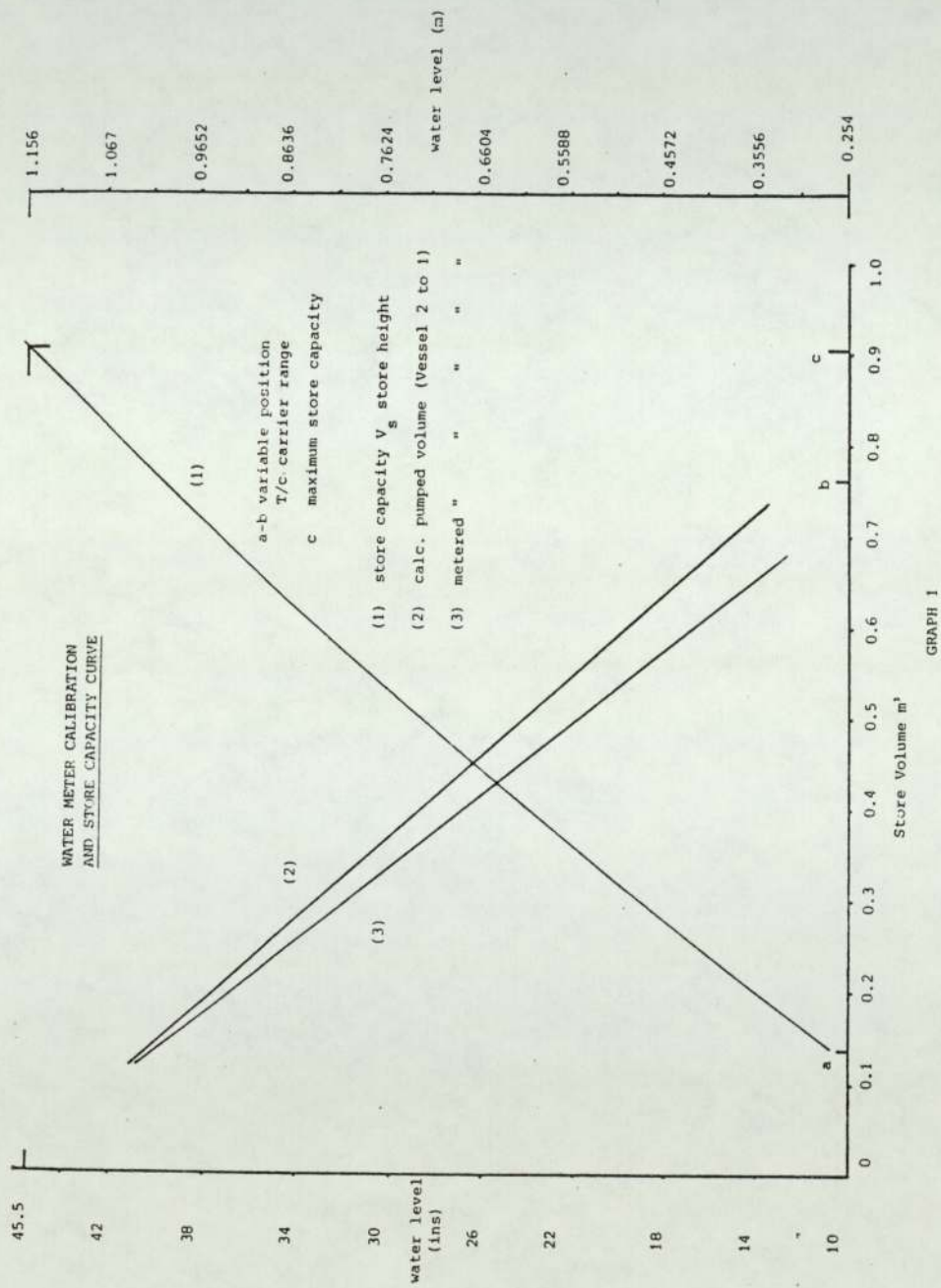
The condenser coil was enclosed in a suitably constructed container, and was insulated against heat loss using expanded polystyrene. An external view of the rectangular container is shown in Fig. 7, situated between the heat pump and the two water store vessels.

The appropriate high temperature refrigerant vapour and hot water lines were thermally insulated to minimise heat loss to the surrounding atmosphere. Figure 7 shows two



External view of condenser coil housing situated between the heat pump unit in the foreground and store vessels at the rear.

Fig.7.



Graph 1

storage vessels in the water circuit. Each vessel being lined internally with a resin bonded insulant. The vessels have an approximate internal volume of 1.0 m^3 each and can be operated either individually or in parallel.

Because the vessels were of an irregular shape it was necessary to confirm the calculated internal volume by measuring the water content of each vessel.

To establish the storage volumes initially water entered one vessel through the top entry port from the high level header tank, which, in turn, was fed from the mains supply.

At various stages of filling the vessels the water level in the vessel was recorded with the aid of an externally mounted sight-glass.

At intervals the water was pumped from the vessel being filled into the second identical vessel and measured by an in-line volume flow meter. The resultant level in the second vessel was checked to correspond with that of the first.

This process was repeated several times to verify the result. A mathematical relationship of water volume to heights within the vessel was derived for use in the computer model. A graphical representation of the measured and calculated values is shown in Graph 1.



Store vessel graduated above for indicating the internal location of the variable position. Thermocouple carrier.

(The vessel inspection port is also shown)

Fig. 8.

Also, during drain-down of the vessels for internal adjustment/inspection the volume of water pumped from the vessels was further checked.

Located immediately above each vessel was a graduated scale as shown in Fig 8. This scale allowed for precise indication of the variable thermocouple carrier position internal to the vessels.

The thermocouple carrier arrangement and central rod which extends through the top of the vessel is shown in Fig. 9.

A scale model replication of the exact orientation of the cross-rods carrying the thermocouples was attached to the top of the central rod.

This enabled the exact orientated of the internal thermocouples to be displayed externally.

Water from the base of the vessel(s) discharges into a "header" vessel located between the vessel outlet and the water circulating pump suction. The "header" vessel provides a buffer to the pump suction and also allows for more complete mixing of the water discharging from the vessels. This mixing process assists in obtaining a more uniform water temperature at the pump suction and therefore at the condenser coil inlet.



The variable position thermocouple carrier located at the base of the vessel with thermocouple cables attached.

(The Vessel 2 velocity diffuser at the top of the vessel is shown).

Fig. 9.

Water circulates throughout the circuit through copper pipework of varying diameters. The water circuit comprises a series of bends; elbows, Tee sections; valves etc, which partially simulate a practical, physical, construction.

On-line temperature measurements of the water, air and refrigerant circuits were recorded and stored via an Analogue-to-Digital converter, and microcomputer, onto magnetic data disks. Details of the Analogue-to-Digital (A-D) unit are included in Appendix 2. The microcomputer was programmed to control the number and frequency of scans taking place. The microcomputer, magnetic disk drive and on-line printer are shown as Fig. 10.

Arrangement of the water temperature sensors (thermocouples) within the store vessels allows for the temperature measurements by four fixed thermocouples - attached internally at each vessel wall surface - and at five, preset, horizontal positions; these being selectable on-line for any setting along the vertical axis.

Fig. 11 shows the relevant fixed and variable thermocouple positions in each vessel. The thermocouples were assembled by the Author using copper-constantan thermocouple cable.



A CBM model microcomputer, on-line
printer and twin floppy disk drive.

Fig. 10.

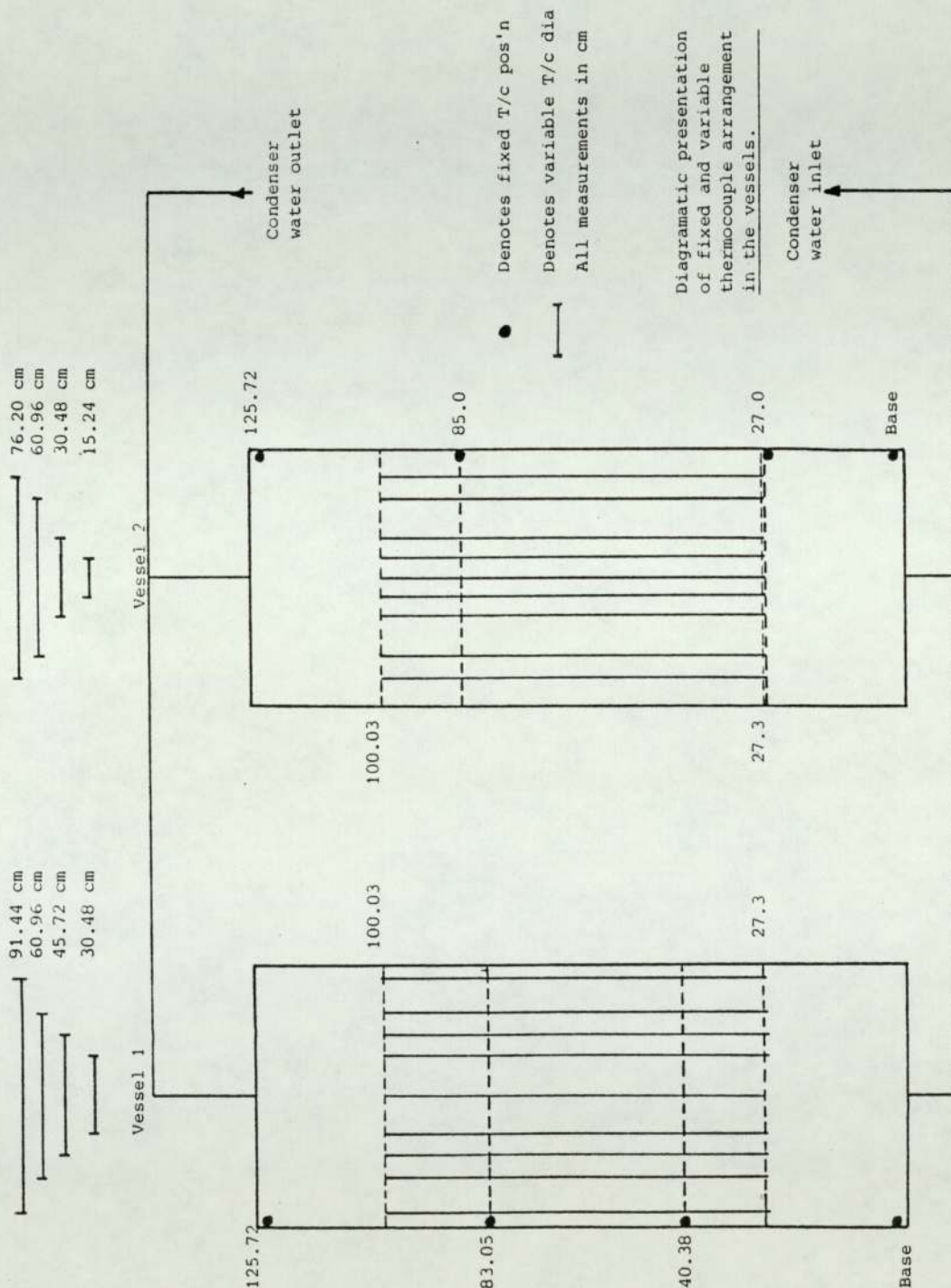


Fig. 11.

A specially designed and constructed thermocouple carrier as outlined above was installed in each vessel to facilitate the vertical and horizontal plane measurements.

The horizontal positions were selected and preset prior to a test taking place whereas the vertical positions could be varied during a test.

Temperatures throughout the system were recorded at the positions shown in Fig. 12. Refrigerant temperature measurements were achieved by bonding copper-constantan thermocouples externally to the refrigerant pipework. The pipework and thermocouples were then encased in a suitable preformed insulation material.

The store vessels, being converted "brewing" vessels, required some initial modification prior to incorporation in the heating system. The modifications required were those of rigidly securing a vortex eliminator over the bottom outlet port and inserting a jet entry velocity diffuser into vessel number 2 at a position below the top entry port - see Figure 9.

The vortex eliminator and velocity diffuser were household plastic kitchen colander and funnel respectively.

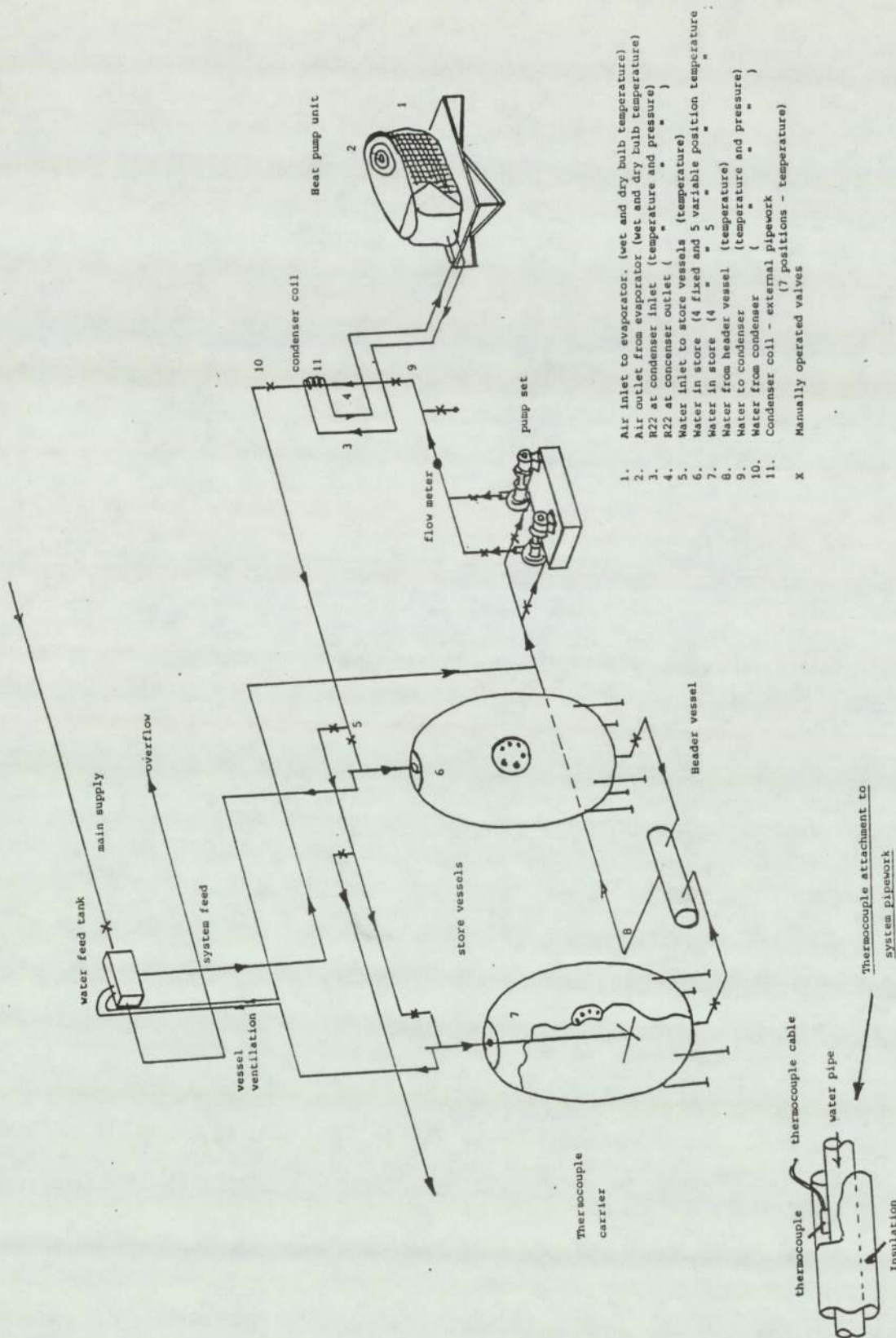


Fig. 12.

The electrical energy consumed at the compressor, the fan and the water pump was monitored individually, and as a total consumption value. A standard Electricity Board integrating meter was connected in the electrical circuit for each component.

Air temperatures at the evaporator inlet and outlet were also recorded during the tests.

Because of the limited number of thermocouple channels available on the A-D converter it was necessary on occasions to record some air temperatures manually.

The complete system was designed and constructed to replicate as far as possible a practical installation. However, several limitations were imposed through being located in the laboratory environment. The most noticeable limitations were the length of system pipework possible in the laboratory and the relatively uniform climatic conditions experienced at the evaporator.

The principle of system operation is one of extracting heat energy from ambient air, via the refrigerant at the evaporator coil, upgrading the heat energy by a compressor, and rejecting the upgraded energy in the refrigerant to water flowing through a condenser coil, into a direct contact thermal water store through a closed loop circuit. The two insulated store vessels each containing 820 litres

(0.82 m³) of water were mounted vertically. Water entering through the top entry port and leaving at the base of the vessel - see Fig. 12.

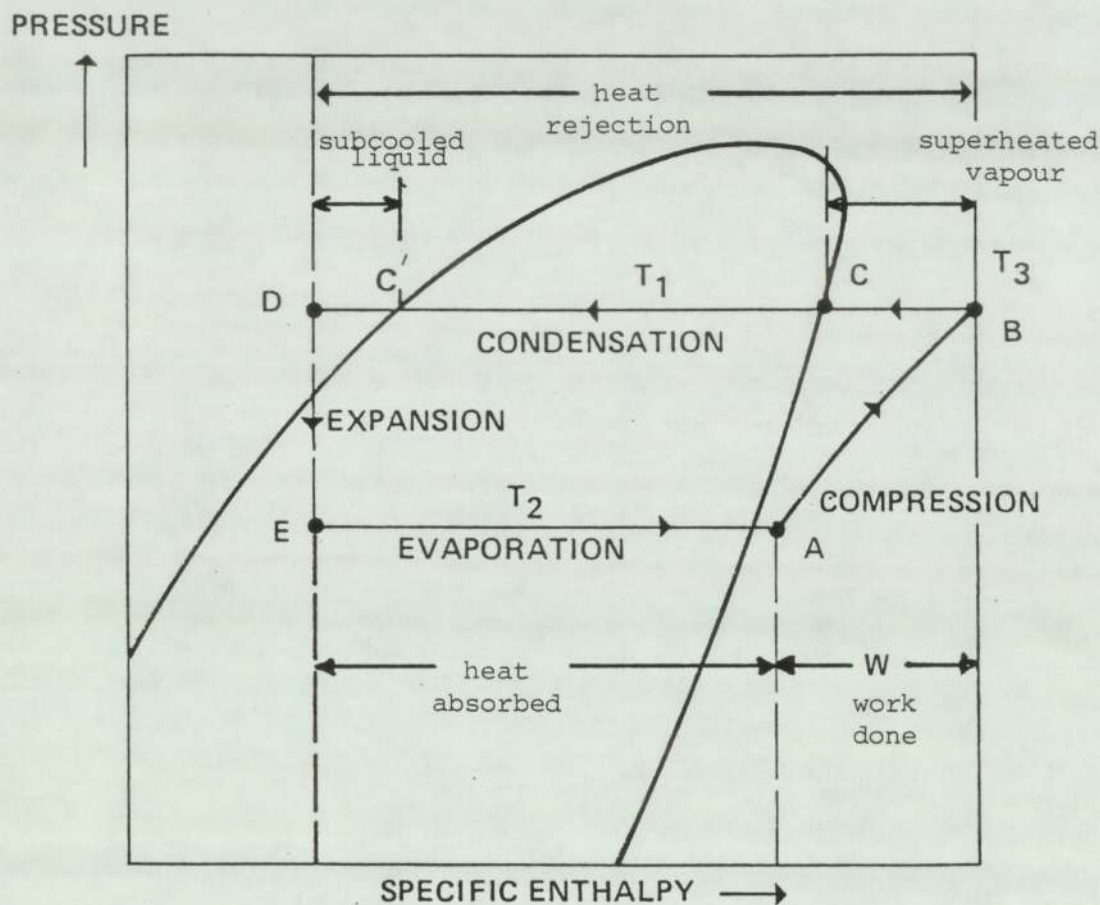
Water drawn from the base of the vessel enters a header vessel prior to the pump suction before passing through to the condenser coil. The heated water then returned through a manually operated flow control valve to the top of each vessel.

The water flow and return pipework is of nominal 22 mm bore whilst the inlet and outlet orifice at the vessels are 17 mm nominal bore (nb).

The various pipework diameters throughout the circuit give rise to differing flow characteristics.

Internal surfaces of all pipework are assumed to be smooth and clean with a nominal degree of roughness present. The vessels are not completely parallel sided as inspection ports are located mid-way up the vessel height, (see Fig. 8). The internal diameter of each vessel was approximately 920 mm.

For the purpose of this study the store vessels are assumed to be vertical tubes.



PRESSURE ENTHALPY DIAGRAM
FOR THE BASIC CYCLE

(Based on Néal W E J^[20] (1980))

Fig.13.

As stated earlier, heat transfer in the vessels is by direct contact between the incoming heated water and the stored mass of water. Heat transfer is considered dependent upon a combination of conduction, convection and possibly mass diffusion.

2.1 The Pressure - Enthalpy Cycle

A simplified pressure - temperature/Enthalpy diagram for an idealized compression cycle based on Neal W E J[20] is shown as Figure 13. For such a cycle it will be noted that for a given mass flow rate of refrigerant the heat absorbed per unit time at the evaporator is

$$\dot{Q} = \dot{M} (h_a - h_e). \quad (1)$$

The power during compression is $\dot{W} = \dot{M} (h_b - h_a).$ (2)

At the condenser the power rejected is $\dot{Q} = \dot{M} (h_b - h_d).$ (3)

The cycle heating performance = $\frac{\text{power out}}{\text{compressor shaft power}}$

and is given by

$$\frac{(h_b - h_d)}{[(h_b - h_d) - (h_a - h_e)]} \quad (4)$$

or $\frac{(h_b - h_d)}{(h_b - h_a)} \quad \text{since } h_d = h_e \quad (5)$

In the idealized situation $\dot{Q}_1 = \dot{Q}_2 + \dot{W} \quad (6)$

Where \dot{Q}_1 = rate of energy released

\dot{Q}_2 = rate of energy extracted

\dot{W} = rate of work done in compression.

The coefficient of performance (COP_H) given by (4) will not be realized in practice because of a variety of factors including:

- (i) pressure drops through the evaporator and condenser
- (ii) Pressure drop through the pipework

(iii) Pressure drop at the suction and exhaust valves of the compressor

(iv) maintenance of temperature gradients at the heat exchangers (evaporator and condenser).

Factors (i) and (ii) assist in maintaining refrigerant flow.

Also for electrically driven systems the compressor shaft power will be less than the power input because of set inefficiencies.

Following compression, heat is rejected in three stages, referring to Figure 13,

(i) from (b) to (c) superheated vapour is cooled

(ii) from (c) to (c¹) condensation takes place

(iii) from (c¹) to (d) sub-cooling of the liquid takes place (after all the vapour has condensed).

Part of the cooling of the superheated vapour may take place between the compressor and the condenser. All three processes (vapour cooling, condensation and sub-cooling) may also be taking place in sections of the condenser.

The pressure/enthalpy cycle of heat pumps is not an area of study for this thesis, therefore further reference would be made to, amongst others, Rogers G F C and Mayhew Y R (1978)[21], ASHRAE (1972)[22] and Dossat R.J.[23] for a fuller account of heat pump cycle operation and performance.

2.2 Refrigerating Capacity

The performance of a heat pump is related to the refrigerating capacity of the compressor used, also upon the range of ambient conditions in which the unit is to operate.

Refrigerating capacity is determined from the mass flow rate of refrigerant and the refrigerating effect per unit mass, which is the amount of heat each unit mass of refrigerant absorbs from the environment. Dossat[23] suggests that in an actual cycle the temperature of liquid entering the refrigerant control (expansion) valve is always higher than the vapourizing temperature in the evaporator and must therefore be reduced before the liquid can vapourize.

The refrigerating effect is therefore always less than the total latent heat of vapourization, however, liquid refrigerant flowing through the evaporator requires to

absorb sufficient heat to complete vapourization. Derivation of the actual amount of heat absorbed by the refrigerant at the evaporator is dependent upon the availability of measured data of high accuracy.

The data would necessarily comprise terminal conditions for the refrigerant and the ambient conditions at evaporator coil inlet and outlet.

Accurate evaluation and the achievement of a system heat balance is largely dependent upon the quality of information recorded at the evaporator.

As stated earlier, liquid refrigerant flowing through the evaporator requires to absorb sufficient heat from the environment to complete vapourization.

If the heat absorbed by, for instance, the evaporator is known, then the refrigerant mass flow rate \dot{M}_F can be determined. An empirical relationship used for calculating the refrigerant mass flow rate from the energy absorbed at the evaporator by the refrigerant \dot{Q}_E is given by:

$$\dot{M}_F = \frac{\dot{Q}_E}{h_A - h_E} \quad (\text{ref Fig 13}) \quad (7)$$

Amongst the more detailed studies carried out for establishing the mass flow rate of refrigerant through a refrigeration cycle is that of Dhar M^[24] (1978). Dhar's mathematical modelling of a refrigerant system

".....involved development of equations to predict the movement of refrigerant in the system and the changes of state of refrigerant in the system components with time".

Dhar's model for the evaporator is summarized as, for refrigerant mass flow rate of vapour refrigerant from the expansion valve to the evaporator:

$$\dot{M}_{O_v} = \dot{M}_O \dot{Q}_e \quad (8)$$

Mass flow rate of liquid refrigerant from the expansion valve to the evaporator:

$$\dot{M}_{O_l} = \dot{M}_O - \dot{M}_{O_v} \quad (9)$$

Enthalpies of vapour and liquid refrigerant from the expansion valve to the evaporator:

$$\text{if } \dot{M}_{O_l} = 0; h_{O_v} = h_O \quad (10)$$

$$\text{if } \dot{M}_{O_v} = 0; h_{O_1} = h_O \quad (11)$$

otherwise,

$$h_{O_v} = h_{v_s} \quad (12)$$

$$\text{and } h_{O_1} = h_{l_s} \quad (13)$$

where

\dot{M}_O = refrigerant mass flow rate

\dot{M}_{O_1} = mass flow rate of liquid refrigerant

\dot{M}_{O_v} = mass flow rate of vapour refrigerant

h_{O_1} = enthalpy of liquid refrigerant flowing from expansion valve to the evaporator (btu/lb_m)

h_{O_v} = enthalpy of vapour refrigerant flowing from expansion valve to the evaporator (btu/lb_m)

h_O = enthalpy of refrigerant flowing through the expansion valve (btu/lb_m)

h_{v_s} = enthalpy of saturated vapour refrigerant
corresponding to the suction pressure P_s
(psia) in (btu/lb_m)

The mass flow rate of refrigerant for the system under study is calculated using ASHRAE[25].

Typical examples of variations in refrigerating effect under differing operating conditions, for the refrigerant R22 as used in the Carlyle 38CQ unit being used, are shown below. These values, extracted from the manufacturers performance data, [Installation Booklet (Fig.8)], apply specifically to the original air-to-air operating mode design and a different refrigerant charge to the present system.

(a) 10°C wet bulb temperature of air entering outdoor unit

Evaporation temperature at

4.086 Bar (50 psi) = - 6.032°C

∴ Δt = 16.032°C.

Enthalpy of vapour (from Tables) = 403.1 Kj Kg⁻¹

Condensing temperature = 45°C

Enthalpy of liquid (from Tables) = 256.396 Kj Kg⁻¹

Refrigerating effect

(403.1 - 256.396) = 146.706 Kj Kg⁻¹

(b) 15°C wet bulb temperature of air entering outdoor unit

Evaporation temperature at

$$4.654 \text{ Bar (67.5 psi)} = - 2.035^{\circ}\text{C}$$

$$\therefore \Delta t = 17.035^{\circ}\text{C}$$

$$\text{Enthalpy of vapour (from Tables)} = 404.612 \text{ Kj Kg}^{-1}$$

$$\text{Condensing temperature} = 45^{\circ}\text{C}$$

$$\text{Enthalpy of liquid (from Tables)} = 256.396 \text{ Kj Kg}^{-1}$$

Refrigerating effect

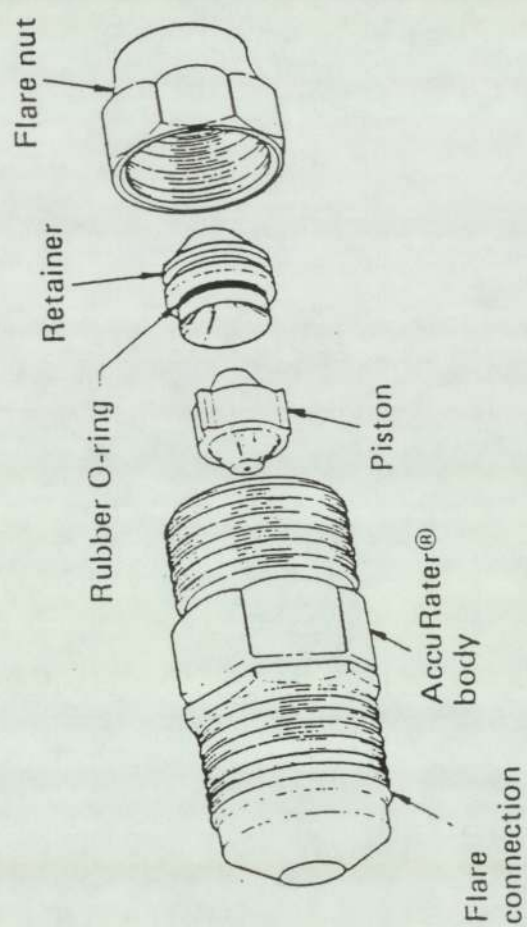
$$(404.612 - 256.396) = 148.216 \text{ Kj Kg}^{-1}$$

It will be noted from the above values that as the temperature difference between air temperature at the evaporator and the evaporation temperature changes, so does the refrigerating effect.

i.e.

$$(a) \quad \Delta t = 16.032^{\circ}\text{C} \quad \text{refrigerating effect} \quad 146.706 \text{ Kj Kg}^{-1}$$

$$(b) \quad \Delta t = 17.035^{\circ}\text{C} \quad \quad \quad " \quad \quad \quad 148.216 \text{ Kj Kg}^{-1}$$



AccuRater® components

Fig.14.

2.3 Evaporator Capacity and Performance

The effectiveness in performance of a thermodynamic cycle is dependent upon the combined performance of the four main components of a heat pump. The evaporator, compressor, condenser and expansion valve.

The type of expansion valve incorporated into the 38 C Q unit is shown in Fig. 14.

The evaporator capacity is equivalent to the heat passing through the evaporator walls. This rate of conductive heat flow is often expressed as:

$$Q \text{ (watts)} = UA T_{ln} \quad (14)$$

for all single flow arrangements,
where,

U is the overall heat transfer coefficient per
unit area. $W(M^2 \text{ } ^\circ C)^{-1}$

A is the total heat transfer area of the heat
exchangers M^2

T_{ln} is the mean temperature difference of the
mediums $^{\circ}\text{C}$

The mean temperature difference is often referred to as the "logarithmic mean temperature difference" (LMTD).

A more complete presentation of the following basic principles of evaporator performance is given by Dossat[23] and the theory of heat exchanger behaviour is covered by Ozisik N M[26] (1985).

The thermal resistance "R" to heat flow across a tube comprises three basic thermal resistances:

$$R = \begin{array}{c} \text{thermal} \\ \text{resistance of} \\ \text{inside flow} \end{array} + \begin{array}{c} \text{thermal} \\ \text{resistance of} \\ \text{tube material} \end{array} + \begin{array}{c} \text{thermal} \\ \text{resistance of} \\ \text{outside flow} \end{array} \quad (15)$$

where the terms are expressed by; (see Ozisik[26]).

$$R = \frac{1}{A_i h_i} + \frac{t}{k A_m} + \frac{1}{A_o h_o} \quad (16)$$

where

A_o, A_i = outside and inside surface areas of tube
respectively M^2

$$A_m = \frac{A_o - A_i}{\ln (A_o / A_i)} = \text{logarithmic mean area} \quad M^2 \quad (17)$$

h_i, h_o = heat transfer coefficient for inside and
outside flow respectively $W(M^2 \text{ } ^\circ C)^{-1}$

k = thermal conductivity of tube material
 $W(M \text{ } ^\circ C)^{-1}$

R = total thermal resistance from inside to
outside flow $^\circ C W^{-1}$

t = thickness of tube $M.$

For general heat exchanger applications it is necessary to account for unclean heat exchange surfaces. These unclean or "fouled" surfaces introduce further thermal resistance to the heat flow path.

A following factor is therefore introduced into equation (16) to give:

$$R = \frac{1}{h_i A_i} + \frac{F_i}{A_i} + \frac{t}{k A_m} + \frac{F_o}{A_o} + \frac{1}{A_o h_o} \quad (18)$$

where F_i and F_o are fouling factors at the inner tube surface and outer surface of the tube respectively. The dimensions for F_i and F_o being $(M^2 {}^0C)W^{-1}$.

The overall heat transfer coefficient "U" is often based on the outside surface of the tube and defined as:

$$U_o = \frac{1}{A_o R} \quad (19)$$

$$U_o = \frac{1}{(D_o/D_i)(1/h_i) + (D_o/D_i)F_i + [D_o/(2k)]\ln(D_o/D_i) + F_o + 1/h_o} \quad (20)$$

However, neglecting the tube wall resistance to heat flow and assuming $D_o \approx D_i$, the overall heat transfer coefficient reduces to:

$$U_o = \frac{1}{1/h_i + 1/h_o} \quad (21)$$

The LMTD, stated as T_{ln} in equation (14), of two quantities ΔT_1 and ΔT_2 is defined as:

$$\Delta T_{ln} = \frac{\Delta T_1 - \Delta T_2}{\ln (\Delta T_1 / \Delta T_2)} \quad (22)$$

where

$$\Delta T_1 = T_w - T_{in} \quad \text{or inlet temperature difference between the fluid and tube wall}$$

and

$$\Delta T_2 = T_w - T_o \quad \text{or outlet temperature difference between the fluid and tube wall}$$

Ozisik[26] suggests that if the temperature ratio of ΔT_1 and ΔT_2 is not greater than 50 percent, then ΔT_{ln} can be approximated by the arithmetic mean difference within about 1.4 percent

$$\text{then} \quad \Delta T_{AM} = \frac{1}{2} (\Delta T_1 + \Delta T_2) \quad (23)$$

ΔT_{AM} being the arithmetic mean temperature.

Dossat^[23] and Pabon-Diaz^[13], amongst others, suggest that an average pressure, hence temperature, of refrigerant in the evaporator suffices for insertion into evaporator performance calculations.

The quantity of air required to pass over the evaporator to maintain a given evaporator performance becomes a function of two main factors:

- (i) the sensible heat ratio of the evaporator,
(ratio of sensible cooling capacity to the
total cooling capacity)
- (ii) the change in air temperature at evaporator
inlet and outlet.

The approach taken for evaluating results of the tests on evaporator capacity and performance in this thesis is discussed more fully in Chapter 3.

2.3.1 Evaporator Fan

The evaporator fan employed in the present work is an integral part of the original standard heat pump unit.

Fan types and sizes are selected, according to Woods [27], to handle a certain quantity of air against a specific pressure, consequently their performance must be determined largely by these two factors. Empirical laws govern the relative performance of fans and reference to Woods [27] provides a comprehensive review of the accepted fan laws.

Amongst the more obvious requirements from the evaporator fan is the need to deliver the specified volume of air across the evaporator and at the lowest possible power consumption level.

The fan must be able to efficiently cope with a considerable variation in the quality of external ambient air (density, temperature, etc) with an acceptably controlled noise level.

Changes in air density are due to changes in air pressure, temperature and composition of gas handled. Fan selection is therefore generally made on the basis of calculated system resistance and an assumed air density.

According to ASHRAE^[22] fan performance data are based on dry air at standard conditions 14.696 psi and 70°F (0.075). $\text{lbs}_m (\text{ft}^3)^{-1}$.

Woods, however, states that performance tables and charts for fans assume that the air is at standard density, which in Great Britain is 0.0764 lbs per cubic foot. This, he continues, is the density of dry air at sea level when the barometric pressure is 30 ins. of mercury and the temperature 60°F.

Whilst the power consumption of the fan is stated to vary in proportion to the air density, there is little need to consider such changes within the range of normal atmospheric conditions.

Woods identifies his stated range of "normal atmospheric conditions" and the effects on power consumption as:

Temperatures down to 32°F (0°C)	Power increase 6%
Temperatures up to 120°F (44°C)	Power decreased 10%
Barometric pressure up to 31.5" Hg	Power increase 5%
Barometric pressure down to 27.0" Hg	Power decrease 10%
Altitudes to 1200 ft below sea level	Power increase 5%
Altitudes to 3000 ft above sea level	Power decrease 10%

Humidity levels up to saturation are normally neglected but saturated air is a little lighter than dry air, e.g. + 2% lighter at 15°C (60°F), + 4.3% lighter at 44°C (120°F).

Since a change in air density results in a proportional change in the power consumed, and in the pressure developed by the fan at constant volume, then the system resistance at constant volume flow will vary in proportion to the density.

However, a fan coupled to a given system normally operates at the same point on the characteristic curve, and delivers a constant volume at a constant speed, irrespective of density.

On the basis of Woods above stated observations the calculated evaporator performance, used for the heat pump and overall system performance evaluation, as shown on page 257, is based on the equipment manufacturers published data.

2.4 Condenser

The condenser unit installed on the system is of Truco (TM) manufacture, model K7-13WT. This unit is not an integral part of the original Carlyle heat pump and has therefore been specially selected because of its "matching" characteristic. The specification for the condenser is included as Appendix 3.

The helical coiled, co-axial unit shown as Fig. 4 is of counterflow design with the cooling medium (water) passing through the inner tube and the refrigerant (condensing medium) flowing between the finned outer surface of the inner tube and the inner surface of the outer tube. The design of this coil allows for effective use of the cooling of superheated refrigerant gas, the vapour condensation and the sub-cooling of the liquid refrigerant, i.e. from B-D in Fig. 13 (page 64).

As referred to in Sections 2.3, equation 15, when two media of different temperatures are separated by a thin metallic wall the indirect heat exchange is mainly determined by the resistivities to heat transfer of the media boundary layers. Resistivity to heat transfer depends on the combination of physical properties of the media, their velocity of flow and to changes of state of the media during heat transfer. The physical characteristics of the separating wall are also highly relevant.

Lewit E H^[28] (1957) suggests the rate of heat transfer varies approximately with the square root of liquid velocity in the tubes. Increasing the velocity of water flow leads to an increase of heat flow but this, in turn, necessitates an increase in circulating water pump power and results in a lower water outlet temperature.

The heat transfer coefficient, denoted K , in JS^{-1} by Lewit^[28] can be calculated using the relationship:

$$K = M \frac{(H_{f1} - H_{f2})}{A T_D} \quad (24)$$

where \dot{M} is the mass flow rate of freon (Kg s^{-1}) passing through the system.

Enthalpy change across the condenser is defined as the difference $H_{f1} - H_{f2}$. The total surface area of the condensing tube is denoted by A whilst T_D is the logarithmic mean temperature difference, refrigerant to mean water temperature, across the condenser.

The operating performance of the Truco coil used in this work has been based solely on the performance data published by the manufacturer, interpreted for use in the evaluation routine by the Author.

An interpretation of the coil manufacturers performance data is presented in detail in section 3.2, of this thesis.

2.5 Empirical Laws (Pressure - Enthalpy)

In an earlier section (section 2.2) reference was made to the use of enthalpy values in heat pump performance calculation. Enthalpy changes reflect the performance of the system and therefore are an essential ingredient in any system model.

As it has been necessary to contain the complete system performance evaluation routines within the capacity of the available computer operating memory it was impractical to incorporate tabulated refrigerant properties data. The relationships referred to as (a - d) below have therefore been derived as a series of quadratic equations by the least squares method for use in the computer model.

The relationships, based on tabulated data for absolute pressure-temperature/enthalpy conditions experienced at the evaporator and condenser, are presented in Appendix 4 and some typical examples of the accuracy obtained using the derived relationships with tabulated data are shown.

The relationships cater for:

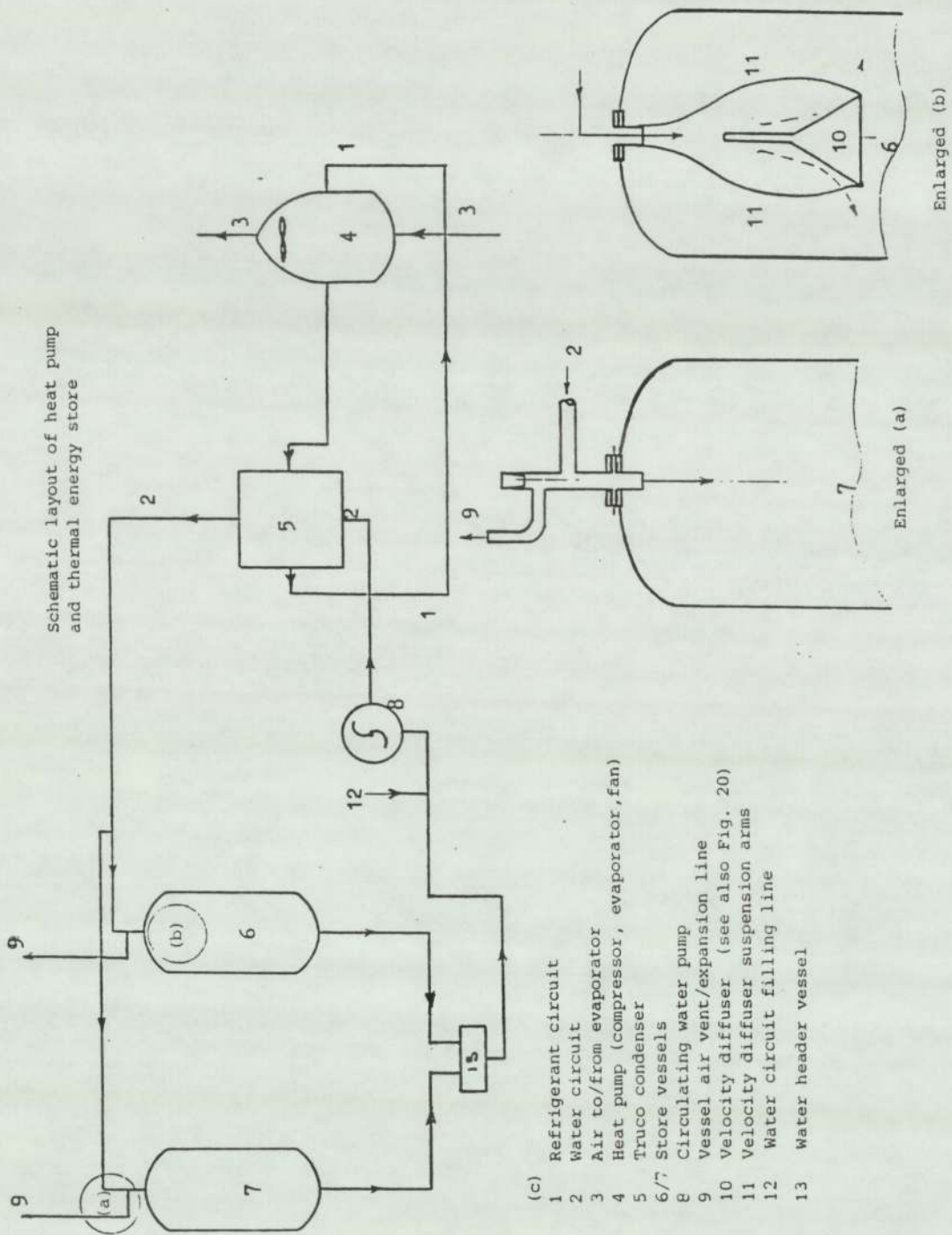
- | | | |
|-----|-------------------|--------------------------|
| (a) | Evaporating phase | (saturated liquid state) |
| (b) | " " | (saturated vapour state) |
| (c) | Condensing phase | (saturated liquid state) |
| (d) | " " | (saturated vapour state) |

Two further relationships have been derived for determining the absolute evaporation pressure and condensing pressure, from known (measured) temperatures of the refrigerant during tests.

Comparisons of enthalpy values, calculated using the derived laws, with those of published tabulated data (from Kinetic Chemicals Inc^[29] and IHVE published data^[30]) show that an accuracy in calculation of greater than 98% is achieved.

2.6 Water Circulating pump

In evaluating the overall system performance it is important to determine the energy use or loss in all components including the water circulating pump. The water pump operating on the test system is an SMC Commodore 130-45 model. The pump is located in the circuit as shown in Fig. 15c. The pump suction is at ground level, i.e. below the



Figs.15. (a) (b) (c)

vessel outlets, connected between the "header" vessel and the condenser coil inlet. Water entering the pump is therefore well mixed at a temperature approaching that of an average value of the discharge temperatures from vessels 1 and 2, when both are in circuit.

It will be shown later in the thesis that with both vessels in circuit there is a noticeable temperature difference at the outlet of each vessel - this results from the different heat transfer conditions taking place within the vessels. The "header" or "mixer" vessel is designed to eliminate initial temperature differences prior to water entering the water pump suction.

The water pump was required to be of sufficient capacity, and capable of developing sufficient delivery pressure to meet the resistive forces of the system. It catered for the range 0.55 ms^{-1} to 1.47 ms^{-1} of flow rate and the pressure drop anticipated from the system.

A further requirement from the circulating water pump was that it performed efficiently; meeting the demand placed upon it with a minimum consumption of energy.

Water volume flow rates through the system, for individual tests conducted, were regulated at the commencement of each test with the aid of a manually operated "gate" type valve at the condenser outlet. The flow rate was normally unaltered during a test.

The volume flow was monitored with the aid of an on-line mechanical type water flow meter incorporating an integrater. The integrated meter was used for measurements upon which Graph 1 was based, and discussed on page 53.

As stated previously the volume flow rate was not normally altered during the course of a test, however, some variation in flow rate may have occurred as a result of water temperature (hence density) changes in the water.

However, during the initial series of tests adjustment to the flow rates were carried out to witness the limited effects on heat transfer rates at the stores when operating within the range of the coil design.

No adjustments are taken into account for the mass flow rate variation due to temperature change during the course of a test.

A more comprehensive discussion of water pumps, their design features and performance characteristics is presented by Addison H^[31] and Karassik I J and Carter R^[32]. (1960).

However, included below is a resume of some of the important criteria to be considered when water pump selection is necessary.

The pump "head" or the pressure against which a pump works, is in general terms the vertical height through which the pumped liquid is raised. The head difference is generally measured at the pump flanges. In practice it is often greater than this value as friction losses in the system have to be overcome. These losses include friction in pipework bends, tee-sections, pipe diameter restrictions etc. Other considerations are the length of pipework involved and the flow rate of water required. Detailed discussions on the characteristics of flow regimes and the relevant flow formulae for different conditions are presented by reference to Douglas, J F[33], Blair J S[34] and the C.E.G.B. memoranda GDM 38 (DM 023/3)[35], amongst other literature.

Amongst the many published formulae used for calculating flow through pipes is that by D'Arcy and Chezy[36].

Karassik[32] et al have subsequently stated that, in practice, the loss of head with turbulent flow does not vary as the square of the velocity but to some power in the range 1.7 to greater than 2.

The friction coefficient or fouling factor as it is sometimes referred to, will not, therefore, be constant for a given pipe for all flow rates.

It has been assumed that for the series of tests undertaken here the pipework "fouling" factor does not vary sufficiently to warrant special consideration in the evaluation routines.

In conditions of turbulent flow, that is, where the Reynolds^[37] Number is greater than 3500, the modified Colebrook and White^[38] formula can be used to ascertain flow rates, e.g:

$$W_{(m^3 \text{ Hr}^{-1})} = -4 (N_1 H d^5)^{1/2} \log_{10} \left[\frac{k_s}{3.7d} + \frac{N_2 d}{(N_1 H d^5)^{1/2}} \right] \frac{1}{2208.48}$$

(25)

Where:

H = Head lost per 100 ft run with water at 62°F (ins)

d = Internal diameter of pipe (ins)

N₁ = 26.87 ρ (≅ 1645 for water at 150°F)

ρ = Density of water at appropriate temperature
(kg dm⁻³)

μ = Absolute viscosity of water at applicable
temperature (10⁶ Kg m⁻¹ s)

$$N_2 = 0.08213\mu \ (\cong 0.0854 \text{ for water at } 150^\circ\text{F})$$

$$k_s = \text{Absolute roughness of pipe wall} \quad (\text{ins})$$

$$(0.00006 \text{ for copper (IHVE)})$$

According to Karassik^[32] several relationships have been established for full scale models, based largely on tests of scale models. The discharge rate Q (ft³/minute) for a pump is the product of the rotative speed N and the third power of the rotor diameter D .

$$Q = ND^3 \quad (26)$$

D being in feet

N in rpm

The delivery head (H) or hydraulic head of the pump is stated as the product of the rotative speed raised to the 2nd power and the 2nd power of the rotor diameter i.e.

$$H = N^2 D^2 \quad (27)$$

Two of the most significant losses in centrifugal pumps results from fluid friction and disk friction, hence the losses varying with viscosity of the liquid.

The effect of increasing the liquid viscosity above that of cold water of approximately 10°C is to lower the head, to increase the power input and to lower the overall efficiency of the pump.

As indicated in the "Pump Users Handbook"[30], the effects of the above are limited unless the liquid viscosity is some 30 times greater than that of cold water - a situation which does not arise in this series of tests.

A method of calculating the pump hydraulic power output (whp) and hence pump efficiency is offered in SIHLBERG[39]. The useful power transferred by the pump to the liquid is:

$$\text{whp} = \rho \frac{QH}{367} \text{ (kw)} \quad (28)$$

ρ = density of water in Kg dm^{-3} ($1 \text{ kg dm}^{-3} = 1000 \text{ kg m}^{-3}$)

Q = flow rate $\text{m}^3 \text{ hr}^{-1}$

H = head of system m

The pump efficiency therefore becomes:

$$\eta = \frac{\text{hydraulic power output}}{\text{shaft horsepower absorbed}} = \frac{\text{whp}}{\text{shp}} \quad (29)$$



View of vessel inspection port
(showing partially filled vessel
with thermocouples entering
from above).

Fig. 16.

Karassik^[32] suggests however,

"Estimations of pump performance generally suffice because the designing of centrifugal pumps is not an exact science - many of the inter-related factors whose combined effect cannot be accurately foreseen, must be determined experimentally".

2.7 Sensible heat store vessels

Two identical storage vessels are installed in the system under test. Construction of the vessels is of fibre glass having an internal smooth lining of epoxy resin. The vessels are mounted vertically on steel cradles. Internal dimensions are 1.156m in height at the maximum dimension and approximately 0.92m diameter.

An approximate diameter is given because the vessels have an inspection port on the vertical face - see (Fig. 16).

Because of the existence of these inspection ports the vessels do not fully replicate a long tube with parallel wall surfaces. This variation in physical construction from a tube with parallel sides renders direct comparison between

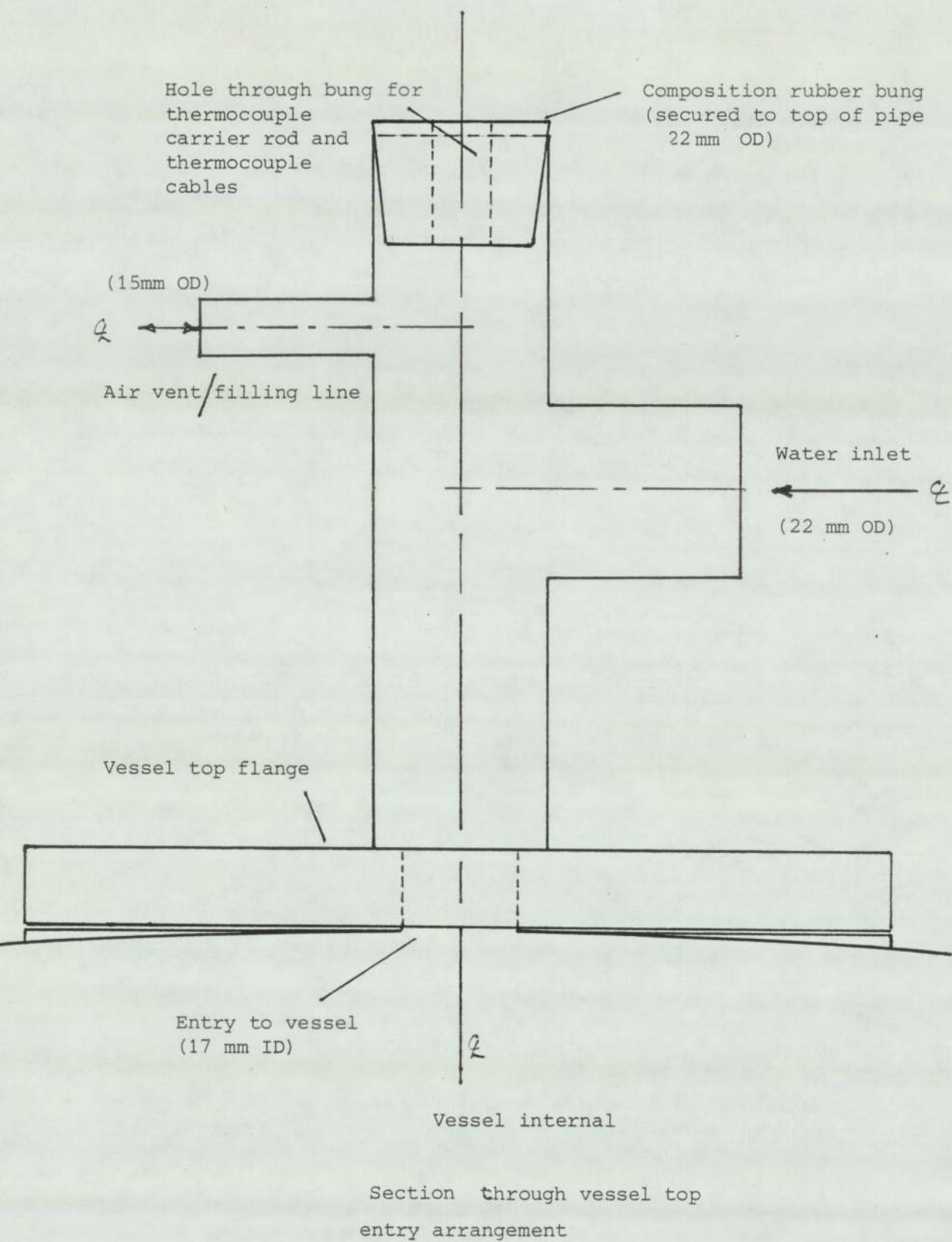


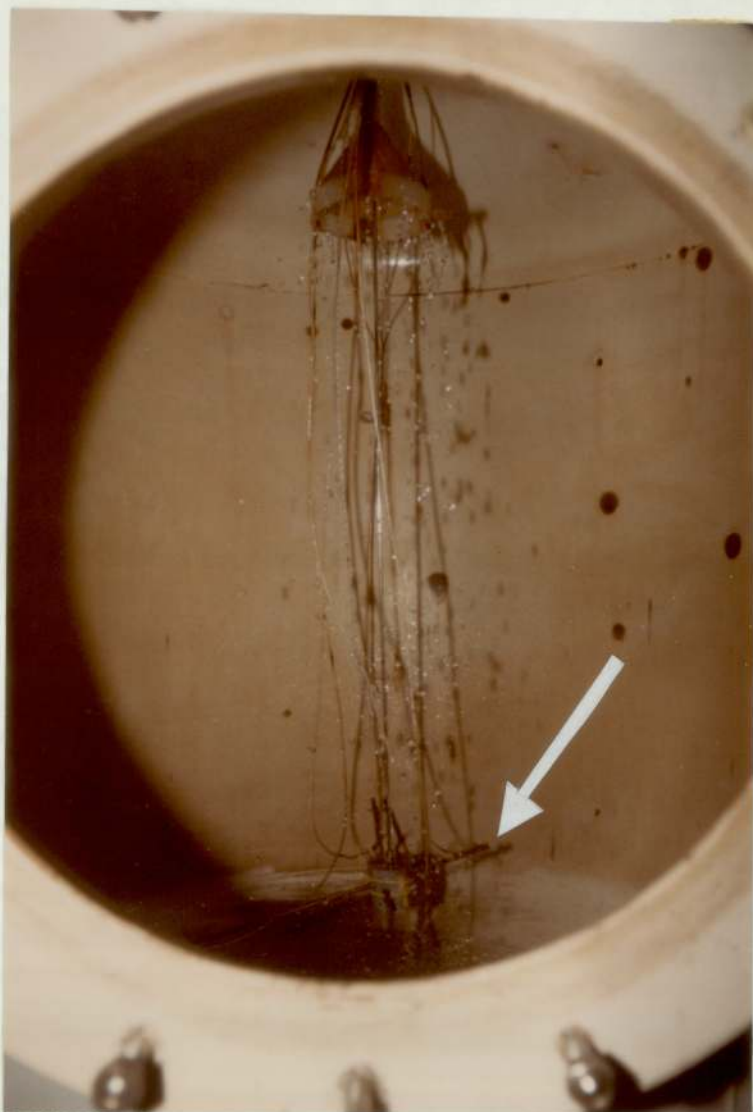
Fig. 17.

established theory and actual performance impossible. The effects on store water temperature distribution down the vessels resulting from the departure from a straight tube, are discussed later.

The heated water from the condenser enters the vessel(s) through a top entry port and is drawn from the vessels at the base. Because the vessels are basically "closed" vessels - operating as direct contact type in a closed loop system - and under a slight working pressure it has been necessary to construct a specially designed fitment to the top entry point.

The fitting, shown as Fig's. 15(b) and 17, allows for the circulating water to enter the vessel under pump pressure. In the event that pressure builds up in the vessels sufficiently to create a "back-pressure" greater than the pump delivery pressure, then the circulating water is pumped to a header or expansion tank situated above the vessels. Under normal operating conditions this expansion line allows for air/gases to escape from the system to atmosphere. This specially designed top entry fitment can also be used when filling the vessel(s) with water.

A separate system "make-up" line is installed prior to the pump suction - see Fig. 15(a). It will also be noted from Fig. 16 - illustrations of the vessels and Fig. 17 that all internally located thermocouple cables enter the vessels at the top entry point.



Variable position thermocouple
carrier internal to the vessel
with a thermocouple bonded at
the radius.

Fig. 18.

Reference to Figure 11 shows the physical location of thermocouples in the vessels which are bonded to the inner surface of the vessels. The thermocouples are of copper-constantan construction. Additional to the four thermocouples bonded to the vessel surface internally are five thermocouples capable of monitoring the temperature of water at various horizontal and vertical positions during a test.

Fig. 18 shows a thermocouple bonded to the variable position carrier mechanism. The velocity diffuser is also shown at the top of the vessel.

A "variable position" carrier as depicted in Fig. 18, was constructed comprising a stainless steel rod of 4mm diameter which protrudes through the inlet port at the top of the vessel. This vertically mounted rod can be raised and lowered through the height of the vessel - a marker device is mounted on the top of the rod and therefore indicates, on an adjacent marker board (with graduations marked at 1cm intervals), the actual position of the base of the rod within the vessel.

At the base of the vertically mounted rod is a solid cylindrical block of plastic through which two holes are drilled across the diameter (Ref. Fig. 19). Through these holes are inserted two further stainless steel rods, these being on the horizontal plane. The extremes of these rods

HEAT STORE VESSEL
(with fixed internal thermocouples)

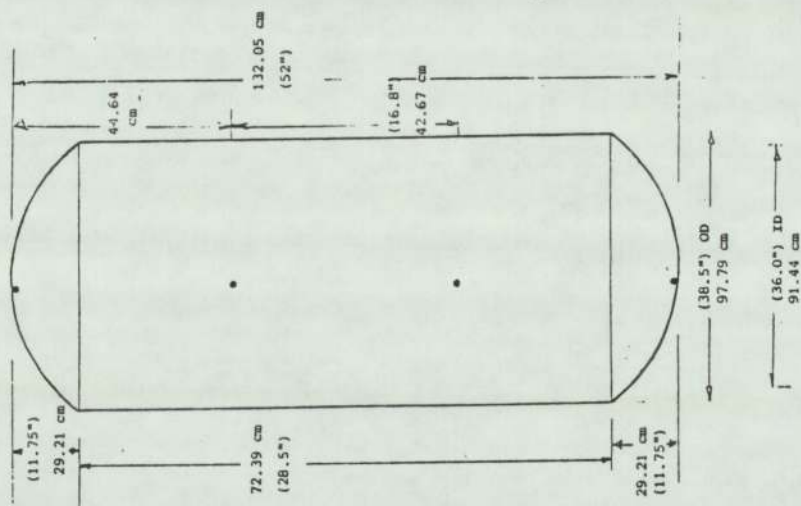


DIAGRAM OF VESSEL
DIMENSIONS AND
THERMOCOUPLE CARRIER

THERMOCOUPLE CARRIER
DEVICE

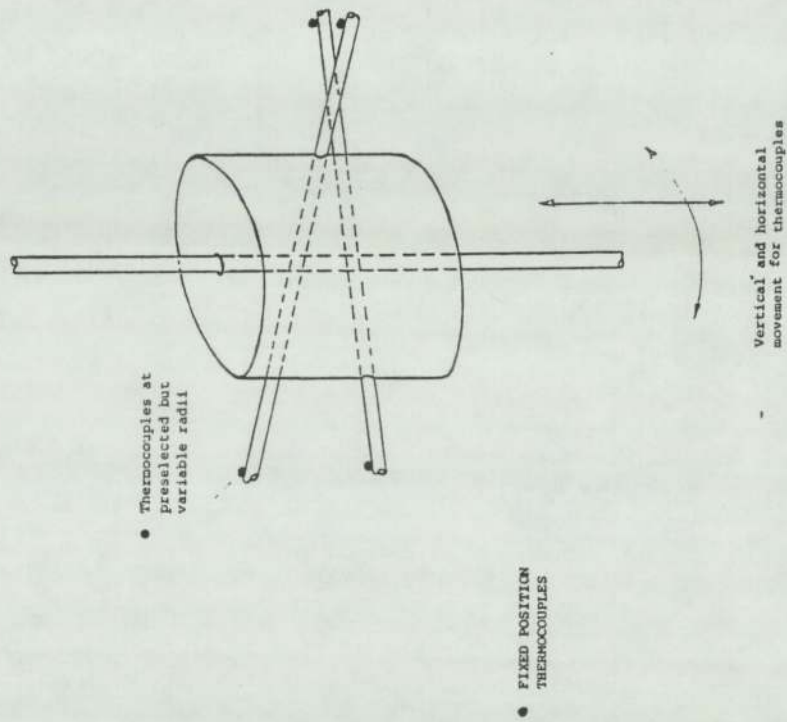


Fig. 19.

carry bonded thermocouples. Each of these four thermocouples are at different radii, (Ref. Fig. 11). A fifth thermocouple is bonded to the central position, i.e. on the plastic block. The four thermocouples at the extremes of the horizontally mounted steel rods can be positioned at a finite number of radii in the vessel - limited by the physical dimensions of the vessel and rods. These positions cannot however be altered during a test operation. Any vertical height can be selected, and changed, during the course of a test.

Stainless steel rods were selected as being suitable for withstanding constant immersion in the water and also because the mass of the steel rods ensured that conduction along the rods was not taking place during a test as they would not be sensitive to changes in water temperature.

Further additions internally to the vessels are a vortex eliminator and a velocity diffuser (one vessel only). The vortex eliminators are basic commercially available plastic kitchen colanders bonded over the orifice at the base of the vessel in an inverted position. The numerous small holes located around the colander ensured the pump suction acted in a relatively uniform manner at the base of the store.

The velocity diffuser is located into vessel 2 only. The location of this diffuser within the vessel can be witnessed from Fig. 18. It is again a commercially

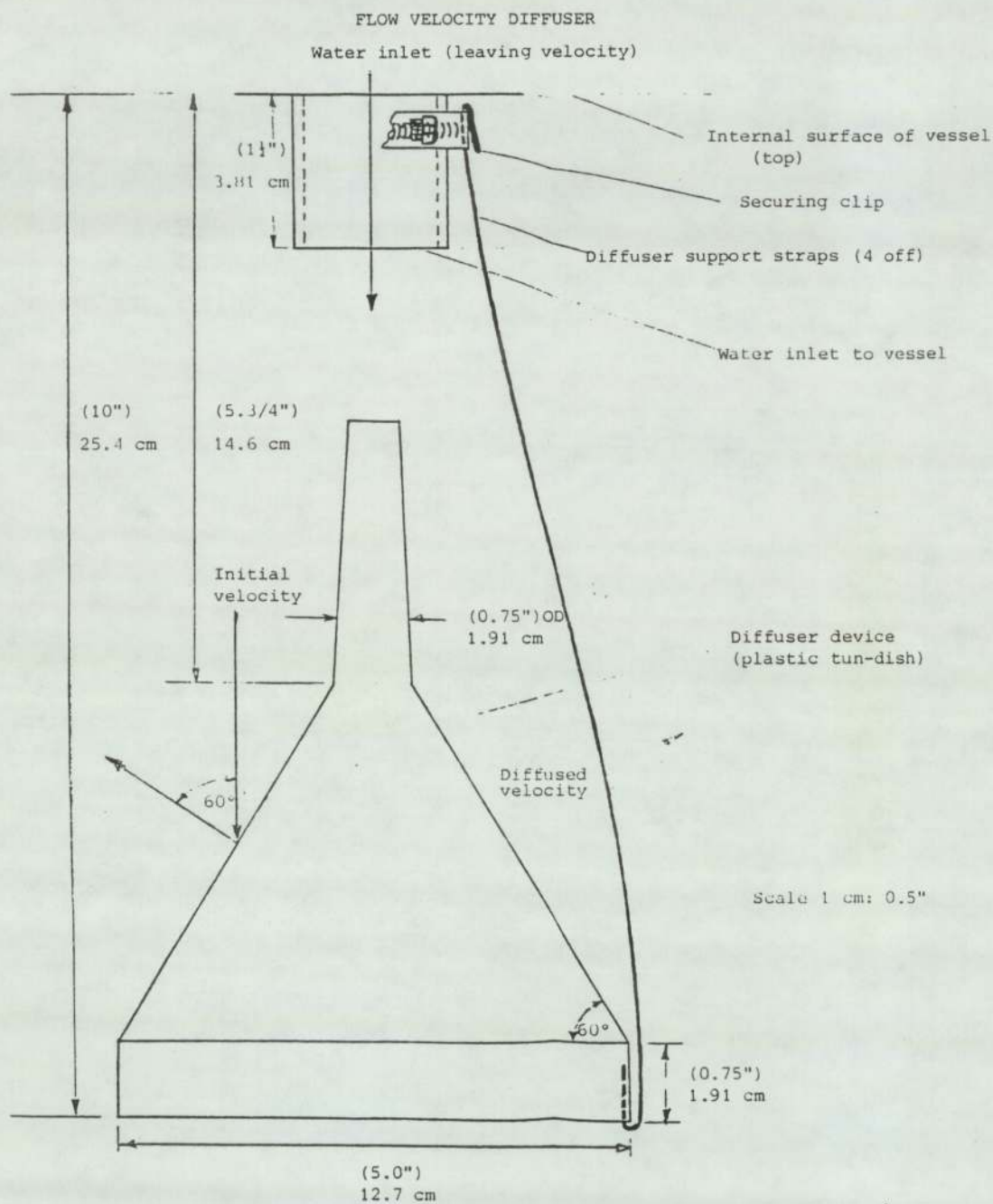


Fig.20.

available appliance, namely a plastic funnel mounted in an inverted position. The purpose of this device, which is situated immediately below the top entry port, is to deflect the inlet jet of water over a greater portion of the store water surface. This action assists in the prevention of jet velocity disturbance at the upper section of the store. The physical dimensions of the funnel are shown as Fig. 20.

The profile of this plastic funnel was not specifically matched to the dimensions of the store vessel and therefore would not be expected to provide optimum results. Nevertheless, inclusion of the velocity diffuser has been identified as a contributory factor towards achieving stratification in the thermal store - comparison of test results with and without the aid of a diffuser are made and discussed more fully in section 4.7 of this thesis.

Relevant to, but not directly an integral part of the store vessels is the circulating water "header" vessel.

The header, as depicted in Figure 21 is a 4 inch diameter plastic drain pipe 28 inches in length specially adapted with a sealing cap at each end. At mid-position along the length of pipe is the outlet port which connects to the pump suction. Directly opposite but equally spaced either side of the outlet port are the two inlet ports; one from each vessel.

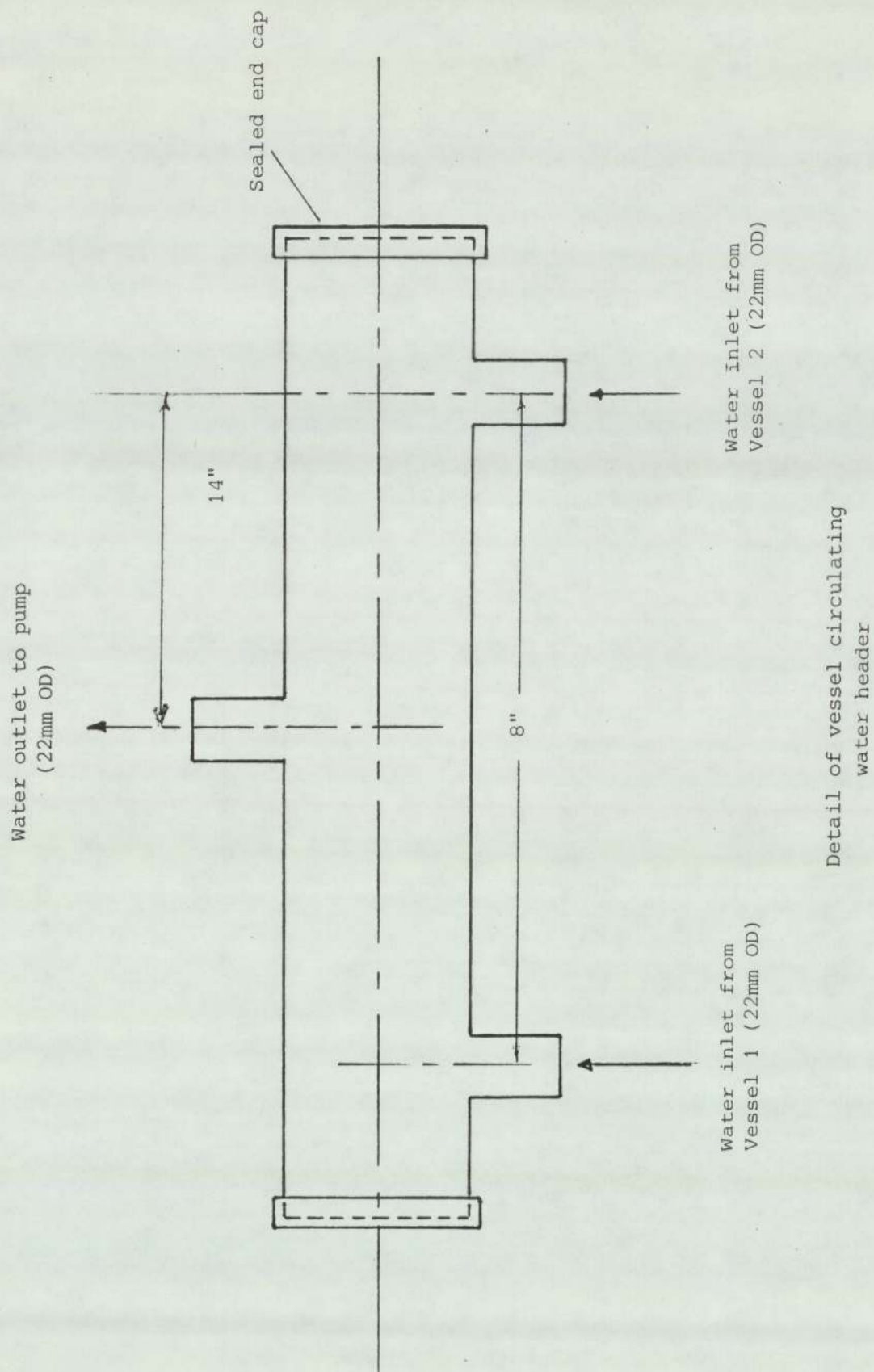


Fig. 21.

As stated earlier the header acts as a reservoir where water at two different temperatures is mixed thoroughly before entering the pump suction prior to re-entering the condenser coil. The header also assists in balancing the flow of water through each vessel when both are in circuit.

2.8 System Monitoring and Instrumentation

System performance is evaluated using specially written computer software and data monitored and recorded during test runs. Temperatures are measured by thermocouples of copper-constantan and by mercury-in-glass thermometers. A number of thermocouples are located in the medium being measured whilst the remainder are bonded externally to the system pipework. Output from the thermocouples is retained on magnetic store devices through an Analogue to Digital (A-D) unit, Appendix 2 summarizes the A-D specification. The readings from mercury-in-glass thermometers is recorded manually.

Pressure gauges of the Bourdon tube type are inserted into the refrigerant and water circuits at selected points. Readings from the pressure gauges are recorded manually.

Electrical consumption of the compressor, the evaporator fan and the water pump is measured individually, and collectively, with the aid of standard type watt-hour integrating meters. Water volume flow rate is measured using a mechanical integrating meter. Both electrical consumption and water flow rates are recorded manually.

Data recorded automatically through the A-D unit, which has been programmed to control the scan length (number of thermocouples) and scan interval (period between scans), can be selected from a combination of the 36 available thermocouples. The combination is limited to 13 channels at any one time. The final combination is dependant upon the system configuration chosen, i.e. whether one or both vessels are employed and the purpose of the test. A diagram of the complete heating system showing the points at which the operational data is recorded is included as Fig. 12.

The microprocessor used for controlling the A-D unit and data storage is a CBM model 4032 - Commodore Business Machine - as shown in Fig. 10, having 40 column screen and 32K bytes of RAM (Random Access Memory). The data storage device is a CBM model 2031 single disk drive, having 175K bytes capacity per disk. As noted earlier the microprocessors, through appropriate software, controls the scanning period of the CIL Analogue to Digital converter.

Data recorded during each test and stored onto magnetic disks can also be printed to paper via a suitable on-line printer.

This data is then manipulated with the aid of software to produce system performance results. A complete discussion of the software specially written for this evaluation is included in Chapter 5.

CHAPTER THREE

3. Evaporator Performance - Psychrometric Properties

The quantity of sensible heat transferred when a mass of air is heated, or cooled, between an initial and final dry bulb (D_b) temperature is, assuming specific heat at constant pressure, calculated using

$$\dot{Q}_s = \dot{M} c_p \Delta D_b \text{ (Kj)} \quad (30)$$

where \dot{M} is mass of dry air (Kg sec^{-1}); C_p is taken as 1 Kj Kg^{-1} for dry air.

The sensible heat content of air is a function of the dry bulb (D_b) temperature whereas the latent heat content of air is a function of the dew point (D_p) temperature.

The total heat content of air is a function of wet bulb (W_b) temperature.

The manner in which each of the D_b , W_b , and D_p temperatures are combined to derive the heat absorbed at the evaporator is discussed below.

3.1 Theoretical Approach Towards Sensible and Latent Heat Availability

Reference has been made to the analysis of moist air by Loveday, D L^[40] using relations given in the National Engineering Steam Tables, 1964^[41]; Section C1 of the IHVE Guide, Book C, 1970^[42]. "Air Conditioning Engineering" by Jones (1973)^[43], and the Handbook of Chemistry and Physics, 1973/74^[44].

The water vapour pressure in saturated air (P_{ss}) at any temperature t °C is given by the following relationship.

$$\log_{10} P_{ss} = 28.59051 - 8.2 \log_{10} (t + 273.16) + 0.0024804 (t + 273.16) - \left(\frac{3142.31}{(t + 273.16)} \right) \quad (31)$$

With the water vapour pressure in dry air (P_s) being:

$$P_s = P_{ss} \frac{\phi}{100} \quad (32)$$

$$\text{where } \phi = \frac{P_s 100}{P_{ss}} \quad (\text{relative humidity of air } (\%)) \quad (33)$$

P_{ss} and P_s = pressure (Bar).

The moisture content of air (g), in Kg Kg^{-1} dry air, at the evaporator inlet and outlet, and at atmospheric pressure, is calculated from:

$$g = \frac{0.622 P_s}{(P_{at} - P_s)} \quad (34)$$

where P_{at} = atmospheric pressure

Substituting for " P_{ss} " and "g" the specific enthalpy of moist air, (h), in Kj Kg^{-1} is calculated

$$h = 1.007 T - 0.026 + g(2501 + 1.84 t) \quad (35)$$

where t = air temperature $^{\circ}\text{C}$ at inlet and/or outlet of evaporator.

Density of moist air (ρ_m), in Kg m^{-3} is then calculated:

$$\rho_m = 1.2929 [273.16/(t + 273.16)] [(P_{at} - 0.3783 P_s)/760] \quad (36)$$

The mass flow rate of air (\dot{M}_{moist}), in Kg s^{-1} across the evaporator would be calculated using:

$$\dot{M}_{\text{moist}} = \dot{V}_{\text{moist}} \rho_{\text{moist}} \quad (37)$$

where \dot{M}_{moist} = mass flow rate of moist air

\dot{V}_{moist} = volume flow rate of moist air

ρ_{moist} = density of moist air

From the heat pump manufacturers data the volume flow rate of air over the evaporator is stated as $1.275 \text{ m}^3 \text{ s}^{-1}$ hence equation 37 becomes:

$$\dot{M}_{\text{moist}} = 1.275 \rho_{\text{moist}} \quad (38)$$

The total energy rate extracted from air over the evaporator becomes:

$$\dot{Q}_2 = \dot{M}_{\text{moist}} (h_{\text{in}} - h_{\text{out}}) \quad (39)$$

where \dot{Q}_2 = sensible + latent heat (kW)

\dot{M}_{moist} = mass flow rate of air over the evaporator (Kg s⁻¹)

h_{in} = specific enthalpy of air at evaporator inlet (Kj Kg⁻¹)

h_{out} = specific enthalpy of air at evaporator outlet (Kj Kg⁻¹)

As the total energy extracted comprises the components of sensible heat and latent heat it is appropriate to identify these contributions separately therefore the total sensible heat component (\dot{Q}_s) of \dot{Q}_2 becomes:

$$\dot{Q}_s = \dot{M}_{\text{dry}} C_p (t_{\text{in}} - t_{\text{out}}) \text{ (Kw)} \quad (40)$$

where \dot{M}_{dry} = mass flow rate of dry air

C_p = specific heat of dry air at constant pressure (Kj Kg⁻¹ K⁻¹)

t_{in} and t_{out} = air temperature ($^{\circ}\text{C}$) at evaporator
inlet and outlet

The mass flow rate of dry air (Kg s^{-1}) over the evaporator is based on:

$$\dot{M}_{dry} = V_{dry} \rho_{dry} \text{ Kg s}^{-1} \quad (41)$$

where

$$\rho_{dry} = \rho_o \left(\frac{T_o}{T_{in}} \right) \left(\frac{P_{at}}{P_o} \right) \text{ Kg m}^{-3} \quad (42)$$

The values T_o and P_o in the above equation (42) are the known absolute temperature and air pressure respectively. ρ_o is the density of air at T_o and P_o .

The value ρ_{dry} reflects the density of air at the evaporator inlet, at the operating inlet temperature and prevailing atmospheric pressure.

The value \dot{M}_{dry} is appropriate for mass flow rate because the units of $(g_{in} - g_{out})$ (moisture content of air) are in Kg Kg^{-1} dry air.

The latent heat component (\dot{Q}_L) of \dot{Q}_2 (total heat) can be derived from

$$\dot{Q}_L = \dot{M}_{\text{dry}} L(g_{\text{in}} - g_{\text{out}}) \quad (43)$$

where L = specific latent heat of evaporation
of water Kj Kg^{-1}

Using the above equations the instantaneous heat pump coefficient of performance, (COP_H) , in the heating mode, can be obtained from:

$$\text{COP}_H = (\dot{Q}_2 + P_c)/P_t \quad (44)$$

where P_c = energy consumption of compressor (kW)
 P_t = energy consumption of compressor
and fan (kW)

$$\text{However, } \dot{Q}_2 = \dot{Q}_s + \dot{Q}_L \quad (45)$$

therefore $\text{COP}_H = [(\dot{Q}_s + \dot{Q}_L) + P_c]/P_t$ (compressor only)

or

$$\text{CoP}_H = [\dot{M}_{\text{dry}} C_p(t_{\text{in}} - t_{\text{out}}) + \dot{M}_{\text{dry}} L(g_{\text{in}} - g_{\text{out}}) + P_c] / P_t$$

(46)

The overall system coefficient of performance in the heating mode (COP_{HS}) can be calculated using the above derivation if the value P_t is substituted by P_{ts} .

Where $P_{\text{ts}} = (\text{compressor power} + \text{fan power} + \text{water circulating pump power})$.

Reference to Appendix 8 will highlight the results of tests undertaken to establish representative positions at the evaporator for monitoring air temperatures. These single point temperatures being ultimately used in the computer model.

Chapters 4 and 5 indicate how the above formulae have been incorporated into the system computer model.

3.1.2 Design Data - Manufacturers Formulae

The formulae presented in this section have been derived from the equipment manufacturers limited published design data^[45]. The formulae can be used for calculating the sensible and total heat capacities (\dot{Q}_s and \dot{Q}_t respectively) of the evaporator coil at temperatures other than design temperature of air entering the coil, i.e. 26.7°C D_b . (Dry bulb temperature).

It will be noted that throughout the remainder of the thesis reference is occasionally made to quantities, e.g. sensible heat and total heat capacities by different abbreviated notation. In Section 3.1 (Equation 45, Page 115) the total heat is denoted by \dot{Q}_2 whereas in this section the total heat is denoted \dot{Q}_t ; in the computer program both notations are used.

This situation results from the fact that the necessary reference material uses different notations which, it was considered, advisable to retain. A further reason being the relatively limited facility of the microcomputer language known as "Beginners All-purpose Symbolic Instruction Code" (BASIC) for handling the variables involved.

Amongst the many published introductions to the BASIC computer language are those by Sack, J and Meadows, J^[46]; Pegels, C^[47] and Albrecht, Finkle and Brown^[48].

As these mixed notations occur the associated derivation is intended to clarify the issue.

Where the derived formulae are used in the computer program they are presented in the thesis in exactly the same format, that is, without being condensed to a scientific notation.

Equations 47 and 50, below are modified versions of manufacturers published material.

- (i) Sensible heat capacity (\dot{Q}_s): (based on dry bulb temperature (Db) of air leaving the evaporator coil).

$$\dot{Q}_s = [1.214 V_a (t_{eDb} - t_{lDb})] - [C_f (\frac{V_a}{3600})] \quad (Kw)$$

(47)

The value C_f is a correction factor derived from a family of relationship curves supplied by the manufacturer. The curves are constructed for coil by-pass factor and actual dry bulb (Db) temperature of air entering the evaporator.

The coil by-pass factor (B_f) is evaluated using:

$$B_f = 1 - \left[\frac{(\text{LMTD at the evaporator} - \text{temp air to evap})}{(\text{LMTD at the evaporator} - \text{temp air from evap})} \right] \quad (48)$$

where LMTD (logarithmic mean temperature difference) is calculated using Equation (22), Section 2.3, Page 79.

therefore

$$C_f = [0.29 (1 - B_f)(26.7 - \text{temp of air entering evap})] \quad (49)$$

(ii) Total heat capacity (\dot{Q}_t): (based on wet bulb (w_b) temperature) of air leaving the evaporator coil, corresponding to enthalpy of air leaving the coil).

$$\dot{Q}_t = 1.18 V_a (h_{ewb} - h_{lwb}) \quad (\text{kW}) \quad (50)$$

where:

t_{eDb} = dry bulb temperature of air entering evaporator °C

t_{lDb} = dry bulb temperature of air leaving evaporator °C

V_a = volume flow rate of air over evaporator $M^3 s^{-1}$

h_{ewb} = enthalpy of air entering evaporator $Kj Kg^{-1}$

h_{lwb} = enthalpy of air leaving evaporator $Kj Kg^{-1}$

1.214 = universal value for specific
heat of air $Kj m^{-3} ^\circ C$

1.18 = universal value for specific density of
standard air $Kg m^{-3}$

3.2 Condenser Performance - Manufacturers Design Data

The condenser coil installed in the system is the model K7-13WT, manufactured by Truco Limited and is designed for use with refrigerant R22 and a condensing temperature of 45°C (with water as the cooling medium).

Condensing capacity and pressure loss of Truco coaxial condensers

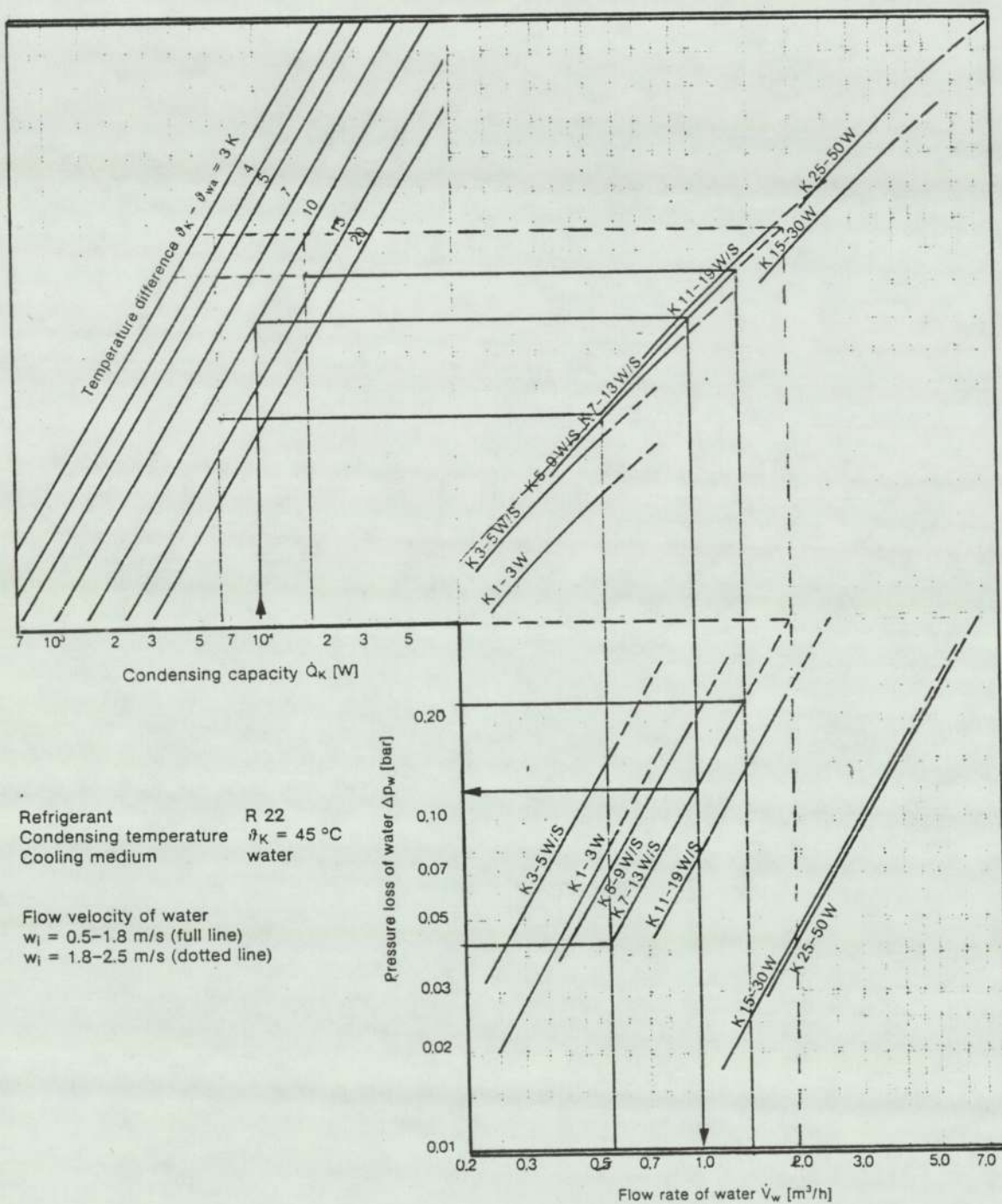


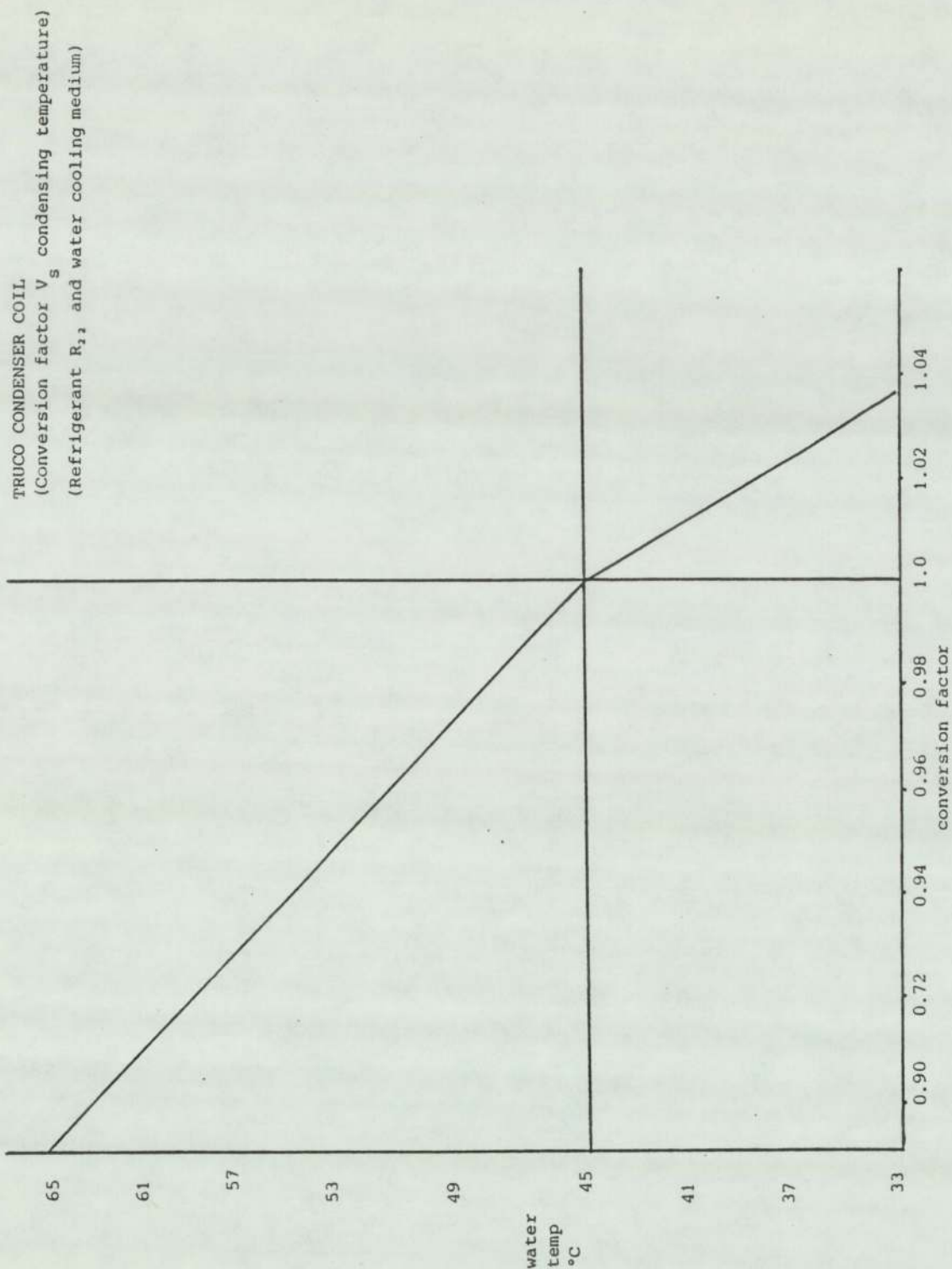
Fig. 22.

This particular model has a design flow rate of water in the range $0.55 - 1.475 \text{ m}^3 \text{ h}^{-1}$, to give a condensing capacity in the range 6.4 to 17.6 kW. The water flow velocity to be in the range 0.5 to 1.8 ms^{-1} .

The manufacturers published design data comprises a series of relation curves in the form of a nomogram (Ref. Fig. 22) - these curves relate water flow rate with water pressure drop through the condenser to the condensing capacity for temperature differences, in °K, from water inlet to refrigerant condensing temperature.

Whilst these curves provide an indication of the various parameter values under specific conditions interpretation from such material, for other than specified conditions, could lead to inaccuracies in final evaluated results. However, the published material necessarily forms the basis of the calculations employed in the computerized heat pump evaluation procedure.

Two approaches have been pursued for interpreting the relation curves, these approaches are outlined below.



Graph 2

Approach 1 (Manufacturers Published Method)

The real condensing capacity Q_E is calculated from

$$Q_E = f_k f_m Q_k \text{ (watts)} \quad (51)$$

where f_k and f_m are conversion factors and Q_k is the condensing capacity, according to manufacturers curves, for data obtained from tests. The correction factor (f_k) corrects for deviation of refrigerant condensing temperature from the design value of 45°C and (f_m) corrects for the mean medium cooling temperature for a cooling medium other than water.

An interpretation of the manufacturers data for (f_k) is shown as Graph 2.

For condensing temperatures less than 45°C the value

$$f_k = 1 + ((C_3 - 45) (-0.003)) \quad (52)$$

for condensing temperatures greater than 45°C the value

$$f_k = 1 + ((C_3 - 45) (-0.0053)). \quad (53)$$

Where C_3 is the condensing temperature (calculated) based on R22 pressure at the condenser inlet.

Calculations for water pressure loss Δp (bar) through the condenser, when the flow rate is within the range $0.55 \text{ m}^3 \text{ hr}^{-1}$ and $1.475 \text{ m}^3 \text{ hr}^{-1}$ is derived as:

$$\Delta p = 0.0433 + \left(\left(\frac{M_w - 0.55}{0.1} \right) (0.0202 \times 0.8746) \right) \text{ (bar)} \quad (54)$$

where M_w is the water flow rate in $\text{m}^3 \text{ hr}^{-1}$

$0.8746 \equiv \cos Q^0 \equiv$ based on manufacturers curve.

Water flow velocity can be calculated by modifying manufacturers data to:

$$F_v = (0.5 + \left(\left(\frac{M_w - 0.55}{0.1} \right) (0.14) \right)) \quad (55)$$

The corrected condensing capacity (CC) based on an interpretation of the manufacturers curve is derived using:

$$CC = ((23040 + \left(\left(\frac{F_v - 0.5}{0.1} \right) (4904.62 \times 0.7314) \right)) / 3600) \text{ kW}$$

(56)

where

F_v = water flow velocity through condenser
0.7314 = $\sin Q^\circ$ based on the manufacturers
velocity curve.

As an indication of the accuracy of results obtainable using the above derivations, (Equations 55 and 56) and assuming a water flow rate of $0.7 \text{ m}^3 \text{ hr}^{-1}$ the following values are achieved:

- (i) F_v (water flow velocity) 0.71 ms^{-1}
(cf. 0.70 ms^{-1} as read from supplied curve).
- (ii) CC (corrected condensing capacity) 8.49 kW
(compared to 8.5 kW read directly from manufacturers published curves)

Approach 2 (Derived equations based on
manufacturers curves)

This approach for calculating the condensing capacity (cc) for the Truco coil is to use a series of derived equations.

The equations are based on manufacturers data for design minimum and maximum volume flow rate of water ($\text{m}^3 \text{hr}^{-1}$) through the coil, and the range of temperature differences applicable, i.e. between the condensing temperature and the water inlet temperature to the condenser.

From the limited data available for condenser coil performance evaluation, the design minimum and maximum volume flow rates of water have been deduced, and referred to earlier as $0.55 \text{ m}^3 \text{hr}^{-1}$ and $1.475 \text{ m}^3 \text{hr}^{-1}$ respectively.

The values for volume flow rate and temperature difference have again been used to derive equations for calculating corrected condenser capacities. The general formulae are included as Appendix 6.

This alternative approach, Approach 2, for the calculation of condensing capacity may be less accurate than Approach 1 when catering for conditions other than those experienced at either the minimum or maximum water volume flow rate, as the basic data used for calculating the equations is susceptible to greater transposition errors (reading from manufacturers curves) than the data used in Approach 1. A comparison of calculated results, based on test data, is presented in Section 4.3.

The approach adopted within the computer program for evaluation of heat energy rejected by the refrigerant to water at the condenser, is based on the heat loss from the refrigerant at various states of phase change. An example calculation is presented in Section 4.3.

3.3 Heat Transfer Mechanisms in Thermal Store Vessels

The transfer of thermal energy as sensible heat occurs in three distinct forms:

- (a) Convection
- (b) Conduction
- (c) Radiation

The evaporation process is a further method of thermal energy transfer but involves a phase change in the substance which, in turn, renders it a latent heat transfer.

Convection: heat transferred by convection occurs in a fluid when the heat moves from one place to another by means of mass flow - convection currents - and results from a change in density brought about by a temperature difference or gradient.

Convective heat transfer adversely affects attempts at stratification within a water source sensible heat store. However, for storage systems where stratification is not an objective, convection becomes an essential feature, i.e. where mixing is required.

Newton's Law is associated with the convective heat transfer.

$$\text{i.e. } \dot{Q} = h A \Delta T \quad (57)$$

Conduction: heat transfer by conduction in non-metallic materials occurs when energy is transmitted by direct contact between molecules of a single body or between the molecules of two or more bodies in good thermal contact with each other.

The increased energy of the heated molecules causes them to strike adjacent molecules. At the moment of impact, and resulting from it, the faster moving molecules transmit some of their energy to the slower moving ones.

When the difference in energy between molecules ceases to exist then a thermal equilibrium state exists throughout the body. As the conduction process takes place in a water store heat is also conducted to the walls of the container in which water is stored. The rate of heat transfer by

conduction is in direct proportion to the difference in temperature between bodies. The relative capacity of a material to conduct heat is known as its conductivity.

The relationship between the heat transfer rate by conduction and the temperature distribution in the fluid is the Fourier Law,

$$\dot{Q} = - KA \frac{\partial T}{\partial x} \quad (58)$$

$\frac{\partial T}{\partial x}$ being the temperature gradient.

Radiation: all materials emit and absorb heat in the form of radiant energy. When a body gives off heat its internal energy decreases. Radiant energy is not dependent on a material medium as a transmittant. Radiant heat can be transmitted in a vacuum.

The amount of radiant energy that is either reflected or absorbed by a material depends on the nature of the materials surface, its texture and colour. Light coloured, highly polished surfaces reflect the maximum of radiant energy.

The law governing heat transfer through radiation is known as Stefans Law:

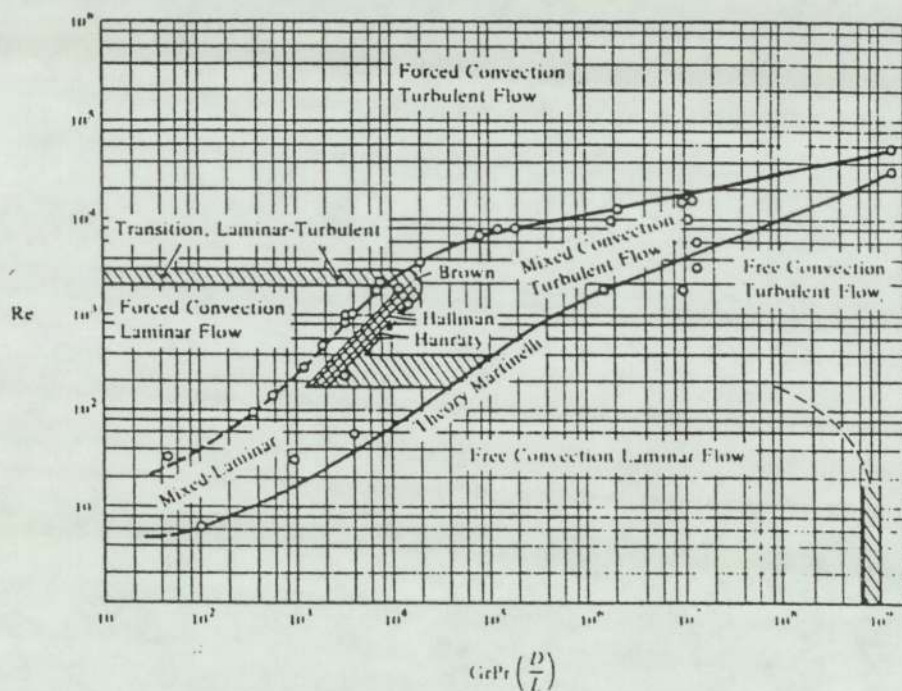
$$\text{i.e. } \dot{Q} = \sigma A (T_1^4 - T_2^4) \quad (59)$$

Karlekar and Desmond^[49] provide an indepth study of heat transfer mechanisms in systems similar to the one under investigation. They conclude that the transfer of heat in thermal stores is based largely on the effectiveness of the convection process. They state that the two major factors contributing towards convection in a stored fluid are:

- (a) the conduction of heat from the solid surface to a thin layer of adjacent fluid which attains a lower density than the fluid layers above it.
- (b) movement of the hot fluid away from a solid surface.

Three modes of convection which prevail are summarized as:

- (i) Free convection. In free convection the motive force comes from density differences in the fluid, which in turn result from its contact with a surface at a different temperature and gives rise to buoyancy forces. The velocity of flow depends also on the magnitude of the temperature difference between the surface and



Regimes of natural, forced and mixed convection for flow through *vertical* tubes [$10^{-2} < Pr(D/L) < 1$] according to Metais, B. and E. R. G. Eckert

Fig. 23

the fluid, the coefficient of thermal expansion of the fluid and the gravitational force acting on the fluid.

- (ii) Forced convection. This results from work done on the heat transfer fluid by, for, example, a water pump. Since the fluid velocity in forced convection is generally greater than in free convection more heat can be transferred at a given temperature difference between a solid and a fluid.
- (iii) Mixed convection. This deals with a superposition of forced and free (natural) convection. Metais and Eckert^[50] have identified the regime's of forced, mixed and free or natural convection for flow through tubes.

The figure opposite, Fig 23, identifies, according to Metais^[50] et al., regimes of natural, forced and mixed convection for flow through vertical tubes within the range $[10^{-2} < P_r (D/L) < 1]$

Regardless of whether the convection is "free" or "forced" the rate of heat transfer "Q" can be written in the form of Newton's law.

The surface convective heat transfer coefficient will, of course be different in the two flow regimes, i.e. "free" and "forced".

3.4 Jet Entry Theory

For an investigation into the transfer of heat from hot water flowing into a vessel having a relatively stable mass of stored water, it is necessary to take account of the available jet theory.

A major feature of the system configuration under investigation is that water of increasing temperature is drawn from the base of the store vessels and returned to the top of the store after further heating at the condenser.

Water re-enters the store vessels as a turbulent jet.

Abramovich^[51] in his studies of jet theory states:

".....a fundamental property of a jet of the turbulent, or submerged, type is that the static pressure is constant throughout the flow except when the jet interacts with an obstacle whereby the pressure may not remain constant.

If the static pressure remains constant then so the velocity within the central core of the jet remains constant".

The obstacle with which the entry jet interacts in this particular instance is the upper surface of store water. A fuller discussion on the effects of entrance velocity on store behaviour and performance has been included in Section 4.7.6. For each of the store vessels under investigation the water inlet jet profiles, and static pressures, are assumed identical at the initial entry point. After entry neither the jets or the static pressure are considered to be identical as Vessel 2 has the velocity diffuser installed, see Fig. 20. Consequently the jet impinges upon the diffuser at full entry velocity and is dispersed across a horizontal plane thus limiting the effect of the central core pressure and velocity, as referred to by Abramovich.

Alternatively the entry velocity entering Vessel 1 impinges directly upon the top surface of the water and creates a disturbance down the vessel until the velocity is dissipated - this depth being generally referred to as an "entry length".

The apparent pattern of behaviour of the jet's penetration into Vessel 2 is a pronounced version of that referred to in turbulent or submerged jet theory where it is established that the velocity field at the initial cross

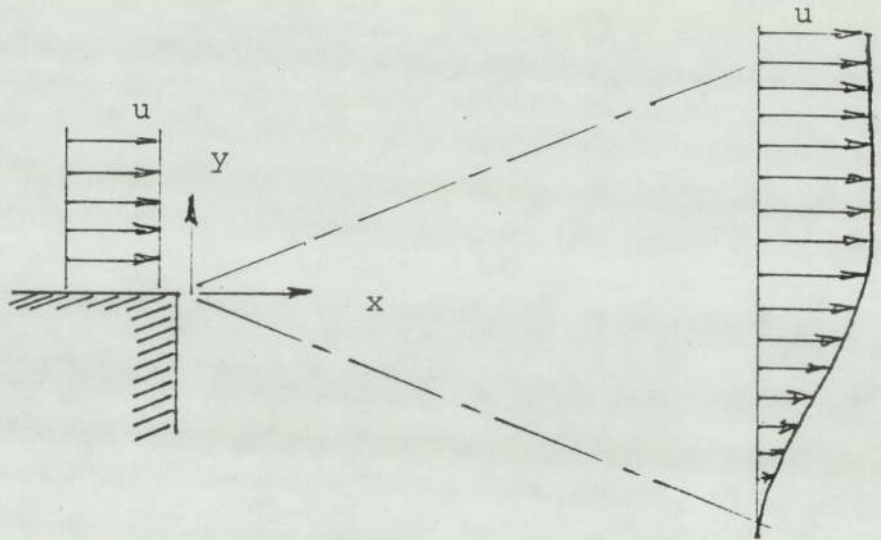
section of the jet is uniform, (see Fig. 24), and the boundaries of the mixing layers form diverging surfaces. The outside boundary layer, which comes into contact with stationary liquid, is taken to be the surface on all points of which the velocity component, with respect to the x-axis, is equal to zero.

The promotion of stratification in Vessel 2 should therefore be aided through significantly reducing the distance, from the entry point, at which turbulence would be experienced, i.e. reducing the entry or mixing length in the fluid store.

As the pump draws water from the store, the tendency would be, without a limiting device, to create a vortex effect in the lower central store region, this again could produce turbulence in the store. This is a further detriment to establishing thermal stratification.

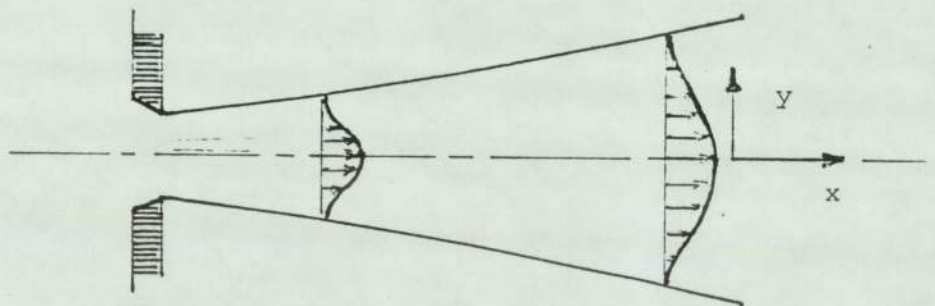
In an attempt at eliminating the vortex effect a device, as referred to earlier (page 60), is fitted internally at the base of each vessel.

It is apparant from the above comments that the extent of stratification capable of taking place in a thermal store would be determined through interpretation of the complex relationship existing between water entry and exit velocities, the effects of water jet entry profile and suction vortex conditions, and of course fluid conditions.



Jet boundary occurrence between two streams moving at different speeds in the same general direction. Mass flow increases in a downstream direction. The jet spreads out and its velocity decreases.

(Total momentum remains constant)



Velocity field at the initial cross-section of a turbulent or submerged jet.

Fig 24.

Account must therefore be taken of the changes in water temperature throughout the vessel, the physical dimensions and construction features of the vessel and the pressures present throughout the water circuit.

To further understand the complex relationship of heat transfer during fluid flow through a store it is useful to consider several of the more widely known dimensionless values.

3.4.1 Dimensionless Group Analysis

Dimensionless analysis simplifies the examination of many variable properties affecting heat transfer in fluids.

The groups are arranged to be dimensionless in order that the relationships between them are not a function of the measuring units employed.

Dimensionless groups; a brief review of appropriate dimensionless groups is given below. The relevance of dimensionless groups to heat transfer mechanisms is also briefly explained.

Dimensionless groups as presented by Cornwell K^[52] (1977) include the following:

$$(a) \quad \text{the Peclet number} \quad P_e = \frac{\rho C_p U d}{k} = R_e P_r \quad (60)$$

$$(b) \quad \text{the Reynolds number} \quad R_e = \frac{\rho U d}{\mu} \quad (61)$$

$$(c) \quad \text{the Prandtl number} \quad P_r = \frac{C_p \mu}{k} \quad (62)$$

$$(d) \quad \text{the Nusselt number} \quad N_u = \frac{h d}{k} \quad (63)$$

$$(e) \quad \text{the Grashof number} \quad G_r = \frac{g \beta \Delta T d^3}{\nu^2} \quad (64)$$

$$(f) \quad \text{the Stanton number} \quad S_t = \frac{h}{\rho C_p U} = \frac{N_u}{R_e P_r} \quad (65)$$

Table 1

Properties of Common Fluids

Water	at 20°C	at 100°C
$\rho \text{ Kg m}^{-3}$	998	958
$k \text{ WM}^{-1} \text{ K}$	0.60	0.68
$C_p \text{ Kj Kg}^{-1} \text{ K}$	4.18	4.22
$\mu \text{ } 10^6 \text{ Kg m}^{-1} \text{ s}$	1002	279
$Pr (C_p \mu k^{-1})$	7.0	1.7

The Peclet number is a measure of the ratio of the thermal energy convected by a fluid to the thermal energy conducted by the fluid. The Peclet number can be approximated to the product of Reynolds number and Prandtl's number.

Reynolds number is the ratio of the inertial forces to the viscous forces. The value of the Reynolds number determines the nature of the flow. In laminar flows the viscous forces dominate the inertia forces. Flow inside circular tubes is always laminar flow for a Reynolds number less than 2300. Turbulent flow will commonly result if the Reynolds number is greater than 4000. Between these values flow is considered as being transitional.

It will be noted that the Colebrook and White formula, Eqn. 25. (page 92) for ascertaining flow rates in pipes is based on turbulent flow resulting when Reynolds Number is "greater than 3500".

Prandtl's number is a measure of how rapidly momentum is dissipated compared to the rate of diffusion of heat through the fluid. Saturated water has a Prandtl number of 13.35 at 32°F (0°C) which drops to 1.0 at 400°F (204°C). Prandtl derived his law for the mixing (entry) length of a jet moving through a medium, from the study of boundary layer theory, and this derived linear law for the increase in jet thickness and mixing length along the stream apparently holds for jets of different shapes.

The Nusselt number is the dimensionless temperature gradient for the fluid evaluated at the wall-fluid interface. The correlations for forced convection heat transfer, analytical or experimental, are expressed in terms of the Nusselt number and the Reynolds number. The

correlation $N_u = \frac{hD}{k}$ is applicable to heat transfer for laminar flow in circular tubes at points that are beyond the thermal energy length (L_c). In thermal entry length problems the Nusselt number is a function of both the Reynold's and Prandtl's number ($R_e P_r \frac{D}{L}$).

The Nusselt number for circular ducts with uniform wall temperature peripherally and axially is 3.657 (Table 8.1 Karlekar^[49] et al). Correlation for the Nusselt number for heat transfer for turbulent flow through circular tubes is discussed further on page 159.

The Grashof number is the relevant dimensionless group for free or natural convection. It can be interpreted physically as the ratio of the buoyancy forces to the viscous forces. The Grashof number is to natural convection what the Reynolds number is to forced convection. The magnitude of the Grashof number serves to indicate what region the flow is in, laminar, transitional or turbulent.

The critical Grashof number for transitional flow ranges between 10^8 and 10^9 . A number greater than 10^9 would indicate turbulent flow in natural convection whilst a value less than 10^8 would signify laminar flow. Figure 23 due to Metais and Eckert^[50] delineates regions of natural (free), forced and mixed convection for flow through vertical tubes.

As the pertinent dimensionless groups for forced and free convection are the Reynolds number and Grashof number respectively, the mixed convection criteria involves both these two groups.

An order of magnitude analysis of the boundary layer, as referred to earlier, shows that when $(G_r/R_e^2) \ll 1$ the condition for free convection is of greater significance than forced convection.

3.4.2 Heat Transfer Coefficients

Heat transfer coefficients are derived using the equation:

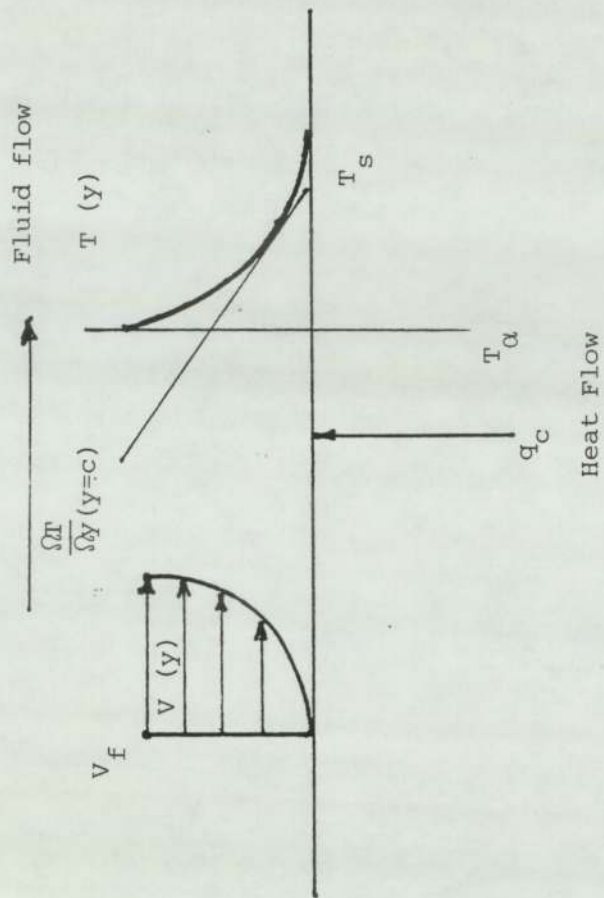
$$\dot{Q}_C = \bar{h}_C A (T_s - T_{f\alpha}) \quad (66)$$

where

\dot{Q}_C is the rate of heat transfer per unit length of vessel or duct.

\bar{h}_C is the unit thermal convective conductance or average convection heat transfer coefficient at the liquid/solid interface ($WM^{-2} K$).

examples of the value for \bar{h}_C are:



Velocity and temperature distribution
for forced convection over a heated
plate

Fig. 25.

for forced convection $\bar{h}_c = 50-10,000$,

for free convection $\bar{h}_c = 20-100$.

A is the surface area in contact with fluid (m^2)

T_s is the surface temperature (K)

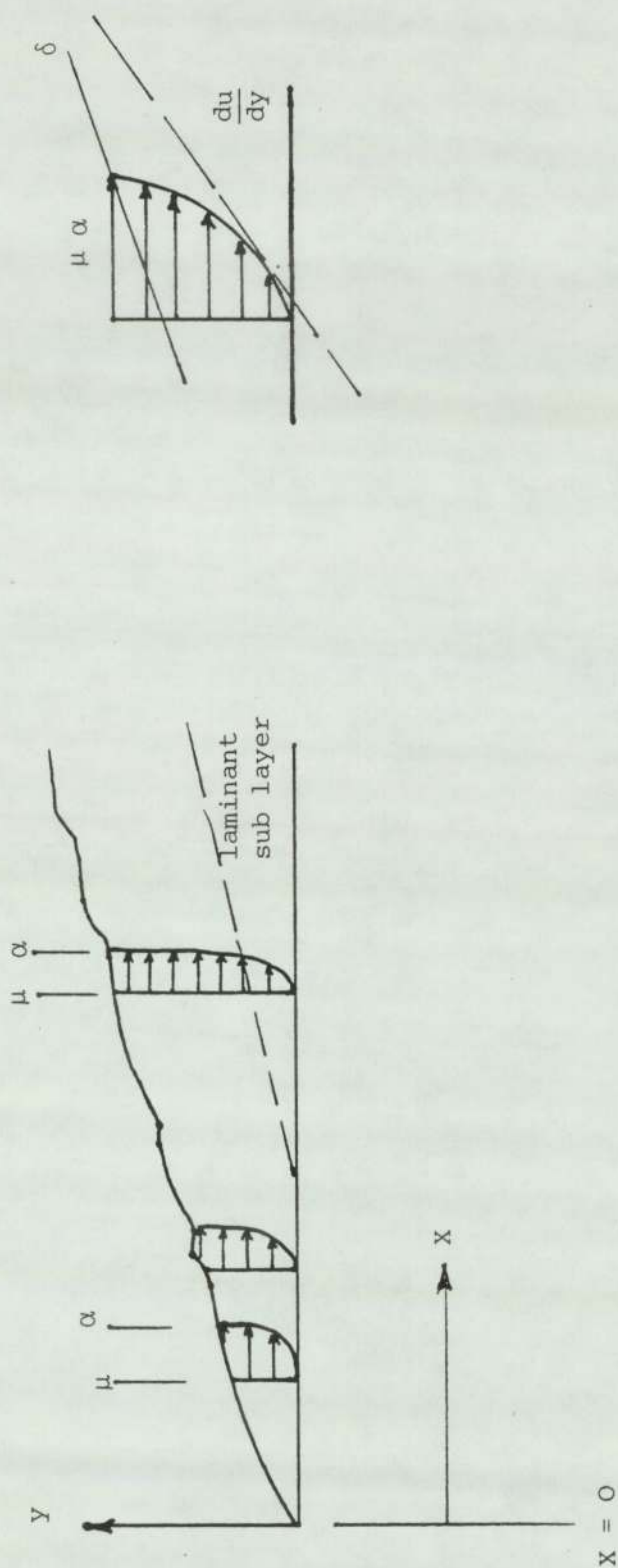
$T_{f\alpha}$ is the temperature of the undisturbed fluid layer at a distance beyond the layer from the heat transfer surface (K).

The numerical value of \bar{h}_c must be determined analytically or experimentally (see example on Appendix 7). Parameters affecting the value of \bar{h}_c for natural or free convection are the properties of the store fluid (specific heat (C_p); viscosity (μ); thermal conductivity (k); coefficient of thermal expansion (β); density (ρ).

Also relevant is the gravitational acceleration (g); the temperature difference ($T_s - T_{f\alpha}$); mean temperature of the store fluid (T_b) and the characteristic length (L_c) to the entry jet profile.

Before attempts are made at calculating a heat transfer co-efficient an examination of the convection process is necessary and must relate the convection of heat to the flow of fluid.

From Figure 25 it will be noted that when a heated surface is cooled by a medium flowing over the surface the velocity decreases in the direction towards the surface, as a result of viscous forces.



Variations in flow regimes at distances from the leading edge of a flat plate.

Fig. 26.

Since the velocity of the fluid layer adjacent to the wall is zero, the heat transfer between the surface and this fluid layer must be by conduction alone, i.e.

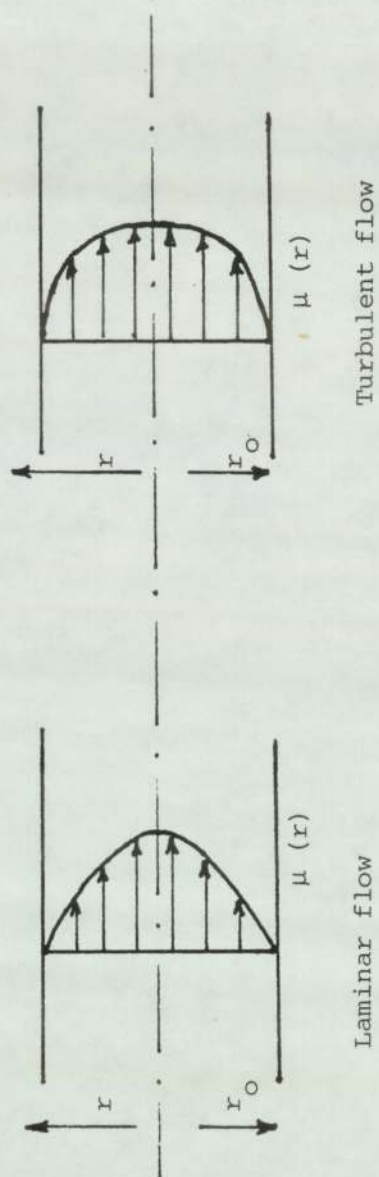
$$q_c'' - K_f \frac{dT}{dy}_{(y=0)} = \bar{h}_c (T_s - T_{f\alpha}) \quad (67)$$

where q_c'' is per unit area.

Although this may suggest the process can be viewed as one of conduction, the temperature gradient at the surface, $(\frac{dT}{dy}_{(y=0)})$ is determined by the rate at which the fluid further from the wall can transport the energy into the mainstream.

The temperature gradient at the wall therefore depends on the flow field; higher velocities being able to produce larger temperature gradients and higher rates of heat transfer. At the same time, however, the thermal conductivity of the fluid plays a role. To gain an understanding of behaviour and the significance of some parameters in forced flow regimes it is useful to refer to Figure 26. This shows how the regimes in flow vary as distance increases from the leading edge of a flat plate.

The region in the flow near the plate, where the fluid velocity is reduced by viscous forces is called the boundary layer. The distance from the plate at which the velocity reached 99% of the free stream velocity is arbitrarily termed



Flow geometries in a tube or duct.

Fig. 27.

the "boundary layer thickness" whilst the region beyond this point is called the "undisturbed" or mainstream flow regime.

Initially the flow in the boundary layer is completely laminar and at some critical distance along the plate (x_c) the inertial effects become sufficiently large compared to the viscous forces (damping action) that small disturbances in the flow begining to grow until the distance builds up to a fully turbulent flow.

Another flow geomtry of importance is the "tube" or "duct". Flow in a tube (or pipework) can be laminar or turbulent, as shown in Fig. 27, depending on the Reynolds number. The Reynolds number for a tube being calculated from

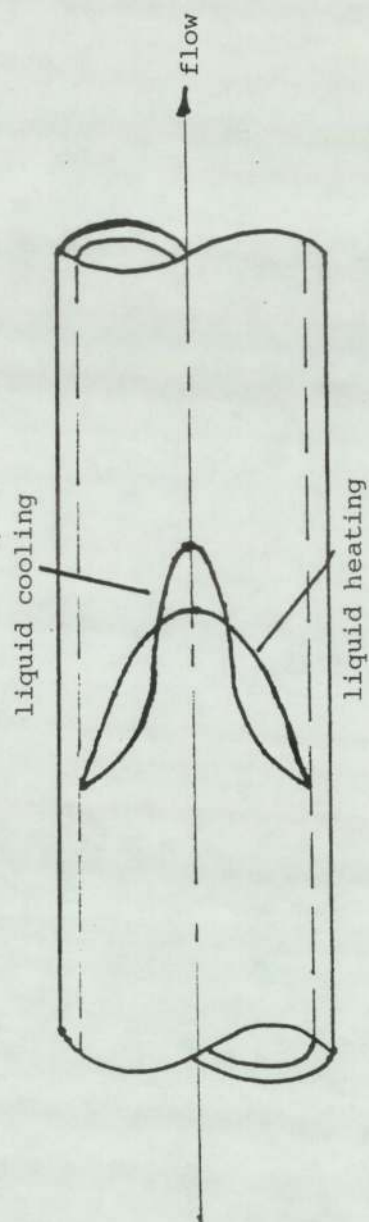
$$Re_D = \frac{V_m D}{\nu} \quad (68)$$

where V_m = mean velocity of flow

D = inside diameter of pipework

ν = kinematic viscosity

The velocity profiles for flow in a tube where liquids are being heated are shown in Fig. 28.



Velocity distribution in laminar
flow of a liquid with heating and
cooling

Fig.28.

When the flow is turbulent the mean velocity of fluid is approximately 83% of the centre velocity. Under laminar flow the mean velocity is 50% of centre velocity and the velocity profile is parabolic.

The Reynolds number can be related to the mass flow per unit area which is defined as:

$$\xi = \rho V_m = \frac{\dot{M}}{A_c} \quad (69)$$

where \dot{M} = mass flow rate of water

A_c = cross sectional area of tube

V_m = mean velocity of flow

The convective heat transfer coefficient varies with the position from the entrance of the tube. The parameters depicting spatial variation is the local heat transfer coefficient (h_l) where "l" is the distance from tube entry. According to Karlekar^[49] et al the relationship between the value h_{cl} and \bar{h}_c is:

$$\bar{h}_c = \frac{1}{L} \int_{l=0}^{l=L} h_{cl} \, dl \quad (70)$$

A local friction coefficient must also be taken into account i.e.

$$C_{fl} = \frac{T_1}{(\rho \frac{\mu^2 \alpha}{2})} \quad (71)$$

the friction coefficient is a dimensionless group giving a measure of fluid shear or drag, on a solid boundary, e.g. tube wall.

The heat transfer coefficient for tubular section turbulent flow is given by:

$$\bar{h}_c = \frac{k}{d} 0.023 Re_D^{0.8} Pr^{0.33} \quad (72)$$

Ignoring changes in heat transfer coefficient caused by changes in the fluid properties, the rate of heat transfer per metre tube length is:

$$\dot{q}_1 = \bar{h}_c \pi D (T_s - T_B) \quad (73)$$

(See also Eqn. 66. page 142).

Where T_B is the bulk fluid temperature.

For fluid flow through long tubes with fluids having a Prandtl number $0.5 < Pr < 100$ a Nusselt number can be correlated by the relation referred to in Colburn[53],

$$N_{U_D} = 0.023 R_{e_D}^{0.8} P_r^{0.33} \quad (74)$$

where all physical properties are evaluated at the mean film temperature, (the average temperature between wall temperature and bulk fluid temperature) evaluated halfway between inlet and outlet of the tube or vessel.

$$\bar{T}_f = \frac{T_s + T_{b_{av}}}{2} \quad (75)$$

where

$$T_{b_{av}} = \frac{T_{b_{in}} + T_{b_{out}}}{2} \quad (76)$$

The bulk fluid temperature (T_b) referred to above is the mean temperature of the fluid at a given cross-section of the tube (vessel). For example, if the flow from a cross-section of the tube were to be collected in a container for a short period of time thoroughly mixed without allowing it to exchange energy with the surroundings, the resulting temperature of the fluid would be the bulk temperature.

Because many practical problems have tubes of insufficient length to have fully developed flow, a relationship taking account of the entrance region is:

$$N_{U_{DH}} = 0.036 R_{e_{DH}}^{0.8} P_r^{0.33} \left(\frac{D_H}{L}\right)^{0.055} \quad (77)$$

which is valid for $10 < \frac{L}{D_H} < 400$ where L is the length of tube and D_H is the hydraulic diameter. $N_{U_{DH}}$ is to be evaluated at the mean film temperature. The Nusselt number can be calculated, according to Webb using Petukhov-Popov equation - which is referred to and illustrated later in a "worked example". The Petukhov-Popov equation is also used in the computer model of the system.

A major assumption made in the study of heat transfer for turbulent flow in circular tubes is that the fluid has constant properties and that the flow is fully developed.

Seider and Tate^[54] (1936) recommended a correlation to account for variations in viscosity values in a fully developed turbulent flow because whenever the fluid temperature changes its viscosity also changes. The Seider and Tate correlation is presented as Eqn. 83 (page 157).

Conductivity of the fluid is considered to be increased due to turbulence.

When convective heat transfer takes place in a turbulent flow a significant contribution to the heat diffusion in the fluid is made by macroscopic transport owing to the eddy motion and is characterized by the eddy diffusivity for heat. If the eddy diffusivity for heat and momentum are assumed equal ($P_{r_t} = 1$) then the velocity profile and temperature profile will be similar. P_{r_t} is referred to as the turbulent Prandtl number and is the ratio:

$$\frac{\text{eddy diffusivity for momentum}}{\text{eddy diffusivity for heat}}$$

The similarity of velocity profile and temperature profile results in a heat flux distribution $q_{(y)}$ which is identical to the shear stress distribution $\tau_{(y)}$. This is known as the Reynolds Analogy.

$$\tau = \frac{\rho}{g_c} (E_m + \nu) \frac{du}{dy} \quad (78)$$

where subscript "m" denotes momentum transfer

$$q = \rho c_p (E_m + \alpha) \frac{dT}{dy} \quad (79)$$

where the quantity $\rho C_p E_H$ may be considered, as suggested earlier, as an increase in the conductivity of the fluid due to turbulence. The ratio $\frac{E_m}{E_H}$ is the turbulent Prandtl number.

An associated problem with turbulent heat transfer in tubes is one whereby heat transfer occurs in the entrance (mixing) length.

At this point a fully developed temperature profile is considered not to be established. A fully developed temperature profile refers to a generalized temperature profile the shape of which does not change with the "x" co-ordinate and is expressed as:

$$\frac{d}{dx} \left(\frac{T_s - T}{T_s - T_b} \right) = 0 \quad (80)$$

This however does not mean that the fluid temperature for a given value of radial co-ordinate does not change as one moves downstream because if the fluid receives a uniform heat flux the temperature would increase linearly.

For distances beyond the thermal entry length the difference between the temperature of fluid at the wall interface (T_s) and the bulk temperature (T_b) is constant.

In general the bulk temperature varies from one cross-section of the tube to another.

Sleicher and Tribus^[55] solved cases where the velocity profile is fully developed and the temperature profile not fully developed for tubes with constant surface temperature by obtaining a solution in the form of an infinite series.

Stephenson^[56] in his studies succeeded in obtaining good agreement between his predictions and experimental data for the velocity profile and the dimensionless quantity $(\frac{Nu}{Re Pr})$ which is known as the Stanton number. See also Eqn. 65 (page 139).

Results for combined thermal and hydrodynamic entry length problems, where neither the temperature nor velocity profile is fully developed are presented by Sellars S R et al^[57].

Webb^[58] recommends that the Petukhov-Popov equation be used to calculate the Nusselt number (N_u) for intermediate Prandtl numbers in the range 1 to 50.

The analytical solution obtained by Petukhov-Popov for circular tubes with uniform heat flux uses the equation:

$$Nu = \frac{\frac{f}{8} Re Pr}{1.07 + 12.7 \sqrt{f}/8 (Pr^{0.66} - 1)} \quad (81)$$

$$\text{where } f = (1.82 \log_{10} Re - 1.64)^{-2} \quad (82)$$

this being known as Filonenko[59] equation for friction.

The fluid properties associated with the above calculations are evaluated at the mean bulk temperature.

Seider and Tate[54] recommended the following Nusselt correlation for laminar flow in tubes:

$$[\bar{Nu}_D = 1.86 (Re_D Pr)^{0.33} \left(\frac{D}{L}\right)^{0.33} \left(\frac{\mu_b}{\mu_s}\right)^{0.14}] \quad (83)$$

to account for variations in viscosity values in a fully developed flow.

According to Cornwell[52] the Sieder and Tate expression for heat transfer (Eqn. 83) in flow through tubes is only used when the predicted heat transfer coefficient is greater than $Nu_u = 3.685$.

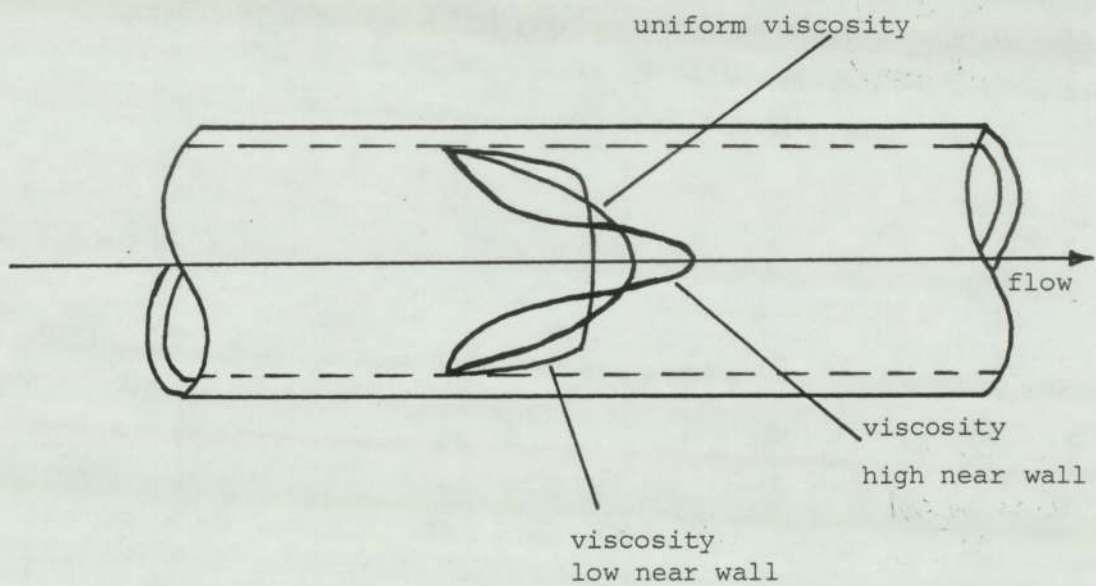


Fig. 29.

Diagram showing relationship of viscosity,
velocity and temperature in fluid flow.
(see also Fig. 28)

A variation to the correlation Eqn. 83 has been proposed by Kundsen J G and Katz D L^[60], (1958) as being one of the simplest to use for turbulent flow in a tube.

The expression:

$$N_u = 0.027 R_e^{0.8} P_r^{0.33} \left(\frac{\mu}{\mu_o} \right)^{0.14} \quad (84)$$

is applicable to fluids with Prandtl numbers in the range 0.7 to 16,700 and over a wide range of temperatures.

For comparison purposes the Hansen A G^[61] (1967) correlation for Nusselt's number can be used, this being:

$$Nu_{av} = 3.66 + \left(\frac{0.0668 \left(\frac{D}{L} \right) Re Pr}{1 + 0.04 \left[\left(\frac{D}{L} \right) Re Pr \right]^{2/3}} \right) \quad (85)$$

where all properties are evaluated at the bulk temperature. The empirical correction factor accounts for the effects temperature variations have on the viscosity.

As shown in the diagram opposite, (Fig. 29) for liquids, the viscosity decreases (velocity increases) with increasing temperature.

The above observations and derivations suggests that for a heated liquid, the fluid near the wall is less viscous than fluid in the centre of the flow. Consequently the velocity of the heated liquid is larger.

Whilst the above comments reflect on approaches for calculating heat transfer coefficients in fluid flows the following aspects, (a-e) inclusive, also have to be taken into account when evaluating test data from this study.

- (a) The actual store vessels are assumed to be at a constant external wall temperature therefore no heat is added from external sources to the water as it flows down the vessel.
- (b) A constantly changing bulk fluid temperature prevails as the water is circulated in a closed-loop circuit with heat constantly being added as the water passes through the condenser coil.
- (c) Water enters the vessel through a top entry point resulting in jet entry effects. The jet profile contributes to disturbances of the stored water - though conditions are different in each vessel because of the installed diffuser.

(d) The effects of jet entry upon velocity and temperature profiles also differs between vessels and will be further affected through not having fully parallel vessel walls.

(e) The heat transfer taking place in the vessels results from a combination of forced convection and possibly from mass transfer.

Mass transfer being the transport of a component of a mixture from the region of high concentration of that component to a region of lower concentration.

The two broad categories of mass transfer are:

(a) diffusion mass transfer (molecular mass transfer)

(b) convective mass transfer.

According to Kreith F and Black W Z^[62] (1980).

"Diffusion of one component in an essentially stationary mixture in the direction of decreasing concentration of that component is analogous to the transfer of heat by conduction in the direction of decreasing temperature".

They also identify convective mass transfer as:

"..... the transport of a component due to the motion of the bulk fluid".

A situation that possibly exists in the system under examination.

3.5 Stratification in sensible heat store vessels

Amongst the published documentation which refers specifically to aspects of sensible heat storage Blay D^[63] (1981) provides some pertinent observations, for example,

"The mechanical stability which results from the superposition of hot fluid layers above colder ones allows, under specific conditions, to establish an important thermal stratification inside a fluid in a tank. It makes possible the storage of both hot and cold fluid in the same container in restricting their mixing".

Without referring specifically to the duration one could expect a suitable storage period under stratification to be Blay continues:

".....during thermal relaxation, due to heat conduction through the walls and free convection inside the tank, degradation of energy occurs which increases the thermocline (stratified band) thickness and leads to a homogenization of temperature".

Blay also suggests that free convection inside the store vessel is characterized by high Grashof and Prandtl numbers.

As mentioned earlier, (page 136) the successful accomplishment of thermal stratification of fluid in a vessel is governed by a set of complex interactions amongst which are:

- (a) boundary layer phenomena
- (b) conduction heat transfer in the fluid bulk
- (c) speed of fluid flow and velocity profile through the store.
- (d) type of fluid flow (turbulent, laminar, transitional)
- (e) jet entry profile (mixing length)

Welty J R^[64] (1978) suggests turbulent flow regimes are most frequently encountered in practical applications, consequently analytical modelling of turbulent flow has to date, attracted the greater level of attention. The study of fluid flows is comprehensively documented by Schlichting H^[65], Pia S I^[66].

CHAPTER FOUR

4.0 Heat Pump Components

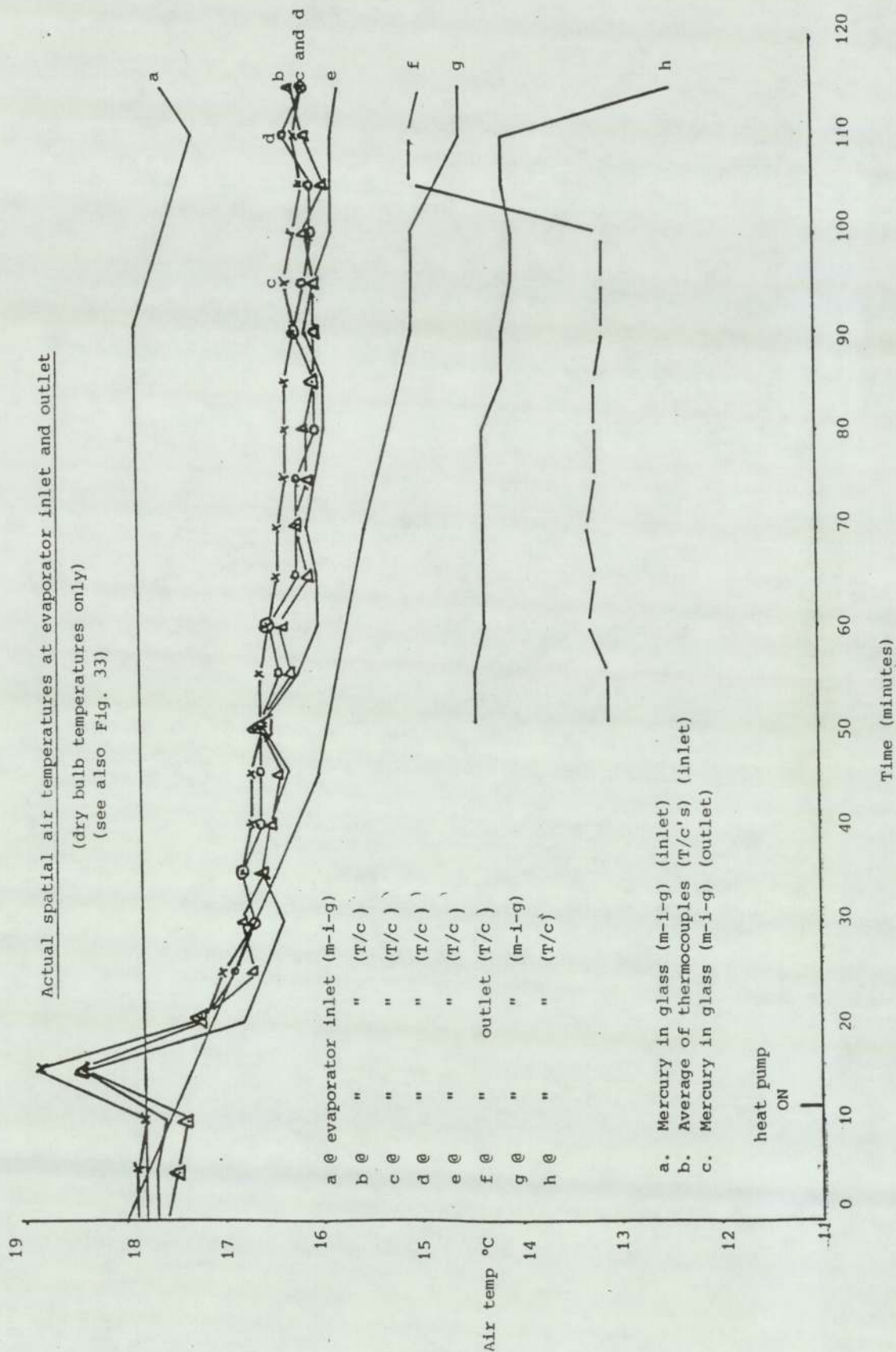
4.1 Evaporator Coil Air Temperature Distribution Patterns

As stated earlier, (page 75) the evaporator is a major component of the heat pump circuit. A correctly designed evaporator is of paramount importance to maximising heat pump performance.

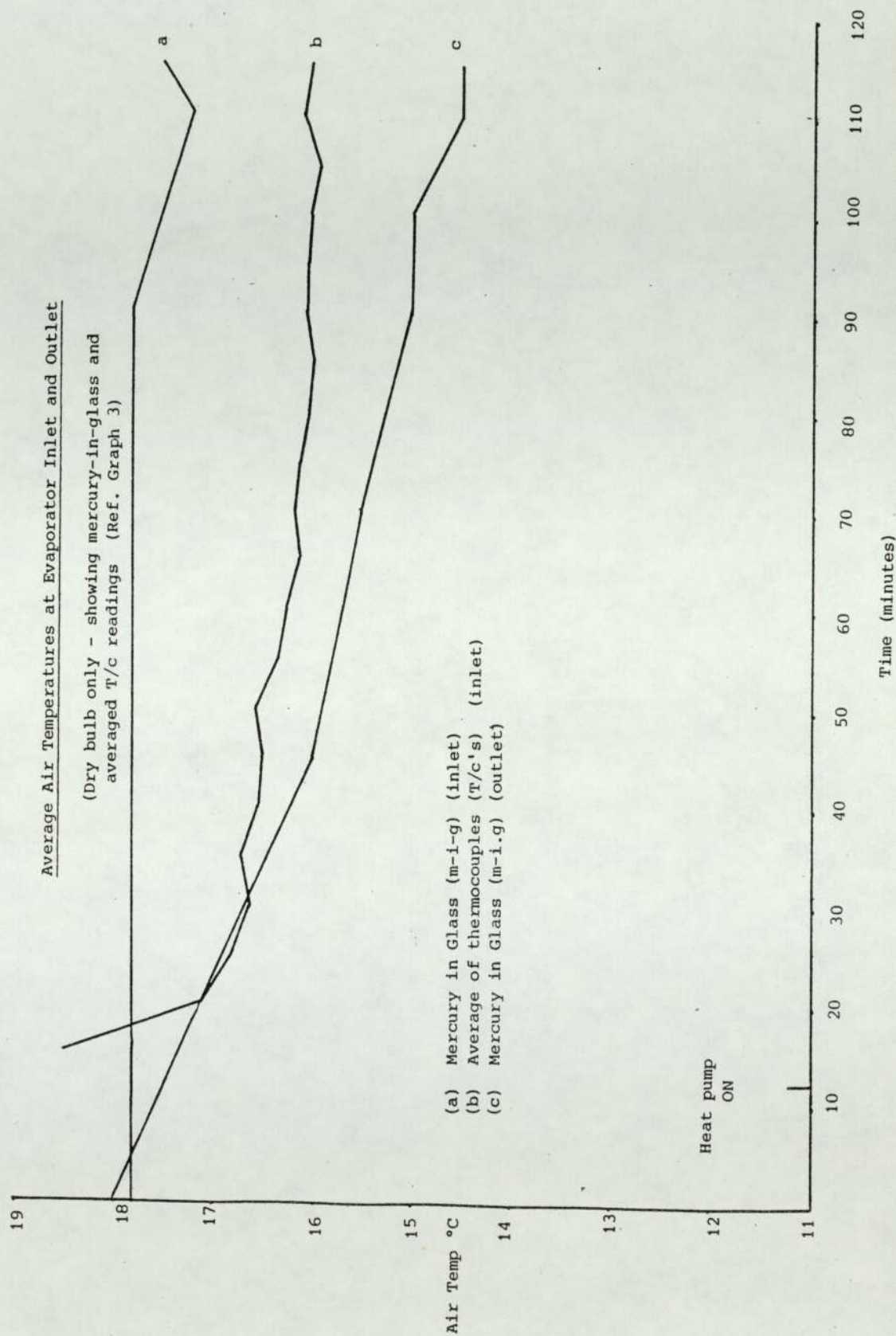
Accurate evaluation of evaporator performance is dependent upon the availability of high quality data recorded at the evaporator refrigerant circuit and at the air circuit.

As the evaporator and associated fan are integral parts of the unit heat pump in this system it has been assumed, for this thesis, that the fan performance is as suggested by the manufacturer. However, it has been necessary to establish representative air temperatures at the evaporator inlet and outlet.

To continually monitor and process the air temperatures at points other than a single representative position (one for inlet and one for outlet) would require computing capacities greater than those immediately available.



Graph 3



Graph 4

Consequently Appendix 5 to this thesis contains a discussion on the air temperature distribution patterns, experienced under test conditions, at the evaporator coil inlet and outlet.

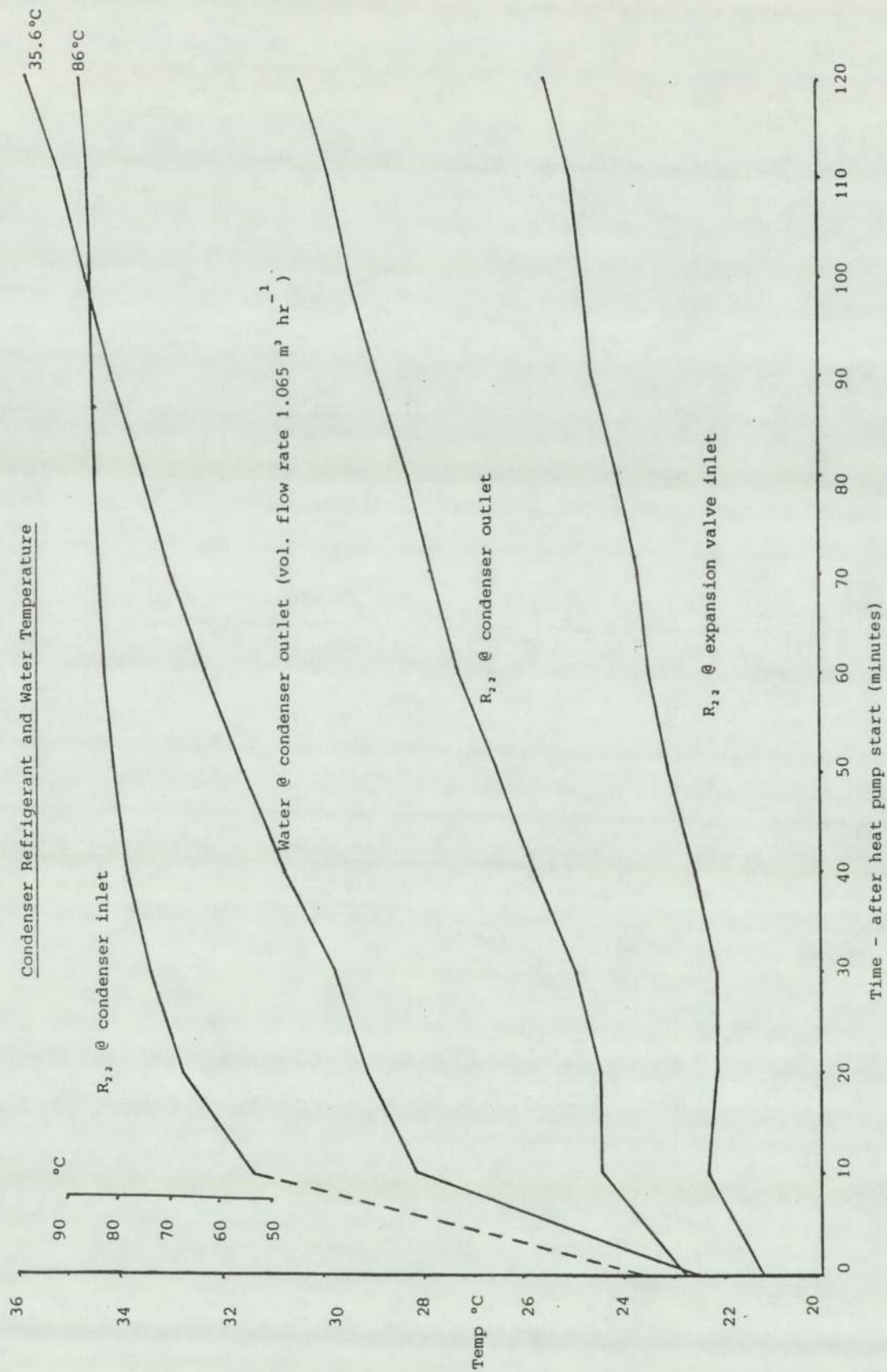
It will be noted in Appendix 5 that positioning of the thermocouples used for measuring air inlet and outlet temperatures at the evaporator coil is not too critical for achieving representative temperatures.

A central position at both the inlet and outlet grills appears suitable for recording the respective temperatures. Graphs 3 and 4 provide examples of some typical test results.

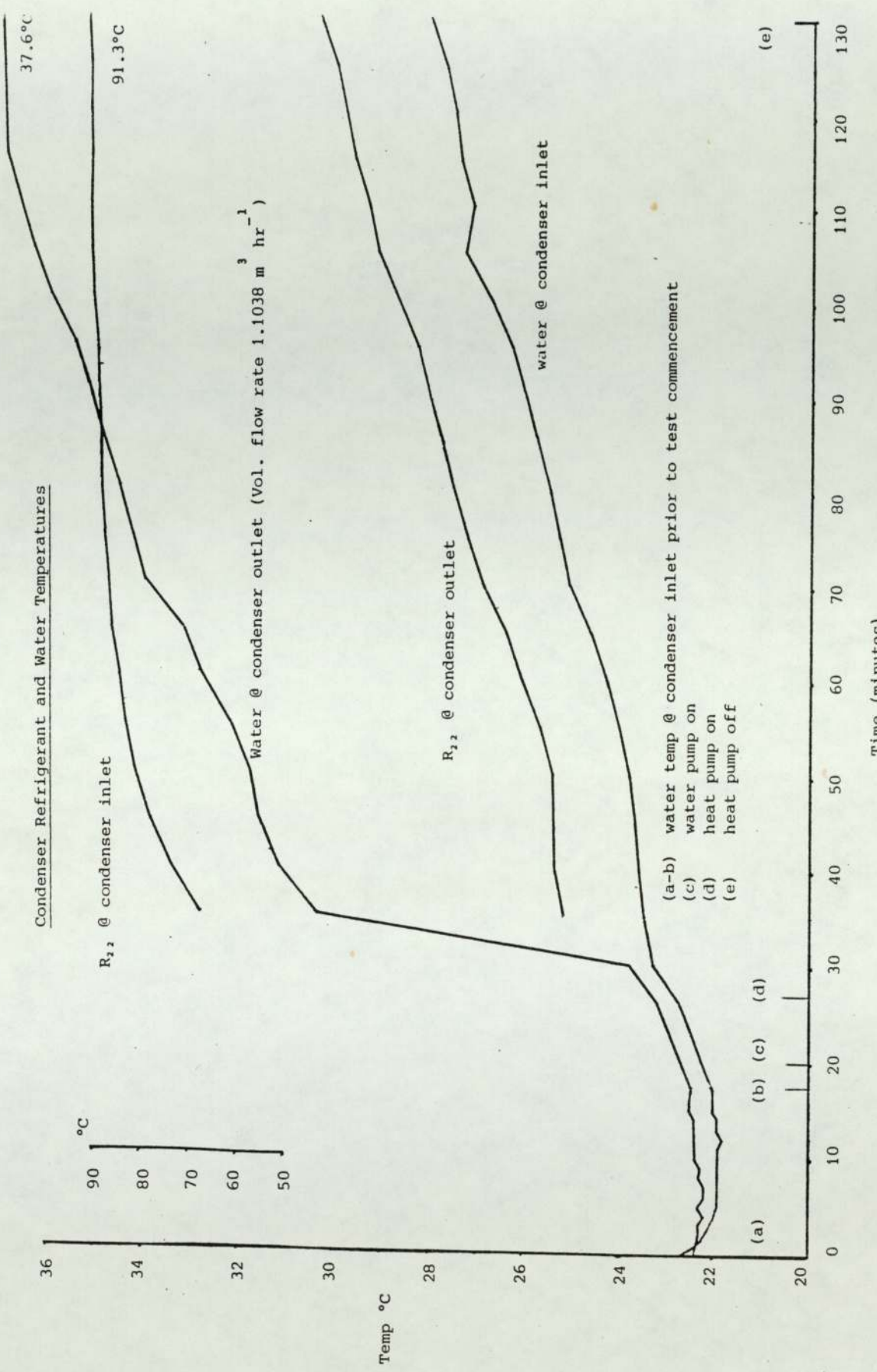
4.2 Condenser Coil Temperature Pattern

Results from the series of tests conducted for establishing condenser performance, under varying water flow rates and with differing initial bulk store temperatures, are represented by Graphs 5 - 8 inclusive.

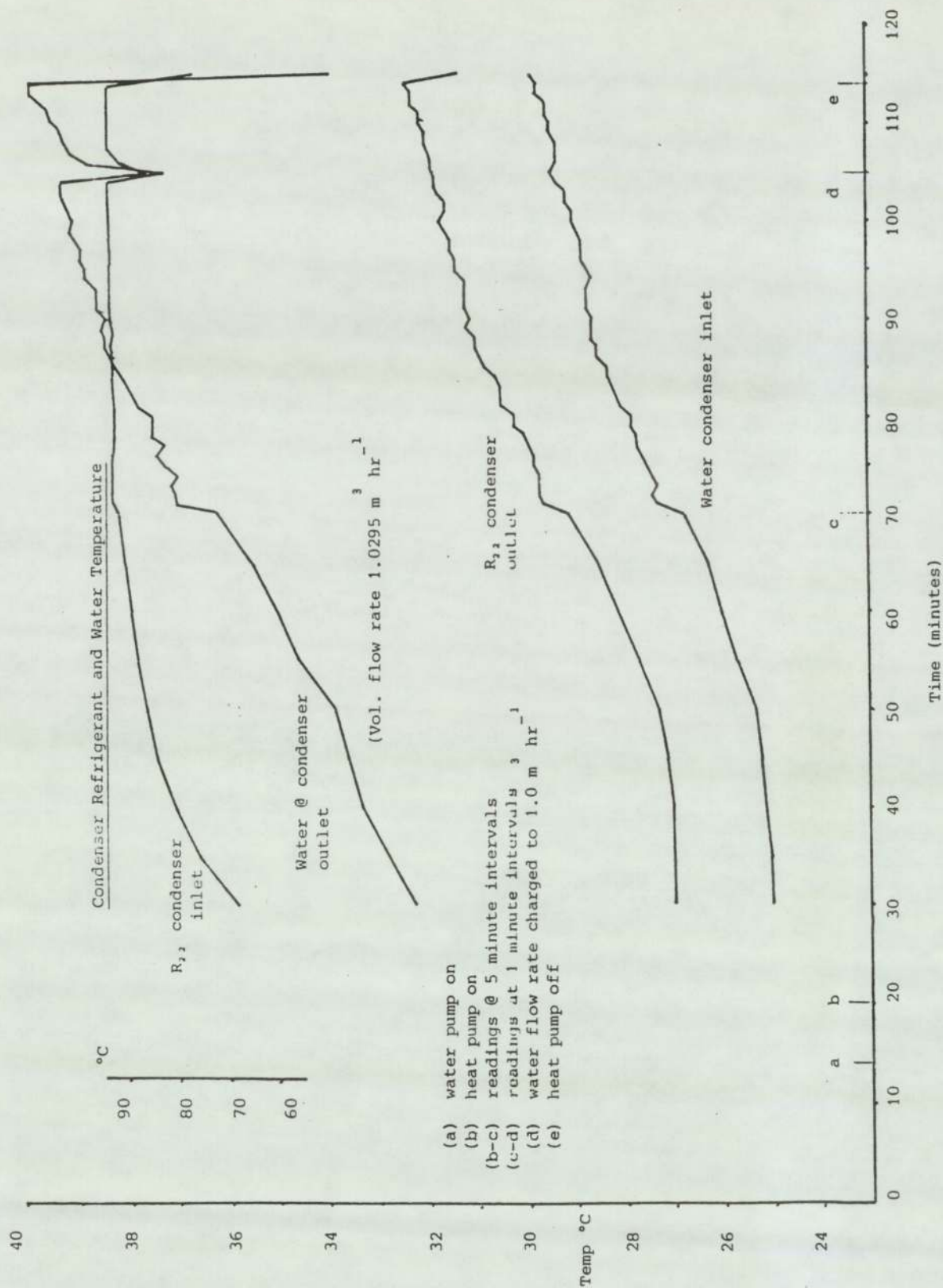
The variations in ambient conditions in the laboratory prior to each test were within a temperature range $\pm 1.5^{\circ}\text{C}$ and therefore the effects on store water bulk temperatures were slight.



Graph 5

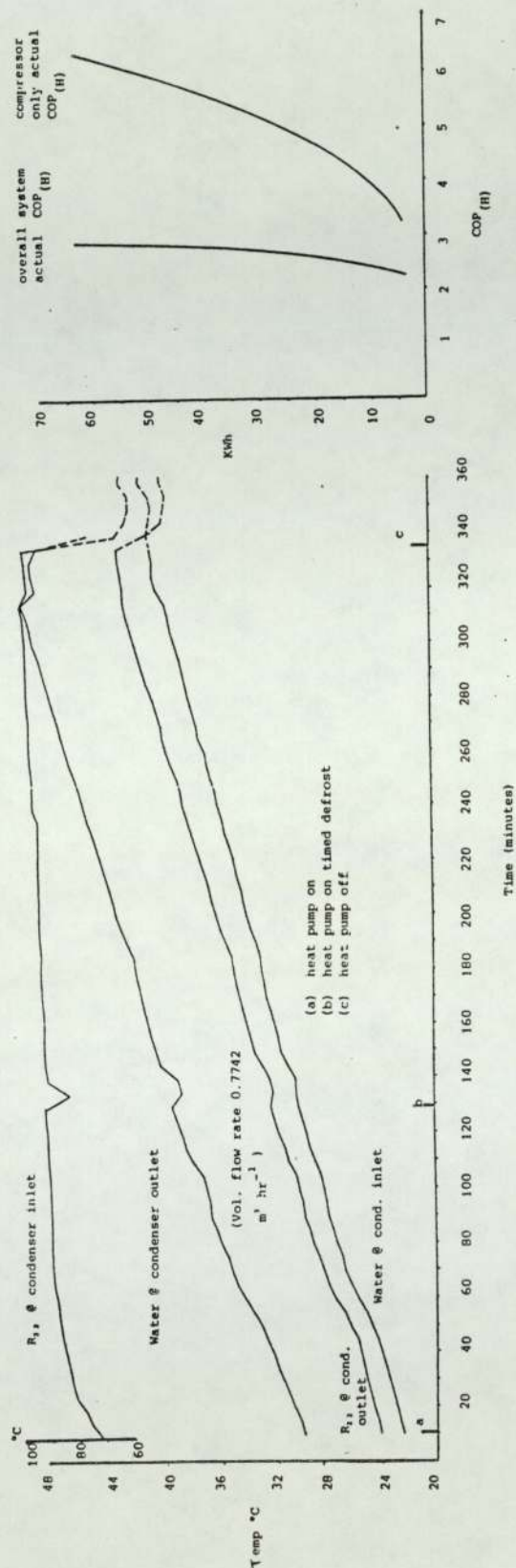


Graph 6



Graph 7

Condenser Refrigerant and Water Temperature



Graph 8

The initial store temperatures top to bottom of the vessel were consistently within 1.2°C.

Refrigerant and water temperature changes during tests exhibited a familar pattern.

The data summarized below is more fully represented on the relevant graph.

From heat pump start-up the refrigerant temperatures recorded at the condenser inlet were, over four selected tests:

Table 2

Refrigerant Temperatures at Condenser Inlet

	Test 1	Test 2	Test 3	Test 4
	(Graph 5)	(Graph 6)	(Graph 7)	(Graph 8)
Initial store temp °C	22.5	22.5	23.2	22
Vol flow rate $\text{m}^3 \text{hr}^{-1}$	1.065	1.1038	1.0295	0.7742
R ₂₂ temp at condenser inlet				
after 10 mins °C	54	70	67	72
" 50 mins	80	87	91	89
" 120 mins	86	91	94	91
" 230 mins	-	-	-	94
" 310 mins	-	-	-	98

The rate of heat rejection, refrigerant to water, again showed consistency as indicated by the following.

Table 3

Rate of Heat Rejection (Refrigerant to water)

Test 1						Test 2			
R ₂₂ temp						R ₂₂ @			
at cond.out °C						at cond.out °C			
water						water			
Δt ⁰ C						Δt ⁰ C			
after 10 min ht pump op.	54				5.8	70			7.1
" 50 " " " "	80				6.5	87			8.9
" 120 " " " "	86				7.2	91			9.5
" 310 " " " "	-				-	-			-
Test 3						Test 4			
after 10 min ht pump op.	67				7.3	72			7.1
" 50 " " " "	91				9.5	89			8
" 120 " " " "	94				10	91			9
" 310 " " " "	-				-	98			10.3

For this selection of tests the water volume flow rate through the condenser varied within $1 \text{ m}^3 \text{ h}^{-1} \pm 11.0\%$ - 22.0% therefore always remaining within the manufacturers design limits.

The condenser capacity under full system test is discussed more fully in Section 4.3.

4.3 System Performance (Corrected Condenser Design Capacity)

Aspects of the condenser - type, size and performance characteristics - have been referred to in previous sections. See sections 2.4 and 3.2.

The basic principle adopted for evaluation of system performance is one of determining the heat energy available at the condenser based on terminal conditions prevailing, i.e. refrigerant pressure/temperatures; water temperatures, the mass flow rate of refrigerant and water.

Calculation of corrected condenser capacity, correcting for actual operating conditions, is undertaken in the computer evaluation routine.

From data, inserted manually to the computer, for operating pressure of refrigerant at condenser inlet, the condenser temperature is calculated using the derived equation, Eqn. 86, which is presented in program syntax and discussed further in Appendix 6.

$$C_3 = \frac{(-.17836 + (\text{Sqr}((0.17836^2) - ((4 \times 0.0138)(56.82 - G2))))}{(2 \times 0.0138)}$$

(86)

where C_3 = condensing temperature $^{\circ}\text{C}$

G_2 = refrigerant pressure at condenser inlet (Psig)

The corrected condenser capacity, corrected for water volume flow rate, condensing temperature and water inlet temperature is calculated as the example below using Eqn. 55, Eqn. 56 (page 125) and Eqn. 53 (page 124).

Corrected condensing capacity kW.

$$\text{CC} = ((23040 + ((F_v - 0.5)/0.1)(4904.62 \times 0.7314)))/3600 \times F_K$$

where F_v = calculated actual water flow velocity ms^{-1}

$$\sin\theta = 0.7314$$

F_K = correction factors for R_{22}

Typically for water flow at $0.927 \text{ m}^3 \text{ hr}^{-1}$ and condensing temperature of 32.6°C then

$$F_v = (0.5 + ((0.927 - 0.55)/0.1)(0.14)) = 1.03$$

$$F_K = 1.0 + ((32.6 - 45)(-0.003)) = 103.72$$

therefore CC becomes:

$$\begin{aligned} \text{CC} &= ((23040 + (((1.03 - 0.5)/0.1)(4904.62 \times 0.7314)))/3600 \\ &\quad \times 103.72 = 12.055 \text{ kW.} \end{aligned}$$

Derivation of the above formulae is discussed more fully in Appendix 6.

4.3.1 Heat Transfer at Condenser

The heat energy delivered to the condenser is determined from refrigerant mass flow rate, the condensing temperature and the refrigerant temperature and pressure at the condenser inlet and outlet.

From data collated under test for the above parameters the heat transferred at the refrigerant vapour, vapour/liquid and liquid stages in the condenser is calculated using the following expressions; (in program syntax)

(i) vapour phase

$$V_L = R_F ((12.52 +)(.022 \times B_1))/86.5)(B_1 - C_3) \quad \text{kW} \quad (87)$$

(ii) vapour/liquid phase

$$M_L = R_F (R_3 - R_4) \quad \text{kW} \quad (88)$$

(iii) liquid phase

$$S_L = R_F \times 0.3 (C_3 - B_2) \quad \text{kW} \quad (89)$$

where R_F = refrigerant flow rate (ASHRAE method) Kg s^{-1}
 B_1 = refrigerant temperature at condenser inlet $^{\circ}\text{C}$
 C_3 = condensing temperature (pressure based) $^{\circ}\text{C}$
 R_3 = enthalpy of refrigerant (saturated
 vapour at condensing pressure) Kj Kg^{-1}
 R_4 = enthalpy of refrigerant (saturated
 liquid at condensing pressure) Kj Kg^{-1}
 B_2 = refrigerant temperature at condenser outlet $^{\circ}\text{C}$

a typical calculation would be:

$$V_L = (0.0573((12.52 + (0.022 \times 78.2))/86.5)(78.2 - 32.6)$$

$$V_L = 0.43 \text{ kW}$$

$$M_L = 0.0573 (263.95 - 88.95)$$

$$M_L = 10.027 \text{ kW}$$

$$S_L = 0.0573 \times 0.3 \times (32.6 - 26.8)$$

$$= 0.093 \text{ kW}$$

i.e. Total energy transferred at the condenser = 10.55 kW.

From the procedure included as Section 4.3 and based on a calculated condensing temperature of 32.6°C the corrected condenser design capacity was determined as 12.055 kW.

Again, using the condensing temperature 32.6°C the actual energy transferred at the condenser is calculated as 10.55 kW. Suggesting a condenser performance of 87.5% at the stated conditions.

4.3.2 Heat Transfer to Store

A value for the total energy in store is obtained from the heat energy transferred from the refrigerant to the circulating water - see Section 4.3.1 - less the calculated heat loss from;

- (a) the condenser coil
- (b) the system pipework (condenser to store)
- (c) the store vessels

Heat losses are calculated for conditions prevailing during each test.

Calculation of the amount of energy transferred to store is based on the store water temperature rise over the test period.

Prior to a test commencing the relevant water temperatures are monitored and recorded, these temperatures being monitored continually throughout the test. Increased temperature of the store water within each temperature band, along with the volume of water within each band is then used for deriving the energy stored, at each band, and therefore the vessel as a whole. Limitation on the accuracy of this approach is discussed in Section 5.5.

The temperature band referred to above is dictated in this system by the fixed thermocouples positions in the store vessels. Each vessel is considered as having three temperature bands. However with the facility for raising/lowering the variable position thermocouple carrier a maximum of six "bands" could be specified.

The following calculations are typical of the test data recorded; (in program syntax).

Energy stored in vessel 1 (top band) between fixed thermocouples No. 3 and No. 4

$$Q_w = ((164.33 \times 4.187(L_y - ((w_3 + w_4)/2)))/3600) \text{ kW} \quad (90)$$

where 164.33 is volume of water, in litres in the band between T/c's 3 and 4 in vessel 1.

$$L_y = (x_3 + x_4)/2 \quad (91)$$

x_3 and x_4 being water temperature at T/c's 3 and 4 at completion of test.

w_3 and w_4 being water temperature at T/c's 3 and 4 at commencement of test.

$$Q_w = ((164.33 \times 4.187(((29.2 + 29.8)/2 - ((22.8 + 23.4)/2))))/3600$$

$$\begin{aligned}
 Q_w &= ((688.05 \times (29.5 - 23.1))/3600 \\
 &= 1.22 \text{ kW}
 \end{aligned}$$

A further series of calculations, based on the above procedure, are carried out within the computer program to establish the energy stored for the remaining temperature bands (or nodes) in each vessel. A more comprehensive sample of calculation for the energy in store is included as Appendix 8.

4.4 Heat Pump Coefficient of Performance

The heat pump coefficient of performance, in the heating mode, as calculated with the computer model, takes account of the energy absorbed at the evaporator and the compressor power consumed during a test.

The calculation, in program syntax.

Coefficient of performance (compressor only)

$$COP_H = P = (\dot{Q}_E + S_Y)/S_Y \quad (92)$$

where

$$\dot{Q}_E = (\dot{Q}_S + \dot{Q}_D) \quad (93)$$

\dot{Q}_S and \dot{Q}_D being the calculated values (see Chapter 3 for the rate of sensible heat extracted (dry air at evaporators) and for the rate of latent heat extracted at the evaporator respectively (in kW).

$S_Y = (S_Z / \text{Hr})$ where S_Z is the energy, in kWh consumed and measured at the compressor motor.

H_R = duration of heat pump operation (hours).

Typical test values give:

$$\begin{aligned} P &= ((\dot{Q}_S + \dot{Q}_D) + (S_Z / \text{Hr})) / (S_Z / \text{Hr}) \\ &= ((1.84 + 2.51) + (2.65 / 1.25)) / (2.65 / 1.25) \\ &= (4.35 + 2.12) / 2.12 \end{aligned}$$

$\text{COP}_H = (3.05 \text{ COP (compressor only)})$.

4.5 Auxiliary Power Consumption

The extent of energy consumed by the auxiliary equipment during a test is limited to that required by the evaporator fan and the circulating water pump. The energy consumed in each case being measured independently.

The energy consumed by the evaporator fan was within the range indicated by the manufacturers. The water pump was slightly oversized for the system being investigated as the intention was for ultimately extending the pipework installed. However, whilst the pumping power was greater than one would normally expect, or design for, it was accepted for the test performance calculations. The effects of auxiliary plant energy consumption on the overall system coefficient of performance can be seen in the following section.

4.6 Overall System Coefficient of Performance (COP_H)

As indicated in the previous two sections the coefficient of performance for the system will be different from that of the compressor only, by virtue of the auxiliary energy consumed. Calculation of the overall COP is, in program syntax;

Coefficient of performance (overall, inc fan and pump)

$$= OP = ((\dot{Q}_E + S_Y)/P_C) \quad (94)$$

where \dot{Q}_E is the sum of sensible heat extracted (dry air at evaporator) and the latent heat extracted at the evaporator, as calculated from test conditions.

P_C is the sum of compressor, fan and water pump energy consumed

S_Y is the energy consumed by the compressor alone.

Typical calculations give:

$$\begin{aligned} O_p &= ((1.84 + 2.51) + (2.65/1.25))/ \\ &\quad ((2.65 + 0.55 + 0.55)/1.25) \\ &= (4.35 + 2.12)/3 \end{aligned}$$

$$CoP_H = 2.16 \text{ (overall system)}$$

4.7 Temperature Distribution in Water Store

4.7.1 Fixed Position Thermocouples

The test results discussed below and reproduced as Graphs 9 - 14 inclusive are typical of those recorded whilst establishing temperature profiles of the water in store - these measurements being taken at the water/vessel interface using fixed thermocouple data.

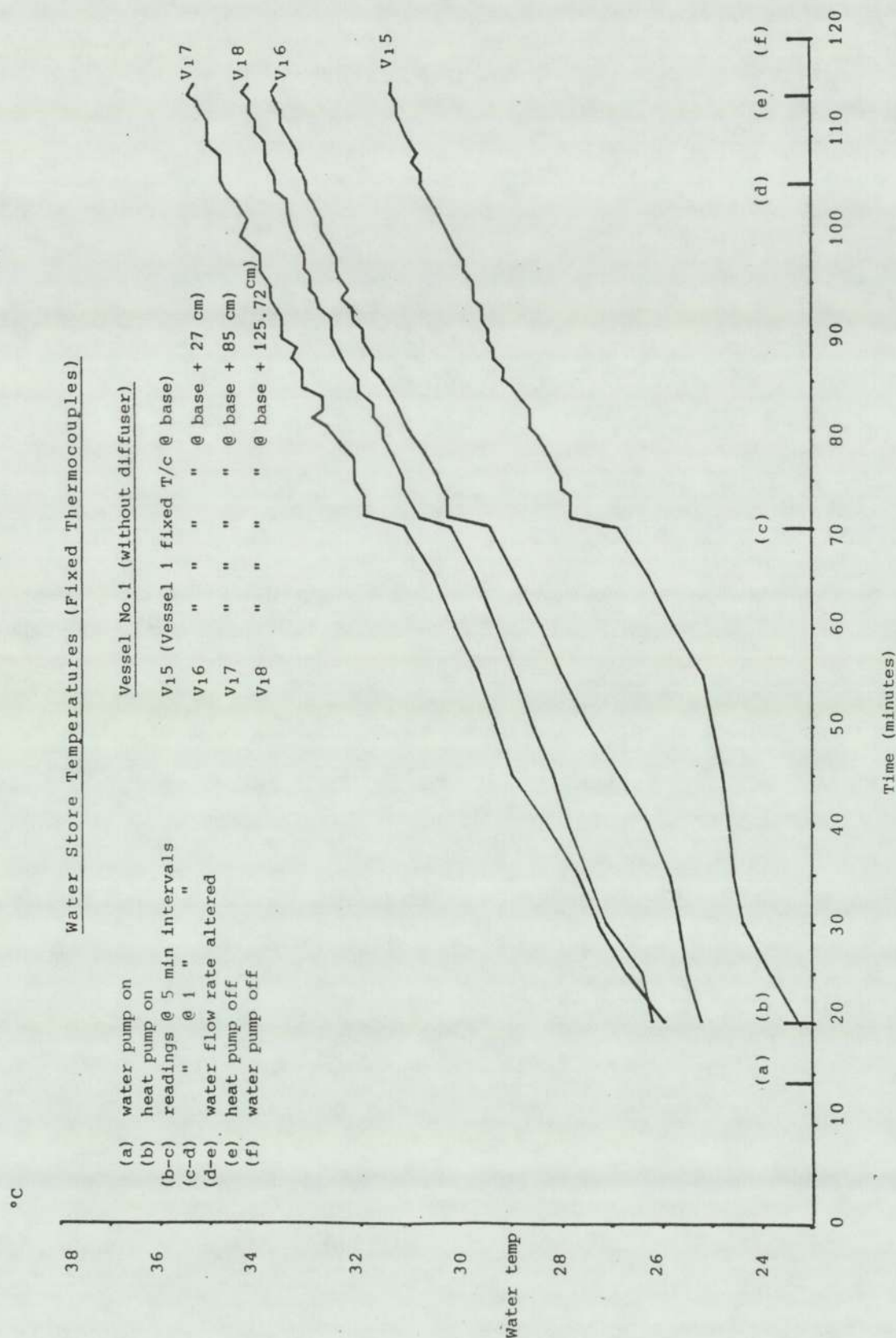
The series of tests involving only the fixed thermocouple readings aimed at identifying the likely patterns of store behaviour and establishing that the behaviour pattern remained stable under changing operating conditions.

As indicated earlier each of the two vessels contain four thermocouples (T/c's) bonded to the internal surface of the vessels at heights as shown in Figure 11.

The position of each T/c was selected to provide a comparison of temperature distribution down the vessels.

Direct comparison of the readings at the top and bottom of the vessels can be made whereas the T/c's at positions 27.0 cm and 85 cm (vessel 1) and positions 40.38 cm and 83.05 cm (vessel 2) reflect changes in depthwise distributions. Further discussion of depthwise distribution is included on page 200.

Water Store Temperatures (Fixed Thermocouples)



Graph 9

Test durations varied from 90 minutes of heat pump operation to over 5.5 hours operation.

The extended periods of operation allowed for time-dependent conditions to manifest themselves.

Prior to commencement of each monitoring period the volume flow rate of water was established and the water circuit allowed to stabilize.

This stabilization period also allowed for any turbulence of water in the stores, brought about by the initial disturbance due primarily to initiating the water pump to be eliminated.

A discussion on the effects of pumping on the temperature distribution is included on page 227. The volume flow rate of water for each full system test was always selected within the range $1 \text{ m}^3 \text{ hr}^{-1} \pm 20\%$. A test for condenser performance was carried out beyond this range. The series of graphs presented - Graphs 9 to 27 inclusive - show typical test results.

Graph 9 shows the effect on store temperature change in vessel 1 throughout the duration of tests when the thermocouple scan intervals differ.

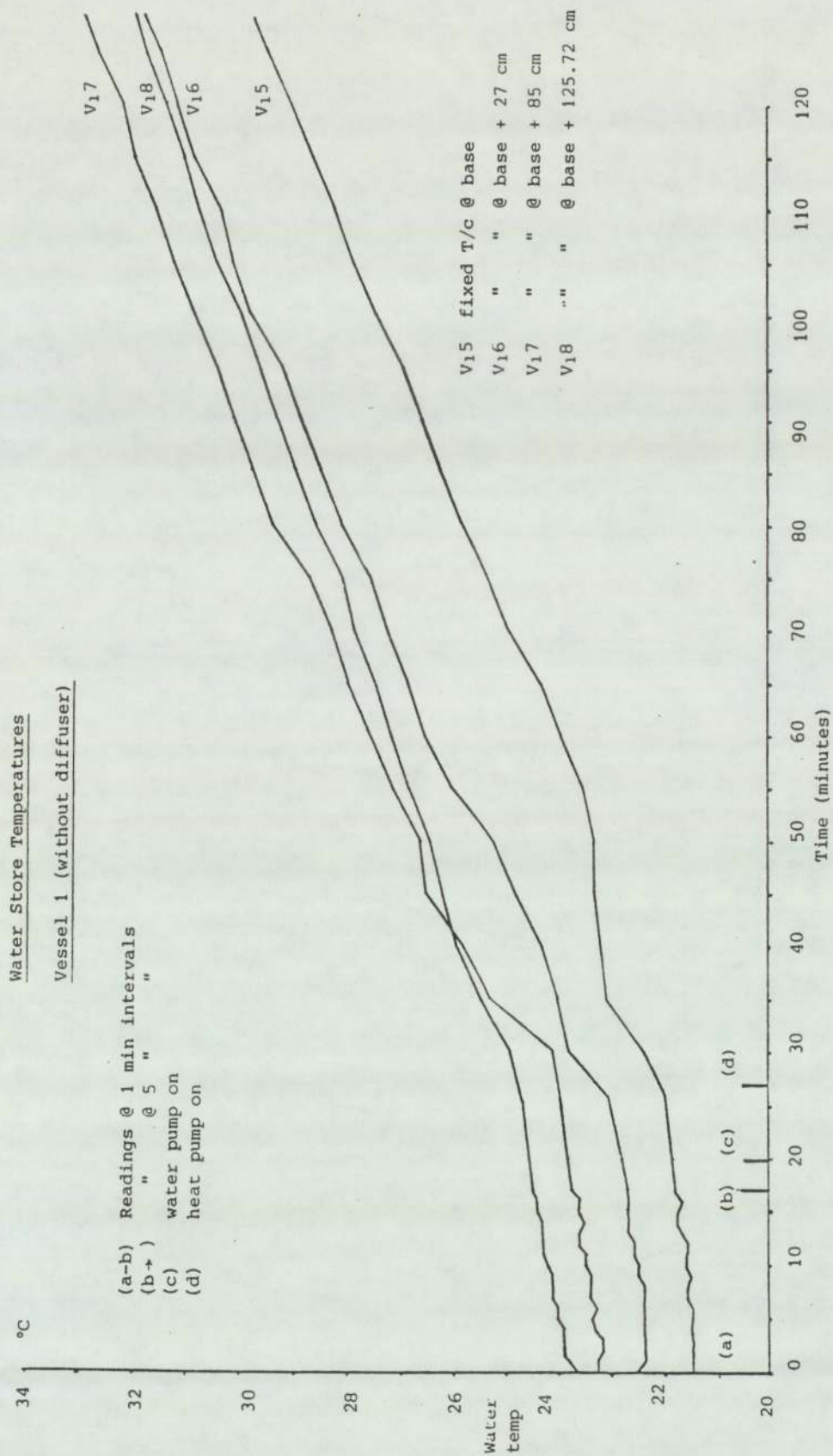
Prior to switching on the water circulation pump the computer controlled analogue-to-digital (A-D) monitoring system commenced scanning the relevant temperatures. This procedure enabled visual checks on equipment response to be made prior to the actual performance test commencing.

The water pump was operated following a 14 minute period during which the A-D equipment was being checked and the water volume flow rate adjusted manually to settle within the designated range. The volume flow rate for this test was $1.029 \text{ m}^3/\text{hr}$.

Ten minutes after water pump start-up the heat pump was activated. This time lapse allowed for the water circuit within the store vessels to "settle down".

For the period covering the initial 50 minutes after heat pump start-up (position 70 minutes on graph 1) the thermocouples were automatically scanned at 5 minute intervals. For the remaining 44 minutes of heat pump operation the thermocouples were scanned at 1 minute intervals.

The 5 minute scan interval noticeably "smoothes out" temperature variations. Throughout the course of the test a series of additional readings were monitored and recorded manually. These are referred to in Appendix 13.



Graph 10

Altering the water volume flow rate at 105 minutes from start of test from the originally set value of $1.029 \text{ m}^3 \text{ hr}^{-1}$ to $1.10 \text{ m}^3 \text{ hr}^{-1}$ did not significantly affect the rate of temperature rise in the vessel.

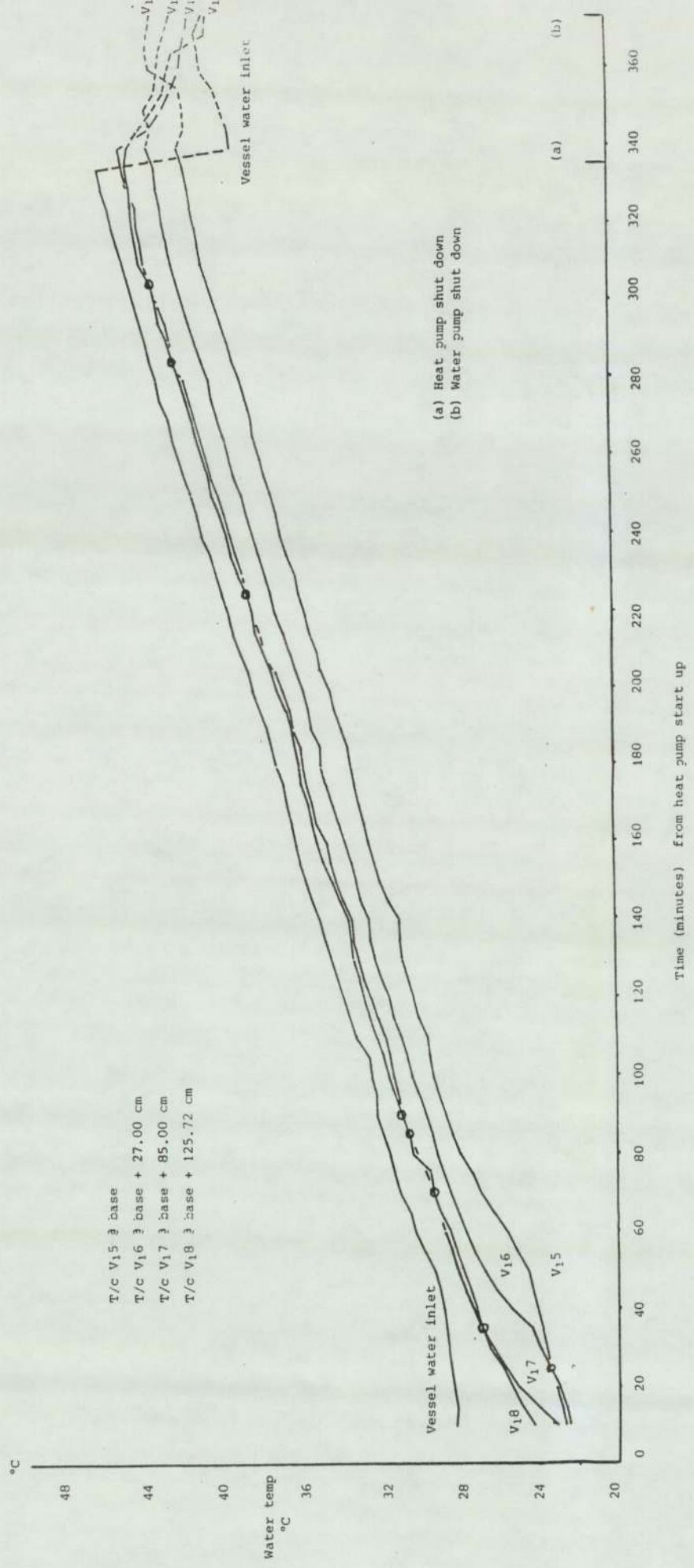
Graph 10 shows the water store temperatures in vessel 1 prior to starting the water pump (at 20 minutes on graph 10) and the heat pump (at 24 minutes). Temperatures recorded up to 17 minutes were scanned at 1 minute intervals. Thereafter the scan was at 5 minute intervals.

Graphs 9 and 10 indicate that the water temperature at thermocouple (t/c) position 8 is invariably lower than that at T/c position 7. This results from the effects of disturbance at the water surface caused by the jet entry effect. Jet entry effects were discussed in Section 3.4.

The t/c scan intervals do not appear to be a critical feature of overall store performance assessment.

The rate of water temperature rise at each t/c position shown on graphs 9 and 10 are basically identical. The initial store temperature does not apparently affect the rate of temperature rise when measured to the degree of accuracy obtainable with the present test equipment.

Store Water Temperature Vessel 1
(fixed thermocouple data;



Graph 11

The tendency for temperatures at positions t/c 5; 6; 7 and 8, on graph 10, not to diverge at the latter stages of the test period suggests that temperature stratification would not occur within the vessel.

Tests of greater duration were therefore conducted to identify likely changes in store behaviour. Graph 11 shows results typical of those obtained from vessel 1 during a test of 330 minutes duration.

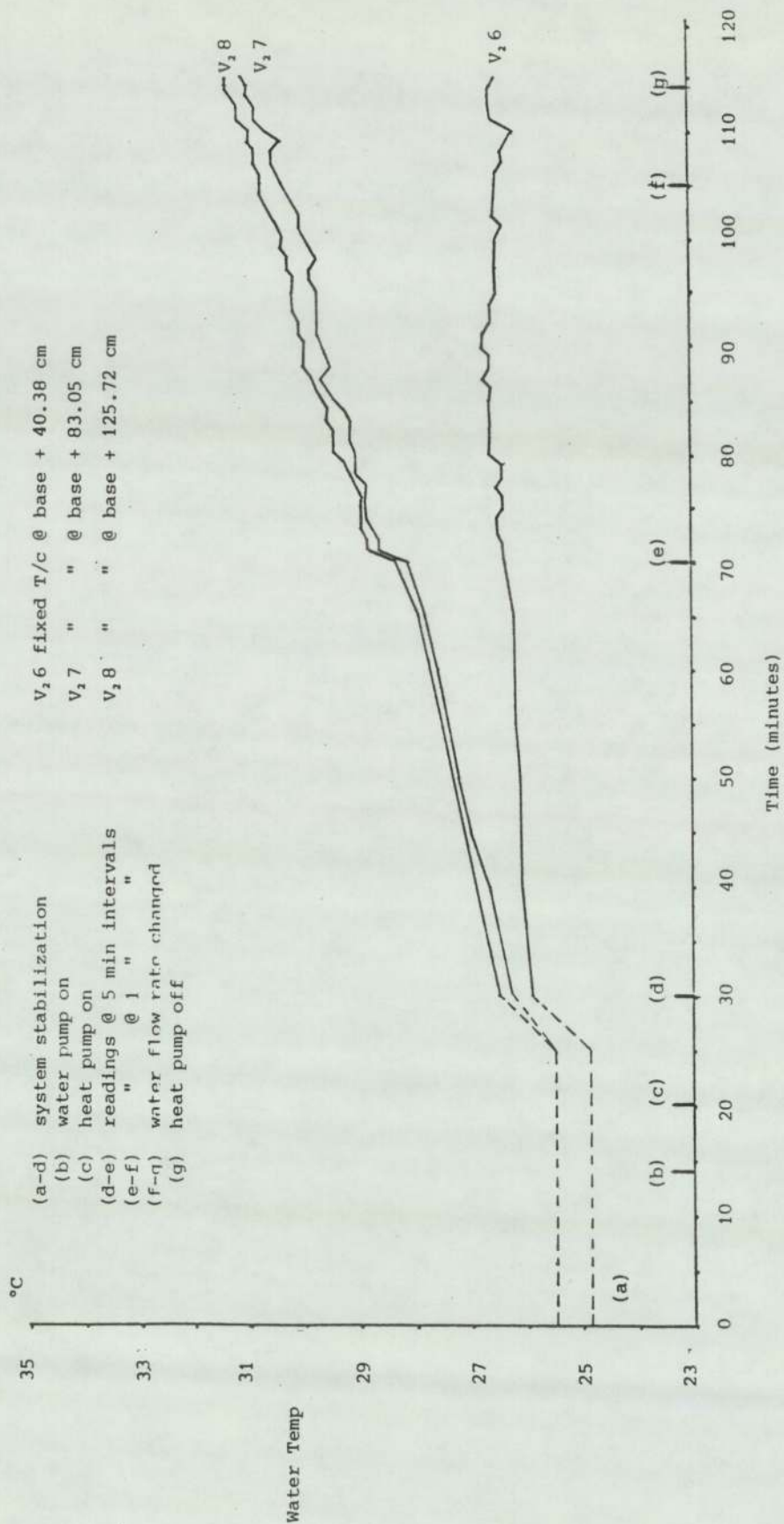
The vessel water inlet temperature (condenser outlet) measurements were monitored by a thermocouple secured externally to the water pipework. The pipework, and therefore the thermocouple, were insulated with a suitable pre-formed insulating material.

With readings recorded at each thermocouple on a 5 minute scan interval there is a tendency, as seen from graphs 9 and 10, to obtain a relatively smooth progressive curve. These particular curves (Graph 11) exhibit similar patterns to those of tests of lesser duration.

At commencement of each heat pump test the store temperature variation throughout the height of the vessel reflects some convection taking place whilst the vessels are not in use - the water at the upper surface being marginally greater than temperatures down the vessel. Vessels constructed of different thermal insulation properties and

Water Store Temperature

Vessel 2 (with diffuser)



Graph 12

sited in different locations would not necessarily exhibit the same degree of initial temperature variances.

Upon commencement of a test (Ref. Graph 11) the temperature at t/c 7 rapidly approaches that recorded at t/c 8. This being affected by jet entry disturbance and possibly due to the sudden change in suction conditions at the base of the vessel. Resulting from data collected during this series of tests the jet entry effect appears to impinge to a point at least 40 cm below the store water surface.

As the test duration progresses so the temperature changes more-or-less uniformly down the vessel. At the point of heat pump shut down the vessel water inlet temperature decreases rapidly. This rate is approximately 7°C in a 5 minute time interval. For the period between heat pump shut down and cessation of the test, during which period the circulating pump was in operation, some temperature equalization throughout the vessel was taking place.

The results presented as graph 12 are those recorded at vessel 2 - the vessel with an entry jet velocity diffuser fitted. These results were recorded during the same test from which graph 9 (for vessel 1) was compiled.

By taking a complete set of data for both vessels during the early series of tests it enabled direct comparisons of internal conditions to be observed. Comparable external conditions also applied to both instances.

The store temperatures recorded at the base of vessel 2, t/c V₂₅, Graph 12 produce meaningless values through either a transient fault in the A-D unit or difficulties with the mains power supply.

A comparison of temperature profiles for vessels 1 and 2 indicates the effectiveness of reduced jet entry velocity on the promotion of temperature stratification.

Over the 114 minute duration of the test represented by Graph 12 the water temperature in the lower band of vessel 2 gained 0.6°C whereas the average final temperature of water in the upper band of the vessel was raised 4.75°C.

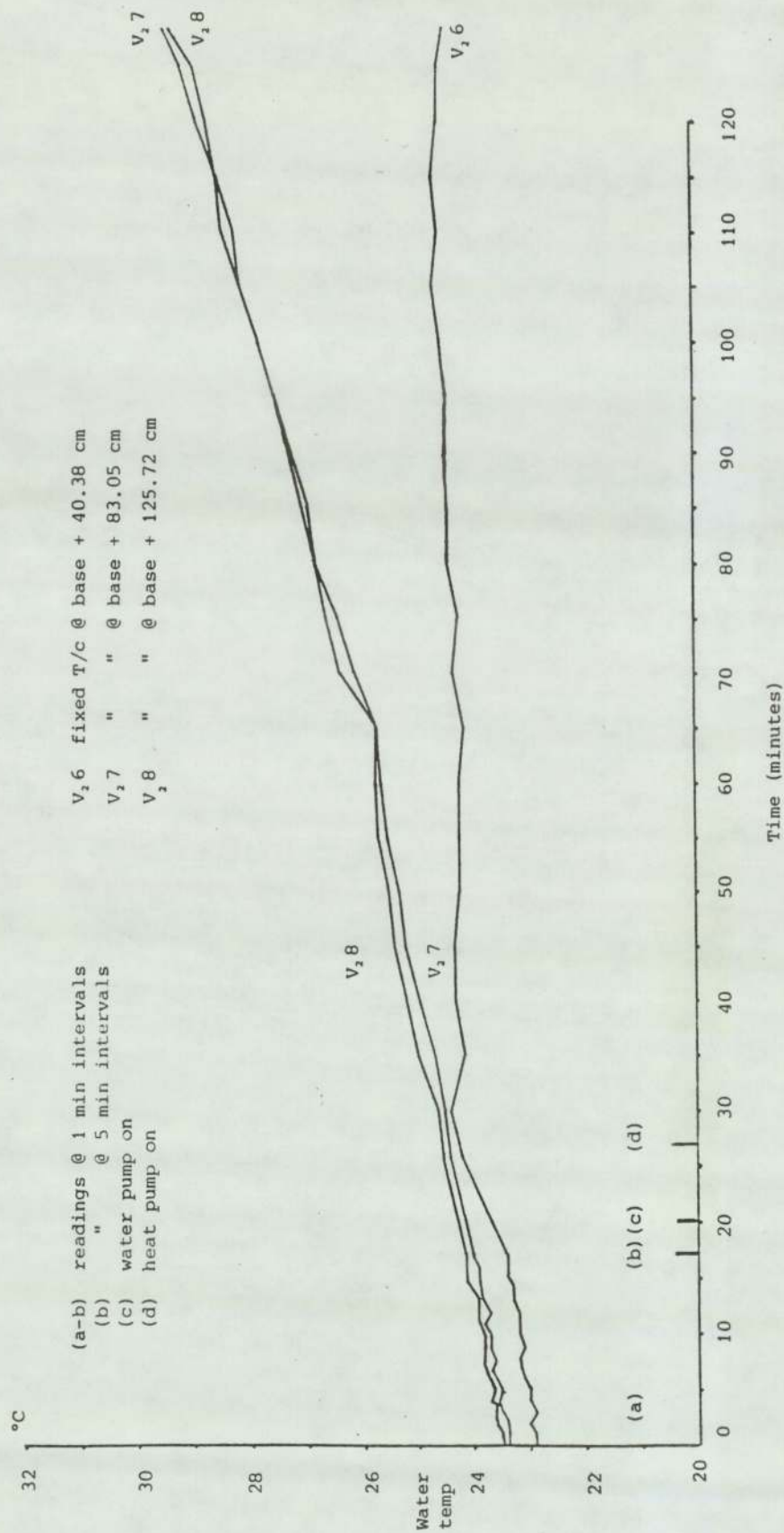
The change in temperature scan times from 5 minutes to 1 minute intervals is again noticeable, i.e. at the 70 minute position, especially in the upper section of the vessel.

The overall rate of change of temperature was however retained.

Water Store Temperature

Vessel 2

(with diffuser)



Graph 13

At position 110 minutes on graph 12, a drop in water temperature at thermocouple position t/c V₂₆ and V₂₇ is clearly defined. A lesser variation in temperature at t/c V₁₅ thermocouple on graph 9 can also be identified.

The reason for such a temperature change is attributed to the heat pump reverting to its timed auto defrost cycle. The effect of this occurrence is reflected to a greater degree in the vessel where stratification is more pronounced - vessel 2.

Graph 13 also reflects the water store temperatures in vessel 2. The test data plotted as graph 13 was recorded during the tests upon which graph 10 is produced. Graph 13 depicts the pattern of store temperature shown in graph 12 but readings in this test were taken at 1 minute intervals for an initial 17 minute period prior to switching the water circulating pump on.

It will be noted from graph 13 that a significant change in temperature at t/c V₂₆ takes place during the first 10 minute period following switch-on of the heat pump. This pattern of change was not experienced during the test from which graph 12 was produced or during the remaining tests of this initial series. The temperature profile for the remaining duration of the test followed identically that of earlier tests.

Tests of extended duration, where the heat pump was in operation for 335 minutes were undertaken. The results of one such test was reproduced as graph 11, discussed earlier, and graph 14.

When comparing graph 14 with graphs 12 and 13 it will be noted that different patterns of store temperature exists.

The variation of temperature at t/c V₂₆ (graph 14) after 95 minutes heat pump operation is + 4.5°C whereas in previous tests discussed, namely those from which graphs 12 and 13 have been reproduced, the temperature at t/c V₂₆ did not rise after 95 minutes heat pump operation.

The major difference in test conditions between the two tests referred to is the volume flow rate of water through the system.

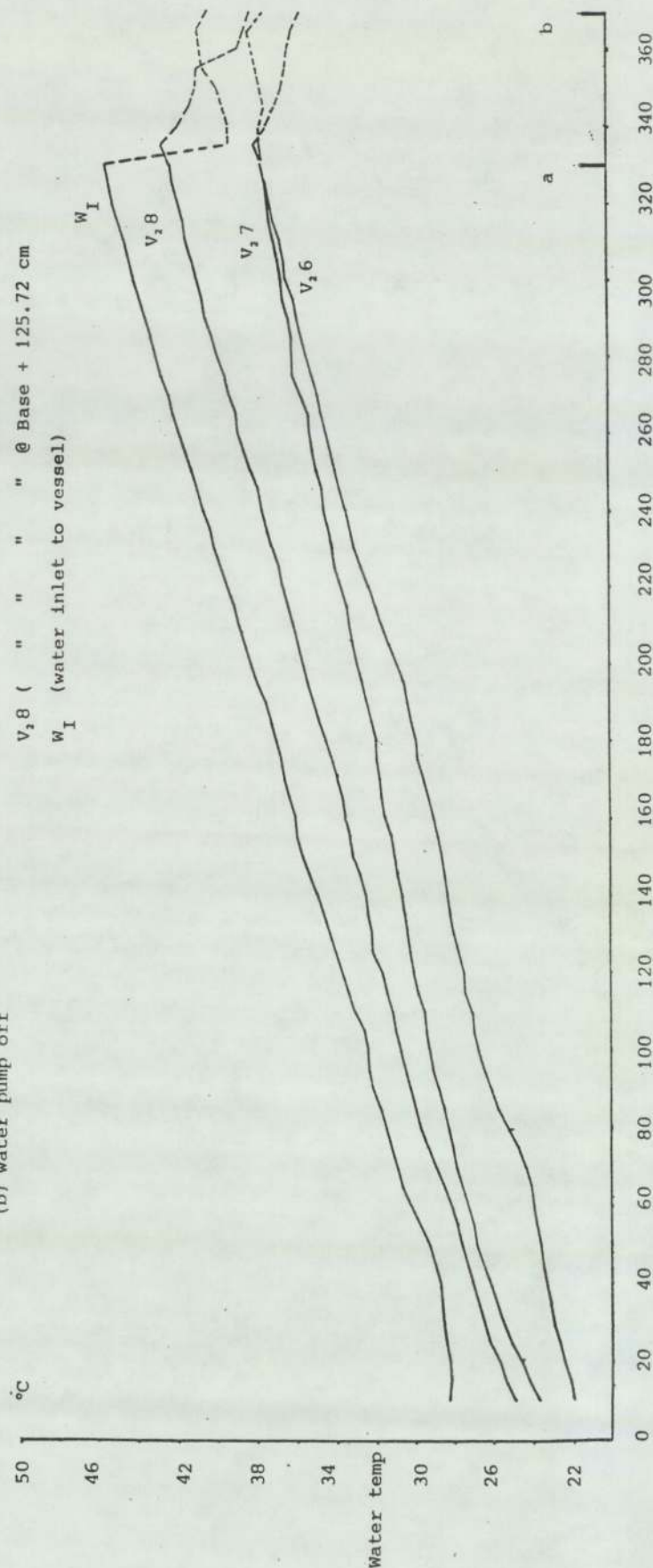
For tests from which the data for graphs 12 and 13 was compiled the water volume flow rate was 1.0295 m³ hr⁻¹ and 1.0817 m³ hr⁻¹ respectively whilst for the test upon which graph 14 was based the water volume flow rate was 0.8912 m³ hr⁻¹.

Water Store Temperature

Vessel No. 2 (with diffuser)

Readings at 5 min intervals
(a) heat pump off
(b) water pump off

V₂6 (Vessel 2, fixed T/c @ Base + 40.38 cm)
V₂7 (" " " @ Base + 83.05 cm)
V₂8 (" " " @ Base + 125.72 cm)
W_I (water inlet to vessel)



Time (minutes) - from heat pump start

Graph 14

Reference to Graph 14 suggests that for tests of duration greater than approximately 5 hours the temperature distribution changes significantly. During this period the apparent stratification patterns change from an initial 3 band, or node, to two distinctive bands.

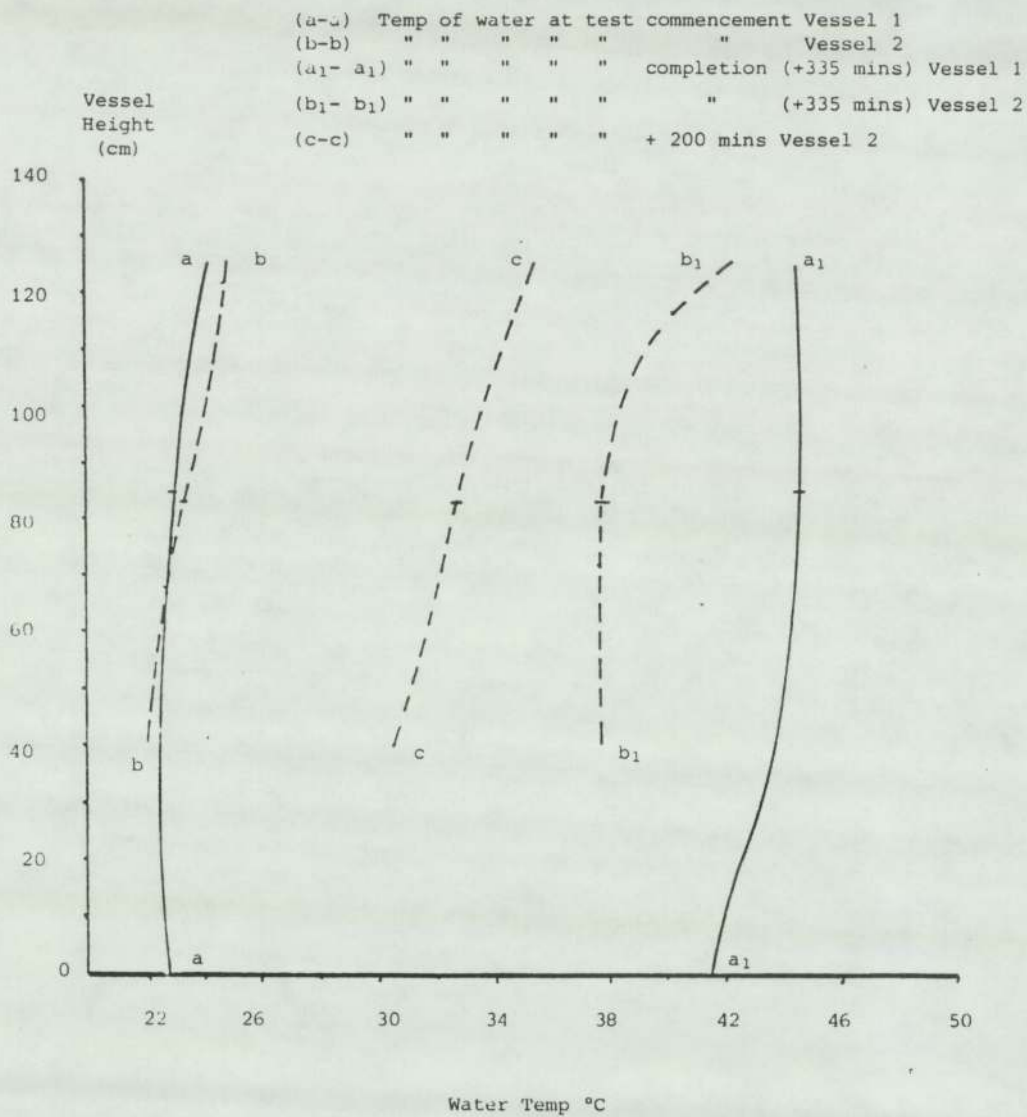
A greater number of fixed position T/c would provide a more conclusive pattern of behaviour with respect to the band thicknesses.

As the rate of temperature rise at fixed T/c 7 reduces, whilst that of T/c 6 (lower down the wall) increases, with respect to time, it indicates that the incoming heated water commences to have an effect at the greater depths as the test progresses.

This condition is not necessarily brought about as a direct consequence of the pump suction effect on the base of the vessel otherwise the base temperature would also be expected to show signs of increase at a similar rate.

Graph 15 presents, in a different format, one of the test results previously plotted as graphs 9 to 14 inclusive. This reflects the depth-wise distribution of temperature achieved in each vessel. To ensure that the results are comparable both vessels were in the test circuit thereby receiving identical inlet water conditions.

Depthwise Temperature
Distribution of Water (Vessels 1 & 2 - Fixed T/c's)



Graph 15

Curves "a" and "a₁" reflect the changed conditions in Vessel 1 - without a velocity diffuser installed - over a test period of 335 minutes.

The temperature of the store water at the fixed thermocouple positions of base, base + 27 cm, base + 85 cm and base + 125.72 cm, are shown as curves "a" and "a₁" .

At the commencement of the test the water temperatures at Vessel 1 were:

base	22.7°C
base + 27 cm	22.5°C
base + 85 cm	23.0°C
base + 125.72 cm	24.3°C

giving a variation from top to bottom of + 1.6°C.

At the conclusion of the test the water temperatures at Vessel 1 were:

base	41.5°C
base + 27 cm	43.0°C
base + 85 cm	44.6°C
base + 125.72 cm	44.5°C

giving a variation from bottom to top of + 3°C, and raised temperatures at each of the fixed thermocouple positions of:

base	+ 18.8°C	after 335 minutes operation				
base + 27 cm	+ 20.5°C	"	"	"	"	"
base + 85 cm	+ 21.6°C	"	"	"	"	"
base + 125.72 cm	+ 20.2°C	"	"	"	"	"

Similarly the variations experienced at Vessel 2, under the same operating conditions prevailing for Vessel 1, are shown on Graph 15 as curves "b" and "b₁" .

At the commencement of the test the water temperatures at Vessel 2 were:

base	unreliable data
base + 40.38 cm	22.0°C
base + 83.05 cm	23.3°C
base + 125.72 cm	24.9°C

At the conclusion of the test the water temperatures at Vessel 2 were:

base	unreliable data
base + 40.38 cm	37.7°C
base + 83.05 cm	37.7°C
base + 125.72 cm	42.4°C

The temperature change at each fixed thermocouple position was:

base + 40.38 cm	+ 15.7°C	after 335 minutes operation
base + 83.05 cm	+ 14.4°C	" " " "
base + 125.72 cm	+ 17.5°C	" " " "

A comparison of the above tabulated data recorded at Vessels 1 and 2, curves a - a₁ and b - b₁ respectively on graph 15, would indicate that, from basically similar store conditions at the commencement of the test, noticeable changes in temperature occurs throughout the test.

Whilst the major changes are taking place in the upper region of the stores, Vessel 1 shows a more uniformly changing condition occurs throughout the vessel height whereas in Vessel 2 the temperature profile changes in a non-uniform manner. From further analysis of the test results it was found that a greater amount of energy is stored in vessel 1 over a time period, albeit at a lower average temperature, than is stored in Vessel 2.

These differing conditions could result from a number of factors. For example, the volume water flow through each vessel could be slightly different even though the water temperature entering the vessels would be identical. Also, on the basis of the theory of heat transfer mechanisms discussed in Sections 3.3, 3.4 and 3.5 it is concluded that the rate of heat transfer in each vessel is influenced by the entry jet velocity conditions.

The volume of water to be heated in each of the three band or nodal regions does not differ sufficiently to have an influence on temperature changes. The volume of water stored in the upper nodal regions, i.e. between thermo-

couples at 85 cm and 125.72 cm (Vessel 1) and thermocouples at 83.05 cm and 125.72 cm (Vessel 2) is sufficiently similar to have no major influence on the different temperature profiles experienced in this region.

In the central nodal region, between thermocouples at 27 cm and 85 cm (Vessel 1) and those at 40.38 cm and 83.05 cm (Vessel 2) the volume of stored water is $.475 \text{ m}^3$ and $.355 \text{ m}^3$ respectively.

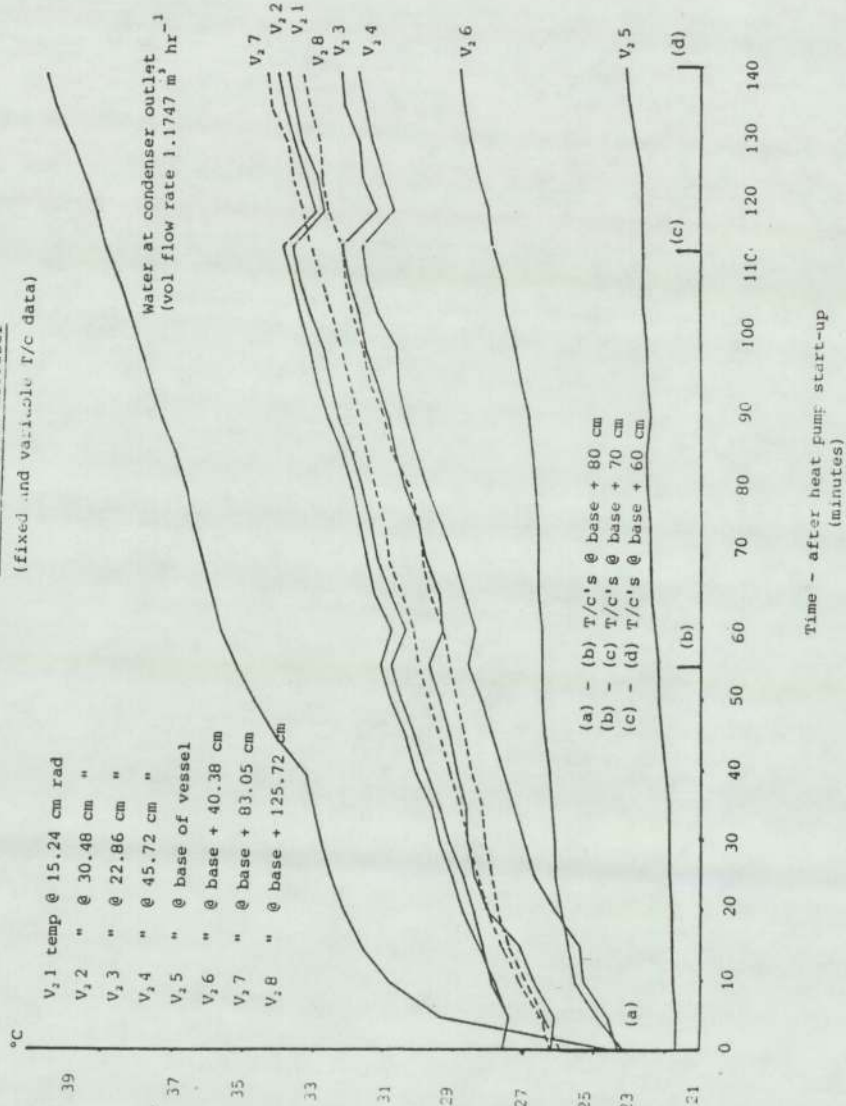
The variation in volume of stored water in the third and lower nodal region is $.135 \text{ m}^3$ in Vessel 1 and $.235 \text{ m}^3$ in Vessel 2.

4.7.2 Variable Position Thermocouples

A series of tests were conducted for identifying patterns of temperature variation along a horizontal plane at various vertical positions within the store. As previously described a specially designed thermocouple carrier was constructed and located in the vessel as shown in Figure 18.

Each carrier ultimately supported five thermocouples bonded to the extension arm as:

Water Store Temperature
Vessel 2 - with diffuser
 (fixed and variable T/c data)



Graph 16

Vessel 1 T/c 1 @ 7.62 cm radius
 T/c 2 @ 30.48 cm "
 T/c 3 @ 15.24 cm "
 T/c 4 @ 38.10 cm "
 T/c 5 @ central position.

Vessel 2 T/c 1 @ 15.24 cm radius
 T/c 2 @ 30.48 cm "
 T/c 3 @ 22.86 cm "
 T/c 4 @ 45.72 cm "
 T/c 5 @ central position.

Radial locations of T/c's 1-4 inclusive in each vessel could be varied within the physical limits of each vessel. The chosen radii are selectable only between test runs, that is, when the vessels were drained of water.

The vertical positions of the T/c's was however totally variable and capable of being repositioned at anytime during a test run.

The results shown as graph 16 depict typical radial temperature variations experienced in Vessel 2. The readings being taken at three different heights within the vessel and in the same spatial position.

Readings plotted as graph 16 were those recorded consecutively during a test, i.e. the T/c carrier height being adjusted during the course of the test. A discussion on the implications of this manoeuvre is referred to later (see page 222).

Four different radial positions were employed at each of the three chosen heights, these radial positions being set prior to commencement of the tests. Readings taken at the fixed T/c positions during the test have also been included on graph 16 for comparison purposes.

Reference again to graph 16 shows that measurements were recorded initially at a height of + 80 cm, which is within 3 cm of fixed T/c 7.

Examination of the spread of temperature across the vessel diameter shows that at the two "inner" radii (curves 2.1 and 2.3), irrespective of vertical position, the temperatures remain in close proximity. At the two "outer" radii (curves 2.2 and 2.4) there are noticeably larger differences in recorded values. These two latter readings are consistently the maximum and minimum radial temperatures recorded.

Temperature distributions at the radial positions 2.2 and 2.4 remain relatively constant at each of the chosen heights whereas the temperature change between positions 2.1 and 2.4 varies with a change in vertical position.

Temperatures at 2.4 and 2.1 show a converging trend as the distance from the jet inlet increases. A similar temperature trend occurs at T/c positions 2.3 and 2.4. This condition may result from a more uniform water flow velocity distribution across the vessel diameter.

Again, from reference to graph 16, it will be noted that the rate of change of temperature at T/c positions 2.6 and 2.5, after approximately 85 minutes and 125 minutes respectively, is approaching the rate of temperature change at radial positions 2.1 - 2.4 inclusive for a vertical height of 60 cm. This suggests that an increase in stratification band thickness is developing.

Also included in Graph 16 is an indication of the average hourly rate of water temperature rise in the store at heights through the vessel.

An examination of the test data upon which Graph 16 is produced shows that for a water volume flow rate of $1.1747 \text{ m}^3 \text{ hr}^{-1}$ the water temperature rise (Δt) across the condenser was:

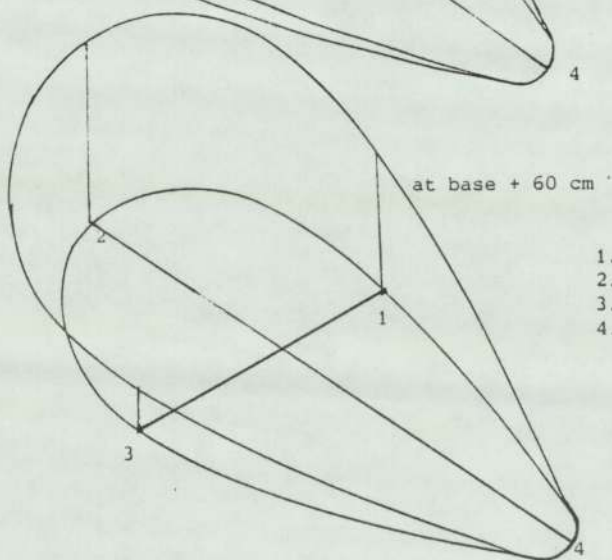
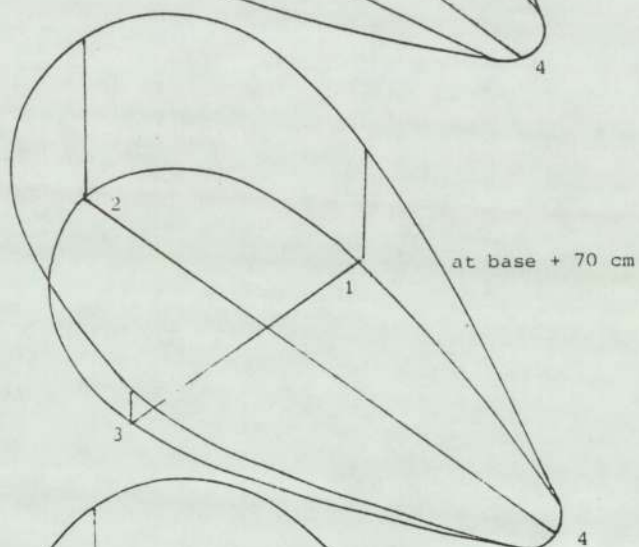
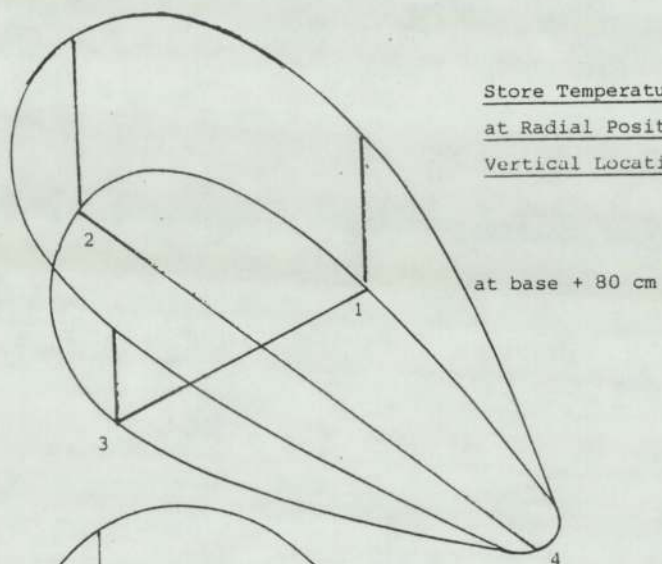
after 10 minutes heat pump operation $\Delta t = 6.0^\circ\text{C}$

" 50 " " " " $\Delta t = 7.6^\circ\text{C}$

" 150 " " " " $\Delta t = 8.6^\circ\text{C}$

which compares favourably with the data in Section 4.2.

Store Temperature Variations
at Radial Positions and Three
Vertical Locations (Vessel 2)



- 1. T/c @ 15.24 cm radius
- 2. T/c @ 30.48 cm "
- 3. T/c @ 22.86 cm "
- 4. T/c @ 45.72 cm "

(drawn to scale)

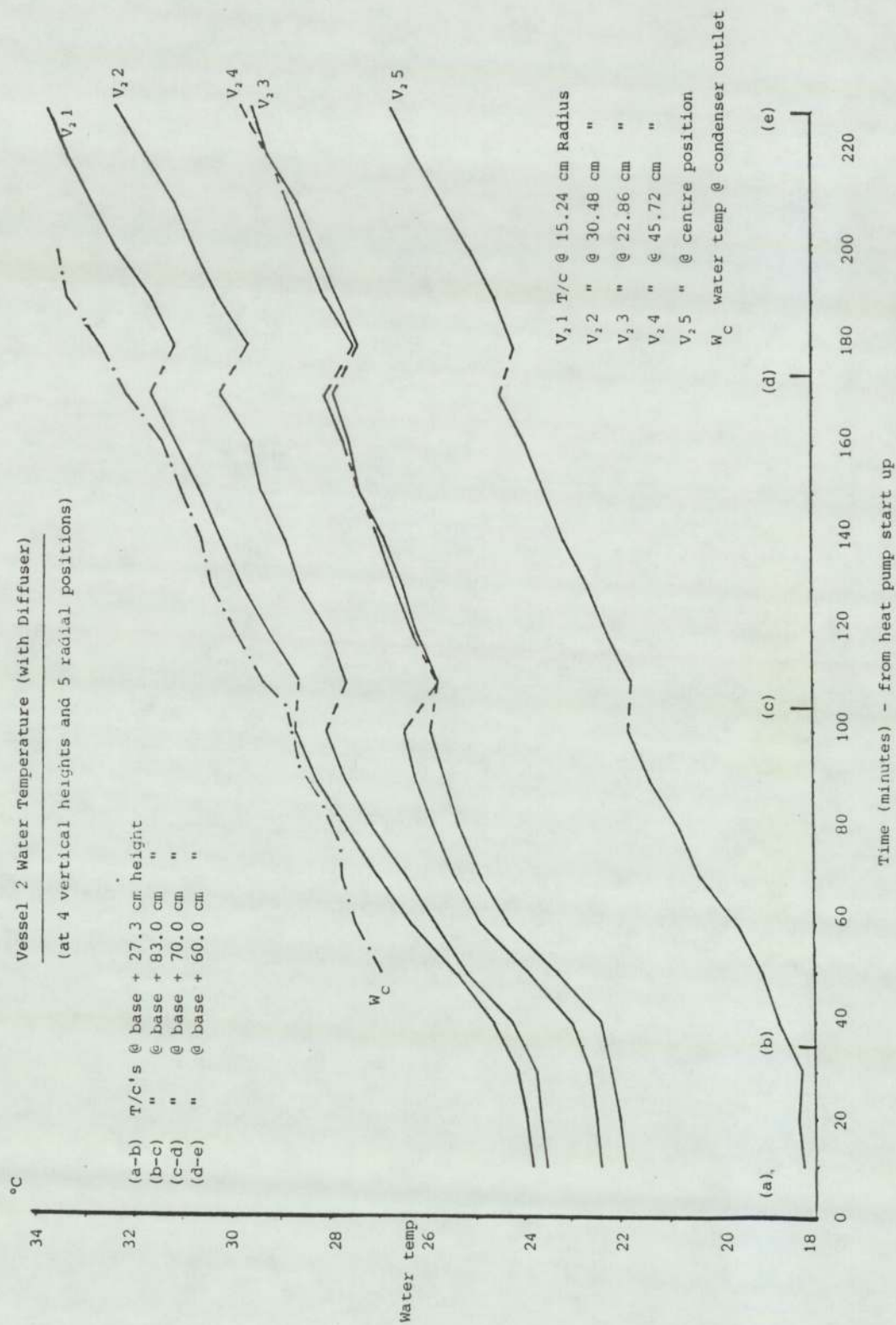
Graphs 17 is a reproduction of the radial temperature distribution used for constructing graph 16. Radial position T/c 4, being consistently the lower reading of T/c's 1-4 inclusive, represents the "reference" point on graph 17.

The remaining temperatures are plotted vertically to scale at their respective radii and at their actual spatial displacement from each other.

The differing interpretation of profiles at each T/c carrier height is quite apparent.

4.7.3 Temperature Distribution along Horizontal Plane (Radial Distribution)

A further series of tests were conducted on Vessel 2 (where stratification was more apparent), for establishing a range of "relation curves" for forming the basis of a mathematical model for use in predicting the temperature of water in the store, at any selectable vertical height and after a defined period of heat pump operation.



Graph 18

In order to reduce test result inconsistencies, several vertical positions were monitored during each test. Inconsistencies were possible as a result of such features as differences in initial stored water temperature, ambient conditions at the time of a test and from a change in the volume flow rate of water.

Earlier series of tests had, however, indicated that these inconsistencies were not sufficiently significant so as to greatly distort the results obtained.

From tests undertaken some typical results are presented and discussed below. A summary of conditions prevailing during a typical test are included as Appendix 9.

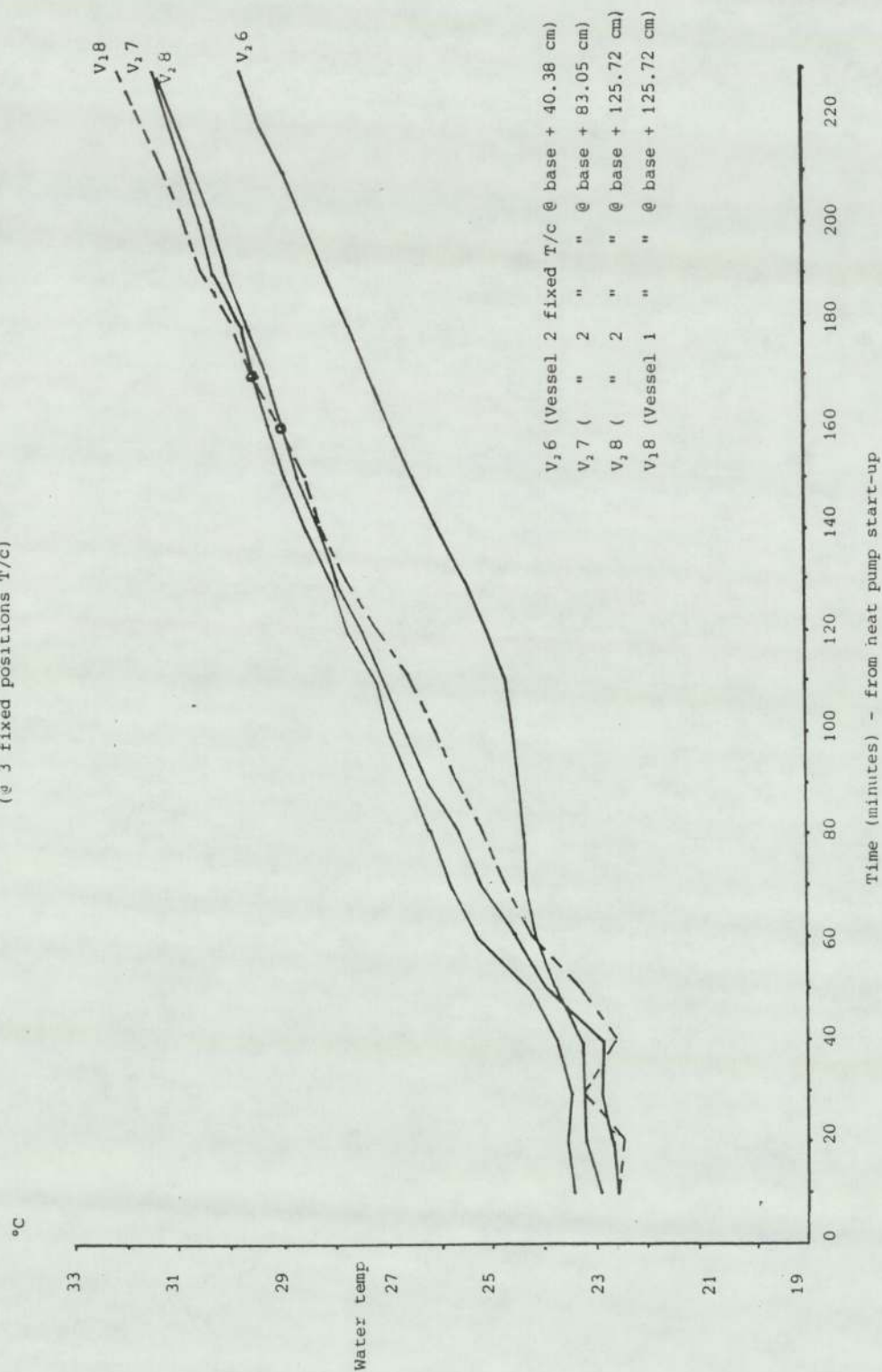
Graphical presentations of some results are included as graphs 18 - 24 inclusive.

An additional thermocouple, T/c 2.5, had been attached for these tests. This is located centrally on the carrier.

Graph 18 shows the temperature distribution at four distinct vertical positions of the T/c carrier.

From the five radial measurements, these average T/c readings were selected for further examination and form the basis of the model development.

Vessel 2 Water Temperature (with diffuser)
(@ 3 fixed positions T/c)



Graph 19

The average readings were selected because they are considered most representative of typical test conditions at the respective heights.

Each series of average recorded data at the respective vertical positions has been projected using a straight line approach to represent the likely trend of temperature change over a full test duration.

The straight line approach has been assumed acceptable based on the findings of earlier tests. Typical of such tests were used to reproduce graphs 9 - 14 inclusive.

A similar extrapolation approach to that employed above applied to the actual data recorded at thermocouples V2.1 (15.24 cm radius) V2.2 (30.48 cm radius), V2.3 (22.86 cm radius), V2.4 (45.72 cm radius) and V2.5, the thermocouple placed centrally, would provide for a full suite of curves typifying the conditions experienced in the store.

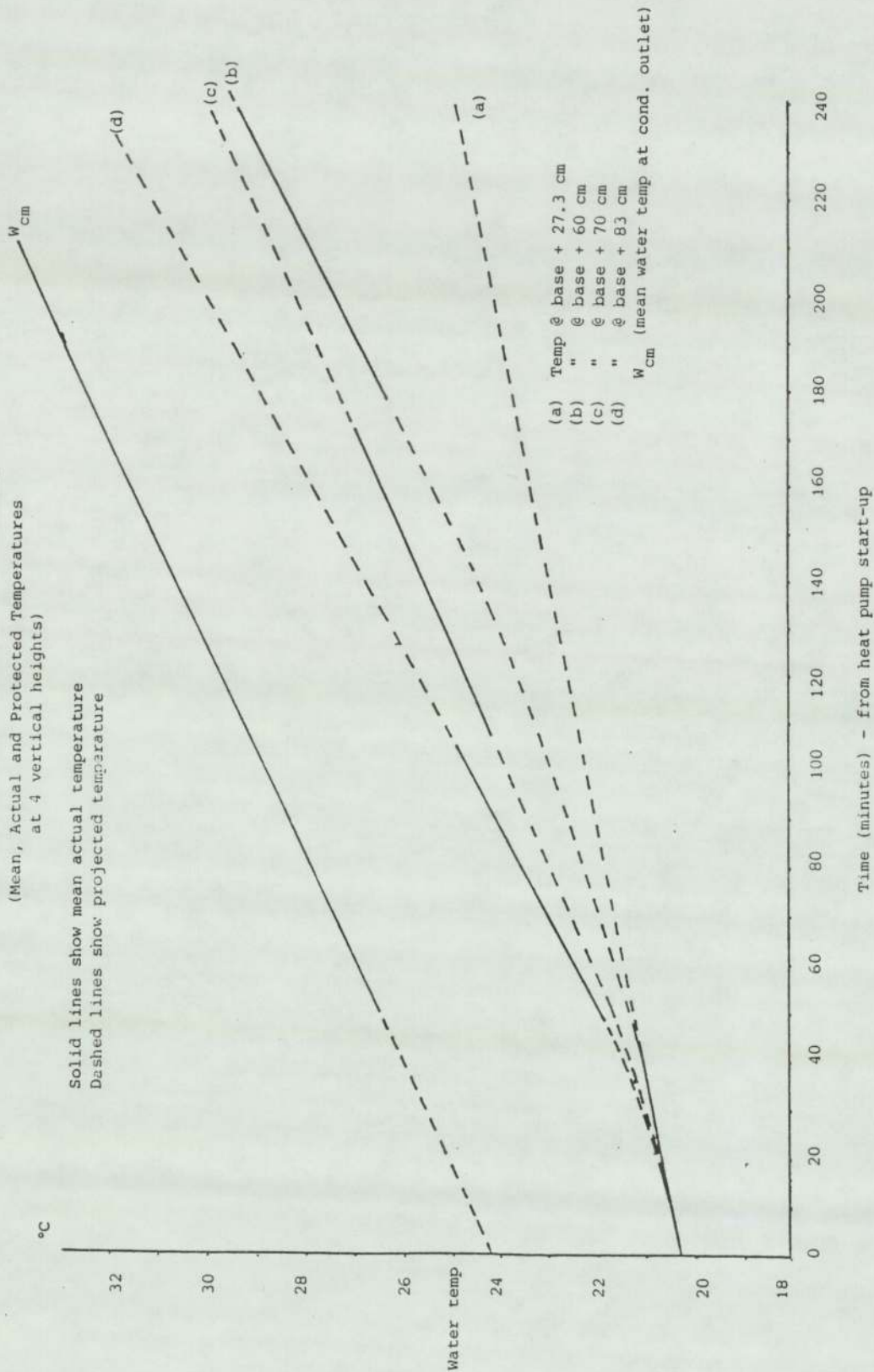
Graph 19 shows the temperature profiles at the fixed thermocouple positions in Vessel 2 recorded during the test which Graph 18 represents.

Being located at the fluid/vessel interface, i.e. at the extreme radius of the vessel these thermocouple readings, along with those from the variable height T/c's

Vessel 2 Water Temperature (with diffuser)

(Mean, Actual and Protected Temperatures
at 4 vertical heights)

Solid lines show mean actual temperature
Dashed lines show projected temperature



Graph 20

provide a view of the temperature profile fully across a horizontal plane in the vessel.

The temperatures recorded at radial positions T/c 1-5 inclusive were used to determine a typical numerical average value for temperature on the horizontal plane at each of the four vertical heights identified above. These values, included as Table 4, form the basis for the curves shown as graph 20.

An "average value" curve has been presented so that clarity in presentation can be achieved. In practice a family of curves would be required for portraying temperature distribution throughout the vessels.

The curves referred to as (+70) and (+60) on graph 20 exhibit a condition which is discussed further on page 296.

Graph 21 is a further representation of the values used for constructing graph 18. This graph, as with graph 22, highlights the variation in temperature across the horizontal plane at selected vertical positions in Vessel 2. The points on the curves denoted by the encircled T/c number at the base of the graphs are actual recorded temperatures, whilst the remaining points speculate on the likely "mirror" image that could be taking place if the flow velocity through the vessel followed the profiles presented in section 3.4.2.

Table 4

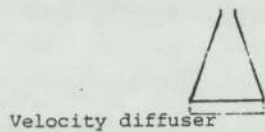
Test Data showing averaged store temperature
used for compiling Graph 20

T/c position (cm radius)		T/c carrier height 27.3 cm		
1 @ 15.24		23.8	23.9	24.1
2 @ 30.48		23.5	23.6	23.7
3 @ 22.86		22.4	22.5	22.6
4 @ 45.72		21.9	22.0	22.2
5 @ centre		18.3	18.4	18.3
	average 20.6	20.7	20.73	

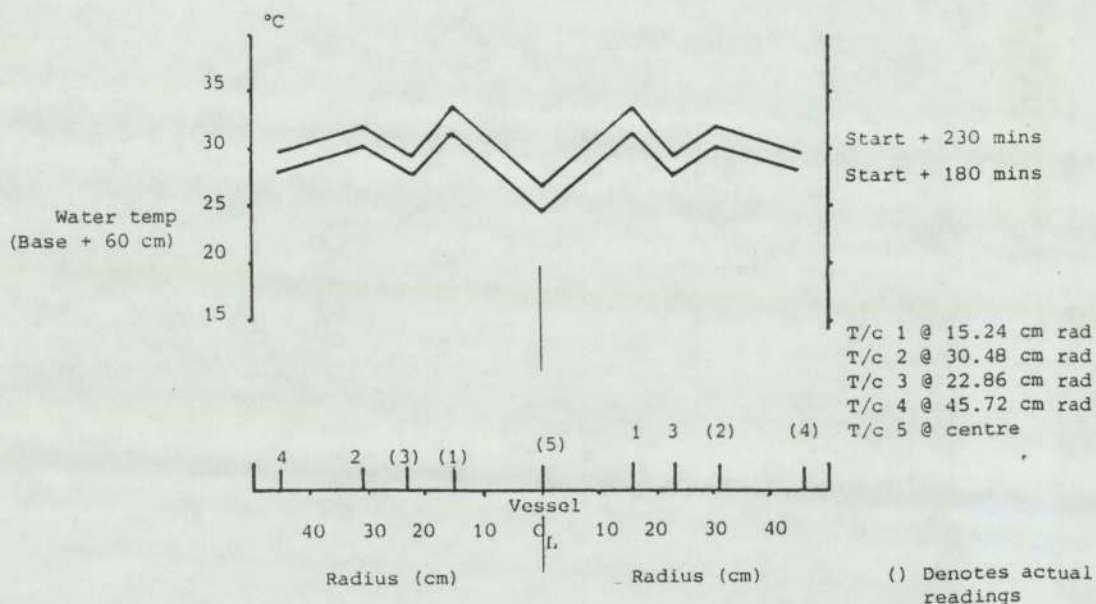
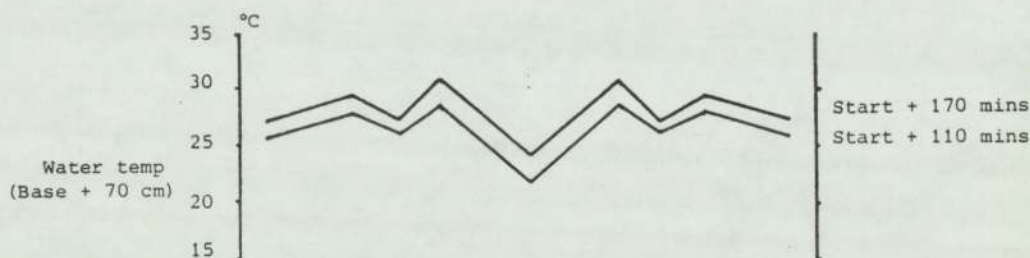
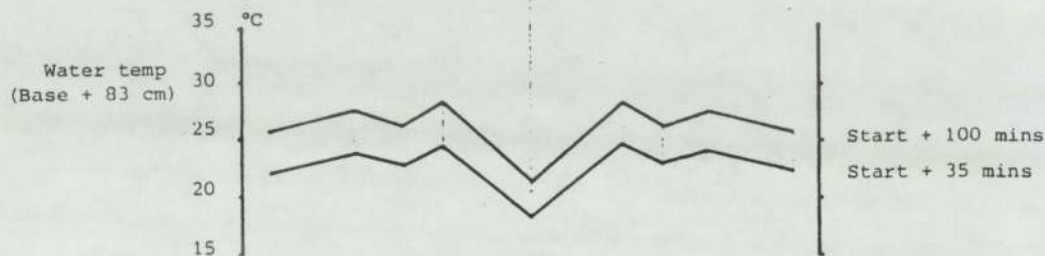
T/c carrier height 83 cm							
1 @ 15.24	24.6	25.4	26.3	27.0	27.6	28.2	28.6
2 @ 30.48	24.2	25.2	25.8	26.4	27.1	27.6	28.0
3 @ 22.86	23.0	23.9	24.9	25.4	25.8	26.2	26.4
4 @ 45.72	22.4	23.3	24.3	24.9	25.3	25.6	25.9
5 @ centre	18.8	19.1	19.6	20.4	20.8	21.4	21.8
average	21.18	21.78	22.47	23.17	23.63	24.15	24.52

		T/c carrier height 70 cm					
1 @ 15.24		28.5	29.1	29.7	30.1	30.5	31.0
2 @ 30.48		27.6	27.9	28.5	28.8	29.3	29.5
3 @ 22.86		25.7	26.2	26.6	26.9	27.3	27.6
4 @ 45.72		25.7	26.1	26.4	26.8	27.3	27.5
5 @ centre		21.7	22.2	22.6	23.1	23.5	23.9
	average	24.29	24.77	25.2	25.63	26.05	26.4

T/c carrier height 60 cm							
1 @ 15.24	31.0	31.5	32.2	32.7	33.2	33.6	
2 @ 30.48	29.5	30.1	30.6	31.0	31.5	32.2	
3 @ 22.86	27.4	28.0	28.4	28.7	29.1	29.6	
4 @ 45.72	27.3	27.7	28.1	28.5	29.1	29.4	
5 @ centre	24.1	24.5	25.0	25.6	26.1	26.6	
average	26.45	26.92	27.42	27.91	28.42	28.9	



Temperature Distribution
on Horizontal Plane at
Three Vertical Heights
(Vessel 2)

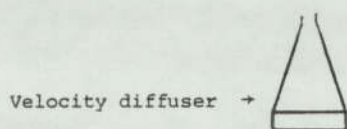


Graph 21

The time period over which readings were monitored is stated on the extreme right of the curves. On graph 21, for example, readings commenced at the 83 cm vertical height after 35 minutes from heat pump start-up. Readings commenced following a 35 minute settling down period because, as experienced in the earlier series of tests, those upon which graphs 9 - 14 inclusive, after 35 minutes of heat pump operation definite patterns of stratification were being exhibited within the vessel (Vessel 2).

This degree of stabilization would, it is assessed, also be taking place in the velocity profile and therefore makes the prospects of achieving a "mirror image" more likely. After 100 minutes from start-up the thermocouple carrier was moved and relocated at 70 cm height. Readings commenced again at 110 minutes and held for a further 60 minutes during which time the store temperature rose by approximately 1.5°C (cf approximately 3.5°C over 65 minute period at the higher thermocouple position of 83 cm).

Direct comparisons between the rates of temperature change at each thermocouple height are difficult to qualify as the readings have, through necessity, been recorded at consecutive intervals of time rather than as a set of concurrent readings.

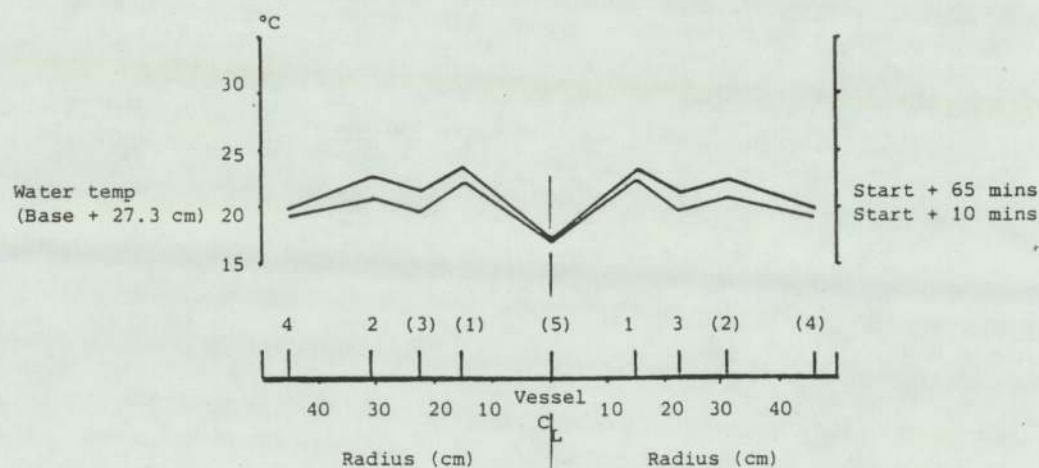
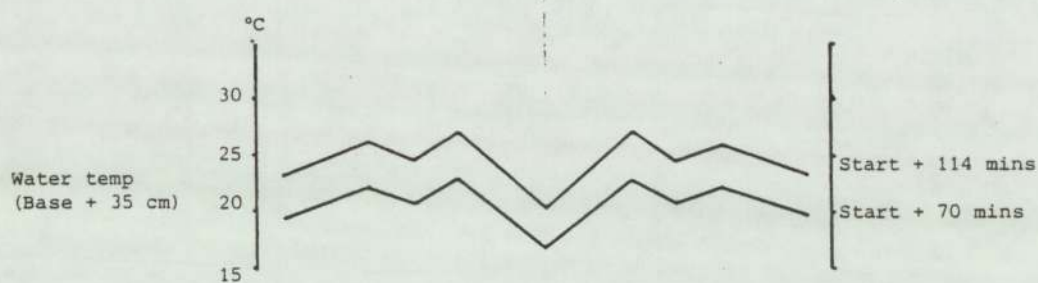


Temperature Distribution
on Horizontal Plane at
Two Vertical Heights

(Vessel 2)

T/c 1 @ 15.24 cm rad
T/c 2 @ 30.48 cm "
T/c 3 @ 22.86 cm "
T/c 4 @ 45.72 cm "
T/c 5 @ centre

() denotes actual readings



Graph 22

Consecutive readings of water temperature are subjected to changes in heat transfer rate brought about by the continually changing bulk water temperature which in turn changes the condenser inlet temperature. This is a direct result of operating a store in a closed loop system and having restrictions on the number of data recording positions available at any one time.

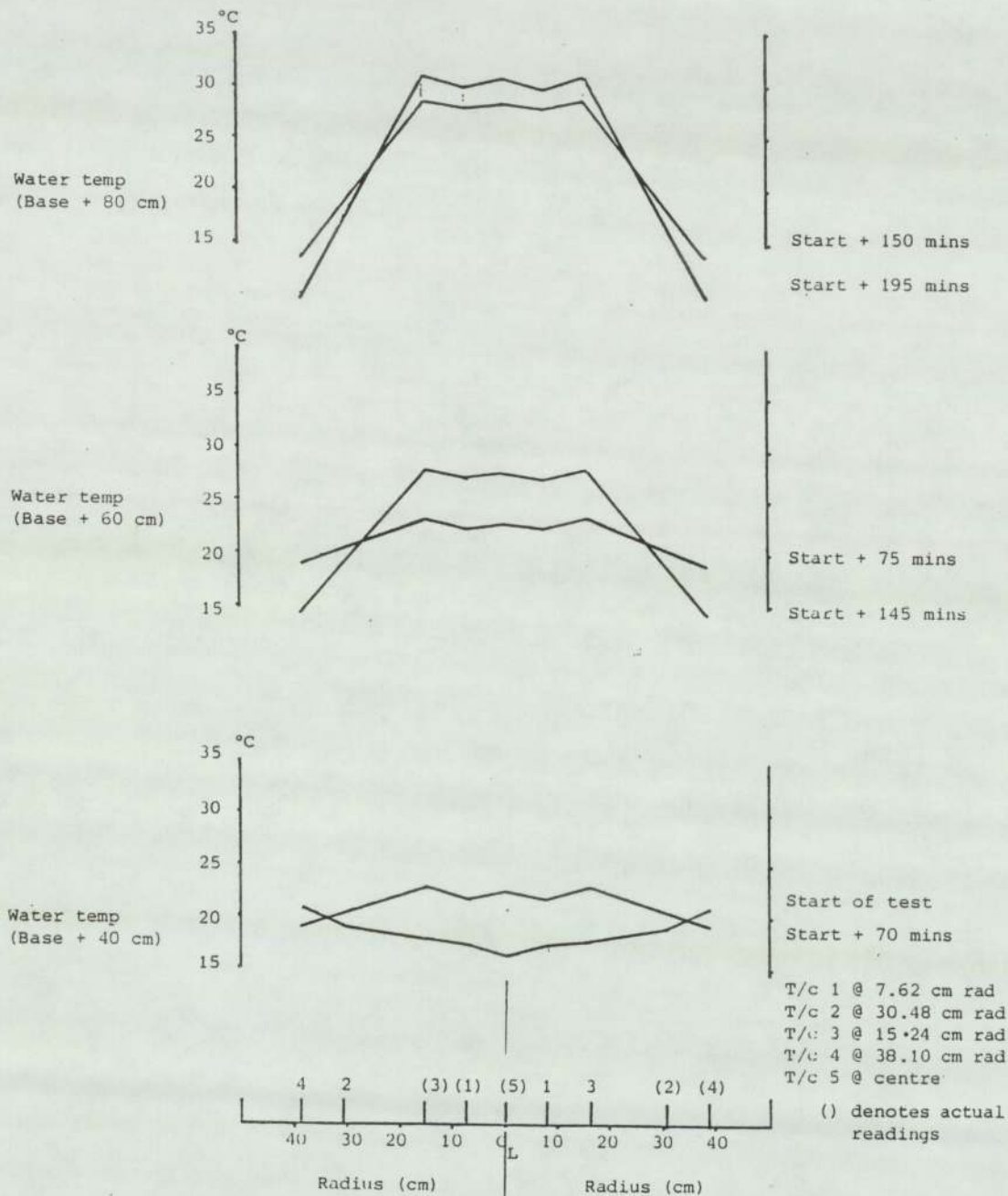
Graph 22 shows the results of a further series of tests where test conditions (ambient temperature, water flow rates etc) differed from those experienced during tests from which graph 21 was produced.

Having established that the pattern of store behaviour in Vessel 2 remained consistent under differing test conditions, similar tests were undertaken on vessel 1. Graph 23 reflects the results of typical tests on Vessel 1. The plotted values on graph 23 at each of the three vertical positions represents the readings taken at the time intervals shown and at the respective heights.

An examination of graphs 21 and 22, and graph 23 (Vessels 2 and 1 respectively) indicates the difference in the pattern of radial temperature distribution in the respective vessels. These differences are discussed later on page 224 and page 251.

Temperature Distribution on
Horizontal Plane at three
Vertical Heights

(Vessel 1)



Graph 23

The differences in values and distribution patterns of store water temperatures between each vessel results mainly from:

- (a) differences in the initial stored water temperature prior to commencement of each test resulting from the physical location of the vessels in the laboratory.
- (b) the different heat input rates, hence heat transfer rates to the stored water resulting from different conditions prevailing internally to each vessel.
- (c) the duration of each test run.

The difference in temperature profiles across the horizontal plane within each vessel would appear to be a direct result of the water entry conditions at the top of the vessels. Graph 23 shows that for the initial 70 minutes of the tests, when the T/c carrier was at "base + 40 cm" height, an increase of approximately 5.5°C in water temperature was experienced in the central core area of the store. Little change in temperature was noted at the water/vessel surface interface between start and finish reading.

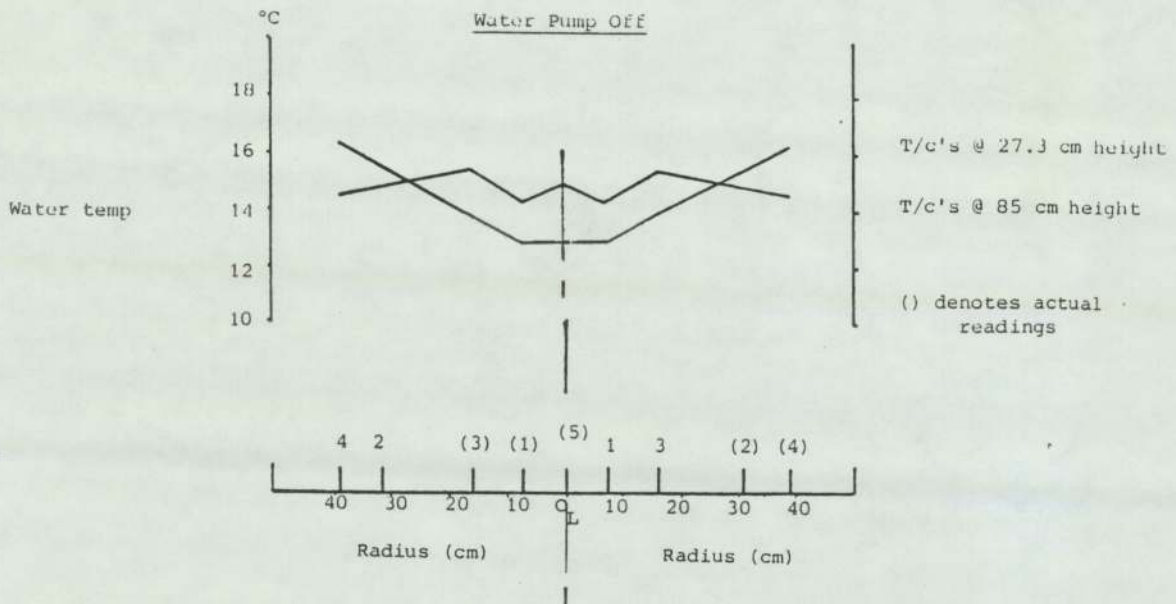
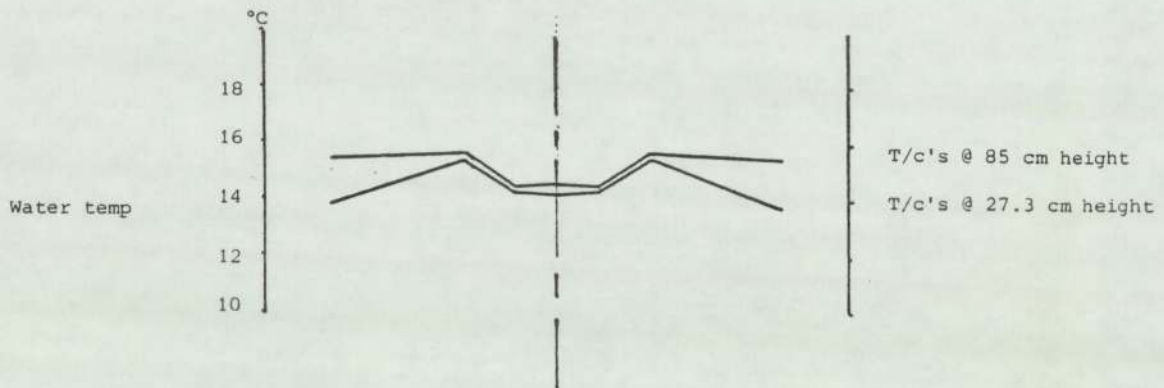
At the intermediate height of +60 cm, monitored again over a 70 minute period immediately following the period at + 40 cm, a significant change in radial temperature distribution was discernable. Again, an increased temperature of approximately 5.5°C was experienced in the central core region over the 70 minute period whilst the temperature at the outer radii shows a much reduced value from the "mean" of the readings in the central area.

The difference being in the order of 7.5°C for "mean centre" readings to "mean outer" reading. The variation in central core temperature over the period of 45 minutes, when the T/c carrier was located at + 80 cm, is considerably less than experienced at the previous heights. However, the time interval between start and finish readings was also less by 25 minutes.

Temperature variation at this height, in the central core, was approximately 2.5°C ; at the outer radii a difference of approximately 15°C was recorded. (Some doubt exists on authenticity of the latter readings but no apparent fault was found to exist on either the T/c's or on the recording instrument when subsequently recalibrated). The occurrence may be attributed to interference on the mains power supply.

Temperature Distribution on
Horizontal Plane at two
Vertical Heights
 (Vessel 1)

Water Pump in Service



Graph 24

As suggested earlier a noticeable change in the pattern of radial temperature distribution exists between Vessels 1 and 2. In order to identify likely reasons for such conditions a further series of tests were conducted. The results of these tests are shown as graph 24. Both vessels remained in circuit but the majority of readings were monitored at Vessel 1. A series of radial position readings were taken at vertical heights of + 80 cm and + 27.3 cm.

Reference to graph 24, lower curves, shows that some variations in store temperature exists under non-circulating conditions. Reference to the upper curve (graph 24) shows, with the water pump operating and heat pump off, that a noticeable difference in radial temperature distribution is experienced compared to that distribution resulting from a non-circulation condition.

Examination of the curves for graphs 21 - 23 inclusive also suggests that the pump suction may be having minor effects on temperature distribution in the early stages of a test but these effects are consistent to both vessels.

Referring to graph 25 and to Appendix 10 it will be noted that a similar pattern of store temperature emerges to that shown as graph 18 - (for tests where operating conditions are different - see Appendix 9 and 10).

Vessel 2 Water Temperature (with diffuser)
(variable position thermocouple)

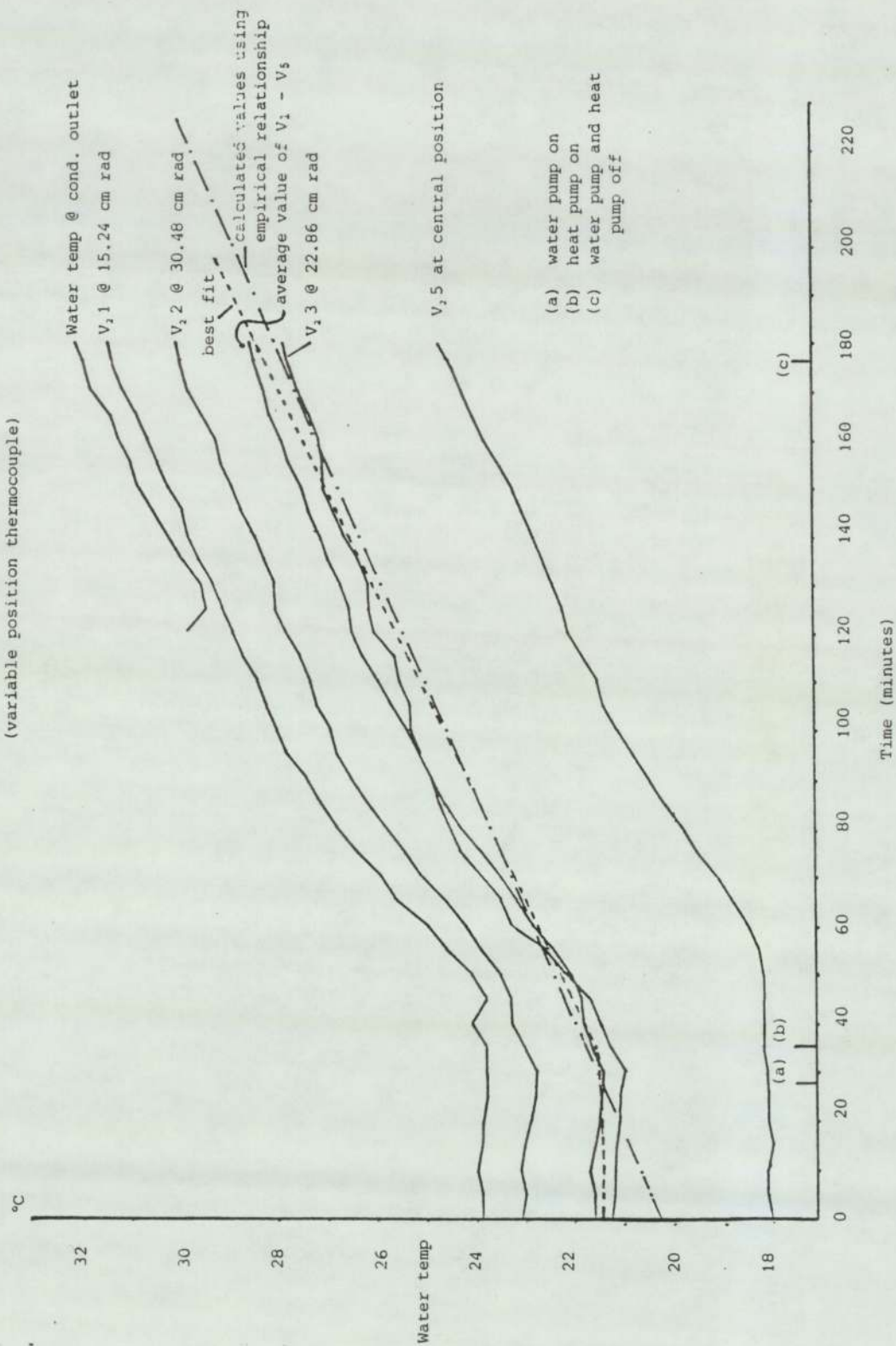


Table 5

Calculated values for water temperature in
store compared to average recorded temperatures

@ height in vessel 27.3

Time after HP start up	calculated temp °C	average recorded temp °C	Diff
10	20.47	20.5	-0.03
30	20.78	20.8	-0.02
50	21.10	21.2	-0.10
80	21.57	21.8	-0.23
120	22.19	22.6	-0.41
150	22.66	23.15	-0.49
190	23.29	23.9	-0.61
210	26.60	24.3	-0.70

@ height 60 cm

10	20.63	20.5	+0.13
30	21.24	20.9	+0.34
50	21.86	21.4	+0.46
80	22.79	22.25	+0.54
120	24.02	23.6	+0.42
150	24.95	24.9	+0.05
190	26.19	26.9	-0.71
210	26.80	27.9	-1.10

@ height 70 cm

10	20.74	20.5	+0.24
30	21.59	21.0	+0.59
50	22.44	21.7	+0.74
80	23.71	23.0	+0.71
120	25.40	24.7	+0.7
150	26.68	26.0	+0.68
190	28.37	27.8	+0.57
210	29.22	28.65	+0.57

@ height 83 cm

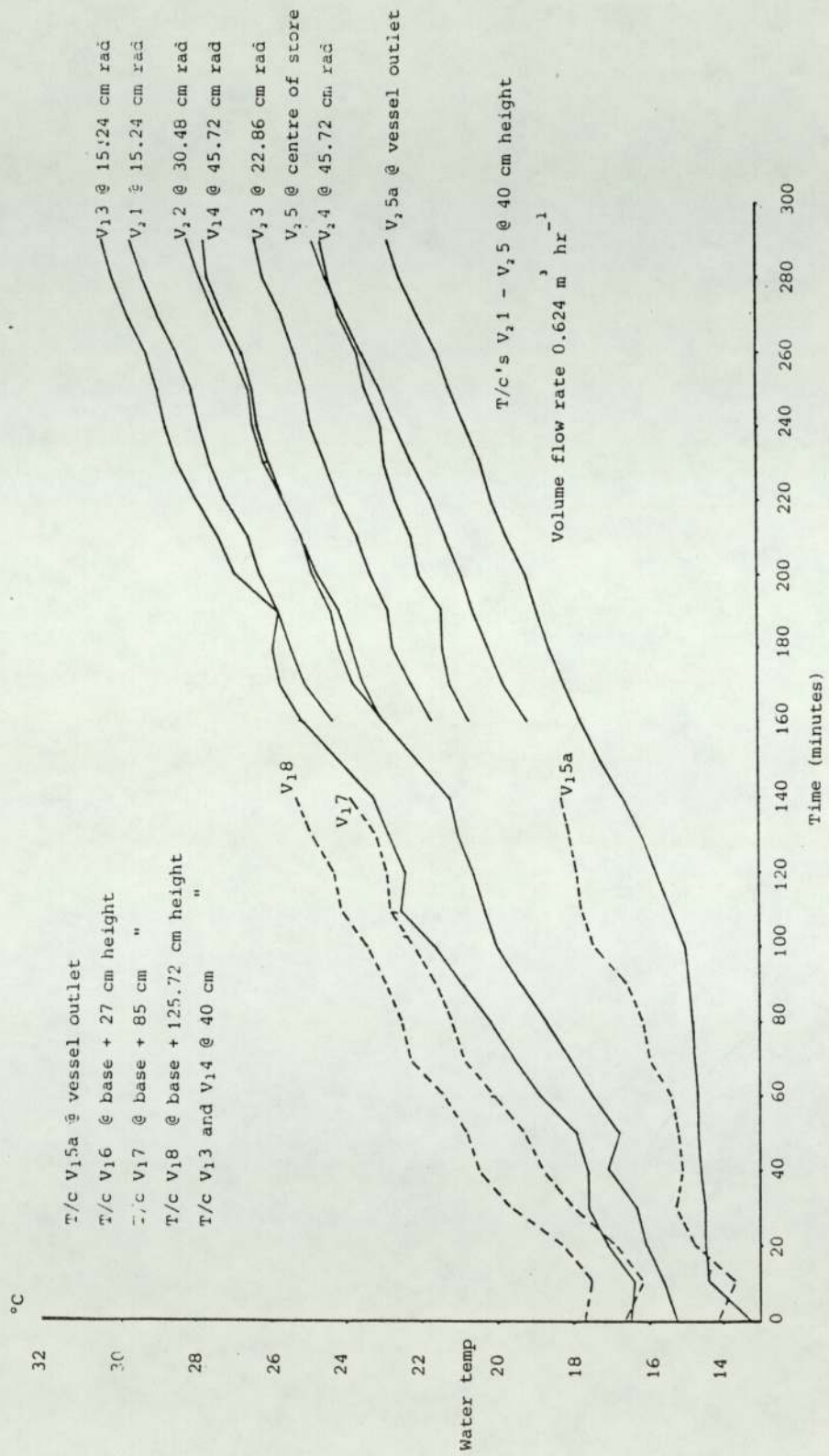
10	20.80	20.5	+0.3
30	21.77	21.1	+0.67
50	22.74	21.95	+0.79
80	24.20	23.5	+0.70
120	26.14	25.7	+0.44
150	27.60	27.3	+0.30
190	29.54	29.5	+0.04
210	30.52	30.55	+0.03

Amongst the differences referred to in test conditions is the water entry velocity (0.52 ms^{-1} for graph 18 and 0.56 ms^{-1} for graph 25); the store temperature at commencement of tests differed and also the duration of the test at T/c height of 70 cm.

The data for graph 25 was recorded over a longer period of time (120 minutes cf 70 minutes for the results plotted as graph 18). Nevertheless, the store temperature distribution at both the vertical and radial positions show clear similarities. The close similarity between test results support the view that the empirical correlation for calculating water temperature at vertical positions, after defined running periods, is representative of conditions being experienced. Table 5 shows comparative data. The remaining curves plotted on graph 25, referred to as "best fit" and "calculated", are the best fit through the numerical average values of T/c's 1 - 5 inclusive and through the calculated values for temperature at 70 cm after the time intervals shown. These two curves should be compared with the (+70) curve of graph 20.

It will be noted that a variation in water velocity of approximately 7.5% has no apparent effect upon the results as displayed by graphs 18 and 25.

Water Temperature - Vessels 1 and 2
(fixed and variable T/c data)



Graph 26

4.7.4 Temperature patterns with the store vessels in parallel

This series of tests were for monitoring the store behaviour in two vessels simultaneously. The typical results presented were recorded concurrently and consecutively over a test durations of 5 hours. For these tests a volume flow rate of water of $0.624 \text{ m}^3 \text{ hr}^{-1}$ was maintained.

From graph 26 it will be seen that the initial period of the test portrayed was used for monitoring store temperatures in Vessel 1 whilst the remainder of the test was used predominantly for measuring conditions in Vessel 2. The variable height T/c carriers in both vessels were maintained at 40 cm height throughout.

From the initial readings taken at fixed T/c's (V_{15a} ; V_{17} and V_{18}) one would suggest that where a velocity diffuser is not employed the temperature distribution down the vessel increases at a more-or-less constant rate, except perhaps at the base position (V_{15a}) which reflects a slower rate of increase compared to the other low positions monitored, i.e. at T/c's V_{13} and V_{14} . However, the base temperature in Vessel 1 (V_{15a}) increases at a rate greater than the base temperature (V_{25a}) of Vessel 2 for at least the initial 90 minute period.

This may result partly from marginally differing flow rates through the vessel but is more likely to be a direct result of the diffuser located in vessel 2. The header situated at the outlets of the vessels would help to eliminate different flow rates.

From graph 26 it will be noted that the readings for Vessel 1 (at 40 cm - depicted by curves V_{13} and V_{14}) are, on average, greater than those at the same height in Vessel 2, (V_{21} - V_{25} inclusive). This again tends to support the view that the diffuser of Vessel 2 is effecting the rate of temperature change in a depthwise direction.

A further interesting feature of the results discussed is the variations in temperature across the horizontal plane. Graph 26 shows that in both vessels, at the same vertical height of 40 cm, there is little difference in temperature between t/c V_{13} and V_{21} (vessels 1 and 2 respectively), both sets of readings being recorded at a radius of 15.25 cm.

Again, the readings at V_{14} (Vessel 1 at 45.72 cm radius) is only marginally different to that temperature experienced at V_{22} (Vessel 2, 30.48 cm radius).

The range and general pattern of temperature distribution across the diameter of Vessel 2 is basically identical with those experienced on other tests where the flow rate of water through the circuit was appreciably greater e.g. $0.909 \text{ m}^3 \text{ hr}^{-1}$ cf $0.624 \text{ m}^3 \text{ hr}^{-1}$.

This further supports the view that for the range of flow rates applied throughout this research the actual flow rate of water has had limited effect upon the temperature distributions obtained for the same total heat pump output.

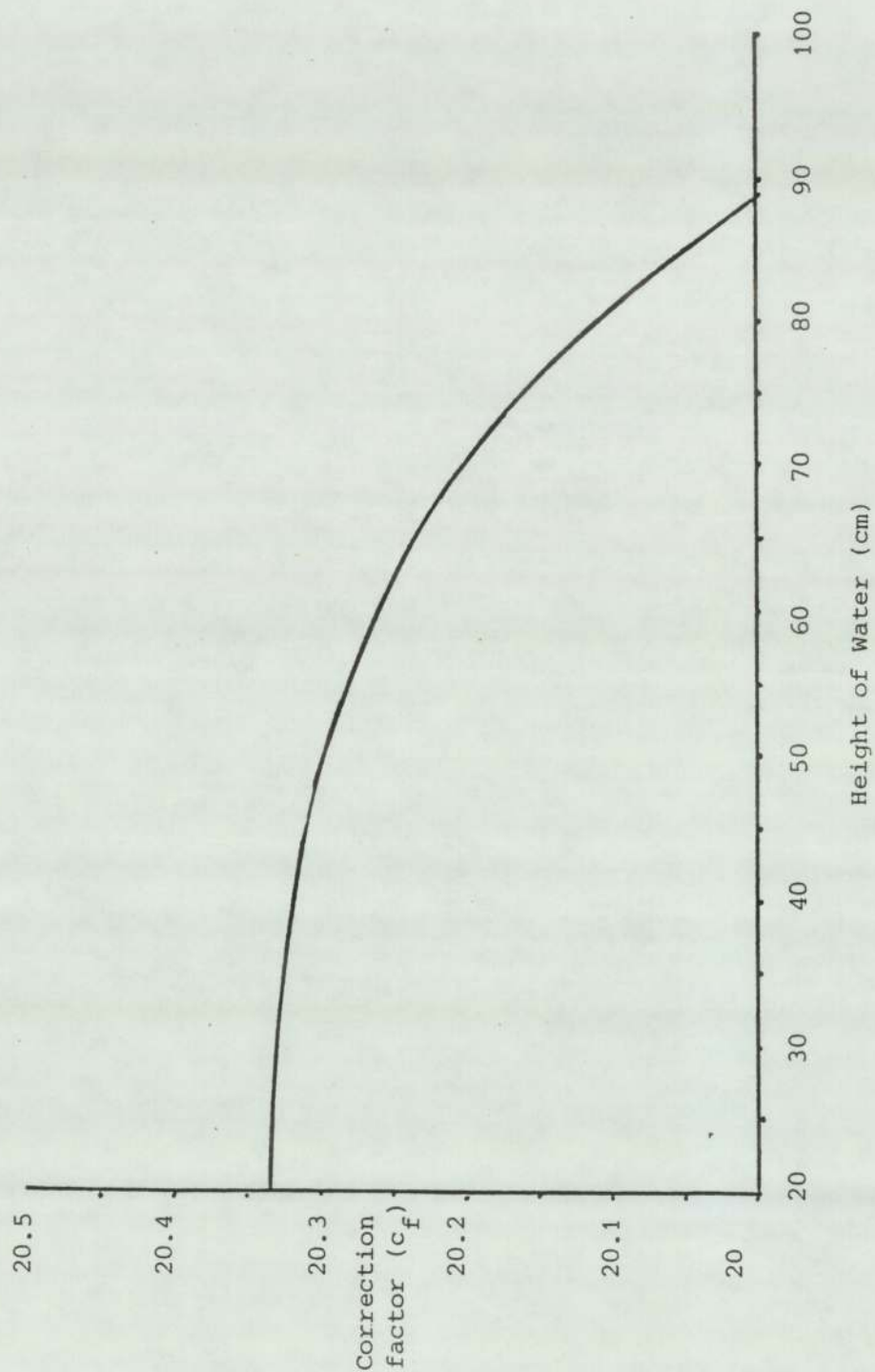
4.7.5. Mathematical Model of Store Temperature Patterns

As referred to earlier (page 211) the test data used in constructing graphs 18 and 20 were also used for derivation of a series of mathematical relationships for the curves plotted.

A general relationship for each of the curves depicted as + 83 cm; + 70 cm etc on Graph 20 has been produced for determining water temperature in store, in °C, against heat pump running time (in minutes). Reference to Appendix 11 shows the general relationship for each curve.

Derivation of First Term Correction Factor (c_f)
against Height of Water in Vessel

(based on Graph 20 data)



Graph 27

The first term of each general equation was replotted as graph 27 and a further general equation established which is basically a correction factor of the first term in the expression.

The corrected first term becoming:

$$Cf_1 = 20.32 + 0.0017 h - 0.000044 h^2 \quad (95)$$

Cf_1 being the first correction factor

h being the height of water in store at which the temperature is sought (cm)

The second term of the original equations (the four general relationships) was replotted as graph 28 (curve Cf_{2a}) 2a). A further relationship being established from the best fit curve, (Cf_2) as:

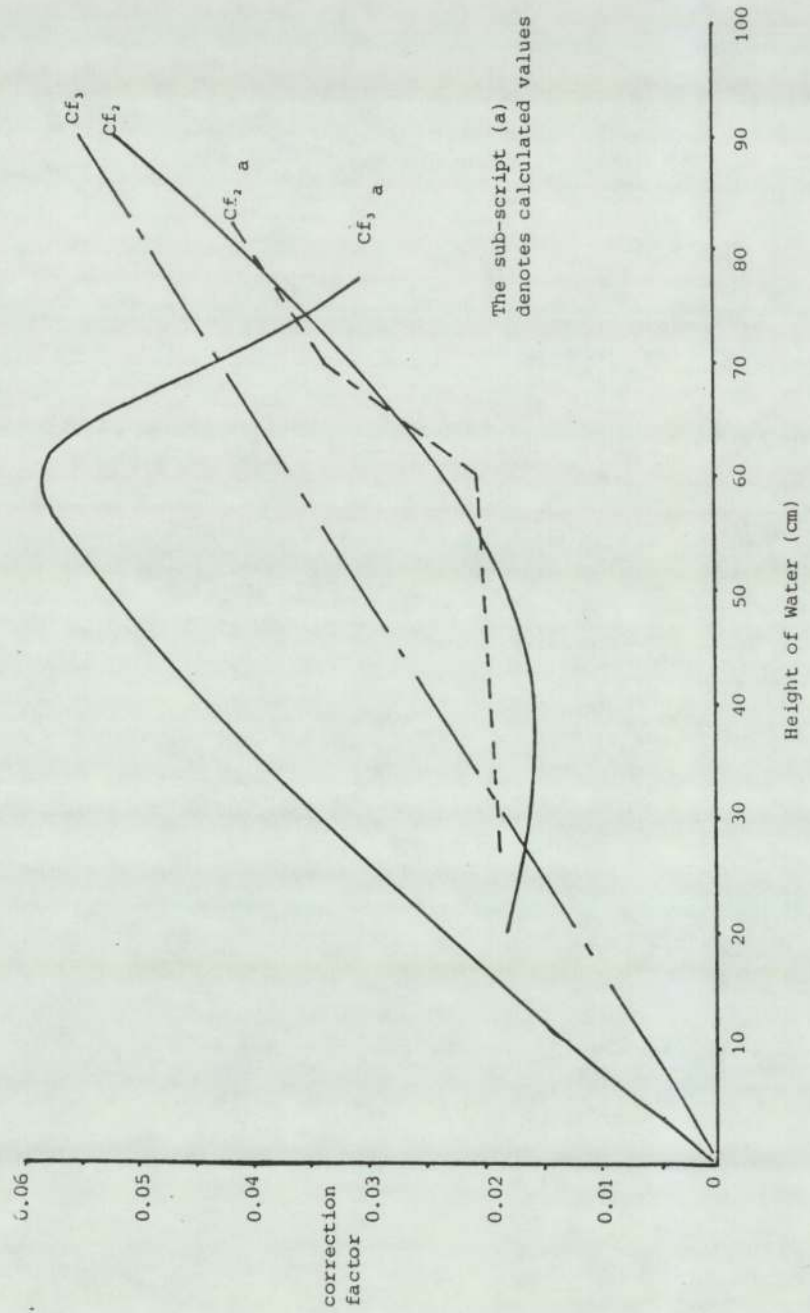
$$Cf_2 = 0.02882 - 0.000769 h + 0.0000114 h^2 \quad (96)$$

Cf_2 being the second term correction factor

h being the height of water in store at which the temperature is sought (cm).

Basis for 2nd and 3rd Term Correction Factors
against Height of Water in Vessei

(Based on Graph 20)



Graph 28

The third term of the original equations was also plotted on graph 28 and a further general relationship was developed as the third term correction factor (Cf_{3a}) the ultimate relationship being, for $h \leq 60$ cm; a best fit curve (Cf_3).

At a height of 60 cm and above the non-parallel vessel sides adversely influenced the model structure.

$$Cf_3 = 0.0000005 + 0.0000012 h - 0.000000005 h^2 \quad (97)$$

Cf_3 being the third term correction factor .

h being the height at which temperature is sought (cm).

The general relationships for correction factors Cf_1 , Cf_2 and Cf_3 have been used to construct an overall relationship for evaluation of the temperature of water in store, at any prescribed height in the vessel, after a defined heat pump running period.

The overall relationship being:

$$t = (Cf_1 + Cf_2 M + Cf_3 M^2) \quad (98)$$

t = the water temperature $^{\circ}\text{C}$
 h = height of water in vessel at
 which $t^{\circ}\text{C}$ applies (cm)
 Cf_1, Cf_2
 and Cf_3 are correction terms
 M = minutes after heat pump start-up.

Reference to Table 3 (page 174) will show the comparative values of temperature as measured to those evaluated using the above derived expressions.

4.7.6. Discussion on Test Results

The closed-loop water circuit was employed for each series of tests undertaken. Where tests have been conducted with only one vessel in circuit these have been clearly identified. When both vessels were used they operated in parallel.

The water volume flow rate was held constant throughout a test and remained always within the range $1 \text{ m}^3 \text{ h}^{-1} \pm 20\%$ for each of the series of system tests. A sample test on condenser performance was undertaken with the volume flow rate at $1 \text{ m}^3 \text{ h}^{-1} - 22\%$.

Vessels 1 and 2 were fitted with a device at the vessel bottom outlet (internally) to reduce any vortex effect due to pump suction on the stored water.

The water circuit was allowed a "settling down" period after water pump start-up, prior to any readings for temperature being recorded. Invariably the initial store bulk water temperature differed from test to test.

Vessel 2 was fitted internally with a velocity diffuser at the water entry position. This device reduced the water entry velocity effect on the stored water surface, i.e. reduced the effects of "mixing length" phenomena as discussed in Section 3.5.

Examination of graphs 9 - 11 inclusive shows that the pattern of temperature distribution in Vessel 1, at each of the fixed thermocouple positions, alters only marginally whatever the heat pump operating period. The rate of temperature increase remains relatively steady at all times.

Tests of similar duration on Vessel 2 however show that a significantly different situation occurs. Graphs 12 - 14 inclusive indicate that the heated incoming water has a lesser effect on the lower section of the vessel than was experienced in Vessel 1.

The pattern of temperature change in Vessel 2 did, however, vary over tests having a duration in excess of 3 hours - see graph 14.

During longer test runs it was apparent that the store temperature increased and tended to approach that of the incoming water at greater depth down the vessel. The results from this series of tests supports the view that pump suction effect on the stored water was not a major influence on temperature profiles.

From the series of tests designed to establish the rate of change of temperature at various vertical positions in the store vessel significant features emerged, amongst which is the pattern of radial temperature distribution.

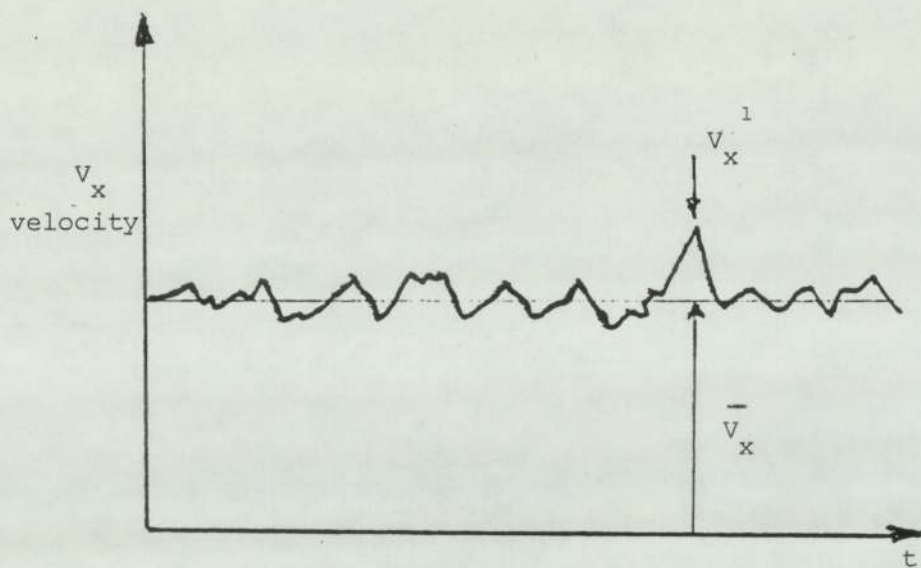
Graphs 15 - 17 inclusive along with Graphs 21 and 22 portray the variations in radial temperature distribution experienced in Vessel 2. The temperatures recorded at the outer radii (45.72 cm) were consistently close to those recorded at the central position.

As would be expected the velocity diffuser alters the generally accepted velocity/temperature profile through the vessel as presented for flow regimes through tubes - see Sections 3.3 and 3.4.

Because of the large variation (often in the order 7.5°C) of temperature distribution along the horizontal plane in the vessel the numerical average temperature was used as providing a "typical" bulk store temperature at the heights chosen for further analysis. These heights being 27.3 cm; 60 cm; 70 cm and 83 cm. Graph 20 displays the "typical" temperatures referred to. The "typical" values were used primarily as a result of the limited computer capacity available. A more refined method of analysis would have been to treat each set of T/c readings individually and derive a series of mathematical models.

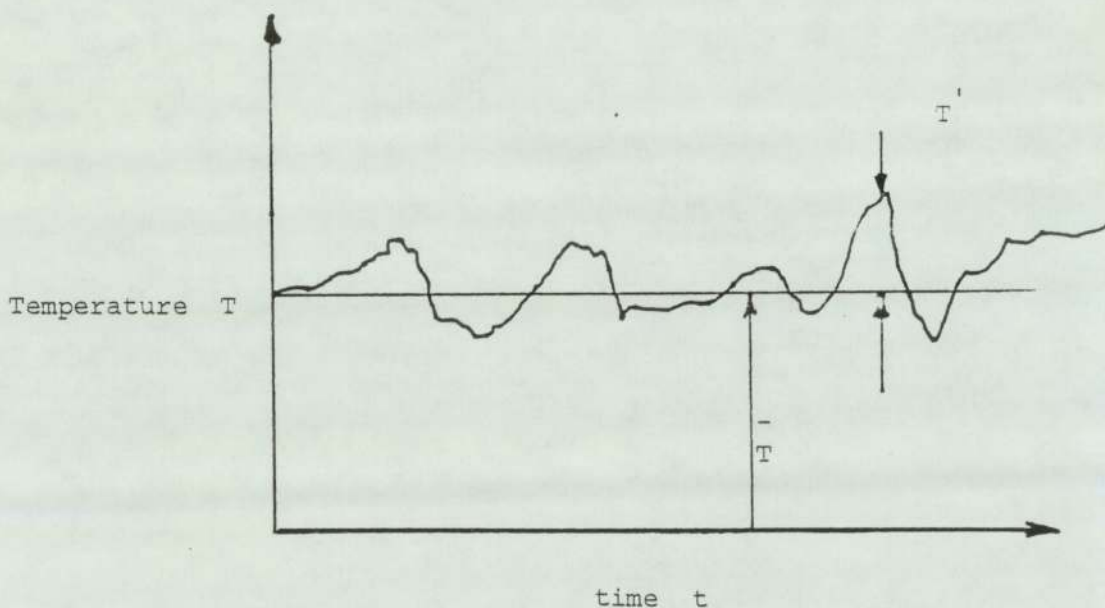
The results plotted as graph 20 form the basis of the mathematical model developed for determining the bulk store temperature at vertical heights in the vessel after a determined heat pump running period.

Graphs 21 - 23 inclusive show the range of radial temperatures experienced. Comparing the graph profiles of graph 21 and 22 with those of graph 23 (Vessel 2 and Vessel 1 respectively), it can be assessed that the velocity diffuser in Vessel 2 has an effect on the water flow through the vessels, and, consequently upon the temperature distribution. Future tests could be undertaken with a range of diffuser types (angles of deflection and physical dimensions) to determine an optimum solution for angle of deflection versus flow velocity.



Time dependence of velocity in turbulent flow
(Welty J R)

The mean value of V_x is constant, indicating steady flow, however, at any instant in time the actual velocity differs from the mean value by the relatively small amount V_x^1 .



Variability in recorded temperature (Bayley et al)

Fig. 30

Welty J R (1978)^[64] makes reference to radial and axial velocity components and provides the illustration in Fig. 30.

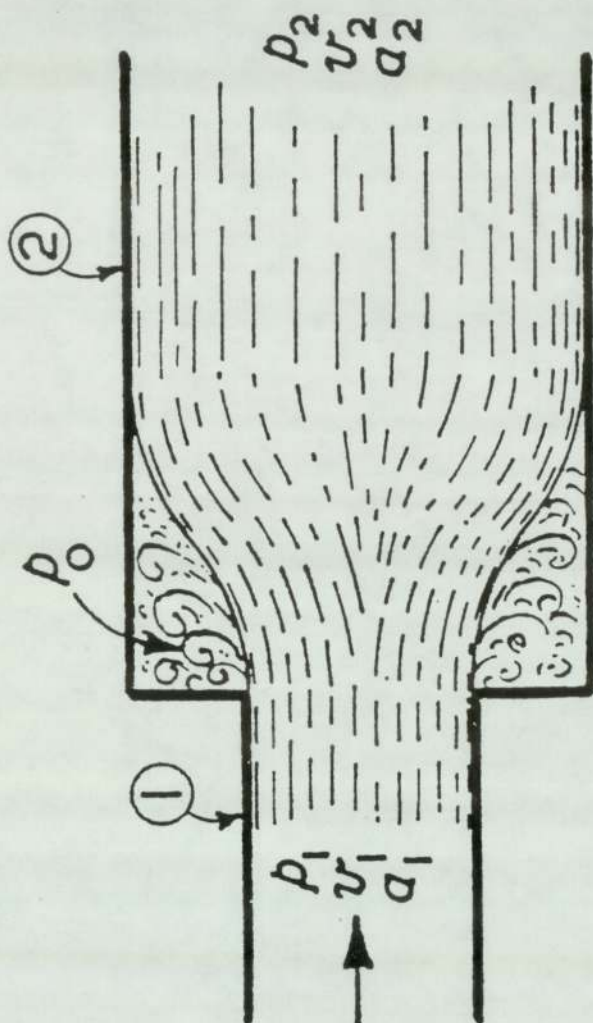
The inter-relationship between velocity and temperature profiles for flow through circular tubes referred to by Welty^[64] and Bayley et al^[67] is summarized as:

"....whereas in turbulent flow the fluctuations superimposed upon mean velocity vary continuously with time. The instantaneous radial and axial velocity components "u" and "v" respectively can be represented by $u = \bar{u} + u^1$ and $v = \bar{v} + v^1$.

Where the bars (-) represent time averaged velocities and primes (¹) denote the time-dependent fluctuating components. Similarly for the pressure, density and temperature e.g.

$$T = \bar{T} + T^1 ."$$

Reference was made earlier, (page 63), to the water circuit which comprised pipework of various diameter. The greater variation being at the water inlet to the vessels. The jet orifice is 17 mm diameter whereas the jet enters the vessel to a diameter of 0.92 m. This sudden enlargement significantly affects "upstream" and "downstream" water pressures and fluid velocity. An illustration of the effects is shown in Fig. 31.



Loss of energy in pipes due to
sudden enlargement in diameter

Fig. 31.

According to Douglas J F^[33] the actual rate of fluid discharge under such circumstances is less than the theoretical value due to:

- (a) the theoretical velocity value being reduced due to frictional resistance
- (b) the area of the issuing jet is less than the area of the orifice.

These conditions contribute to energy loss from the system - often referred to as "shock" losses. The influence of these losses on flow velocity can be seen from Figure 31.

A region of "dead" water occurs where the pressure is (P_0) . There is also a rate of change of momentum between sections 1 and 2 which is produced by the forces due to pressures P_0 , P_1 and P_2 , which have a resultant opposing motion.

The system "head" loss at the enlargement (H_L) is found to be:

$$\left(\frac{V_1 - V_2}{2g} \right)^2 . \quad (99)$$

Since, for continuity of flow, $a_1 v_1 = a_2 v_2$

so that
$$H_L = \left(1 - \frac{a_1^2}{a_2^2}\right) \frac{v_1^2}{2g} + \text{ or } K \frac{v_1^2}{2g} \quad (100)$$

$a_1 v_1 = a_2 v_2$). (being the volumetric flow rate).

The interference due to "head loss" on the flow profile, and therefore on velocity and temperature distribution will, according to Douglas, be noticeable.

Whilst the results plotted on graphs 21 and 22 (Vessel 2) and graph 23 (vessel 1) show limited resemblance to the profiles presented as Figure 27, the curves do reflect a different condition in each vessel.

On the basis that "increased velocity is matched by increased temperature" (see pages 146 and 159) then a marginally higher flow velocity should be experienced away from the central core of Vessel 2 whereas for Vessel 1 the highest velocity of flow is in the central core region, at the top section of the vessel. At the 40 cm height the jet effect has been mostly eliminated - see graph 23 - due to the fluid bulk.

As stated, the temperature profiles for graphs 21 and 22 show a resemblance to the velocity profile referred to in Section 3.4.2. i.e. "velocity profile in laminar flow through tubes".

Fully developed flow however is not apparent.

A reason for the limited similarity to both Bayley's observation and the laminar flow profile could be the non-uniform nature of the vessel, i.e. the walls are not wholly parallel and the flow is not strictly representative of flow through a circular tube. Non-symmetry of the vessel results from the inspection port at the side of the vessel.

The variability in recorded temperatures at each T/c is apparent. However, the magnitude of the variation cannot be fully established because of the conditions to which Bayley refers, namely:

"....that a thermocouple, with sufficiently small time constants, placed at a fixed location in a turbulent fluid would record an output similar to,....." (see Fig. 30).

On the basis of Bayley's comments it may be appropriate to assign a tolerance value to the T/c readings taken throughout the series of tests. This would remove some of the variations depicted on graphs 21 - 23 inclusive.

Karlekar and Desmond^[49] recommend that for turbulent heat transfer in tubes account has to be taken of heat transfer conditions in the entry (mixing) length. They also state that where neither the velocity profile nor the temperature profile is established a combined thermal and hydrodynamic entry length exists.

This would imply that a steady state heat transfer condition does not apply to the store vessel under examination, therefore, the rate of change of bulk store temperature at different vertical locations, will not be constant over time.

Nikuradse^[68], in his extensive study of pipe flows found that fully developed turbulent velocity profiles existed after an inlet mixing length of "25 to 40 diameter".

The physical dimensions of the present system would, on this basis give a mixing length of between 4 and 7 cm, if Nikurdase assumption is based on the diameter at the jet entry rather than on the larger vessel diameter.

If the assumption is based on 25 to 40 diameters of the receiving vessel then a mixing length could not be achieved using the present equipment.

Direct comparison of the three sets of curves on Graph 23 for the absolute value of temperature and the temperature rise over time, is not totally meaningful because they

reflect readings taken in consecutive time intervals rather than for concurrent periods. The continuously changing condition of water inlet temperature distorts interpretations. A significant feature of the curves is the temperature profiles - the "central core" temperatures are more uniform than those experienced in Vessel 2.

The sequence of tests for ascertaining whether or not the pump suction vortex had an influence on temperature distribution in the vessels gave results similar to those depicted as graph 24. The patterns of behaviour on temperature distribution, under conditions with the pump in operation, and without the pump operating, are very similar. It is therefore concluded that the pumping action did not significantly effect the results of previously referred to tests.

It may be appropriate to assume therefore that an amount of thermal cycling, due to natural convection processes, gave rise to the temperature profiles resulting from the pump not being in operation.

Graph 25, which was discussed in detail on page 230, was selected for highlighting the accuracy of the mathematical model referred to earlier.

Graph 26 presents test data recorded at Vessels 1 and 2. Employing both the fixed thermocouple data and that from selected variable position thermocouples. For comparative

purposes data was recorded at the five variable position thermocouples of Vessel 2 and at the base fixed position thermocouple. Each curve on Graph 26 is identified by the thermocouple reference.

It will be noted from Graph 26 that for an initial 60 minutes after heat pump start-up the fixed thermocouple reading at Vessel 1, (V_{15_a}) and Vessel 2 (V_{25_a}) were in close proximity. After this initial period the curves diverged as in previously presented test data.

The variable position thermocouple carriers were positioned at base + 40 cm in both Vessel 1 and Vessel 2 for the period 160 minutes after heat pump start-up to the completion of the test, i.e. at 300 minutes after start-up.

Direct comparison of results between thermocouple readings V_{13} and V_{21} can be made as they were both at 40 cm height and at a radius of 15.25 cm.

Similarly, the results obtained from Vessel 1 (V_{14} at 45.72 cm radius) and Vessel 2 (V_{22} at 30.48 cm radius) confirm the temperature profiles presented as Graphs 21 and 22 (Vessel 2) and graph 23 (Vessel 1), namely, the temperature distribution patterns tend to be opposing. Higher temperatures tend to be towards the outer diameter down through Vessel 2.

CHAPTER FIVE

5. The Computer Model

5.1. The Model - an Overview

The computer model comprises two distinct programs namely:

- (a) for data collection
- (b) for calculating system performance

Each of the program routines are written in CBM Basic 4.0 computer language. The programs require a CBM system comprising not less than

- (i) a CBM 32K microprocessor
- (ii) a CBM 2031 (175K) disk drive
- (ii) a suitable 80 column dot-matrix printer.

An additional requirement for conducting a monitoring and recording sequence is an Analogue to Digital (A-D) conversion unit for transposing thermocouple output to temperature in °C. The A-D unit employed on this system was the CIL model PCI 1002 having 15 input terminals, Ref. Appendix 2.

Development of the computer model has been a major activity in this research.

Each relevant system component including the evaporator, the condenser, the water store vessels, the water distribution circuit to the refrigerant circuit, have been modelled individually and collectively.

As discussed in previous chapters modelling individual components has necessitated manipulation of manufacturers design specification data, where provided, into suitable computational routines capable of converting actual recorded values into component performance at conditions other than design conditions.

Comparison of the store vessel performance was not possible as these were modified brewing vessels and therefore not purpose designed for the system.

Where possible a routine has been incorporated into the computer program employing universally accepted calculation methods. These routines are for comparing the results obtained from using modified manufacturers procedure.

A typical example being that of sensible and latent heat contents of water in store.

To conserve the limited computer operating memory for data manipulations and necessary iteration of the many variable data, it has been desirable to include the maximum possible fixed data items.

Fixed data in this context means that the values do not change with changing test conditions. Changes to fixed data would be necessary if the system construction alters.

A further method for conserving valuable computer memory has been the inclusion of derived formula, derived by the Author for calculating such data as pressure/enthalpy relationships for refrigerant.

By employing derived formulae the need for storing tabulated data for the refrigerant has been removed.

As data collection employed a separate program routine to that of the system performance calculation, and was a significantly smaller program, it was possible to provide on-line facilities.

The on-line facility, in conjunction with the analogue-to-digital conversion unit, controlled the majority of data monitoring and recording sequences.

Being an on-line facility enabled the operator to view system conditions throughout the duration of a test.

The computer model provides ultimately for a Coefficient of Performance (CoP_H) in the heating mode for the system overall. The Coefficient of Performance for the compressor unit is also calculated.

5.2 Inputs to Model

5.2.1 Data Collection

The data collection routine comprises a combination of manual entries, through the keyboard, and inputs directly from thermocouples via the A-D unit. Keyboard entries are reduced to a minimum and include such items as the date of the test; the time the tests commenced (and ceased) and the time intervals derived between automatic scanning of thermocouples.

Identification of thermocouple positioning is also manually entered. An output of test data which is of a typical test run is included as Appendix 12 and referred to again in Section 5.4.

5.2.2. Calculation of System Performance

Inputs for calculating system performance, as itemized in Appendix 13, are entered through the keyboard. The values entered manually are those monitored manually and include line pressures, volume flow rate, power consumptions etc, as well as such information as averaged values from the automatically recorded data.

The system performance evaluations are, through necessity, strictly off-line calculations, that is, results are not immediately registered on the computer display screen whilst the system (heat pump) is in operation. Some of the data collected on-line is however displayed whilst the thermocouples are scanned. This allows for a visual check on system behaviour as the tests progress. A typical performance calculation print out is included as Appendix 14.

5.3 Data Manipulation within the Model

The operating performance of each major component of the heat pump and store system is evaluated as an individual item and also collectively in order that an "energy balance" condition can be attained i.e:

(a) energy absorbed at the evaporator
plus compressor

equals (b) energy rejected at the condenser

equals (c) energy transferred to the heat store.

The manner in which each evaluation is executed is detailed below.

(a) The Evaporator - energy absorbed at the evaporator is calculated from the enthalpy change of air at evaporator inlet and outlet.

The calculation routine, being a development of Eqns. 31 (page 110); 34 and 35 (page 111) and presented in program syntax as:

Enthalpy of air leaving evaporator

$$= \text{Int}((1.007 \times F_2 - 0.026 + N_7 \times (2501 + 1.84 \times F_2))) \quad \text{Kj Kg}^{-1} \quad (101)$$

where

- F_2 = dry bulb temperature of air leaving evaporator
- N_7 = moisture content of air leaving evaporator
 $= ((0.622 \times N_6) / ((P_p / 29.92) - N_6))$
- N_6 = $H_Z \times N_5 / 100$
- H_Z = relative humidity of air at evaporator outlet
- N_5 = $10 + (28.591 - 8.2 \times \ln(T_Z) / \ln(10) + 0.00248 \times (T_Z) - 3412.31 / T_Z)$
- T_Z = absolute dry bulb temperature of air leaving evaporator
- INT = BASIC instruction for containing the degree of calculation accuracy.

The enthalpy value of air entering the evaporator is calculated using the same procedure.

Heat extracted from dry air at the evaporator becomes a function of mass flow rate of dry air over the evaporator and the change in enthalpy.

e.g. $Q_s = \text{Int} (M_D \times (F_1 - F_2))$ [Eqn. 40 (page 113)]

where $M_D = \text{Int} ((1.275 \times D_A) \text{ Kgs}^{-1})$ (Eqn. 41 (page 114))

and 1.275 being the manufacturers designed volume flow rate $\text{m}^3 \text{s}^{-1}$ for the evaporator.

Density of dry air, based on Eqn. 42 (page 114) =

$$D_A = \text{Int} ((1.2014 \times (294.1 / (F_1 + 273))) \times (B_p / 29.92)) \text{ Kgm}^{-3}$$

B_p = measured barometric pressure. ins Hg.

F_1 being air inlet temperature. °C.

The heat pump manufacturer's published calculation procedures, which were discussed in section 3.1.2 (pages 117-120) are reproduced below, in program syntax for comparison with the approach presented above, i.e. sensible heat capacity;

$$(Q_s = ((F_1 - F_2) \times 1.214 \times (4590/3600)) - (C_f \times (4590/3600)) \text{ kW}$$

where

$$C_f = \text{correction factor for air temperature} \\ = (0.29 \times (1 - B_F) \times (26.7 - F_1))/1000$$

$$B_F = \text{coil by-pass factor} \\ = \text{Int} (1 - ((\text{LMTD} - F_1)/(\text{LMTD} - F_2)))$$

where LMTD is log mean temperature difference at coil

$$= \text{Int}((F_1 - E) - (F_2 - E))/(\text{Log}((F_1 - E)/(F_2 - E))).$$

where E is the evaporating temperature of the refrigerant (pressure based).

$$E = \frac{-32 + (-0.7958 + (\text{SQR}((0.7958 + 2) - ((4 \times 0.00819) \times (37.986 - G_1))))}{2 \times 0.00819}$$

The above enthalpy formula being derived by the Author from temperature/pressure V_s enthalpy curves for refrigerant R_{22} (above saturated liquid at -40°F) based on data from Kinetic Chemicals Incorporated and IHVE See also Appendix 4.

where

G_1 = pressure of R_{22} recorded at evaporator outlet (Psig).

The total heat extracted at the evaporator is evaluated using flow rate of moist air over the evaporator and the enthalpy change - e.g. in program syntax,

$$Q_2 = M_F \times (ESE - LSE)$$

where

$$M_F = \text{Int} (1.275 \times R_M)$$

1.275 being volume flow rate of air ($\text{m}^3 \text{s}^{-1}$)

R_M is density of moist air to the evaporator

$$R_M = \frac{(1.2929 \times (273.13 / (F_1 + 273.13))) \times ((BP / 29.92) - (0.3783 \times N_2))}{1.101325}$$

where

$$N_Z = H_Y \times N_1/100$$

H_Y being RH% of air at evaporator inlet

$$N_1 = 10 + (28.591 - 8.2 \times \log(T_Y) / \log(10) + 0.00248 \times (T_Y - 3142.41/T_Y))$$

and ESE; LSE are the specific enthalpy of moist air to the evaporator and leaving the evaporator respectively in $Kj Kg^{-1}$.

The manufacturers' corrected design total heat capacity (QT) based on wet bulb temperature leaving evaporator coil corresponding to enthalpy of air leaving evaporator coil becomes:

$$Q_T = \text{Int} ((\text{ESE} - \text{LSE}) \times (1.18 \times (4590/3600)))$$

(b) The Condenser - the heat rejected to the cooling water at the condenser is calculated using an approach discussed by Neal W E J as follows: (in program syntax).

Energy delivered to condenser

$$\dot{E}_T = \text{Int} ((\dot{V}_L + \dot{M}_L + \dot{S}_L)) \quad (102)$$

Each of the three terms are considered in (i - iii) below:

(i) \dot{V}_L is heat loss from vapour

$$\dot{V}_L = R_F \times ((12.52 + (0.022 \times B_1))/86.5) \times (B_1 - C_3)$$

(103)

The values for B_1 and C_3 (in the heat loss from vapour equation (Eqn. 103) are the refrigerant temperature at condenser inlet and condensing temperature, ($^{\circ}\text{C}$) evaluated from measured pressure respectively.

where

$$C_3 = (-0.17836 + (\text{SQR}((0.17836^2) - ((4 \times 0.0138) \times (56.82 - G_2))))/2 \times 0.0132 \quad (104)$$

(and being derived formula based on R_{22} pressure-enthalpy data applicable to the condenser inlet pressure (G_2).

Where R_F is refrigerant flow rate calculated using ASHRAE.

$$R_F = \text{Int} \left(\frac{((MQ \times (SW \times 1000 \times (C_2 - C_1))) + (A_u \times (S_{4T} - F_1)))}{((R_3 - R_5) \times 10^3)} \right) \times 10^4$$

(105)

where

$$\dot{M}_Q = \text{Int} ((M_w / 3.6) \times R_O)$$

and M_w = metered volume flow rate of water

R_O = density of water

S_w = specific heat of water

C_1 and

C_2 = condenser water inlet and outlet
temperature respectively

A_u = coefficient of thermal conductivity
of tube material

S_{4T} = mean temperature of condenser pipework

F_1 = dry bulb temperature of air to evaporator

R_3 = enthalpy of saturated vapour at
condenser pressure

$$= \text{Int} (104.91093 + (0.10925 \times 0_1) + (0.0001875 \times (10^2)) \times 2.33) \quad (106)$$

R_5 = enthalpy of sub cooled liquid

$$= \text{Int} (9.6502 + (0.287675 \times 0_4) + (0_4^2)) \times 2.33 \quad (107)$$

The formulae for R_3 and R_5 have been derived using the least squares method and based on temperature/pressure V_s enthalpy curves for R_{22} refrigerant for use in the computer model.

The values O_1 and O_4 are the condensing temperature and condenser outlet refrigerant temperature ($^{\circ}F$) respectively.

$$\begin{aligned} \text{(ii)} \quad \dot{M}_L &= \text{heat loss from vapour/liquid phase} \\ &= R_F (R_3 - R_4) \end{aligned} \quad (108)$$

where

$$\begin{aligned} R_4 &= \text{enthalpy of saturated liquid at} \\ &\quad \text{the condensing pressure} \\ &= \text{Int} ((9.6502 + (0.287675 \times O_2) + \\ &\quad (0.0002555 \times (O_2 + 2))) \times 2.33 \end{aligned} \quad (109)$$

being derived formula based on R_{22} pressure - enthalpy data applicable to the measured condenser inlet pressure (G_2).

$$\begin{aligned} \text{(iii)} \quad \dot{S}_L &= \text{heat loss from sub cooled liquid} \\ &= R_F (0.3 \times (C_3 - B_2)) \end{aligned} \quad (110)$$

where

$$\begin{aligned} B_2 &= R_{22} \text{ temperature at condenser outlet.} & ^{\circ}C \\ C_3 &= \text{condensing pressure} & ^{\circ}C \end{aligned}$$

As suggested in Section 2.1 (page 67), part of the cooling of superheated vapour may take place in the circuit between the compressor and the condenser this energy will be lost, therefore a complete energy balance throughout the system may not always prevail.

- (c) The Heat Store - The amount of energy transferred to store is based on the change in store temperature over the test duration.

A three "node" arrangement is considered for each vessel i.e. the temperature change between four fixed internal thermocouples is monitored, then, based on the known volume of water relevant to each node a value for the increase in energy stored between the fixed thermocouples is calculated as shown in the following example; (in program syntax)

(values based on Vessel 2 - top node between T/c's at 83.05 cm and 125.72 cm).

Energy stored Vessel 2 top layer

$$Q_k = \text{Int}((((192.69 \times 4.187 \times (L_6 - ((W_8 + W_7)/2))))/3600) \quad (111)$$

where

192.69 = volume of water in top node (litres)

4.187 = specific heat of water (Kj Kg^{-1})

$L_6 = (x_7 + x_8)/2$

where

x_7 and x_8 = final temperature of water ($^{\circ}\text{C}$) at 83.05 cm and 125.72 cm respectively

w_7 and w_8 = initial temperature of water ($^{\circ}\text{C}$) at 83.05 cm and 125.72 cm respectively.

An additional facility available in the program allows for the selection of vertical positions between 27.3 cm and 100.03 cm in either vessel at which further thermocouple readings may be monitored.

The volume of water above the chosen vertical position, within the range base + 27.3 cm and base + 100.03 cm, is then calculated using the formula:

$$V_6 = \text{volume of water above carrier} \\ = (0.0331 + (0.579 \times (1.003 - T_{1P})) + (0.207 \times ((1.003 - T_{1P}) + 2)))$$

(112)

where

T_{1P} = chosen vertical height of T/c carrier.

The equation (Eqn 112) has been derived using the simultaneous equation method and data collected when quantifying the volume capacity of the store vessels.

The curves shown in Graph 1 indicate the store capacity with respect to height of water in the store and also the metered volume of water passing from one tank to another compared to the calculated volume based on Eqn (112).

The amount of energy stored in the volume of water applicable to the chosen position of the variable position thermocouple carrier can therefore be established.

5.4. Outputs from the Model

The computer model is designed to calculate the energy transferred to store during operation of the heat pump in an air-to-water mode.

The overall system performance is calculated and presented as a coefficient of performance (COP_H) value. A COP for the compressor only is also calculated.

A typical printed data output sheet would include a comprehensive summary of inputted variables to the model. The variables being those monitored and recorded both manually and in an on-line mode via the A - D unit.

A discussion on input data, and methods of collection, has been included earlier in this thesis (page 255). A summary of system evaluations is also included on the data output sheet.

Because the model allows for calculation of the energy stored between the fixed thermocouple positions and/or the energy stored in the volume of water located above the variable thermocouple carrier, the output document will reflect the option chosen. A further series of options would include an analysis of the energy storage in each of the vessels individually or jointly.

The extent of output data provided has been restricted by the operating capacity of the computing facilities available.

A fuller presentation of a typical output from the model is included as Appendix 12.

5.5 Limitations of the Model

The computer model, designed specifically for use with the heat pump system presented and discussed in this thesis, has operational limitations which includes:

- (i) the program is executed in an off-line mode
 - (ii) the number of parameters, including fixed parameters and variable parameters capable of being processed is limited
 - (iii) some essential data has to be input manually.
-
- (i) On-line performance evaluations would have been possible if additional monitoring facilities had been available. These additional facilities would necessarily include a series of pressure transducers located in the refrigerant circuit; a facility for continuous measurement of water volume flow, electrical power consumption monitoring and the measurement of relative humidity at the evaporator air inlet and outlet.
 - (ii) The number of data variables capable of being handled by the computer was limited only by the random access memory (RAM) capacity incorporated into the machine.

The data variables required in the model included, for example:

- (a) Wet and dry bulb temperatures of air to and from the evaporator.
- (b) Water temperatures throughout the circuit, i.e. at the condenser, at the pipework and within each store vessel.
- (c) Refrigerant temperatures and pressures at the evaporator and at the condenser.

Inclusion of a facility for increased numbers of variables to be catered for in the model structure would have been possible only at the expense of some calculation routines and/or a number of screen or printer options; purely as a result of machine memory limitations. The screen and printer options were retained primarily because it was considered they aided the understanding of the program mechanics.

A reduction in the number, and extent of calculation routines would have necessitated the input, through the keyboard, of a greater number of values.

Fixed data presently included in the model are such items as pipework lengths, pipework diameters, number of bends, tee-sections etc. The "fixed" values can be altered by accessing the program data files and thereby allow the program to be applied to other system or for examining the effects of varying the piping system dimensions for example.

The extent of usage of "fixed" data was purposefully limited as an increase in the number of fixed data values would, it is believed, result in the evaluation of system performance being significantly less representative than is desirable.

- (iii) The manual entry of data was made necessary through limited computer capacity. Non-manual inputs would require a greater amount of monitoring equipment installed on the test system and therefore the facility for accepting continuously recorded data, manipulation of this data and suitable methods for extracting the relevant data for insertion into the evaluation routine.

Examples of data being recorded automatically through the duration of a test, manually interpreted and re-entered via the keyboard is the water store temperatures and single-point air temperature measurements at the evaporator inlet and outlet.

Presently, the computer program is designed to use only "start" and "finish" temperatures of the stored water. These values being extracted from the information continuously retrieved through the A-D unit during the course of a test.

To remove the manual involvement would necessitate a program routine which accepts the measured values, stores the values and ultimately selects the appropriate value(s) for use in the calculation routines.

The mechanics of such an on-line feature are totally feasible, however, the computing capacity needed would be extensive especially when catering for each parameter involved.

A computing facility in the order of at least 40 mb (megabytes) fixed disc capacity would be necessary to cater for the number of parameters included on the system.

CHAPTER SIX

6. Possible Improvements to the System

6.1 The Heat Pump Unit

The outdoor section comprises the evaporator coil, the compressor, four-way reversing valve and the expansion valve, - it is a commercially available unit and therefore subject to continuous development and modification by the equipment manufacturers.

It has not been an objective of this study to examine, in depth, the design features of the components individually or as a whole. It has, however, been essential to assess the performance of the "whole" against the manufacturers published material.

Where possible manufacturers published design criteria have been compared to performance values based on known, conventional, calculation procedures.

Reference to Appendix 12, which shows a typical test data output format, highlights results evaluated using the manufacturers published procedures, manipulated for use in the computational routine and corrected for test conditions,

and results obtained using other, known, routines as discussed in Chapter 3. From Appendix 14 the following four abbreviated results have been extracted.

(a)	Sen' Ht Ext'd (Dry Air @ evap) (kW)	0.91
(b)	Mfr. corr'd design S'HT capacity (kW)	0.92
(c)	Sen' + Lat' HT extracted @ evap (kW)	4.85
(d)	Mfr. corr'd design TOT HT capacity (kW)	5.32

Throughout the tests conducted the results for sensible heat capacities (a and b above) showed compatible values. The values obtained for total heat capacity, (c and d above) were consistently at variance by 6% to 8%.

Further investigations based on the results of this study, but outside the objectives of this thesis could be devised to examine, in depth, the design criteria of each of the four major heat pump components.

This may however be a duplication of effort if the manufacturers data can be relied upon. An overall objective for this study was to assess the suitability of a system for use in commercial environments; the results obtained in this investigation suggests manufacturers data could be used to construct a suitable system.

It would seem appropriate to undertake additional research for the evaluation of evaporator coil performance. The results produced here in securing an energy balance, i.e. matching the heat absorbed at the evaporator and generated by the compressor with that rejected at the condenser and ultimately transferred to store, have been subjected to relatively stable ambient conditions.

Constantly varying ambient conditions as would be experienced in a commercial installation, along with changing refrigerant flow conditions, resulting from changing heat exchange rates at the condenser for example, influences evaporator efficiency performance.

Conditions prevailing at the coil should therefore be constantly and extensively monitored so that more precise enthalpy values can be defined. This would best be achieved by expanding the computational facilities - as outlined in the previous section. A discussion relating to evaporator performance is included as Section 2.3.

Refrigerant flow rates could be more precisely assessed. Whether this is achieved by the inclusion of a suitable volume flow meter or by achieving a more accurate initial refrigerant charge is worthy of further investigation. Adopting an alternative method for determining refrigerant flow rate could remove the

calculation routine incorporated into this system model and thereby allow more computer memory for processing other equally important data.

The changed approach towards determining refrigerant flow rates could result in a more accurate value of "refrigeration effect". The refrigeration effect being a measure of the amount of heat each unit mass of refrigerant absorbs from the environment. However the problems associated with the measurement of refrigerant flow rate are considerable as has been identified in Section 2.1.

A thorough analysis of compressor performance would be necessary if greater accuracy of heat pump performance was desired. Amongst the many facets of the compressor behaviour to be considered further would be that of compressor compression ratio. Continuous monitoring of refrigerant pressures would however require the availability of greater computing power.

Considerable attention is currently given by manufacturers to the performance of expansion valves. Response of the expansion valve to changing operational conditions can play a major role in the maintenance of optimum heat pump performance. This, in turn, affects the economics of a heat pump installation.

6.2 The System

6.2.1 The System - Condenser Coil

The condenser coil was selected for its compatibility of performance with that performance attributed to the compressor and evaporator, by the manufacturer. The condenser is a commercially available unit.

The counter flow co-axial coil design was considered suitable for use in the closed-loop water circuit. Each test of the system was conducted so that the operating conditions always remained within the coil design parameters specified by the manufacturer, (water flow velocity; water temperature rise across to coil, water volume flow rate etc).

Interpretations of the manufacturers published performance criteria have been undertaken - see Section 3.2, and a method for evaluating the coil performance devised, suitable for insertion into the computer model. To achieve a more comprehensive awareness of coil behaviour it would be necessary to increase the amount of instrumentation at the coil beyond the level employed for these tests.

As with the evaporator coil, an on-line evaluation would prove beneficial when attempting to verify the system heat balance (evaporator, condenser, store), but again greater computing capacity would be essential.

Through increased computing capability and instrumentation one could examine, in detail, areas within the coil where refrigerant superheating takes place - and the results of such phenomenon on heat transfer rates. Likewise identifying the region (and effects) within the coil where phase change and sub-cooling of the refrigerant occurs could prove valuable for future coil design.

Tests similar to these undertaken throughout this research on condenser coils of different types and configuration would assist in establishing the optimum coil construction for similar systems. Amongst the different types of coils available are the shell and tube design and the parallel flow type.

6.2.2 The System - Pipework

The pipework configuration was designed to replicate, in a confined environment, that of a practical, commercial system layout. A number of circuit restrictions (bends, elbows, valves etc) were incorporated and the pipework was encased in an appropriate thermal insulation layer.

Because of enforced limitations on the extent of pipework used the circuit restrictions were less than one would generally experience in practice, consequently, the circuit "head" loss was much lower than a normal domestic/commercial circuit. The pumping power was therefore much lower.

The computer program is however capable of being run with manually preset pipe resistance which simulates various pipework configuration without any extra experimental work. A facility of this nature would be beneficial for system design purposes.

Low pumping power requirements with marginal circuit pressure losses, and reduced heat losses from pipework to atmosphere were contributory factors towards achieving the heat balance results discussed in section 5.4.

The level of instrumentation around the water circuit appeared adequate to meet the objectives of this study.

As stated earlier the facilities for processing all data capable of being collected was limited.

On-line computer monitoring of water temperatures was completed with the aid of the A-D conversion unit referred to earlier, this was controlled by one of the programs specially written for this research activity .

All water temperatures recorded at the circuit pipework were from thermocouples bonded externally to the pipework and encased in an insulation material.

6.2.3. The System - Storage Vessels

The storage vessels used were not purpose designed for this research activity and could therefore be usefully improved upon if further series of tests were embarked upon.

Improvements to the vessels would include a more regular shaped vessel, that is, with full parallel sides and an inlet orifice designed specifically for meeting the desired results. The desired results would be either the promotion of thermal stratification throughout the vessel

length or complete equilibrium of temperature distribution within the vessel.

If thermal stratification is the desired objective then it would be appropriate to design an inlet which further aided the diffusion of the inlet jet profile to further reduce the "mixing length" to a minimum, or totally eradicate it.

Whilst the pump suction had little discernable effect on the temperature distribution in either of the two vessels employed it would be useful to incorporate a practical precaution against such an occurrence. This could be a device similar to the one used in this research.

The ultimate physical usable volume of storage vessel to be used must obviously be compatible with the system's overall requirements, however, one important criteria is that for a stratified condition, the smaller the diameter and longer the vessel the better for creating significant temperature differences between the top and bottom of the vessel. A pre-requisite being that heated water is input at the top of the vessel.

Limitations on store suitability will ultimately be the cost of design, construction etc, because once the desired stratification has been achieved quite sophisticated controls could be incorporated at the vessel for drawing-off water at pre-selected locations.

Basic Schematic Arrangement
of Vessel with multi draw off
Points (stratified energy store)

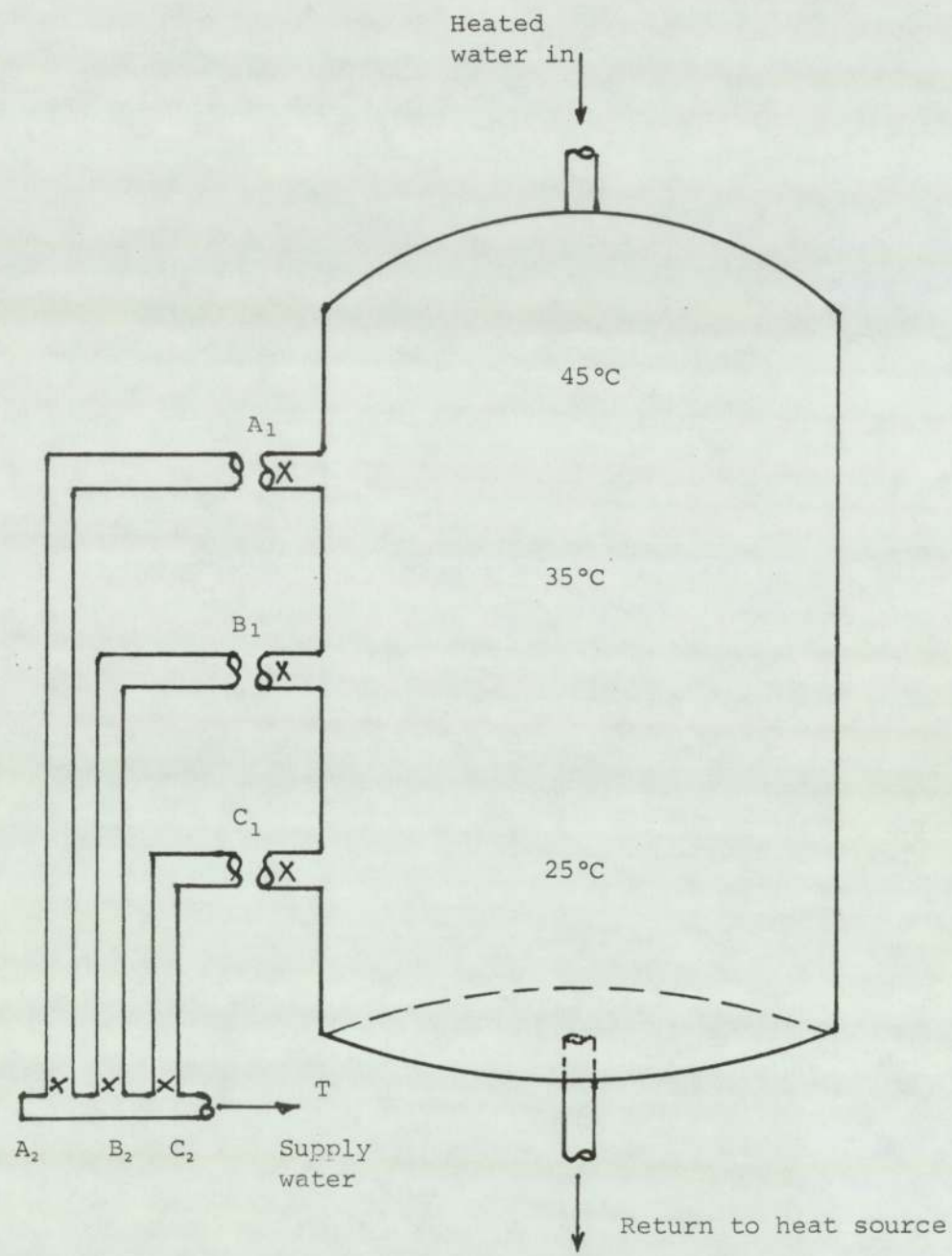


Fig.32.

6.3 Basis of a System for Commercial Application

Figure 32 is a basic schematic arrangement of a vessel with several draw-off points which allows the user to call for warm, tepid or preheated water when required. The degree of sophistication of control features can be extensive. The store vessel shown has a three nodal arrangement; when the desired temperature is selected on tap "T" then, through a feed back control circuit, two pairs of valves - say ($A_1 A_2$) and ($C_1 C_2$) remain closed whilst water is drawn from tap B_1 through B_2 . Depending on the amount of water drawn there could be a change in the bulk store temperature of the "band" or stratified layer above the 35°C layer. If the change was significant then further hot water would be pumped into the top of the vessel.

The greater the number of draw-off points available the greater the range of temperatures become available. The result being less disturbance to the remaining thermoclines which, in turn, makes the system more acceptable to some applications, i.e. small to medium hotel kitchens. The degree of sophistication of the control system would need to be cost effective.

Larger systems would have fewer thermoclines which renders the control system less costly. A two-nodal system could usefully satisfy, as an example DH water requirement in an office complex or a preheat to a warehouse heating system.

CHAPTER SEVEN

7. Future Possible Applications for Heat Pumps with Thermal Energy Storage in the U.K.

The prospects for adopting thermal energy store systems in the U.K. may have been advanced through the rapidly changing design of light commercial developments.

Light commercial developments, or more specifically, large retail developments, sports complexes, hotels with conference facilities and large office/warehouse sites, provide a greater opportunity for the incorporation of sensible heat stores than purely residential or major industrial establishments.

Over the last decade many thermal energy storage schemes have been examined for potential development.

An examination of the performance of a residential annual energy storage scheme utilizing a three coil heat pump was carried out by Miller R S^[69] (1980). He concluded that annual energy storage was uneconomic.

A study by Vasilakis A D^[70] et al (1984) of space heating and domestic hot water systems for a multi-unit housing scheme in the USA suggested that a triple-integrated-appliance (TIA) scheme would be an efficient solution to a housing development where conventional system flue discharge was a problem. A TIA scheme employs electric heat pumps, electric resistance heating and electric air conditioning which are capable of achieving space heating efficiencies of 90% and domestic water efficiencies of approximately 85%.

Whilst the application of a heat pump and storage system in single or small residential establishments has not been a consideration in this study it is interesting to note that Mobil Oil^[71] commissioned a study of the annual heating costs of a modernized heating system, including heat pump, in a one-family house in the Federal Republic of Germany and not surprisingly found the results of this investigation were in favour of a conventional heating fuel oil or gas heating system for a 30 kW - one-family house.

A system similar in principle to the one outlined in Chapter Six is considered technically practical and possibly financially feasible within selected light commercial premises.

Large retail premises do not generally require domestic hot water supplies having water temperatures greater than 55°C to 60°C.

Hotel complexes would require domestic hot water at higher temperatures than those currently achievable using a heat pump alone and consequently a supplementary heat source would be necessary.

Heat pump based space heating systems could operate successfully in modern buildings, where high levels of thermal insulation are now a standard feature, supplying heat energy at much lower temperatures than has hitherto been the case.

Large modern open areas could usefully employ larger than conventional radiators for effective heat dissipation.

The system outlined in Chapter Six would therefore be beneficial in the larger retail shops, especially those situated in the enclosed malls or precincts which are currently in favour throughout the major towns and cities of the U.K.

Modern retail shop design incorporates a high degree of display lighting. These premises almost invariably have an electrical supply as the sole energy source. The shops are basically buildings within a building and have no

external walls. A situation experienced by Vasilakis^[70] and overcome by the TIA principle.

Because the enclosed malls or precincts are subjected to a controlled internal environment, designed to provide personnel comfort year-round, the individual shops do not experience the ambient conditions which shops in the older style High Street still suffer.

The level of ambient temperature and humidity sought in the public areas of malls, i.e. the concourse or walkways is generally in the range $23^{\circ}\text{C} \pm 2^{\circ}\text{C}$ with relative humidity in the range 50% to 65% RH.

With the high level of display lighting referred to earlier in the shops and the greater occupational levels achieved the shop environment can readily approach $28^{\circ}\text{C} - 29^{\circ}\text{C}$, Norrey M J^[72] (1987).

The current range of air conditioning equipment used in the majority of U.K. light commercial establishments to counteract the extreme conditions of enclosed malls include reverse cycle heat pumps. The units are either the outdoor package type, supplying ducted air with a predefined percentage fresh air make-up, or the split-package unit where the condenser is located externally which again requires an air duct system and depends on a change of air which is often drawn through the open shop door, from the mall.

Occasionally it is possible to site outdoor condensing units, similar to the Carrier model used for this research, at a distance external to the area being conditioned, in conjunction with an indoor fan coil unit.

These systems, however, are generally of the air-to-air type units as water supplies for a coil similar to the model discussed earlier is often not available.

Revisions in the thinking of property developers, planners, architects and end-users alike could readily alter the emphasis from air-to-air heat pump systems to a combination of air-to-water and water-to-air systems.

This would allow the use of sensible heat stores, and cooled water stores, to become a standard ingredient in the future design of large enclosed public areas.

Hoffman G H^[73] (1984) describes steps that could be taken to encourage the use of cool storage as referred to above. He argues that cool storage is a "promising" technology when used in conjunction with air conditioning systems.

The store vessel would perform as a "buffer" facility enabling the heat pump system to contend with short-term fluctuations in internal ambient conditions.

Recent developments in compressor design has culminated in the rotary vane compressor:

"The heart of the compressor is the computer generated stator. The complex geometry optimises blade accelerations and provides a large compression arc without affecting suction and discharge areas. the seal zone and careful matching of the blade root reduces the re-expansion volume to a minimum, improving performance at high compression ratios". Rotocold Limited^[74] (1987).

Compressor control systems are now also very sophisticated. The variable speed drive (VSD) units are:

".....designed to vary both frequency and voltage (of the power supply) automatically, and can also be set to provide a voltage boost to help overcome high/low speed starting torques". Mills M^[75] (1987).

The combination of a rotary vane compressor and variable speed drive unit provides even greater scope for the development of an economical heat pump and thermal energy store system by virtue of the following, more obvious, benefits as identified by Mills^[75].

- (i) Capacity control at high efficiency giving energy savings of up to 36%.
- (ii) Improved "seasonal" efficiency.
- (iii) Reduced overdesign capacity - providing savings on capital cost.
- (iv) Close control of temperatures at high overall efficiency.
- (v) Built-in "soft" starting to help reduce peak demand charges.
- (vi) Built-in power factor correction producing up to 12% savings in overall running costs due to reduction in marginal KVA charges.

An effectively designed heat store would also allow for an electrically driven heat pump unit to capitalize on the low tariff electricity periods.

The U.K. Government, through the Energy Technology Support Unit (ETSU) commissioned a study by Harmsworth B^[76] (1983) of sensible heat storage in water for examining the variation in the cost of heat storage with the method of store construction, store volume and store insulation.

Limited interest to date (1987) in the commercial production of such a system is apparent. Major changes in primary fuel price relativities and availabilities along with the prospect for off-setting a portion of the high capital cost of installation would be necessary before sensible heat storage systems become more universally acceptable.

7.1 System Economics

A design and evaluation project is currently being carried out by the Author to integrate a sensible heat store with an air-to-water heat pump based air conditioning system serving a large computer complex. The heat rejected at the computer room, which is operational 24 hours per day, 365 days per year, would be transferred to a water store of approximately 20,000 litres capacity. The heated water would ultimately be used as a pre-heat to a large adjacent warehouse and also for domestic hot water supplies to the attached three storey office block.

With the advent of most major U.K. industrial organisations embarking upon large in-house computer installations, the prospects for other heat recovery systems, employing heat pumps and thermal energy stores, should gain momentum.

Through the availability of an abundance of waste heat from systems where the initial major capital expenditure has been financially justified the additional capital cost of recovering, storing and distributing this heat energy is low in comparison.

Preliminary studies of a similar opportunity, as referred to above, by the Author suggests that a combination system shows paybacks of between 5 and 10 years.

In relation to the payback period of the initial major installation this period should be attractive.

The majority of problems associated with stratification in store vessels may ultimately be resolved and such vessels used in certain practical applications but further experimental work will be required to devise a suitable method for drawing off water at selected thermoclines so that the stratified layers are not distorted.

The effects of water draw-off have not been part of this research activity.

7.2 Summary of Main Results

- (i) The initial objectives established for the research project have been achieved.

Through pursuit of the stated secondary objectives the important physical characteristics of the overall system as identified below, have been discussed in Chapter 4.

Application of the purposed designed and assembled system performance monitoring facility enabled an examination of the heat store to be undertaken when thermal stratification was promoted and also where stratification was not sought.

The monitoring system, albeit limited by the available computing capacity, allowed for store water temperature patterns to be distinguished under different system operating conditions.

It has been possible to establish the changing rates of heat transfer taking place in various regions of the stores when stratification is, and is not, being promoted.

The discussion on test results included in Chapter 4 reveals that in the store where stratification is promoted the water temperature difference, top to bottom, of the store is more pronounced than in the non-stratified store, - see Graph 15 (page 201).

It is considered therefore that the jet entry conditions being experienced in each vessel differ. The heat transfer rate is also affected in accordance with the theoretical presentation in Chapter 3.

A more detailed study of the effects upon heat transfer rates through including a velocity diffuser device in the water flow should be considered.

Any further investigation would ideally "match" the profile of the diffuser to the velocity of flow and the store vessel physical dimensions.

Again, from Graph 15, it will be noted that from basically identical initial store water temperatures throughout the vessel height, the temperatures ultimately achieved in Vessel 1, at the respective monitoring positions were, in each case, greater than the temperatures achieved in Vessel 2.

This condition prevailed throughout tests performed under different operating conditions, e.g. different water flow rates, different running periods and ambient conditions.

Whether the temperature profiles resulted purely from changes in heat transfer performance or whether it was a function of physical construction of the system has not been established.

However, it is concluded that the non-parallel sided vessels distorted the temperature, hence velocity, patterns from those anticipated based on known behaviour for turbulent and/or laminar flow through tubes. The curves shown as (+ 70) and (+ 60) on Graph 20 reflect the temperature distortions.

Whilst it may be argued that similar vessel design applies in both vessels the water entry conditions are not identical, as explained above.

- (ii) An important feature of the research was that of employing standard, commercially available, components of various manufacturers in an overall system design.

Combining components from a number of sources should ultimately allow for systems to be purpose-designed to meet a variety of situations at an acceptable capital cost.

For one single manufacturer to establish short-run production facilities for the multiplicity of systems that could be encountered, would be uneconomic.

Before combining components of different manufacture into a commercial system an approach for matching the various component characteristics is required. Such an approach has been developed and discussed in this thesis.

A computer based routine for calculating individual component performance, using limited specification detail from publicity material, featured by manufacturers, has been prepared.

Where applicable universally accepted approaches for calculating enthalpy changes and heat transfer rates, for example, have also been incorporated into the computer routine for comparison purposes.

The results from using limited manufacturer specification detail, modified by the Author to suit computer terminology and to provide performance values at conditions other than design conditions, shows good agreement with known calculation procedure results.

For each system test undertaken the resultant data was processed and entered to the purpose-designed computer routine for calculating the system heat-balance. Ultimately the coefficient of performance (COP_H) of the compressor only and of the overall system in the heating mode was calculated.

Inaccuracies in either the data recorded under test or in certain of the calculation routines - particularly those manipulating manufacturer material - resulted in the need to occasionally "force" an energy balance.

The inaccuracies encountered however, could readily be overcome by employing a more powerful computer. A computer with greater operating memory would remove the need for curtailing input of operational data.

A typical example of where energy balance inaccuracies manifest themselves would be in the limited amount of data relevant to water store temperature capable of being processed by the computer.

The "spot" temperature readings recorded at commencement and completion of a test are less than representative of overall store behaviour. Average values of the test data recorded at the store vessels during a test would be equally unrepresentative.

Both methods of data entry are however necessary. Amongst the series of tests undertaken on individual system components were those on the evaporator and the condenser. Tests on the evaporator were completed to establish the limitations on system performance calculation accuracy through using single point air on, air off temperatures in the calculation routine. Results presented show that single point temperatures were acceptable.

Test results presented for abbreviating the input data relevant to the condenser also show that the level of inaccuracy from such an approach could be tolerated.

The computer model operation is dependent upon a combination of fixed and variable data availability.

Fixed data, compared to variable data discussed above, fulfills two prime functions in the computational routine. One feature of fixed data statements is that available computer operating memory is economically used. System data which remains unaltered irrespective of the test conditions prevailing is termed "fixed".

For the system under test one terms the length of water and refrigerant pipework as being fixed. Likewise the number of water pipework bends, elbows, valves etc, are all considered as being fixed.

Assigning such data to fixed data removes the need to manually enter the same data through the keyboard each time an evaluation is undertaken. However, the fixed data can be altered by accessing the relevant data statements in the computer program. Altering the data in this manner reduces the need to physically change the system configuration for deriving results for changed system designs. A series of "what if" situations can therefore be explored.

Greater computational facilities would also remove the need for off-line performance evaluation. Off-line performance evaluation can also be readily overcome in future projects.

- (iii) Combining the facilities which the computerised system model provides with data from the programmed sequence of tests it has been possible to develop a mathematical model of temperature stratification taking place in the store.

This model enables predictions of store temperature at various heights in the vessel after stated periods of heat pump operation.

Good agreement is achieved between predicted values and averaged measured values - ref Graph 25.

A limitation of the mathematical model is resultant upon the restricted computational facilities available. The initial data collection for model construction has been based on consecutive time periods for conditions at the selected heights in the store, rather than on the desired concurrent time period data collection.

As store conditions are continually changing during system operation these changing conditions cannot be catered for with the existing non-dynamic model; limitations on accuracy therefore prevail. A further limitation of the model developed during this research is that averaged results have been used for comparative purposes. Ideally, a "family" of curves based on data recorded at the many available monitoring positions during simulation tests would have provided the most appropriate comparative material.

Averaged results have been used primarily through limitations on the available on-line analogue to digital (A-D) equipment and computer capacity to handle concurrent test data.

- (iv) As the research programme progressed through initial system design, construction and operation phases, and the instrumentation and monitoring facilities developed, it became apparent that minor changes to the physical installation were necessary.

Amongst the relevant modifications were the inclusion of a vessel water discharge header situated in the return flow from the vessels to the circulating water pump and the condenser coil, ref. Fig. 21.

This header enabled some equalization of return water temperature to take place when both vessels were in circuit.

It also assisted in finely balancing the flow of water through each vessel.

Flow of water through the vessels was balanced primarily with the aid of handwheel valves at the vessel top entry position.

The specially designed vessel entry fitment - ref. Fig 17 - allowed for a visual indication of whether or not the flow through, one vessel was greater or less than the other. If the flow differed a back pressure built up in one vessel and water became visible in the relief line.

A further, important, modification to the system was the inclusion of a vortex eliminator - a plastic kitchen colander - over the vessels discharge port internally. This had the effect of reducing the influence of the pump suction on the flow regime developing in the store vessels.

- (v) A system for providing a thermal energy store in configuration with an air-to-water heat pump, similar in principle to the system upon which this research is based, can be a viable proposition in selected commercial environments.

As presented in this thesis a system could incorporate a facility for promoting thermal stratification in the store or include storage of a non-stratified condition.

Standard type systems suitable for application into a variety of situations would not necessarily be appropriate at the current stage of development. Each application must therefore be assessed on its merits.

Amongst the current limitations for developing commercially available systems similar to that presented are:

- (a) the relatively high capital cost of installation which adversely affects economic pay-back criteria
- (b) the physical size of an installation. This is primarily the size of storage facilities required. The market in which prototype systems could be employed would not, however, necessarily be limited on space
- (c) the functional features of a closed-loop hot water system.

If there is a requirement for drawing-off water from the storage to be replaced by fresh supplies of make-up water then the effectiveness of the store would be impaired.

7.3 Main Conclusions

- (a) An electrically driven air-to-water heat pump operating at design Coefficients of Performance in the heating mode is a suitable method for providing heat energy to a thermal energy store.

- (b) Results from the present research provide sufficient indication that a system is technically feasible. Component manufacturers plant specifications should be capable of forming the basis of a scheme proposal.

Greater attention to the design of a suitable store vessel is, however, essential.

- (c) A vessel designed to conform more closely with the needs of the system must provide improved heat transfer between fluids. The adverse effect of jet entry velocity upon thermal stratification, where desired, could be reduced or eliminated through improved design features.

- (d) With thermal stores operating in a closed-loop, direct contact mode without draw-off facilities, it is possible to predict reasonably accurately the store effectiveness.

The effects of draw-off have not been considered in this research.

- (e) The ultimate temperature achievable of water heated using an electrically driven heat pump of the type used is currently limited to approximately 55°C.

This temperature could, however, be raised using for example an electric resistive heating element of the immersion type.

This obviously affects both system capital and operating costs.

- (f) In section 1.3.1 it was stated that a major reason for limited use of heat pumps to date had been the higher capital cost in relation to other, conventional, systems.

The capital cost relativity is now reducing in favour of heat pumps.

Also, in many of the more likely instances where heat pumps and thermal storage are beneficial the economic availability of alternative fuels is becoming limited.

Pabon-Diaz has indicated that heat pumps "usually require a three phase electrical supply". This is no longer the case as the new range of equipment is also of single phase design. An inverter unit is also incorporated which reduces significantly the electrical consumption but also allows for a wider range of operating speeds. Amongst the obvious advantages here are the precise load matching

facility and reduced running costs through increased compressor efficiency. This is quoted by manufacturers to be 39% greater than the existing piston compressors.

The effects of the new design compressors on equipment maintenance has yet to be ascertained but through a reduced number of compressor components in the scroll or rotary vane compressor compared to the hermetically sealed piston type units, and the variable speed facility which reduces cyclic operation, as referred to in Chapter 1, the maintenance costs must be considerably reduced.

The need for supplementary heat using resistive type heaters has been removed by the new design of reverse cycle heat pumps. This again reduces the initial capital cost of the equipment and should significantly reduce running costs on an air-to-air based system.

7.4 Recommendations for Future Work

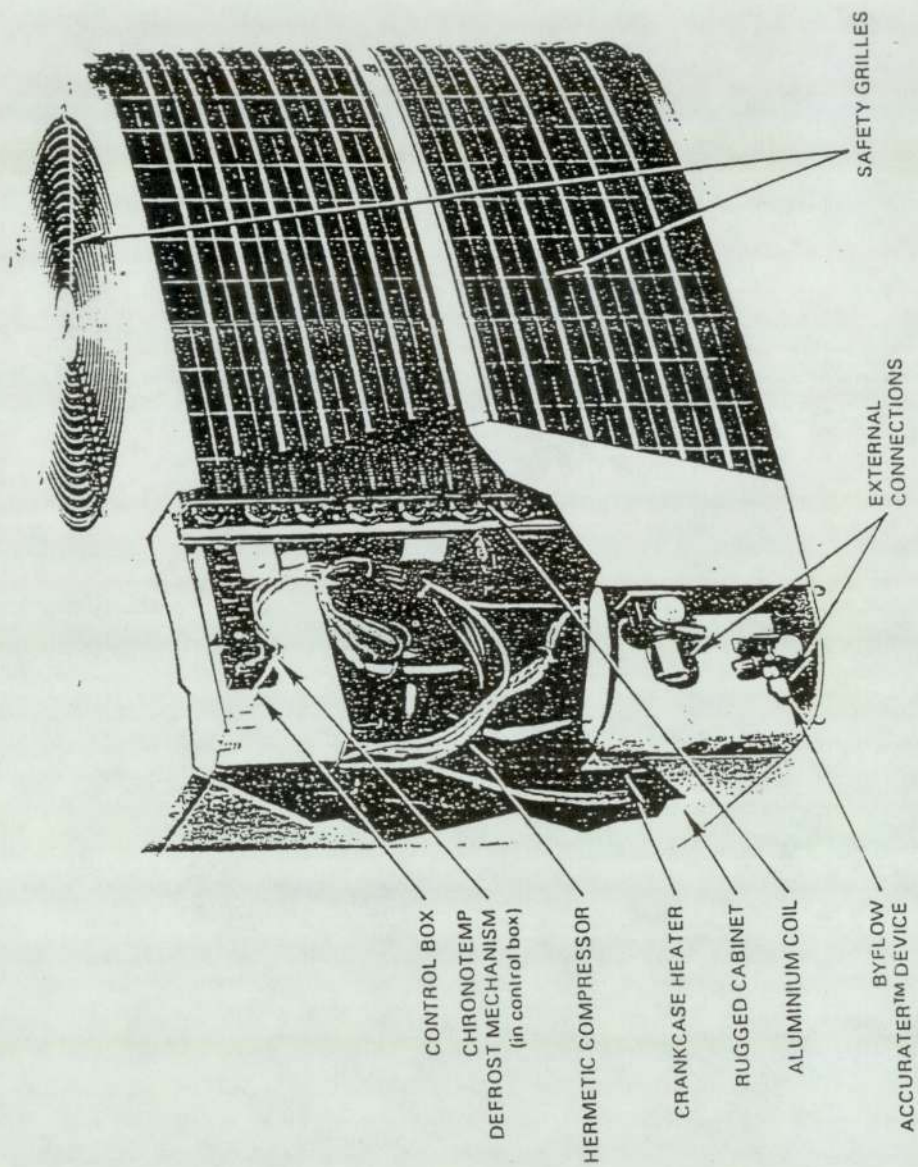
- (a) Develop further the system design, especially related to the physical dimensions of the storage vessel, beyond that design employed here.

Particular emphasis should also be given to increasing the computing capacity, the concurrent monitoring/recording facilities and development of an on-line dynamic system model.

- (b) Increased understanding of actual heat transfer mechanisms, based on improved theoretical understanding of three dimensional unsteady state conditions would further improve the accuracy of a predictive model of store performance.

- (c) Install prototype thermal energy storage systems which incorporate an electrically driven air-to-water heat pump into selected practical applications.

These systems should be evaluated both technically and financially and compared with similar systems employing conventional heating units.



View of 38 CQ heat pump outdoor section

Fig 33

Appendix 1

Heat Pump Specification

Carlyle 38 CQ (split system - outdoor section)

Unit	38 CQ 027
Operating weight	78.1 kg
Nominal cooling capacity	6680 Kcal/h (7.769)kW
Nominal heating capacity	7180 Kcal/h (8.35) kW
Refrigerant	R ₂₂
Refrigerant control	Accurater (Biflow)
Compressor	Hermetic
Cylinders	2
Speed (RPM)	2900
Fan	propellor type, direct drive
Air discharge	vertical
Air quantity	4590 m ³ h ⁻¹
Motor power input	0.19 kW
Motor speed	1100 RPM
Coil	plate fin
Number	1

Appendix 1 cont....

Fin spacing	1.3 mm
Face area	0.65 m ²
Rows	1.5
Connections - vapour	$\frac{3}{4}$ " flare fitting
" - liquid	$\frac{3}{8}$ " compatible fitting
Refrigerant line sizes	
- suction	$\frac{3}{4}$ "
Refrigerant line sizes	
- liquid	$\frac{3}{8}$ "

Appendix 2

Analogue to Digital Conversion Unit - Manufacturers Material

The Analogue to Digital (A-D) unit used was the CIL Model PCI 1002 suitable for use on the IEEE Bus which is compatible with the Commodore Business Machine (CBM) micro-computer.

The CIL units have selectable device numbers, selectable in the range 0 - 14. Device number 4 is reserved for the CBM machine.

In accordance with IEEE recommendations the maximum bus extension from the CBM is 20 metres. The maximum interdevice spacing is 15 metres and the number of devices limited to 15.

Under operating conditions the inputs to the CIL are scanned displaying the output in BITS for channels CH1 and CH2, and in temperature for channels 4 - 15 inclusive.

CH3, the cold junction channel, being added in software, is followed by the range set.

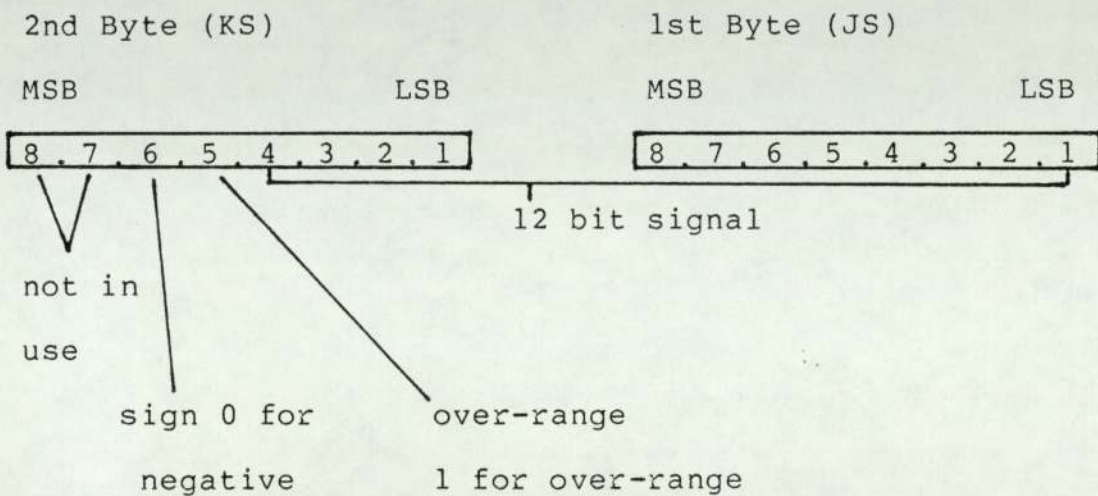
The input range is internally set to 10 mV; 30 mV or 100 mV full scale deflection. The desired range is selected based on the following table.

Table 6

Desired Range for Setting the A-D unit

Thermocouple Type	Range 1 (± 10 mV)	Range 2 (± 30 mV)	Range 3 (± 100 mV)
J	- 210 to + 186	up to 545	up to 1200
K	- 270 " + 245	" " 720	" " 1370
T	- 270 " + 212	" " 400	" " --
S	- 50 " + 1035	" " 1760	" " --
R	- 50 " + 962	" " 1760	" " --
E	- 270 " + 152	" " 413	" " --
B	0 " + 1492	" " 1820	" " --

The analogue to digital conversion is provided by the dual slope converter ICL 7109. The data output of this device consists of two bytes (two eight bit words) as illustrated.



Channel selection is carried out by the secondary address. In CBM program syntax is:

OPEN, 1, 10, X.

```
1 being the file number
10  "      "  device number
X   "      "  channel number.
```

Appendix 2 cont.....

Channel 0 - is internally connected to a proportion of
the power supply.

Values are approx.	4000 bits for	10 mV range	
	1333	" "	30 mV "
	400	" "	100 mV "

Channels 1 and 2 - are directly connected to the multi-
plexer and are high level single
ended input connections.

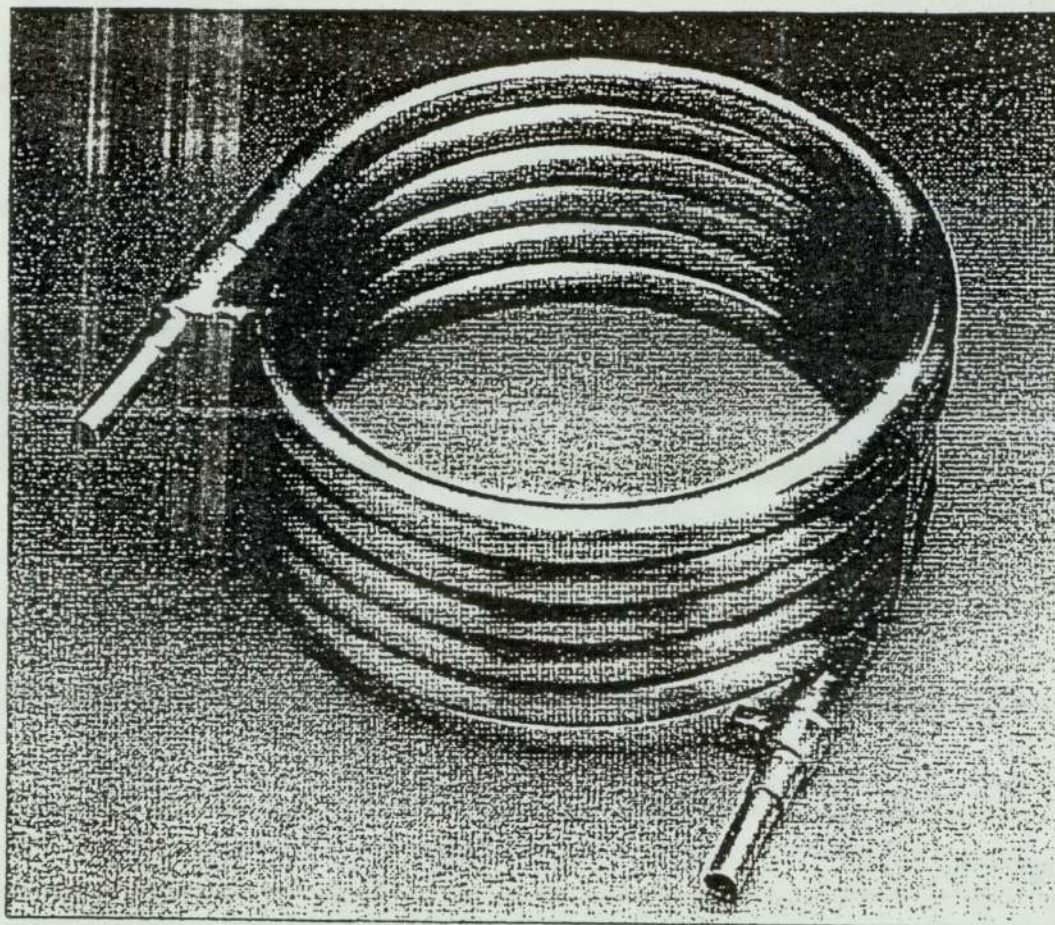
Channel 3 - is internally connected to the platinum
resistance thermometer on the Cold Junction
Circuitry (CJC).

Channels 4 - 13 - are connected via thermocouple material
plugs and socket, and cable to the CJC.

The PCI 1002 produces data which is linear with mV
rather than with temperature. Linearization is carried out
in software by a polynomial expansion (4th Order).

For improved accuracy individual thermocouples require
to be individually calibrated.

Re-calibration is carried out internally to the CIL
unit.



Truco coaxial condenser K 7-13 WT

Fig. 34.

Appendix 3

Truco Co-axial Condenser Coil

Co-axial condenser	K7 - 13WT
Water connection	d_1 22 mm OD
Refrigerant connection	d_2 22mm OD
Maximum dimensions - A	360 mm
- B	355 mm
- H	310 mm
Other dimentions - a	315 mm
- c	29 mm
- h	265 mm
- D	35 mm
Weight (approx)	17 Kg
Capacity range	6400-17630 W

(6.4-17.63) kW

Capacity range - is based on the following:

Refrigerant	R ₂₂
Condensing temperature	45°C
Condensing medium	water
Water inlet temperature	35°C
Water flow velocity	0.55 to 1.475 ms ⁻¹
Pressure loss of water	0.0433 to 0.23 bar
Material type	SF-Cu to DIN 1787
Permissible operating pressure	26 bar

(See also Fig. 4. in text)

Appendix 4

Derived Laws for Determining Absolute Pressure - Temperature/Enthalpy

(a) Evaporating phase (saturated liquid)

$$E_1 = 10.37128 + 0.25825 S_L + 0.0004625 S_L^2$$

Examples:

$S_L = 28^\circ\text{F}$	calculated value	17.96	btu/lb;	Tables	18.17	btu/lb	
$= 10^\circ\text{F}$	"	"	13.00	btu/lb;	"	13.29	btu/lb
$= 36^\circ\text{F}$	"	"	20.26	btu/lb;	"	20.49	btu/lb

(b) Evaporating phase (saturated vapour)

$$E_2 = 104.91093 + 0.10925 S_V - 0.0001875 S_V^2$$

Examples:

$S_V = 28^\circ\text{F}$	calculated value	107.82	btu/lb;	Tables	107.93	btu/lb	
$= 10^\circ\text{F}$	"	"	105.98	btu/lb;	"	106.08	btu/lb
$= 36^\circ\text{F}$	"	"	108.60	btu/lb;	"	108.71	btu/lb

Appendix 4 cont.....

(c) Condensing phase (liquid)

$$E_3 = 9.6502 + 0.287675 C_L + 0.0002555 C_L^2$$

Examples:

C_L = 70°F calculated value 31.04 btu/lb; Tables 30.99 btu/lb
= 116°F " " 46.46 btu/lb; Tables 46.44 btu/lb

(d) Condensing phase (vapour)

$$E_4 = 103.88 + 0.149655 C_V - 0.0005777 C_V^2$$

Examples:

C_V = 70°F calculated value 111.53 btu/lb; Table 111.49 btu/lb
= 116°F " " 113.47 btu/lb; " 113.42 btu/lb

(e) Enthalpy of superheated vapour

(Based on curves within the range 160 psia and 220 psia and
constant temperature lines 100°F - 120°F

$$\text{Enthalpy} = 97.48 + 0.1675 t + 0.00005 t^2$$

t being temperature (°F).

Appendix 5

Air Temperature Distribution at Evaporator Coil (Inlet and Outlet)

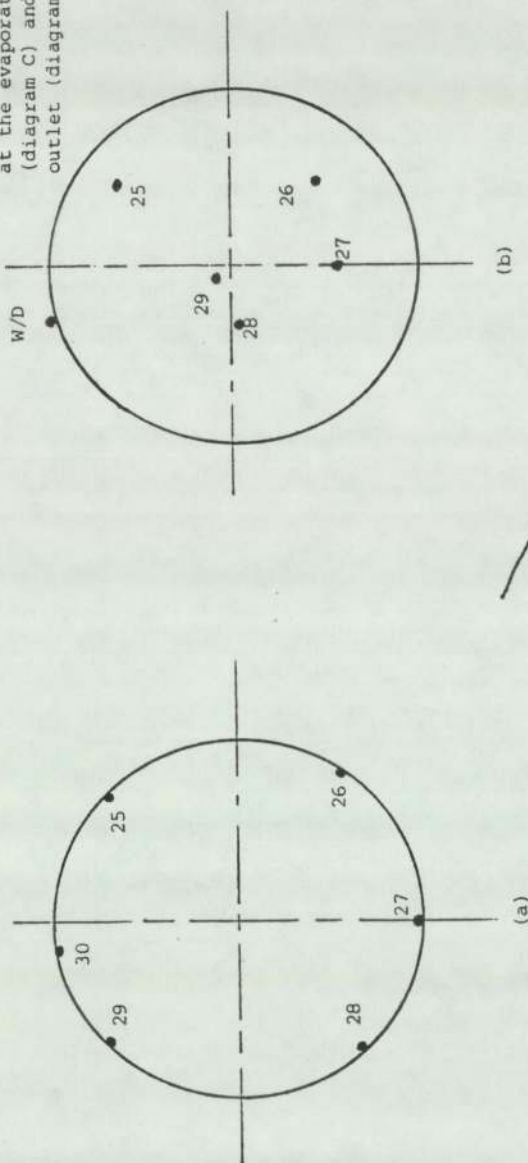
Examination of the air temperature distribution at the evaporator, for ascertaining a representative single-point position for continuous monitoring of air entering and leaving the evaporator, was based on measurements of the following parameters:

- (a) Dry bulb temperature of air to the evaporator
- (b) Wet " " " " " "
- (c) Dry " " " " from the evaporator
- (d) Wet " " " " " "

Initially 6 thermocouples were located selectively across the evaporator fan discharge port. A wet/dry bulb (W/D) thermometer and a single mercury-in-glass (m-i-g) thermometer were also used to register temperatures, these were located at intervals, adjacent to the various thermocouples (T/c) positions for comparative purposes.

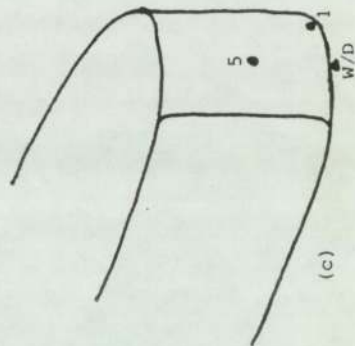
Ultimately, for a different series of test runs, two additional T/c's and a W/D bulb unit were located at the evaporator inlet area.

Location of thermocouples
at the evaporator inlet
(diagram C) and evaporator
outlet (diagrams (a) and (b)).



25 - 30 (thermocouples)
all at outer radius

T/c 25 @ 18.5 cm
T/c 26 @ 13.5 cm
T/c 27 @ 8.5 cm
T/c 28 @ 3.5 cm
T/c 29 @ centre position



1 and 5 (thermocouples)
W/D (Wet/Dry mercury-in-glass) thermometer

Fig 35 (a) (b) (c)

Appendix 5 cont....

The results referred to below are typical of those recorded over a period of 1.5 hours heat pump operation. The readings were recorded at 10 minute intervals and the original 6 T/c's were located at the air outlet as indicated in the sketch (Fig 35 (a) and (b)).

The T/c's were each secured at the outlet grill which is 4" above the discharge fan blade tips.

For the purpose of each test the heat pump was in operation for at least 10 minutes prior to commencement of the recordings via the the T/c's and other instrumentation. This allowed for some stability of air temperature to be achieved and the T/c's to be cross-calibrated. A printout of recorded temperatures, in °C, was obtained. The Analogue to Digital (A-D) unit channels 4 to 9 inclusive were used for T/c positions indicated in Fig. 35 (a).

The readings recorded at T/c 28 - this T/c was not in the air stream but attached to the heat pump body panel and was used primarily to identify any "drift" at the A-D unit; the readings were therefore not used in the manipulations shown below.

Appendix 5 cont....

Table 7 (Relevant to Fig 35a)

T/c number/ position	Average air temp °C	Overall average temp °C	Temp min/ max °C	Mean temp of range °C	Average temp of mean °C	Number of read's
1	-	-	-	-	-	-
5	-	-	-	-	-	-
25	19.16		18.1 19.5	18.8		20
26	17.99		17.8 18.2	18.0		20
27	17.29	17.95	16.9 17.6	17.25	17.86	20
28	-		- -	-		-
29	16.87		16.5 18.0	17.25		20
30	18.38		17.0 19.0	18.0		20

Average wet/dry air temperature at evaporator outlet
16.32/19.92°C

Range of wet and dry air temperature at evaporator outlet
(15.3-19.0) (19.75-20)°C

Average air temperature (mercury-in-glass) at evaporator
outlet 20°C.

Range of air temperature (mercury-in-glass) at evaporator
outlet 19.0 - 21.75°C.

Appendix 5 cont.....

The initial readings on the printout, row 1, columns 5-9 inclusive reflect ambient temperatures in the laboratory at the commencement of a test. The range of readings suggests complete mixing of discharge air is not taking place at the evaporator outlet, whereas the readings in columns 10-15 inclusive reflect the accuracy/stability of the A-D unit. Readings on the printout recorded immediately following heat pump shutdown show a distinct increase from earlier readings.

The trend, and derivation, of readings taken with the heat pump shutdown reflect the effects other equipment, e.g. liquid nitrogen producing plant, installed in the laboratory, has on ambient conditions within the laboratory.

The tabulated data shown as Table 7, is taken from a typical test sequence.

Tests for determining air temperature patterns were also taken for different test durations. The results discussed below are typical for a 2 hour 10 minute duration. In these tests 8 T/c's were employed. Of these, 6 T/c's were located at the air outlet grill (as for the previous discussion) but at different radii on the outlet grill - see the Fig 35 (b). Two T/c's were located at the evaporator inlet grill (Fig.35 (c)).

Table 8 (relevant to Fig's 35 (b) (c)

T/c number/ position	Average air temp °C	Overall average °C	Temp Range (min-max) °C	Mean Temp of range °C	Average temp of °C	Number of reading
1	22.97	22.65	22.7-23.4	23.05		13
5	22.96		22.7-23.4	23.05		13
25	20.5		20.2-20.9	20.55		13
26	18.72		18.6-19.0	18.80		13
27	18.83	19.15	18.7-19.1	18.90	19.24	13
28	-		-	-		--
29	18.5		18.3-19.1	18.70		13
30	19.21		18.9-19.3	19.30		13
Average air temperature	(W/D bulb)	(W/D bulb)	at evaporator outlet		18.13/21.25°C	
Range of air temperature	(W/D bulb)	(W/D bulb)	" "	" "	(16.75-19.5)/(21-21.5)°C	
Average air temperature	(mig)	(mig)	" "	" "	(22.05°C)	
Range of air temperature	(mig)	(mig)	" "	" "	(21.1-23.0)°C	
Average air temperature	(W/D bulb)	(W/D bulb)	evaporator inlet		17.9/21.5°C	
Range of air temperature	(W/D bulb)	(W/D bulb)	" "	" "	(17.5-18.3)/(21.7-22.2)°C	

Appendix 5 cont....

A pair of W/D bulb thermometers were also situated as shown in the figures; a further mercury-in-glass thermometer was positioned as shown.

A printout of test results upon which the following comments are based is shown as page 327. The analysis of test results are summarized in Table (8).

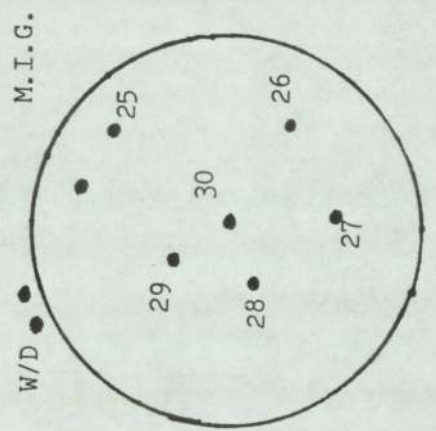
It will be noted that air temperatures leaving the evaporator coil through the outlet port are consistently greater at the outer radii than those recorded elsewhere, however, the centre position temperatures are greater than those recorded at the intermediate radii.

There are only slight variations in the temperature at the outer radius over the test duration - this being confirmed by readings from the T/c, the W/D bulb and mercury-in glass thermometer.

An overall average reading from the readings recorded at all locations gives a value of 19.15°C. This compares closely to the average value of the "mean" of each range, i.e. 19.24°C. Both values referred to above are in close proximity to the average reading taken at the central position of the discharge area, i.e. T/c 30 (channel 6 on the A-D) at 19.21°C.

Spatial air temperatures
at evaporator
(Test 20.06.84)

1200584		System records									
		T/C	27	30	29	26	25	1	5		
9	1	959	24.2	22.6	21.9	21.5	21.7	22.2	22.9	24.2	24.2
7	1	1032	26	19	19.7	18.7	20.6	22.9	22.7	25.9	25.2
5	0	1086	27.3	18.9	18.9	19	20.9	22.9	22.9	27.1	26.5
0	6	1124	28.9	19.1	19.6	18.9	20.9	22.9	22.9	27.4	26.9
0	1	1150	28.9	19.3	18.9	18.6	20.6	22.9	22.9	28.1	26.9
0	1	1164	29.9	18.9	19.9	18.9	20.6	22.9	22.9	28.4	26.9
7	0	1172	29.4	19	19.2	18.5	20.6	22.7	22.9	28.6	26.4
0	2	1176	29.5	18.9	19.1	18.9	20.6	22.9	22.9	28.9	26.5
0	1	1180	29.6	18.9	19	18.4	20.4	22.7	22.9	28.9	26.6
0	6	1180	29.7	18.9	19.1	18.4	20.5	22.9	22.9	29.7	26.7
5	1	1187	29.9	18.7	19	18.9	20.4	22.9	22.9	29.9	26.9
1	6	1191	29.9	18.9	19	18.9	20.9	22.9	22.9	29.9	26.9
0	1	1194	30	18.7	18.9	18.6	20.4	22.9	22.9	29.9	26.9
4	1	1196	30	18.7	18.9	18.7	20.9	22.9	22.9	29.9	26.9
1	1	1204	30.2	23.5	25.1	24.4	26.5	27.1	29.9	30.1	29.2
7	3	1226	30.9	24	26.6	23.9	27.9	24.7	24.6	30.9	29.7
0	1	1251	31.4	24.4	26.1	24.6	27.7	25.2	25	31.6	31.4
-1	2	1276	32	24.9	26.2	24.7	26.9	25.6	25.4	32.2	31.1
0	0	1299	32.5	25.9	25.9	24.9	27.1	25.7	25.8	32.4	31.7
4	7	1320	33.1	25.9	25.5	24.2	26.7	27.5	26.4	32.6	32.2



All readings at 10 minute intervals.

Table 9

Air Temperature Comparisons

(Averaged Spacial viz Central Position)

Average Temp of T/c's (25,26,27,29)	Temp at centre position (T/c 30)
19.35 °C	19.7 °C
19.40	19.6
19.42	19.6
19.15	19.3
19.17	19.3
19.20	19.2
19.0	19.1
19.0	19.0
19.0	19.1
19.0	19.0
19.0	19.0
19.0	18.9
18.9	18.9
19.12	19.2

Appendix 5 cont....

The trend of readings taken at the central position T/c also reflects, more so than those at the outer radius, the change in air temperature to be expected at the air discharge, when the heat pump is operating in the heating mode, in a semi-enclosed (laboratory) environment. Out-of-door conditions would obviously be much different as a result of wind movement etc.

From the table (Table 9) it will be noted that the T/c reading at the central position (T/c 30), for each time interval is very close to the average of readings taken at the remaining T/c positions, excluding T/c 28.

Temperatures recorded manually on the mig thermometer reflects the rather static condition of the laboratory environment referred to earlier but suitably reflects the ambient air temperatures existing when the heat pump is not in operation, i.e. before and after the test period (T/c readings on channels 5-11 inclusive).

Examination of the T/c readings referred to as T/c's 1 and 5 (channels 10 and 11) suggests a very steady state exists at the evaporator inlet with respect to air temperature. This is confirmed by the readings noted at the W/D bulb thermometer. It can be concluded from data in

Appendix 5 cont.....

tables 8 and 9 that average readings, the range of readings and the mean range at both locations are in close proximity.

From further tests of longer duration, i.e. between 3.5 and 4.5 hours of heat pump operation, similar patterns of air temperature variations remained. It is, therefore, concluded that for all subsequent tests and for heat pump performance calculations the air outlet and inlet, wet and dry bulb temperatures, would be recorded central to the air discharge port and from a central position at the front air inlet grill to the evaporator coil.

The graphs presented as Graph 3 and Graph 4 (Section 4.1) show the values recorded during "typical" tests discussed in this Appendix.

Appendix 6

Condenser Coil - Derivation of Formulae

(Based on manufacturers data)

$$\text{Coil condensing capacity } Q_C = \frac{Q_E}{f_k \times f_m}$$

Q_E = real condensing capacity

f_k = correction factor for change in
condensing temperature (from design)

f_m = correction factor for change in cooling
medium (other than water).

For condensing temperatures less than 45°C.

$$f_k = 1.0 + ((C_3 - 45) \times \frac{(1.0 - 1.03)}{10})$$

For condensing temperatures greater than 45°C.

$$f_k = 1.0 + ((C_3 - 45) \times \frac{(0.92 - 1.0)}{15})$$

For the K7 - 13WT coil with a water flow rate in the range $0.55 - 1.475 \text{ m}^3 \text{ h}^{-1}$, and temperature difference of 10°C (between condensing temperature (V_k) and water outlet temperature (V_{wa})), used in conjunction with the manufacturers curves of performance, gives the relevant capacity (CC) Kj Hr^{-1} and ΔP_w (pressure loss of water (Bar)).

Appendix 6 cont....

Derivations (from mfr. curves)

(a) f_k : when $C_3 = 45^0\text{C}$, $f_k = 1.0$; $\Delta t = 10^0\text{C}$: $.f_k = -0.03$

when $C_3 = 35^0\text{C}$, $f_k = 1.03$; $\Delta t = 1^0\text{C}$: $.f_k = -0.003$

so $f_k = 1.0 + ((35 - 45) \times (-0.003))$
 $= 1.0 + ((-10) \times (-0.003))$
 $= 1.03$

(b) Δp : (calculated from water flow rates W_r)

$1.475 - 0.55 = 0.925 \text{ m}^3 \text{ hr}^{-1}$

$0.23 - 0.0433 = 0.1867 \text{ Bar}$

therefore it is assumed that for a linear relationship
 $0.1 \text{ m}^3 \text{ hr}^{-1}$ variation within the stated
range $\equiv 0.0202 \text{ Bar}$

so for water flow rate $x \text{ m}^3 \text{ hr}^{-1}$

$$\Delta p \equiv (0.0433 + ((\frac{W_r - 0.55}{0.1}) \times (0.0202 \times 0.8746))) \text{ Bar}$$

where $0.8746 = \cos Q^\circ$ (or slope of the manufacturers
water flow rate curve).

Appendix 6 cont....

As an example:

when

$$W_R = 0.7 \text{ m}^3 \text{ hr}^{-1} : \Delta p = 0.0433 + \left(\frac{0.7 - 0.55}{0.1} \right) \times (0.0202 \times 0.8746)$$

$$\Delta p = 0.0433 + (0.02651)$$

$$\Delta p = \underline{0.0698} \text{ cf } \underline{0.07} \text{ Bar (taken from}$$

manufacturers published curves).

(c) Relationship between water flow rate (W_R); water flow velocity (F_V) and condensing capacity (CC).

$$0.5 \text{ ms}^{-1} \equiv 23040 \text{ Kj (6400 W) and } 0.55 \text{ m}^3 \text{ hr}^{-1}$$

$$1.8 \text{ ms}^{-1} \equiv 63468 \text{ Kj (17630 W) and } 1.475 \text{ m}^3 \text{ hr}^{-1}$$

therefore it is assumed that a linear relationship exists
so for difference of

$$1.3 \text{ ms}^{-1} \equiv 40468 \text{ Kj and } 0.925 \text{ m}^3 \text{ hr}^{-1}$$

$$\text{so } 0.1 \text{ ms}^{-1} \equiv 4904.62 \text{ Kj and}$$

$$0.1 \text{ m}^3 \text{ hr}^{-1} \equiv 0.14 \text{ ms}^{-1}$$

Appendix 6 cont....

with the water flow rate (W_R) within the stated range then

$$F_V \text{ (flow velocity)} = (0.5 + (\frac{W_r - 0.55}{0.1}) \times 0.14)$$

$$\text{for } W_R = 0.7 \text{ m}^3 \text{ hr}^{-1}; F_V = (0.5 + (\frac{0.7 - 0.55}{0.1}) \times 0.14)$$

$$= \underline{0.71 \text{ m/s}} \text{ cf } \underline{0.7 \text{ m/s}}$$

(taken from manufacturers published curves).

also condensing capacity (CC) Kj/hr

becomes

$$CC = (23040 + (\frac{F_V - 0.5}{0.1}) \times (4904.62 \times \sin Q))$$

$$\sin Q = 0.7314 \text{ or slope of curve,}$$

therefore

$$CC = (23040 + (\frac{0.71 - 0.5}{0.1}) \times ((4904.62 \times 0.7314)))$$

$$= \underline{30573 \text{ Kj}} \text{ cf } \underline{30600 \text{ Kj}} \text{ from manufacturers}$$

published curves.

Thus the computed values using the above procedure can be used in the system model.

Appendix 7

Sample Calculations Based on Actual Test Data

(Derivation of heat transfer co-efficient)

Measured water volume flow rate	$0.851 \text{ m}^3 \text{ hr}^{-1}$
Vessel external wall surface temperature	20°C
Vessel inlet port diameter	17 mm
Water inlet temperature to vessel (at heat pump start-up)	24.2°C
(after 210 minutes heat pump operation)	33.8°C
Water temperature distribution through vessel	
Thermodynamic properties of water @	30°C (303K)
ρ (density)	995.2 kg m^{-3}
β (thermal expansion co-efficient)	$0.18 \times 10^{-3} \text{ K}^{-1}$
C_p (specific heat @ constant pressure)	$4178.5 \text{ J Kg}^{-1} \text{ K}$
k (thermal conductivity)	$0.615 \text{ WM}^{-1} \text{ K}$
α (thermal diffusivity)	$0.147 \times 10^{-6} \text{ ms}^{-1}$
μ (absolute viscosity)	$8.25 \times 10^{-4} \text{ N.sm}^{-2}$
V (kinematic viscosity)	$0.832 \times 10^{-6} \text{ m}^2 \text{ s}^{-1}$
Pr (Prandtl number) from Tables	5.40

Appendix 7 cont....

$$\begin{aligned} \text{Average water velocity} & \frac{(0.851)}{2} \\ \text{(in supply P/wk)} & \frac{3600}{\left(\frac{\pi 0.017^2}{4}\right)} = \frac{0.000118}{0.000227} \\ & = \underline{0.52 \text{ ms}^{-1}} \end{aligned}$$

$$\text{Reynolds number } \frac{\rho V_{av} D}{\mu} = \frac{995.2 \times 0.52 \times 0.017}{8.25 \times 10^{-4}} = \underline{10664}$$

this suggests a turbulent flow regime at the vessel inlet port.

Prandtl number (calculated)

$$\frac{C_p \rho V}{k} = \frac{4178.5 \times 995.2 \times 0.0832 \times 10^{-6}}{0.615} = \underline{5.41}$$

The calculated Prandtl number compares with the tabulated value of 5.40.

Mass flow rate of water

$$\begin{aligned} \dot{M} &= \rho \frac{\pi D^2}{4} V_{av} \\ &= 995.2 \times \frac{\pi}{4} \times 0.017^2 \times 0.52 = \underline{0.226 \text{ kgs}^{-1}} \end{aligned}$$

Appendix 7 cont.....

For turbulent flow the average convective heat transfer coefficient (\bar{h}_c) is:

$$\bar{h}_c = \frac{k}{D} 0.023 Re^{0.8} Pr^{0.33} \quad (\text{Eqn 72}) \quad (\text{page 151})$$

$$= \frac{0.615}{0.92} \times (0.023 \times (10664 + 0.8)) \times (5.41 + 0.33)$$

$$= 44.78 \text{ WM}^{-1} \text{ K at the vessel wall internal surface.}$$

NB. The value "D" in the above equation is the internal diameter of the vessel - where the heat transfer takes place.

The value " \bar{h}_c " suggests that heat transfer is within the range attributed to free convection and marginally outside the range of forced convection, (see Chapter 3.4.2).

Rate of heat transfer per metre length of vessel

Appendix 7 cont....

$$q^1 = \bar{h}_c \pi D (T_S - T_B) \quad (\text{see Eqn. 73) (page 151).}$$

$$= 44.78 \times \pi 0.92 \times (293 - 303)$$

$$= \underline{- 1295 \text{ W}}$$

where T_S = external wall temperature
of vessel (K)

T_B = average temperature of
incoming water (K)

Nusselt number (Nu) i.e. the ratio of temperature gradients
for the fluid, evaluated at
the wall-fluid interface.

Is calculated:

Nu (for 0.5 Pr 200) Based on eqns. 81 and 82 (page
157).

Appendix 7 cont....

$$= \frac{\left(\frac{(1.82 \log_{10} (Re) - 1.64)^{-2}}{8} \right) \times Re \ Pr}{1.07 + 12.7 \sqrt{\left((1.82 \log_{10} (Re) - 1.64)^{-2} / 8 \right) \times (Pr^{0.66} - 1)}}$$

$$= \frac{3.859 \times 10^{-3} \times 10664 \times 5.41}{1.07 + (12.7((3.859 \times 10^{-3})^{1/2}) \times ((5.41^{0.66} - 1)))}$$

$$= \frac{222.671}{2.6851}$$

$$= \underline{82.92}$$

The local convective heat transfer co-efficient (h_1) becomes

$$h_1 = \frac{k \ N_u}{D} = \frac{0.615 \times 82.92}{0.92} = \underline{55.43} \text{ WM}^{-1} \text{ K}$$

The mean Nusselt number (N_{um}) for an abrupt contracted entrance and for $\frac{L}{D}$ 20 is; (according to Rohsenow et al)

$$N_{um} = \left(1 + \frac{C}{(L/D)} \right) Nu$$

Appendix 7 cont.....

where C for an abrupt contraction entrance = 6

therefore

$$N_{um} = (1 + \frac{6}{(\frac{1.15}{0.17})}) \times 82.92 = \underline{90.27} \text{ WM}^{-1} \text{ K}$$

With a Reynolds number of approximately 10,000 and a vessel "length to diameter" ratio $(\frac{L}{D}) = (\frac{1.15}{0.92}) = 1.25$, it will be noted from Rohsenow's curves that the Nusselt number $82.92 \text{ WM}^{-1} \text{ K}$ is at a point where complete stability of flow has not been achieved and therefore a fully established temperature profile within the vessel does not exist.

A fully developed temperature profile could only exist with the above values for Re and Nu if the vessel "length to diameter" ratio 4.

Appendix 8

Heat Transfer at Store Vessel

Determination of the amount of energy transferred to store during heat pump operations is an important aspect of achieving an energy "balance" throughout the system - as discussed on page 257.

Below are two approaches adopted for these series of tests. The values are typical test results.

Approach (a) (Referred to in program syntax)

Calculation of energy stored based on START/FINISH temperatures of stored water.

Vessel 1

Height of fixed T/c (cm)	Start Temp °C	Finish Temp °C
115	(w ₄) 23.4	(x ₄) 29.8
85	(w ₃) 22.8	(x ₃) 29.2
27.3	(w ₂) 23.1	(x ₂) 26.9
0	(w ₁) <u>20.7</u>	(x ₁) <u>20.9</u>
Average temp °C	<u>22.5</u>	<u>26.7</u>

Appendix 8 cont.....

Vessel 2

Height of fixed T/c (cm)	Start Temp °C	Finish Temp °C
115	(w ₈) 23.9	(x ₈) 28.9
83	(w ₇) 25.0	(x ₇) 29.8
40.3	(w ₆) 24.4	(x ₆) 25.8
0	(w ₅) <u>20.9</u>	(x ₅) <u>20.9</u>
	<u>23.55</u>	<u>26.35</u>

where w₁ - w₈ and x₁ - x₈ refer to start/finish at T/c heights.

The total energy stored in the vessels can be calculated using the following:

$$Q_t = M C_p \Delta t$$

where

M = mass of water

C_p = specific heat of water

Δt = rise in temperature

therefore based on Start/Finish temperatures as above.

Appendix 8 cont.....

Total Energy(Q₁) stored in Vessel 1;

$$\begin{aligned} Q_1 &= 820 \times 4.187 \times \left(\left(\frac{x_1 + x_2}{2} \right) - \left(\frac{w_1 + w_4}{2} \right) \right) / 3600 \\ &= 820 \times 4.187 \times \left(\left(\frac{20.9 + 29.8}{2} \right) - \left(\frac{20.7 + 23.4}{2} \right) \right) / 3600 \\ &= \underline{3.14 \text{ kW h}} \end{aligned}$$

Total Energy(Q₂) stored in Vessel 2;

$$\begin{aligned} Q_2 &= 820 \times 4.187 \times \left(\left(\frac{x_5 + x_8}{2} \right) - \left(\frac{w_5 + w_8}{2} \right) \right) / 3600 \\ &= 820 \times 4.187 \times \left(\left(\frac{20.9 + 29.8}{2} \right) - \left(\frac{20.9 + 23.9}{2} \right) \right) / 3600 \\ &= \underline{2.38 \text{ kW h}} \end{aligned}$$

Total energy (Q_t) stored over the test duration;

$$\begin{aligned} Q_t &= 3.14 + 2.38 \\ &= \underline{5.52 \text{ kW h}} \end{aligned}$$

Appendix 8 cont.....

Approach b (Referred to to program syntax)

Calculation of energy stored based on AVERAGE temperatures of stored water.

Total energy(Q_1) stored in vessel 1;

$$\begin{aligned} Q_1 &= 820 \times 4.187 \times ((26.7 - 22.5))/3600 \\ &= \underline{4.0 \text{ kW h}} \end{aligned}$$

Total energy(Q_2) stored in Vessel 2;

$$\begin{aligned} Q_2 &= 820 \times 4.187 \times ((26.35 - 23.35))/3600 \\ &= \underline{2.67 \text{ kW h}} \end{aligned}$$

Total energy (Q_t) stored over test duration

$$\begin{aligned} Q_t &= 4.0 + 2.67 \\ &= \underline{6.67 \text{ kW h}} \end{aligned}$$

The difference in total energy stored over the test duration as calculated using approach a) and approach b) is 1.15 kW h.

Appendix 8 cont.....

The total energy rejected at the condenser for this particluar test was recorded as 7.39 KW h.

The approaches a) and b) are therefore inadequate for precise calculation of store effectiveness. A more precise approach, using a number of temperature "bands" or "nodes" is therefore more representative of store behaviour.

Appendix 9

Summary of Test Conditions for a Typical Test Period - (Ref: Graph 18)

Water meter advance $2.6539 \text{ m}^3 = 0.851 \text{ m}^3 \text{ hr}^{-1}$

Compressor energy consumption 5.85 kWh)

) 2.7 hours running

Fan energy consumption 1.30 kWh)

Water pump energy consumption 1.16 kWh 3.12 hours running

Water flow velocity 0.52 ms^{-1}

Air temperature @ evaporator

	Wet/Dry bulb inlet °C	Wet/Dry bulb outlet °C
Start	15.6/20	15/19
Finish	15.6/20	15/19

R₂₂ pressure/temperature @ condenser inlet (Psig/°F)

Start	120/69
Start + 2 hrs	175/92
Finish	180/96

Appendix 9 cont....

R₂₂ pressure/temperature @ compressor inlet (Psig/°F)

Start ---*

Start + 2 hrs 37/14

Finish 39/17

*NB. At start-up the pressure/temperature of refrigerant is equalised through the system.

Variable height thermocouple heights (i.e. giving 5 radial temperatures).

Vessel 1 @ 27.3 cm throughout test

Vessel 2 @ 27.3 cm at start of test

 @ 83.0 cm at start + 30 minutes

 @ 70.0 cm at start + 100 minutes

 @ 60.0 cm at start + 170 minutes.

The radial positions within Vessel 2 being:

T/c 1 @ 15.24 cm Rad

T/c 2 @ 30.48 cm "

T/c 3 @ 22.86 cm "

T/c 4 @ 45.72 cm "

T/c 5 @ central position.

Appendix 10

Summary of Test Conditions.

(Ref: Graph 25)

Water meter advance $1.9277 \text{ m}^3 = 0.909 \text{ m}^3 \text{ hr}^{-1}$

Compressor energy consumed 4.02 kWh)

) Running period 2.0 hr

Fan energy consumed 0.92 kWh)

Water pump energy consumed 0.84 kWh Running Period 2.12 hr

Water flow velocity 0.56 ms^{-1}

Air temperatures at evaporator

	W/D (inlet) °C	W/D (outlet) °C
Start	13.9/19.4	14/20
Finish	12.8/18.9	12.5/17.5

R₂₂ pressure/temperature @ condenser inlet (psig/°F)

Start	115/66
Start +	1.167 hrs 155/85
Finish	175/92

Appendix 10 cont.....

R₂₂ pressure/temperature @ compressor inlet (psig/°F)

Start ---

Start + 1.167 hrs 35/12

Finish 37/14

Variable thermocouple carrier height (5 radial positions)

Vessel 1 @ 40.0 cm throughout

Vessel 2 @ 70.0 cm throughout

T/c₁ @ 15.24 cm rad

T/c₂ @ 30.48 cm "

T/c₃ @ 22.86 cm "

T/c₄ @ 45.72 cm "

T/c₅ @ central position.

Appendix 11

Summary of Equations used in the Mathematical Model

From graph 20 the following equations result:

$$@ \text{ height } 27.3 \text{ cm } t = 20.313 + 0.01875 m$$

$$@ \text{ " } 60 \text{ cm } t = 20.29 + 0.02039 m + 0.0000586m^2$$

$$@ \text{ " } 70 \text{ cm } t = 20.166 + 0.03338 m + 0.0000288m^2$$

$$@ \text{ " } 83 \text{ cm } t = 20.08 + 0.04164 m + 0.0000336m^2$$

when the first term of each equation was replotted against the height - see graph 27.

$$Cf_1 = 20.32 + 0.0017 h - 0.000044h^2$$

when the second term of each equation was replotted against the height - see graph 28.

The general law becomes

$$Cf_2 = 0.02882 - 0.000769 h + 0.0000114 h^2$$

when the third term of each equation was replotted against height - see graph 28

The general law becomes

$$Cf_3 = 0.0000005 + 0.0000012 h + 0.000000005h^2$$

The combined law becomes

$$t = ((20.32 + 0.0017 h - 0.000044h^2) + Cf_2 m + Cf_3 m^2$$

t = temperature of water at height (h) after (m) minutes from heat pump start-up.

The following calculation is a sample based on the formula.

Appendix 11 cont....

Based on test data obtained 21.08.84 (Vessel 2), the T/c carrier height at the end of test was 60 cm, the test duration being 1.25 hours.

$$\begin{aligned}Cf_2 &= (0.02882 - 0.000769 \times 60 + 0.0000114 \times 60^2) \\&= 0.02882 - 0.04614 + 0.04104 \\&= \underline{0.02372}\end{aligned}$$

$$\begin{aligned}Cf_3 &= (0.00000005) + 0.0000012 \times 60 - 0.000000005 \times 60^2 \\&= 0.00000005 + 0.000072 - 0.0000018 \\&= \underline{0.0000545}\end{aligned}$$

$$\begin{aligned}t &= ((20.32 + 0.0017 \times 60 - 0.000044 \times 3600) + (0.0237 \\&\quad \times 75) + (0.0000545 \times 75^2) \\&= \underline{22.35^\circ\text{C}} \text{ compared with the measured value } \underline{24.48^\circ\text{C}}\end{aligned}$$

To generalize the "combined law" it is necessary to take account of variations in the initial bulk temperature of the store from the value 20.32°C applicable in the results presented.

Where the initial store water temperature is different to the value 20.32°C an approach would be:

for a starting temperature (t_s)

$$t = ([(20.32 - (20.32 - t_s)) + 0.0017h - 0.000044h^2] + Cf_2m + Cf_3m^2)$$

Appendix 12

Output Format of Test Data and Typical Evaluated Results

** SYSTEM EVALUATIONS **

RELATIVE HUMIDITY @ EVAP INLET	(%)	56.4395
RELATIVE HUMIDITY @ EVAP O'LET	(%)	47.291
MOIST' CON'T OF AIR TO EVAP	(KG/KG)	5.83784276E-03
MOIST' CON'T OF AIR FROM EVAP	(KG/KG)	4.69561318E-03
DENSITY MOIST AIR TO EVAP	(KG/MCU)	1.073
DENSITY OF DRY AIR OVER EVAP	(KG/MCU)	1.19
FLOW RATE MOIST AIR OVER EVAP	(KG/S)	1.37
FLOW RATE OF DRY AIR OVER EVAP	(KG/S)	1.52
CALC'D AIR VELOCITY OVER EVAP	(M/S)	.235
SP ENTH'Y MOIST AIR TO EVAP	(KJ/KG)	28.86
SP ENTH'Y MOIST AIR FROM EVAP	(KJ/KG)	25.34
COIL SENSIBLE HEAT FACTOR		.18
SEN' HEAT EXT'D (DRY AIR @ EVAP)	(KW)	.91
LATENT HEAT EXTRACTED @ EVAP	(KW)	3.94
SEN' + LAT' HT EX'TED @ EVAP	(KW)	4.85
TOT' HEAT EXT'D (ENTH' CHANGE)	(KW)	4.84
MFR CORR'D DESIGN S'HT CAPACITY	(KW)	.92
MFR CORR'D DESIGN T'HT CAPACITY	(KW)	5.32
EVAPORATING TEMPERATURE	(DEGC)	-2.2
REFRIG'T FLOW RATE (ASHRAE)	(KG/S)	.0355
CONDENSING TEMPERATURE	(DEGC)	49.6
MASS FLOW RATE OF WATER	(KG/S)	.267
CALC'D AVE VELOCITY OF WATER	(M/S)	.75
GRAPH'D AVE VELOCITY OF WATER	(M/S)	1.09
CONDENSER CAPACITY (CORRECTED)	(KW)	8.1
INITIAL AVE STORE TEMP V1	(DEGC)	20.3
FINAL AVE STORE TEMP V1	(DEGC)	42.25
INITIAL AVE STORE TEMP V2	(DEGC)	20.3
FINAL AVE STORE TEMP V2	(DEGC)	35.6

ENERGY ST'D IN VES 1	(% OF TOTAL)	
164.33 LITRES @ 46.05 DEGC(AV)	(%)	21.79
496.44 @ 41.35 DEGC(AV)	(%)	60.83
159.23 @ 38.15 DEGC(AV)	(%)	17.38
TOTAL ENERGY STD VES 1	(KWH)	20.995

ENERGY ST'D IN VES 2	(% OF TOTAL)	
192.69 LITRES @ 40.75 DEGC(AV)	(%)	25.44
439.62 @ 38.9 DEGC(AV)	(%)	20.3
187.69 @ 33.75 DEGC(AV)	(%)	18.64
TOTAL ENERGY STD VES 2	(KWH)	16.785
TOTAL ENERGY IN STORE	(KWH)	37.779

COMPRESSOR COMPRESSION RATIO		4.33
COMPRESSOR VOLUMETRIC EFF'Y	(%)	72.63
C.O.P. (COMB' RATING IND - STD RATG CAP)		1.92
C.O.P. (EVALUATED COMP'OR ONLY)		2.592
C.O.P. (EVALUATED COMP' + AUX PWR)		2.273

Appendix 13

Summary of Parameters Monitored during a Test

** SUMMARY OF INPUTTED VARIABLES & SYSTEM EVALUATIONS **

~~DATA AS QUANTITIES, UNLESS INDICATED~~

DATE OF TEST RUN	80384
HEAT PUMP TEST DURATION	(HOURS) 5.33
VOLUME OF LIQUID IN VESSEL 3	(MCU) 1.64
D-BULB TEMP OF AIR TO EVAP	(DEGC) 13.9
W-BULB TEMP OF AIR TO EVAP	(DEGC) 8.89
D-BULB TEMP OF AIR FROM EVAP	(DEGC) 13.3
W-BULB TEMP OF AIR FROM EVAP	(DEGC) 7.22
BAROMETRIC PRESSURE	(INHG) 28.85
R22 TEMP @ CONDENSER INLET	(DEGC) 92.6
R22 TEMP @ CONDENSER OUTLET	(DEGC) 45.2
R22 PRESS @ COMPRESSOR INLET	(PSIG) 49
R22 PRESS @ COMPRESSOR OUTLET	(PSIG) 260
CONDENSER MEAN WATER IN TEMP	(DEGC) 41.1
CONDENSER MEAN WATER OUT TEMP	(DEGC) 48.2
METERED FLOW OF WATER	(MCUH) .971
WATER PRESS @ CONDENSER IN	(BAR) .25
WATER PRESS @ CONDENSER OUT	(BAR) .15
PIPE/W TEMP (COND TO STORE)	(DEGC) 45
PIPE/W TEMP (STORE TO PUMP)	(DEGC) 20
PIPE/W TEMP (PUMP TO COND)	(DEGC) 25
MEAN TEMP OF CONDENSER P/WK	(DEGC) 55
COMPRESSOR MTR ENERGY CONS'	(KWH) 12.56
EVAPORATOR FAN ENERGY CONS'	(KWH) 2.25
WATER PUMP MTR ENERGY CONS'	(KWH) 2.1
VESSEL 1 MEAN EXT SURF'E TEMP	(DEGC) 18
VESSEL 2 MEAN EXT SURF'E TEMP	(DEGC) 18
INT'L FIXED T/C VESSEL 1 NOS(13-16)	
STARTING TEMP @	(BASE) 18.3
	(+ 30.0CM) 18.8
	(+ 90.0CM) 21.1
	(+ 115.0CM) 22.3
FINISH TEMP @	(BASE) 37.8
	(+ 30.0CM) 38.3
	(+ 90.0CM) 45.6
	(+ 115.0CM) 46.5
INT'L FIXED T/C VESSEL 2 NOS(5-8)	
STARTING TEMP @	(BASE) 19.1
	(+ 34.0CM) 19.9
	(+ 87.0CM) 21.8
	(+ 115.0CM) 21.8
FINISH TEMP @	(BASE) 30.4
	(+ 34.0CM) 37.1
	(+ 87.0CM) 40.7
	(+ 115.0CM) 40.7

Appendix 14

Summarized Calculation Output Format

```

20 PRINT"HEAT PUMP & STORAGE SIMULATION PROJECT"
22 FORJ=1TO1000:NEXT
30 PRINT"
35 READXX,PH,L1,P1,L2,P2,L3,P3,L4,P4,NB,NV,NC,NI,NO,ND,NT,IT,DFS,LD,OE
40 READLL,LIT,K1,K3,DV,TVI,VH,K8,SS,PID,SH
45 READSW,SP,FP,ZX,ZY,KV
50 DATA1,4,8,22,1.5,28,3,15,7,22,10,4,3,2,2,1,6,50,0.25,19,80
55 DATA7,50,0.035,0.035,0.5,50,0.75,0.035,1700,.05,.75
60 DATA4,186,3,0.19,100,5,1000,5,6.58E-07
65 CLOSE1:OPEN1,4
80 PRINT"ANSWER THE QUESTIONS WITH NUMERICAL DATA"
83 PRINT"DATA AS @ END OF TEST UNLESS INDICATED"
92 PRINT"VESSEL BEING CONSIDERED 1 2 OR 3(1+2)"
93 GETZ$
94 IFZ$=CHR$(49)THENVV=1:GOTO100
95 IFZ$=CHR$(50)THENVV=2:GOTO100
96 IFZ$=CHR$(51)THENVV=3:GOTO100
97 GOTO93
100 PRINT"DATE OF TEST RUN"
104 PRINT"HEAT PUMP TEST DURATION"
106 GOSUB19000
107 F=F1:F0=F3:DF=(10*(F-F0)):GOSUB119
108 PRINT"RELATIVE HUMIDITY @ EVAP INLET (X) ";HH:HY=HH
114 F=F2:F0=F4:DF=(10*(F-F0)):GOSUB119
115 PRINT"RELATIVE HUMIDITY @ EVAP O'LET (X) ";HH:HZ=HH
116 GOTO129
119 IFF<=18 THENDE=DF:HH=(95-((DE-5)*.855)):GOTO128
120 IFF>18ANDFC19.1 THENDE=DF:HH=(95-((DE-5)*.832)):GOTO128
121 IFF>19ANDFC20.1 THENDE=DF:HH=(95-((DE-5)*.83)):GOTO128
122 IFF>20ANDFC21.1 THENDE=DF:HH=(95-((DE-5)*.817)):GOTO128
123 IFF>21ANDFC22.1 THENDE=DF:HH=(95-((DE-5)*.77)):GOTO128
124 IFF>22ANDFC23.1 THENDE=DF:HH=(95-((DE-5)*.75)):GOTO128
125 IFF>23ANDFC24.1 THENDE=DF:HH=(95-((DE-5)*.735)):GOTO128
126 IFF>24ANDFC25.1 THENDE=DF:HH=(95-((DE-5)*.71)):GOTO128
127 IFF>25ANDFC26.1ANDFO<(F-5.1)THENDE=DF:HH=(95-((DE-5)*.70)):GOTO128
128 RETURN:RETURN
129 TY=(F1+273.16)
130 N1=10*(28.591-8.2*LOG(TY)/LOG(10)+.00248*(TY)-3142.31/TY)
131 N2=HY*N1/100
132 N3=((.622*N2)/((BP/29.92)-N2))
133 N3$="MOIST' CON'T OF AIR TO EVAP (KG/KG)":PRINT""N3$.N3
134 ESE=INT((1.007*F1-.026+N3*(2501+1.84*F1))*ZX)/100
135 TZ=(F2+273.16)
136 N5=10*(28.591-8.2*LOG(TZ)/LOG(10)+.00248*(TZ)-3142.31/TZ)
137 N6=HZ*N5/100
138 N7=((.622*N6)/((BP/29.92)-N6))
139 N7$="MOIST' CON'T OF AIR FROM EVAP(KG/KG)":PRINT""N7$.N7
142 LSE=INT((1.007*F2-.026+N7*(2501+1.8*F2))*ZX)/100
147 RM=(1.2929*(273.15/(F1+273.16))*((BP/29.92)-(.3783*N2))/1.101325))
148 RM=INT(RM*ZX)/1000
149 RM$="DENSITY MOIST AIR TO EVAP (KG/MCU)":PRINT""RM$.RM
150 MF=INT((1.275*RM)*ZX)/100:REM 1.275=VOL FLOW RATE OF AIR MCU/S
155 MF$="FLOW RATE MOIST AIR OVER EVAP(KG/S)":PRINT""MF$.MF
160 DA=INT((1.2014*(294.1/(273+F1))*((BP/29.92))*ZX)/100
165 DA$="DENSITY OF DRY AIR OVER EVAP(KG/MCU)":PRINT""DA$.DA
170 MD=INT((1.275*DA)*ZX)/100
175 MD$="FLOW RATE OF DRY AIR OVER EVAP(KG/S)":PRINT""MD$.MD
180 ESE$="SP ENTH'Y MOIST AIR TO EVAP(KJ/KG)":PRINT""ESE$.ESE
185 LSE$="SP ENTH'Y MOIST AIR FROM EV(KJ/KG)":PRINT""LSE$.LSE
190 QS=INT(MD*(F1-F2)*ZX)/100:REM WE IN
195 QD=INT((MD*2261*(N3-N7))*ZX)/100:REM 2261=SP LAT HT OF VAPOR (WATER)
196 REM ALSO QD=Q2-QS
200 Q2=INT((MF*(ESE-LSE))*ZX)/100
210 QS$="SEN' HT EXT'D (DRY AIR @ EVAP)(KW)":PRINT""QS$.QS
215 QD$="LATENT HEAT EXTRACTED @ EVAP (KW)":PRINT""QD$.QD

```

REFERENCES

1. Tabor H. ISE Congress Solar World Forum. Brighton 1981. Pergammon Press (Pxxiv).
2. Brinkworth B J. Thermal Storage in density stratified fluids and phase change materials. J. Inst. Energy (GB), Vol 52, No. 413, pp 193-6 (Dec 1979).
3. van Koppen C W J. Short and long term sensible storage. Solar Energy Benefits evaluated. Techniques and Results. Conf. Report. The University of Birmingham. M3 (Sept 1982).
4. University of Wisconsin - A parametric study of DHW installations. ISES Congress. The Sun in Service of Mankind, Paris (1973) (Handouts). Gutierrez C et al. Paper E50.
5. Wood R J. Thermally stratified hot water storage systems. Appl. Energy (GB). Vol 9. No.3 pp 231-42 (Nov 1981).
6. ISES Congress, Solar World Forum Conf. Report. Brighton 1981. Pergammon Press (1982).
7. Cox A J., Neal W E J and Yankuba S C S. A study of a heat pump used to heat a Domestic or Commercial service hot water system. Dept of Mathematics and Physics, The University of Aston in Birmingham.
8. Neal W E J. Thermal Energy Storage. Phys. Technol. Vol 12. pp 213-226 (1981).
9. Todd R W. Conf. Rep. UK-ISES C15 1 (1978).
10. Wozniak S T. Conf. Rep. UK-ISES C11 71 (1977).
11. Pearson J. How gas engines can drive heat pumps for profit. Dept of Energy - Energy Management FOCUS. Issue No.1. (1985) pp 12-13.
12. Witt A. Heat pumps penetrate the Industrial Markets. Dept of Energy - Energy Management Focus Issue No.1. (1985) pp4-6.
13. Pabon-Diaz M. A study in the application of domestic solar assisted heat pumps for heating and cooling. Thesis submitted for the Degree of Doctor of Philosophy. The University of Aston in Birmingham (Aug 1982).

14. McDonnell T. Experience with heat pumps in the field. Symposium Report. Inst. of Energy. University of Warwick (Sept. 1983).
15. Tassou S A., Marquand C J and Wilson D R. Modelling of variable speed air-to-water heat pump systems. J. Inst. Energy (June 1982).
16. The Heat Pump and Air Conditioning Bureau. Domestic Heat Pumps. Electricity Council Information. EC4302/9 82.
17. Anderson J A., Bradford R A and Carrington C G. Assessment of a heat pump water heater. J. of Energy Research. Vol. 9. (1985).
18. Carrington C G and Knopp (1983). J. of Energy Research. Vol. 6. pp 233-240. (1982). John Wiley and Sons Limited.
19. Channey S R., Humphrey J A C., Mouth L., Shah A. Flow and heat transfer of a stably stratified fluid through an enclosure. ASME J. of Solar Energy Engineering. Vol. 106. (Aug 1984).
20. Neal W E J. Collecting precious joules. Inaugural Lecture, University of Aston in Birmingham (Oct. 1980).
21. Rogers G F C and Mayhew Y R. Thermodynamic and transport properties of fluids, S I Units, 2nd Edition. Oxford Blackwell (1967).
22. ASHRAE. Pocket handbook for air conditioning, heating, ventilation, refrigeration. (c1987).
23. Dossat R J. Principles of Refrigeration (2nd Edition) - SI Units, Wiley (1978).
24. Dhar Manmohan. Transient analysis of refrigerating systems. Ph.D. Thesis to Purdue University (May 1978).
25. ASHRAE - Compressor Calibration Method. Methods of testing for rating unitary air conditioning and heat pump equipment. Direct heating capacity measurement 4.4 p9. ANSI/ASHRAE 37-1978.
26. Ozisik Necati M. Heat Transfer. A basic approach. McGraw-Hill Book Co. 1985.
27. Woods G. Woods Practical Guide to Fan Engineering (second edition). Woods of Colchester 1969 (5th impression).

28. Lewit E H. Thermodynamics Applied to Heat Engines. (Fifth Edition). Pitman and Sons Ltd, London (1957).
29. Kinetic Chemicals Inc.
30. IHVE. Guide Book C. Sec 17. Table 17-3.
31. Addison H. The pump users handbook. Pitman.
32. Karassik I J., Carter R. Centrifugal Pumps - selection, operation and maintenance. McGraw-Hill. USA. (1960).
33. Douglas J F. Solutions of problems in fluid mechanics. (Part 1). Pitman 1967.
34. Blair J S. New formulae for water flow in pipes. Proc. I. Mech. E. Vol. 165. 1951.
35. C.E.G.B. Memoranda GDM 38 (DM 023/3) (GEN/11/13/9744).
36. D'Arcy and Chezy.
37. Reynolds O A. Proc. Manchester Lit. and Phil. Soc. (1874).
38. Colebrook and White in IHVE Guide. Section 3.
39. The SIHI Group. Basic principles for the design of centrifugal pump installations. SIHI-HALBERG. (West Germany). (1980).
40. Loveday D L. Conventional roofs as collectors in a solar assisted heat pump system. Thesis submitted to the University of Aston in Birmingham. June 1983.
41. National engineering steam tables, 1964.
42. IHVE Guide, Book C. 1970.
43. Jones. Air Conditioning Engineering. (1973).
44. Handbook of Chemistry and Physics (1973/74). Chemical Rubber Co. USA. 1973.
45. Carlyle Air Conditioning Co. Ltd. 38 CQ split system heat pump outdoor sections. From 38CQ-C1P (Revised). Caricor Ltd. London 1976.
46. Sack J., Meadows J. "Entering Basic". Science Research Associates. 1973.
47. Pegels C. BASIC: A Computer Programming Language. Holden-Day Inc. 1973.

48. Albrecht, Finkle, Brown. BASIC. Peoples Computer Co. 1973. 1010 Doyle (P O Box 3100), Menlo Park, CA 94025.
49. Karlekar B V and Desmond R M. Heat Transfer 2nd Ed. St Pauls, Minn West Pub. Co. 1982.
50. Metais B., Eckert E R G. Forced, Mixed and Free Convection Regimes. ASME. J. of Heat Transfer (1986).
51. Abramovich G N. The theory of turbulent jets. Cambridge, Mass MIT Press. 1963.
52. Cornwell K. The flow of heat. Van Nostrand Reinhold Co. (England) 1977.
53. Colburn A P. Trans. A.I. Ch. E. (1933).
54. Seider E N., Tate G E. Ind. Chem. Eng. 28. (1936).
55. Sleicher C A and Tribus M. Heat transfer in a pipe with turbulent flow and arbitrary wall - temperature distribution, Trans ASME (1957).
56. Stephenson
57. Sellars S R, Tribus M and Klein J S. Heat transfer in laminar flow in a round tube or flat plate, Trans. ASME (1956).
58. Webb
59. Filonenko
60. Kundsen James G., Katz Donald L. Fluid dynamics and heat transfer. McGraw-Hill. 1958.
61. Hanson Arthur Gene. Fluid Mechanics. Wiley 1967.
62. Kreith F., Black William Z. Basic heat transfer. Harper Row. 1980.
63. Blay D. Abs. Solar World Forum. Vol. 1. Brighton. 1981. Laboratoire d'Enegetique Solaire - CNRS. France.
64. Welty J R. Engineering Heat Transfer SI Version. Willey 1978.
65. Schlichting H. Boundary Layer Theory. 4th Edition. McGraw-Hill.
66. Pia S I. Fluid Dynamics of Jets. New York 1954.

67. Bayley F J., Owen J M., Turner A B. Heat Transfer. Thomas Nelson and Sons Ltd. 1972.
68. Nikuradse J. Third International Congress of Applied Mechanics (1930), also (1932) (1933).
69. Miller R S., Energy (GB). Vol 5. No.2. Feb 1980.
70. Vasilakis A D., Gerstmann J., Celovier G. Energy Technology XI Applications and Economics. Proc. Eleventh Energy Tech. Con. Washington DC. 1984.
71. Mobil Oil Co. There's no way around oil and gas. Sanit-Heizingstech 1982. Vol. 47. Issue 2. pp 80-82. CODEN: SAKEAO. Federal Republic of Germany.
72. Norrey M J. Report of the performance of a Honeywell Excel DDC unit at Foster Menswear - Sutton Coldfield. June 1987. Report presented to company management - restricted circulation.
73. Hoffman G H., Nimmagadda M. Energy Technology XI. "Applications and Economics". Proc. Eleventh Energy Tech. Con. Washington DC. 1984.
74. Rotocold Ltd. Technical Guide - The use of variable speed drives and rotary compressors in the refrigeration industry. Hereford. Issue No.1. (Feb. 1987).
75. Mills M. Variable speed drives. Refrigeration, air conditioning and heat recovery (Feb 1987).
76. Harmsworth B. Sensible Heat Storage in Water. Heat and Vent Engineer (GB). Vol. 57. No. 659. p 5-10 (July/Aug) 1983.